Investigations into Structure Formation of Dairy Products

vorgelegt von
Diplom-Ingenieur
Monika Stephanie Brückner-Gühmann
aus Overath

Von der Fakultät III – Prozesswissenschaften
der Technischen Universität Berlin
zur Erlangung des akademischen Grades
Doktor der Ingenieurwissenschaften
Dr.-Ing.

genehmigte Dissertation

Zusammenfassung

Eine gleichbleibend hohe Produktqualität determiniert maßgeblich die Akzeptanz beim Verbraucher und den Erhalt der Marktstellung. Dieses Ziel lässt sich nur realisieren, wenn eine Qualitätskontrolle der involvierten Prozesse und Rohmaterialien erfolgt. Vielfach existieren zur Qualitätsbeurteilung nur aufwendige analytische Methoden, die eine schnelle Kontrolle und ein unmittelbares Eingreifen verhindern. Mit dieser Arbeit sollen die Strukturbildung und -änderung im Verlauf verschiedener Prozesse in der Produktionstechnologie der Milchindustrie untersucht und Prüfprocedere entwickelt werden, die als Schnellmethoden ein kurzfristiges Bewerten der Rohstoffe und ein Eingreifen in den Produktionsprozess ermöglichen.

Die labinduzierte Gerinnung wurde sowohl mit Rohmilch gesunder Kühe und Ziegen als auch mit Milch euterkranker Kühe durchgeführt. Ziel der Untersuchungen war eine Analyse der biochemischen Veränderungen des Caseins und der Strukturierungsmechanismen. Der Untersuchungsschwerpunkt umfasst die zeitliche Abfolge und Kopplung zwischen biochemischen Reaktionen am Casein und den Strukturveränderungen von der Milch zum Labgel durch inline-online-Erfassung der Prozessviskosität. Die Kinetik der enzymatischen Reaktion am Beispiel der Freisetzung von Caseinmakropeptid und die resultierenden Strukturbildungsmechanismen wurden untersucht und modelliert. Es zeigt sich ein deutlich abweichendes Verhalten der Milch von euterkranken Kühen. Durch Kopplung der Strukturparameter mit den Ergebnissen der hydrophoben Interaktionschromatographie werden Veränderungen am Caseinprofil der Milch von euterkranken Kühen nachgewiesen. Daher sollte diese im Rahmen der Promotion entwickelte Analytik in eine Eingangskontrolle der Milch aufgenommen werden. Bezüglich der Optimierung der Käseproduktion bietet die rheologische Methode eine Möglichkeit den optimalen Schneidezeitpunkt nicht mehr visuell zu beurteilen, sondern objektiv anhand der Endviskosität zu bestimmen.

Die Untersuchungen zur Labgerinnung von Ziegenmilch dienen der Überprüfung der Übertragbarkeit der rheologischen und spektrophotometrischen Methode. Es werden klare Unterschiede zum Gerinnungsverhalten von Kuhmilch vor allem bei der Gelausbildung gefunden.

Üblicherweise wird bei dem Prozess der Säuregerinnung (Joghurtproduktion) die Trockensubstanz der Prozessmilch erhöht, was unter anderem durch Zugabe von Molkenproteinkonzentratpulvern geschehen kann. Aus der Industrie ist das Auftreten einer erheblichen Anzahl von Fehlfermentationen bekannt, die in einer mangelhaften Funktionalität der Pulver begründet sind. Thermisch denaturierte Molkenproteinpulver bilden Partikelgele aus, was sich wiederum als Störgröße auf den Technologieablauf und die Produktqualität (Synärese) auswirkt. Es besteht daher ein großes wirtschaftliches Interesse an einer Schnellmethode zur Bewertung der Pulverqualität. In der vorliegenden Arbeit wird die Laserdiffraktometrie als Verfahren zur Bewertung des Lösungsverhaltens gewählt und die Anwendbarkeit durch eine umfassende Methodenentwicklung und verschiedene Untersuchungen bestätigt.

Als wichtige dritte Produktionstechnologie in der Milchindustrie wird die Sprühtrocknung am Beispiel der Herstellung von Quarkpulver betrachtet. Hierbei muss besonders beachtet werden, dass es sich um ein plastisches, nicht-NEWTON`sches System handelt. Die Produktionstechnologie wird im Folgenden untersucht, wobei kritisch angemerkt werden muss, dass anstatt der üblichen Zerstäubung für hochkonsistente Produkte über eine Scheibe eine Düse gewählt wurde, die ursprünglich zur Trocknung von Magermilchkonzentrat ausgelegt war. Zudem wurde der Einfluss von Scherenergie und Wärme auf die Destrukturierung vor Trocknung untersucht.

Abstract

The production of dairy products of a consistently high quality significantly determines consumer acceptance and will occupy a similarly important market position in the future. This objective can be realized if a quality control of the involved processes and raw materials is undertaken. In many cases, only elaborate analytical methods exist which represent a barrier to a rapid control and direct intervention. In this work the structure formation and structural changes in the course of various processes in dairy production technology should be examined and methods should be developed, which facilitate a rapid grading of the raw materials and intervention in the production process.

Rennet-induced coagulation was investigated for raw bulk cow and goat milk as well as for milk from infected udder quarters of cows. Experiments were carried out to gain more scientifically-based information on biochemical changes of the casein and the mechanism of structuring during rennet-induced coagulation. The main focus of the research was the time-dependent coupling between the biochemical reaction of the casein and the structural change from the fluid milk to the rennet gel by inline-online detection of the process viscosity. The kinetics of the enzymatic reaction—the release of caseinmacropeptide—and the resulting structuring mechanisms were examined and modeled. A significantly different behavior of milk from infected udder quarters was detected. The structure parameter in combination with the hydrophobic interaction chromatography results proved an altered casein profile. It is imperative that the analytical method which was developed as part of this thesis be included in milk grading. Concerning an optimized cheese production, the rheological method offers the possibility to determine the optimal cutting time not only from a subjective but also from an objective position by calculated projection of the end viscosity after a definite time period.

The investigations dealing with the rennet-induced coagulation of goat milk were done to verify the transferability of the rheological and spectrophotometric method. Significant differences were detected between the rennet-induced coagulation of cow and goat milk especially between the gel formation.

Commonly, during the process of acid-induced coagulation (yoghurt production) dairy powders are used to increase the dry matter of the process milk which is often done by addition of whey protein concentrate powder. It was found that in the production flow a large share of defective fermentations might occur, which are related to defective functionality of the powders. Thermal denaturation of whey proteins leads to the development of particle gels which act as a disturbance variable during the production process and for the product quality (syneresis). As a result, the development of a rapid method for the assessment of the powder quality is of great economic interest. The principle of laser diffraction was chosen in the present work for the assessment of the rehydration behavior and the applicability of this method has been confirmed by an extensive method development and diverse experiments.

The third important production technology in the dairy industry—spray drying—is viewed exemplarily for the production of quark powder. Attention should be paid to the fact that quark is a plastic, non-NEWTONIAN system. In the following, production technology systems are investigated. It has to be remarked here that atomization was done via nozzle instead of the commonly used wheel atomization for highly consistent products. The nozzle geometry typically was designed for the drying of skim milk concentrate. Additionally, the influence of shear energy and temperature on the structure deformation before drying was investigated.

Acknowledgements

Table of Contents

List of Figures

List of Tables

Nomenclature

Abbreviations and acronyms I	
BSA	Bovine serum albumin
C	Percentage concentration of the crosslinker (bisacrylamide) relative to the total concentration T
C.V.	Column volume
Ca	Calcium
CAS	Chemical abstracts service
CMP	Caseinmacropeptide
CN	Casein
CN-No.	Casein number
CSR	Controlled stress rheometry/controlled shear rate
d.m.	Dry mass
D_{65}	Standard illuminant defined by the International Commission on Illumination; also daylight illuminant
DF	Diafiltration
DQ_i	Differential quotient
DSC	Differential scanning calorimetry
GMP	Glycomacropeptide
GPC	Gel permeation chromatography
HCl	Hydrochloric acid
HB	HERSCHEL-BULKLEY
HIC	Hydrophobic interaction chromatography
HPSEC	High performance size exclusion chromatography
IDF	International Dairy Federation
IE	Ion-exchange
Ig	Immunoglobulin
Ip	Isoelectric point
LKV	Landeskontrollverband
MCP	Milk coagulation property
MF	Microfiltration
MFGM	Milk fat globule membrane
Mw	Molecular weight
n.-g. CMP	Non-glycosylated caseinmacropeptide
NCN	Non-casein nitrogen
NF	Nanofiltration
NPN	Non-protein nitrogen
NSI	Nitrogen solubility index
OW	OSTWALD DE WAELE
PAGE	Polyacrylamide gel electrophoresis
PBS	Phosphate buffered saline
pKa	Negative log of the dissociation constant Ka
PS	Protein solubility
PSD	Particle size distribution, based on volume
rehy.	after full rehydration
RO	Reverse osmosis
SCC	Somatic cell count
SD	Spray drying

Abbreviations and acronyms II	
SDS	Sodiumdodecylsulfate
SDS-PAGE	PAGE performed under dissociating and reducing conditions
SEM	Scanning electron microscopy
SHE	Surface heat exchanger
SMP	Skim milk powder
Spec. surf.	Specific surface
Std. dev.	Standard deviation
SWP	Sweet whey powder
T	Total percentage of both monomers (acrylamide/bisacrylamide)
TCA	Trichlor acetic acid
TEMED	Tetramethylethylenediamine
UF	Ultrafiltration
WPC	Whey protein concentrate
WPI	Whey protein isolate
WPNI	Whey protein nitrogen index
ZELMI	Zentralinstitut für Elektronenmikroskopie
α-La	α-Lactalbumin
β-Lg	β-Lactoglobulin

Symbols I		*Unit*
$A_{280\,nm}$	Absorptivity of a 1 % solution measured in a 1 cm light path at 280 nm	%
A_{Th}	Thixotropic area	$Pa \cdot s^{-1}$
a	Distance from scatterer to detector	mm
b	Amount of Chelaplex III	ml
c	Concentration	%; $mg \cdot ml^{-1}$
c_{milk}	Concentration in milk	$g \cdot kg^{-1}$
$c_{Ca^{2+}}$	Calcium concentration	$Ca^{2+} \cdot 100\ ml^{-1}$ milk
D_{10}	Particle diameter for cumulative distribution value 10%	µm
D_{50}	Particle diameter for cumulative distribution value 50%	µm
D_{90}	Particle diameter for cumulative distribution value 90%	µm
d	Diameter	m
E	Weighted sample	ml
F	Factor of the Chelaplex III solution	
g	Acceleration due to gravity	$m \cdot s^{-2}$
h	Groups of samples	m
$I(\theta)$	Total scattered intensity as a function of angle	
I_0	Intensity of the incident light	
i	Indication for imaginary part of refractive index	
K	Consistency index	$Pa \cdot s^{n}$
k	Wave number; $k = \dfrac{2\pi}{\lambda}$	

Symbols II		Unit
k_{IP}	Imaginary (absorption) part of refractive index of particle	
l	Length	m, cm
m	Complex refractive index	
N	Number of experiments/detectors	
n	Flow behavior index	
n_m	Refractive index of dispersion medium	
n_{RP}	Real part of refractive index of particle	
Oh	OHNESORGE number	
$P_{Supernatant}$	Protein content in the supernatant	%
$P_{Solution}$	Protein content in the solution	%
p_c	Capillary pressure; Laplace pressure	Pa
p_w	Pressure drop in the flow direction	
R	Measure for quantification of the quality of the raw data and the calculation of the reported particle size distribution using the chosen real and imaginary parts of the refractive index	
R^2	Coefficient of determination	
Re	REYNOLDS number	
r	Correlation coefficient	
r_c	Capillary radius	m
$S_1(\theta); S_2(\theta)$	Dimensionless, complex functions, describing the change of amplitude in, respectively, the perpendicular and the parallel polarized light as a function of angle and particle diameter	
s	Standard deviation	…
T	Temperature	°C, K
t	Time	min, h
V	Volume	m³, cm³
$\dot{V}$	Flow rate	l·h^{-1}
$\dot{V}_{max}$	Maximum capacity	l·h^{-1}
v	Velocity	m·s^{-1}
v_S	Settling velocity	m·s^{-1}
We	WEBER number	
x	Individual value	
$\bar{x}$	Mean value	
y	Depth of penetration	m
$z(x)$	The calculated scattered light at each channel of the detector based on the chosen refractive index kernel and reported particle size distribution.	
z	The measured scattered light at each channel of the detector	

Greek symbols		Unit
α	Level of significance	
$\dot{\gamma}$	Shear rate	s^{-1}
δ	Contact angle	°
$\delta(v)$	Dynamic contact angle depending on the velocity of the advancing liquid meniscus	°
Δ	Gradient	
η	(Process) viscosity	Pa·s; mPa·s
η_{eff}	Effective viscosity	Pa·s
θ	Angle with respect to forward direction	°
λ	Wavelength of the illuminating source in medium	nm
ρ	Density	$kg·m^{-3}$
σ	Surface/interfacial tension forces	$N·m^{-1}$
τ	Shear stress	Pa
τ_0	Yield point	Pa
χ^2	Measure for quantification of the quality of the raw data and the calculation of the reported particle size distribution using the chosen real and imaginary parts of the refractive index	

Indices	
c	capillary
i	Individual value
L	Liquid
P	Particle

Chapter 1: Introduction

Quality assurance and control play an important role in dairy technology as long as compositional variations exist for the raw material milk and consequently for the products produced from it. Additionally, most of the processing technology involved requires a complex procedure which in itself might cause quality variations or deficits, if the process is not capably undertaken and reliable.

The production of high quality dairy products with respect to taste, smell, consistency, (mouthfeel, stability), and appearance, which maintain a stable structure over storage time, is of primary importance. Therefore, the processes and the raw materials have to be analyzed, optimized, and controlled.

It has to be guaranteed by the manufacturer that the quality of the product meets with strict specifications. Control methods have to be able to monitor and control the quality of the final products and also at an earlier stage so that corrections are possible. These control methods would refer to control of input and output streams as well as of all relevant processing steps in between. Thus, processing would be more effective producing higher yields and less loss of valuable products. To enhance process-effectiveness an inline/online control of the processes might be advantageous, which means that the data are gained very quickly and correction is possible after a short time.

The present work makes an attempt to take a closer look at processes in dairy technology which are, in detail, the acid and rennet-induced coagulation and the drying technology, taking the production of quark powder as an example. The raw material milk itself and its quality for the rennet-induced coagulation as well as further dairy additives like WPC powders and the production technology are viewed. Several parameters are considered for process optimization and quality control. These parameters are:

- the cheese-making parameters of the milk—controlled inline/online—and its dependence of the coagulation process on udder inflammation,

- the solubility/functionality of dairy powders being used in acid coagulation as an input quality control in form of a rapid method, and

- the water retention of quark powder after rehydration to maintain the desired texture.

The focus of the present work is on the investigation into structure formation during various processes in dairy technology and—derived therefrom—the development of control methods for the various processes which provide reliable information at an early stage, thus allowing immediate controlling and correction. Especially for the processes of rennet-induced coagulation and acidification these rapid control methods should be able to assess the input streams like the quality of the raw milk and the functionality of the powders used so that those raw materials can be rejected prior to processing.

To date, visual clotting time is the key parameter for the programming of equipment during cheese production. To gain a maximum cheese yield and quality an exact determination of the gel firmness is needed, because a too-soft gel causes protein and fat losses and a too-firm gel requires unnecessary deceleration of the overall process.

All-in-all, research is needed on the detailed mechanisms of rennet-induced coagulation and the interrelationship with milk composition. Additionally, the rheological measurements of the rennet-induced coagulation should provide a parameter—the process viscosity in relation to time—which can be used as an objective tool for the control of the production process. The results should enable a grading of the rennetability of the milk in dependence on milk composition. The physical changes of milk from healthy cows during rennet-induced coagulation have been published [1-5]. Now, a connection between physical and biochemical parameters should be presented. The biochemical parameters are related to the coagulation parameters and cow health.

Commonly, whey protein powders are used in sour milk production to standardize the non-fat solid content of the milk. Heat treatment in yoghurt production is commonly high to obtain the desired structure [6]. Typically, a degree of whey protein denaturation of about 75 % is achieved [7;8]. It was reported that at a high degree of whey protein denaturation the whey proteins interact with the casein micelle surface, coat it, and—as a result—lead to a decreased surface hydrophobicity and increased water binding capacity [8]. Thus, yoghurt texture and water retention are improved. However, the study of SCHORSCH, WILKINS, JONES, and NORTON (2001) indicates that if pre-denatured whey proteins are present in the yoghurt milk before heat treatment large aggregates exist, which are not able to interact with the casein micelle surface during heat treatment [9]. Thus, those aggregates act as a destructive filler or structure breaker in acid milk gels.

Additionally, practical investigations have led to the conclusion that heat-denatured whey proteins cause particle gels to become a disturbance variable on the production process and the product quality (syneresis) [10-13]. Currently, about 15 to 20 % mis-fermentations are assumed. Therefore, there is an enormous economic and also scientific interest in the development of a rapid method for the assessment of the powder quality—in detail the ability to completely rehydrate—immediately before its use in sour milk technology. But to date no practicable method for the rapid powder analysis including the assessment of functional and structuring properties is known.

Quark powder is a raw material produced for use in bakery products mainly for fillings, pastries, and long-life bakery products (convenience product for bakery) but also for ice cream, chocolate, dressings, sports foods, and desserts. The advantages of a powder compared to the original quark are the ease of handling and transport, the extension of the shelf life, better storage properties, and favorable dosage. Nevertheless, the conversion into a dry product can create additional problems. Quark (18 % dry matter) can be described as a highly structured product. After drying, the resulting product should be easy to rehydrate and the resultant structure/consistency level should be as high and stable as the original quark. A deficient powder quality is characterized by problems in consistency and functional properties such as water retention after rehydration.

In the present work the attempt was made to atomize the highly structured product low fat quark via nozzle atomization instead of the commonly used disc atomization. When quark powder is produced by spray drying, insufficient atomization can cause quality problems of the powder after rehydration. Those quality problems are normally related to separation of very large particles from the atomizer. The time of exposure of the very large particles in the dryer might be too short to result in complete drying. Hence, only the surface is dried. Because of long diffusion path of the water and water vapor to the interface no cooling effect takes place and a crustification occurs at the surface of the quark particles. Additionally, this crustification inhibits a complete drying of the inner part of the particles which very likely negatively influences the wetting of the particles and therefore the functionality.

Chapter 2: Objectives

Overall, the acid and rennet-induced coagulation, and the drying technology, taking the production of quark powder as an example, are viewed in detail.

Regarding rennet-induced coagulation several experiments were carried out in line with the following objectives:

- The structure formation during renneting of cow milk is recorded to determine time-dependent relationships between the sections of the rennet-induced coagulation. The analysis of various samples from bovine bulk milk derived from healthy cows in combination with a spectrophotometric method for the determination of the released CMP and GMP supplies a standard curve of the process viscosity during rennet-induced coagulation. Thus, an enhancement of information on the kinetics involved becomes possible.

- With the use of the rheological measurements a parameter should be developed, which can be used as an objective tool for the control of the production process. The process viscosity after different coagulation times seems to be a good choice for the prediction of the optimal cutting time via pre-calculation of desired end-viscosities.

- In a further step, milk from cows suffering from an udder inflammation should be analyzed. A correlation between chemical changes—release of CMP, protein profile—and rheological parameters—process viscosity, development of the structure—would be possible. Here, the main focus is on the variation of the protein profile in milk from individual cows obtained by hydrophobic interaction chromatography. Variations in milk protein composition and concentration are crucial for the cheese-making properties. For the first time, a classification of milk from infected cows can be made on the basis of the parameter process viscosity to provide information to what extent the altered composition would modify cheese-making properties.

- Milk from individual cows suffering from an udder inflammation should be examined. If mastitis was detected, medication with antibiotics is the common therapy. But to date no information is available on effectiveness regarding cheese-making parameters and on how the milk composition is altered in the case of inflammation and medication.

- Additionally, the structure formation during renneting of goat milk is recorded to determine time-dependent relationships between the stages of the rennet-induced coagulation and to detect differences between bovine and caprine milk. An attempt is made to transfer the rheological measurements and the spectrophotometric analysis from cow to goat milk and to obtain more information regarding the correlation between chemical changes—release of CMP—and rheological parameters—process viscosity, development of the structure.

As long as pre-denatured whey protein aggregates—present in yoghurt milk—have been discussed to act as destructive fillers or structure breakers in acid milk gels, there is an enormous economic and also scientific interest in the development of a rapid method for the assessment of the powder quality, which means the ability to completely rehydrate without remaining aggregates in detail.

Generally, a method of particle size determination is useful for the detection of the rehydration behavior. Depending on the field of activity different methods exist: photon correlation spectroscopy, static laser light scattering (laser diffractometry), or the coulter principle. Because the particles size ranges between 0.07 and 600 µm in the case of whey protein powders the static laser light scattering method was chosen. Admittedly, no absolute number of microparticles per unit volume of dispersion can be stated—as the PCS can—only a relative volume distribution is possible.

Regarding the quality/functionality of the WPC powders several experiments were carried out according to the following objectives:

-   Assessment of the applicability of the static laser light scattering for the monitoring of the rehydration of whey protein concentrate powders, sweet whey powders, and skim milk powder

-   Access of more information about the kinetic properties involved during rehydration of dairy powders

-   Classification of dairy powders regarding their solubility behavior

-   Development of a rapid method for the assessment of the powder quality on the basis of the size distributions

-   Derivation of critical limits which ease the rating of the dairy powders

-   Detection of dairy powders having a disrupted functionality.

The processing technology used for the production of quark powder was examined and water retention was analyzed. The following experiments were conducted:

-   Assessment of the scale up from small-scale to large-scale dryer (4 t h^{-1})

-   Determination of material characteristics of low fat quark with 16 % dry mass relevant for the drying technology

-   Investigation into structure deformation (rheological measurements) of the low fat quark via temperature and shear rate before feeding into the atomizer

-   Assessment of the water-binding capacity of dried quark. An increased water-binding capacity is accompanied by an improved texture of reconstituted cheese, thus leading to a favorable commercial acceptability of the final product.

-   Analysis of the particle morphology and surface properties in relation to processing technology/parameters via laser diffraction and SEM (scanning electron microscopy).

Chapter 3: Theoretical background

3.1 Composition of bovine milk

Milk consists of 87-88 % water. Lactose, protein, fat, and minerals contribute to the dry mass of 12-13 %. The average composition of bovine milk is listed in Table 3-1. The exact components of raw milk vary during lactation. Genetic (breed), physiologic (stage of lactation and age of the cow and state of health), and external factors (feeding, care, and milking) cause variations in the concentration of milk components [14].

Table 3-1: Average composition of bovine milk [15]

Component	Average content in bovine milk %
Water	87.3
Lactose	4.6
Fat	3.9
Protein	3.25
Casein	2.6
Whey protein	0.65
Minerals	0.65
Organic acid	0.18

3.1.1 Caseins

The group of caseins comprises the four main fractions α_{S1}-, α_{S2}-, β-, and κ-casein as well as β-casein fragments (γ-caseins) which result from plasmin cleavage [14;16]. Several genetic variants of caseins are known. The major genetic variants and selected properties are given in Table 3-2.

Table 3-2: Selected properties of the bovine caseins [15-17]

Casein	α_{S1}		α_{S2}	β			κ	
Genetic variants[A]	B	C	A	A^1	A^2	B	A	B
c_{milk} (g·kg^{-1})	12-15		3-4	9-11			2-4	
Average composition of the casein fraction (%)	36-40		9-11	34-41			10-13	
Ip (pH)	4.92-5.05	5.00-5.35		5.41	5.30	5.53	5.77 (5.35)	6.07 (5.37)
Mw (Dalton)	23,615	23,542	25,226	24,023	23,983	24,092	19,037	19,996
$A_{280\,nm}$[B] (%)	10.05	10.03			4.6, 4.7	4.7		10.5
Amino acid residues	199		207	209			169	
Cystein residues	0		2	0			2	
Phosphoserin residues	8-9		10-13	5			1-2	
Carbohydrate	0		0	0			+	
Rennet sensitivity	-		- -	-			+ +	
Ca^{2+} sensitivity	+		+ +	+			-	

[A] Major variants
[B] Absorptivity of a 1% solution measured in a 1 cm light path at 280 nm

Due to the fact that the hydrolysis of κ-casein by rennet during milk clotting is the main reaction during the primary phase, more details on the structure of κ-casein are given below.

The bovine κ-caseins are a divergent group consisting of a major carbohydrate-free component and a minimum of six minor components with varying degrees of phosphorylation and glycosylation [16;18-22].

Generally, the majority of all κ-casein variants was found to be carbohydrate-free, whereas the minor κ-casein components are multiglycosylated and/or multiphosphorylated forms of the major κ-casein [16;18;21;23]. The Phe_{105}-Met_{106} peptide bond of κ-casein is hydrolyzed by rennet [24;25] resulting in the hydrophobic N-terminal para-κ-casein (residues 1…105) and the C-terminal hydrophilic (casein)macropeptide (CMP) (residues 106…169) containing various degrees of glycosylation [16;26;27].

The structures of the different carbohydrate moieties have been investigated by various researchers [28-33]. Basically, the carbohydrates attached to κ-casein consist of galactosyl, N-acetylgalactosamine, and N-acetylneuraminyl [26;30]. SAITO and ITOH (1992) identified five different carbohydrate units isolated from bovine κ-casein [26]. MOLLÉ and LÉONIL (1995) characterized the distribution of glycosyl residues of the caseinmacropeptide A variant by a combination of reversed-phase high-performance liquid chromatography online with electrospray-ionization mass spectrometry [34]. They found at least fourteen glycosylated forms besides the non-glycosylated and multiphosphorylated forms having one, two, or three phosphate groups.

Casein micelles

The individual caseins are aggregated in the form of casein micelles. At least three types of models for the structure of the casein micelles have been proposed [15;35-40] which are described below.

The model proposed by WALSTRA and JENNESS (1984), WALSTRA (1990), and SCHMIDT (1982) is the submicelle model [15;35;39], Figure 3-1.
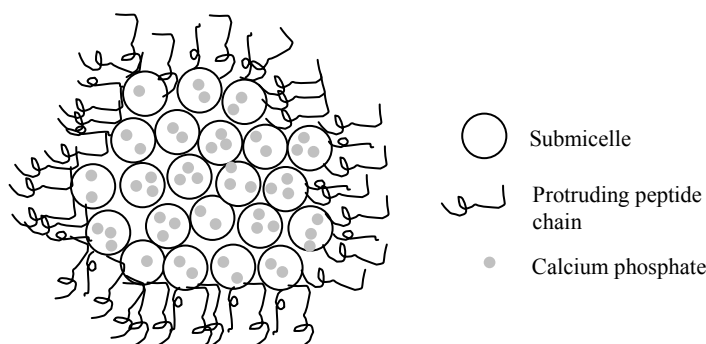
Figure 3-1:   Schematic model of a casein micelle [36]

In this model, casein micelles consist of subunits—the sub-micelles—containing casein but differing in composition. Two main sub-micelle types exist, one primarily consisting of α_S- and β-caseins, the other of α_S- and κ-caseins.

The sub-micelles are connected via calcium phosphate clusters building up micelles. Sub-micelles being rich in κ-casein are located at the outside. The C-terminal end of the κ-caseins is located at the surface of the micelles and builds up the hairy layer which prevents the micelles from aggregation and flocculation. The mechanism therefore is steric and electrostatic repulsion.

HOLT et al. (1992) and HOLT and HORNE (1996) announced a model of the casein micelles in which no quantitative differences exist between the composition of the caseins on the surface and in the inside of the micelles [38;40], Figure 3-2. Casein micelles are described as a mineralized, cross-linked protein gel. The linking agents are calcium phosphate nanoclusters.

●   Calcium phosphate nanocluster
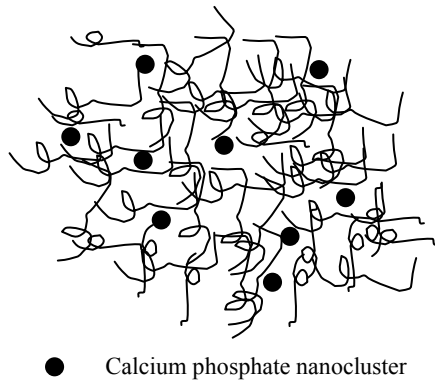
Figure 3-2:   **Model of a casein micelle [38;40]**

HORNE (1998) described the dual bonding model in which the individual caseins are not only connected via colloidal calcium phosphate but additionally hydrophobic interactions [37], Figure 3-3. The rectangular bars indicate hydrophobic regions of the casein molecules. Two types of linkage contribute to the assembling of the casein micelles: first, the formation of casein clusters via hydrophobic interactions and second, the linkage of the phosphoserine residues located at the hydrophilic part of the casein molecules via colloidal calcium phosphate. The model gives an explanation for the location of κ-casein at the outside of the micelle. The size of the casein micelle is limited because κ-casein is attached to the other casein molecules via hydrophobic interaction but it has at maximum 1 to 2 phosphoserine residue and no second hydrophobic region anticipating both types of growth mechanisms.
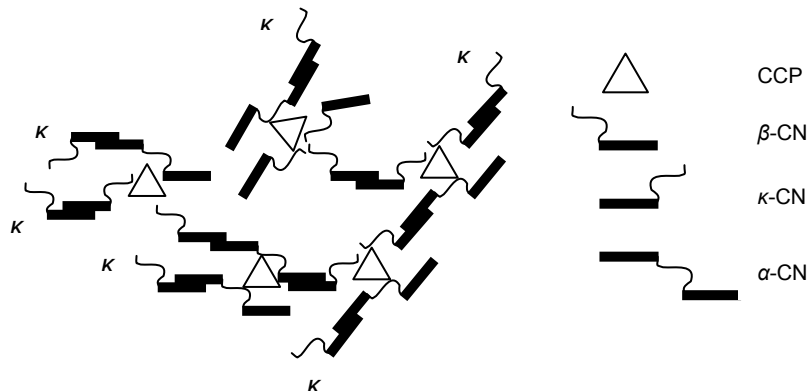
Figure 3-3:   **Model of a casein micelle [37]**

3.1.2 Whey Proteins

On acidification to pH 4.6 at 20 °C or rennet addition, about 80 % of the total protein in bovine milk is precipitated out of solution. The protein which remains soluble under these conditions is referred to as whey protein [41].

The main fractions of whey proteins are β-Lg (β-Lactoglobulin), α-La (α-Lactalbumin), BSA (bovine serum albumin) and several Igs (Immunoglobulins) including IgA, IgG, and IgM [15;16]. Table 3-3 displays selected properties of whey proteins.

Table 3-3:   Selected properties of whey proteins [16]

	Genetic variants[A]	c_{milk} g·kg^{-1}	Ip (pH)	Mw Dalton	$A_{280\ nm}$[B] %
β-Lg	A	2-4	5.13	18,363	9.6
	B		5.13	18,277	10.0, 9.6
α-La	B	0.6-1.7	4.2-4.5	14,178	20.1-20.9
BSA	A	0.4	4.7-4.9	66,399	6.3-6.9
IgG1		0.3-0.6	5.5-6.8	161,000	13.6
IgG2		0.05	7.5-8.3	150,000	13.6
IgA		0.01		385,000-417,000	12.1
IgM		0.09		1,000,000	12.1

[A] Major variants
[B] Absorptivity of a 1 % solution measured in a 1 cm light path at 280 nm

3.2 Composition of caprine milk

The average composition of caprine milk is listed in Table 3-4. Quantitatively similar values are obtained for bovine (Table 3-1) and caprine milk. But as reported for bovine milk the exact content of the components in raw milk vary during lactation and depend on genetic (breed), physiological (stage of lactation, age of the cow, and state of health), and external factors (feeding, care, and milking) [14].

Table 3-4:   Average composition of caprine milk [42]

Component	Average content in caprine milk %
Water	87.8
Lactose	4.1
Fat	3.8
Protein	3.5
Casein	2.11
Whey protein	0.6
Minerals	0.8

The very low content of carotin (vitamin A) and the smaller size of the fat droplets determine the color of caprine milk which seems to be whiter compared to cow milk.

The typical taste of the goat milk originates from a higher proportion of short-chain, volatile fatty acids.

The structure of caprine casein micelles was assumed to be similar to that in bovine milk. Nevertheless, proportions of the individual caseins and size of the micelles differ [15;43].

Table 3-5 displays the average composition of the caprine caseins. Caprine casein is dominated by β-casein whereas in bovine milk α_{S1}-casein dominates (Table 3-2).

Table 3-5: **Average composition of the caprine caseins in % [15;43]**

	α_{S1}	α_{S2}	β	κ
Average composition	4-26	5-19	42-64	10-24

κ-casein was assumed to have the same influence on the size of the micelles for bovine and caprine milk [35;44]. RICHARDSON (1973) reported that the composition of caprine κ-casein was very similar to that of bovine milk [45]. Divergent findings exist about the casein micelle size. The micelle size of caprine milk was reported by ONO and CREAMER (1986) to be larger than that of bovine milk [44]. REMEUF and LENOIR (1986) stated that the caprine micelles were smaller [46].

Although, the casein composition of caprine milk differs from that of bovine milk no differences exist in the physico-chemical properties of the micelles [47].

3.3 Processes of coagulation

In the following sections the processes rennet-induced, acid-induced, and combined acid and rennet-induced coagulation are discussed in detail.

3.3.1 Rennet-induced coagulation

3.3.1.1 Production technology

The production technology is viewed exemplarily for the manufacture of a hard cheese. Figure 3-4 displays the protocol for the manufacture of Emmental cheese with maximum moisture content of 38 %. Starters used are *Lactobacillus helveticus*, *Streptococcus salivarius* ssp. *thermophilus*, and *Propionibacterium freudenreichii* ssp. *shermanii.*
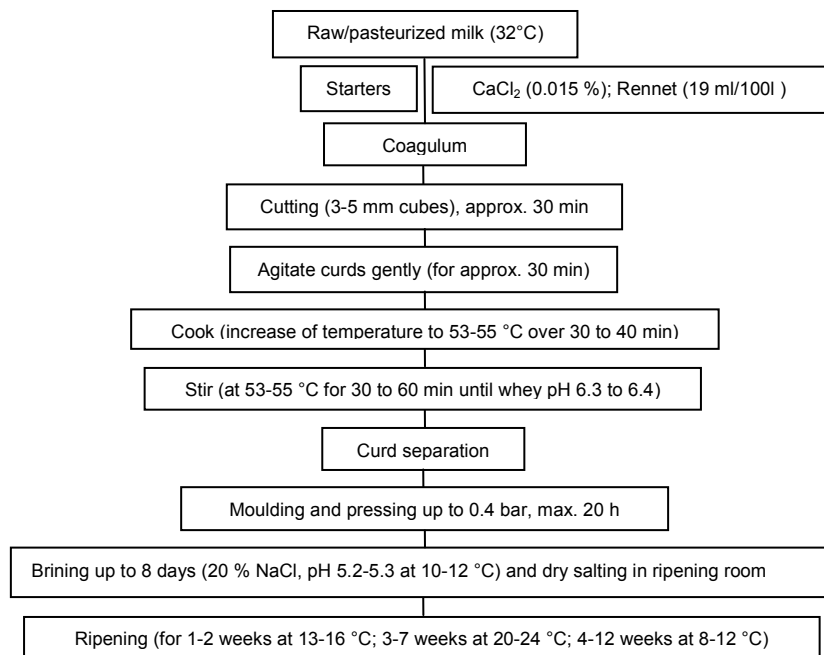
Figure 3-4: **Protocol for the manufacture of Emmental cheese [48]**

3.3.1.2 Mechanism of reaction

Three phases of rennet-induced coagulation were already described by FLUELER (1982) [49]. In principle, the rennet-induced coagulation is divided into:

The primary phase or enzymatic step. During this step the Phe_{105}-Met_{106} peptide bond of κ-casein is hydrolyzed by rennet [24] resulting in the hydrophobic N-terminal para-κ-casein and the C-terminal hydrophilic caseinmacropeptide (CMP) [50] which is released into the milk serum [50]. Some of the macropeptides contain sugars including Galactose, N-acetylgalactosamine, and N-acetylneuramic acid and are therefore referred to as glycosylated caseinmacropeptide or glycomacropeptide (GMP). GMPs correspond to the highly glycosylated, C-terminal sequences which are present on the surface of the casein micelles and stabilize the native micelles in milk [51]. The macropeptides which contain no sugar molecules are referred to as non-glycosylated caseinmacropeptides (n.-g. CMP). In the course of enzymatic splitting, primarily the negatively charged GMP is released into the milk serum [50]. The micelles lose their steric and electrostatic stability and therefore the solubility in the serum. Coagulation begins [4;50-53]. The casein micelles are not destroyed by rennet action [54] but lose hydration.

In the secondary phase the destabilized casein micelles begin to aggregate [49;55]. The aggregated micelles form bead-like, un-branched chains from which the gel network is formed.

In the third phase the network is strengthened. Additionally, the interspaces in the network are minimized resulting in a loss of whey from the gel. A demixing between the coagulum and liquid whey occurs which is called syneresis [56].

3.3.1.3 Influencing factors

The enzymatic coagulation of milk is influenced by many factors. The parameters most important are the milk composition and technological parameters. Milk composition was found to vary in relation to stage of lactation [57-59], age of cow [57;58], feeding, month of sampling [57;58], SCC (somatic cell count) (health of cow) [57;58;60-62], and genetic variants [63], all of these having an enormous influence on coagulating properties [59;64-70].

Milk from healthy udder quarters

The technological parameters having significant influence on rennet gel formation are the pH value, the coagulation temperature, and the rennet concentration.

The structure formation velocity increases with decreasing pH value, because more colloidal calcium becomes soluble and the volume of the casein micelles decreases [14]. Hence, the Phe_{105}-Met_{106} peptide bond of κ-casein becomes less accessible for the rennet [15], leading to a strengthened micelle aggregation [15].

During the enzymatic step of the rennet coagulation the ambient pH value influences the pH optimum of the enzymes chymosin and pepsin, having great influence on the rate of cleavage of the rennet-sensitive peptide bond. The optimum pH value of chymosin is 5.0, whereas the optimum of pepsin is 2.0.

In practice, mixtures of chymosin and pepsin are used. Therefore a decrease in pH leads to a higher activity of pepsin [55;71;72].

The coagulation temperature has a great influence on enzyme activity. The optimum temperature of the enzyme leads to a quicker coagulation. At temperatures > 45 °C chymosin is inactivated [72;73].

The rennet concentration used has an influence on coagulation time. Gel formation and coagulation activity increase until an optimum is reached. After this optimum rennet concentration, the activity decreases due to competitive inhibition of the enzyme molecules [71;72].

Milk from infected udder quarters

The health of the cow has an immense influence on the suitability of milk for the rennet cheese production as long as disease and poor health reduce not only the milk yield but also a changed milk composition. Especially, inflammation of the mammary gland— mastitis—and defects of the secretion cause a changed composition of milk, a reduced synthetic activity, elevated somatic cell counts, and changed technological usability [74-76]. Therefore, mastitis—especially the subclinical type—is one of the most widely spread diseases having a critical effect on milk quality worldwide [75] and causing great economic losses [77].

Mastitis describes an inflammation of the mammary gland primarily caused by a bacterial infection. The most common major pathogens include *Staphylococcus aureus*, *Streptococcus agalactiae,* and coliforms, *streptococci*, and *enterococci* of environmental origin [76]. The parameters somatic cell count and the bacteriological examination of the milk verify the infection [77].

The somatic cells in milk are primarily leukocytes or white blood cells including macrophages, lymphocytes, and polymorphonuclear neutrophil leukocyte [76]. SCC is the most common measurement of milk quality and udder health [76] and can be related to the cellular immune response after an inflammatory stimulus [78-80]. Generally, milk from normal, uninfected quarters contains less than 200,000 somatic cells ml^{-1}.

Usually, the total protein content is independent of SCC below 10^6 cells ml^{-1} [15] but the types of protein present in milk are changed [81]. The synthesis of the major whey proteins β-Lg and α-La is reduced and the content of bovine serum albumin is increased due to leakage from the blood [82]. The content and activity of many enzymes (e. g., lysozyme, lactoperoxidase, NAGase, and plasmin) increase with elevated SCC [81;83;84]. URECH (1999) found about 20 % increased plasmin activity and 30 % increased plasminogen values in quarters with subclinical mastitis without any significant change in the plasminogen-plasmin ratio [81].

HARMON (1994) mentioned that many enzymes have an increased activity [76]. Additionally, an elevated SCC is associated with a decrease in lactose, and some studies have shown a minor decrease in fat content compared to milk with a lower SCC [82].

In Table 3-6 a comparison of the composition of milk from healthy cows and milk from cows suffering from infectious udder inflammation is given.

Table 3-6: **Composition of bovine raw milk from healthy cows and mastitic milk [85][C] and [15;86][D, E]**

	Composition, healthy cow[D, E]	Change mastitic milk[C] tendency (-falling, +increasing)
Fat	3.9 %	-
Lactose	4.6 %	-
Protein	3.25 %	-
Casein	2.6 %	- -
Whey Protein	0.65 %	+ + +
Casein	Relation to total protein content	
$\alpha_{S1,2}$	45 - 55 %	+
β	23 - 35 %	- - -
γ	3 - 7 %	+
κ	8 - 15 %	+
Whey Protein	Relation to total protein content	
β -Lg	7 - 12 %	- -
BSA	0.7 - 1.3 %	+ + +
α -La	2 - 5 %	+ + (decrease reported in [76])
Ig	1.9 - 3.3 %	+ + +
Minerals	0.65 %	
Calcium	136 mg·ml^{-1}	- - -
Sodium	57 mg·dl^{-1}	+ +
Chloride	80-120 mg·ml^{-1}	+ + +
Potassium	173 mg·ml^{-1}	-
Magnesium	18 mg·ml^{-1}	- - -
Phosphate	26 mg·ml^{-1}	- - -

Overall, mastitis or elevated SCC cause a decrease in lactose concentration, alterations of the fat globule membrane promoting lipolysis, a reduction in casein content, an increase in soluble protein and enzyme concentrations (plasmin in particular), and modifications of salt balances [61;75]. Usually, the pH value of the milk of cows suffering from an infectious udder inflammation rises. In case of immense organ injuries, the pH value decreases under 6.5 [85]. There is an increased activation of plasmin from plasminogen in mastitic milk [87-89]. It has been shown that there is elevated plasmin activity in mastitic milk, which causes increased casein hydrolysis [76;90;91].

Subclinical infections are characterized by a decreased milk yield, the presence of bacteria in the secretion, and a changed milk composition, but no visible changes occur in the appearance of the milk or the udder [76]. For cow milk the somatic cell count is often used as predictor of subclinical mastitis to make a statement about milk quality, hygiene, and mastitis control [76]. An increase in SCC comes along with altered protein quality, change in fatty acid composition, lactose, ion, and mineral concentration, increased enzymatic activity, a higher pH of raw milk [75;92], and reduced milk yield, affecting milk processability, e.g., increase of rennet clotting time, loss of moisture in cheese, delayed growth of starter cultured, and reduced curd stability and yield [61;93].

If the infection becomes clinical, visible changes occur in the appearance of the milk (e.g., blood), the udder is swollen or painful, and the cow may show systemic signs such as elevated rectal temperature, lethargy, or anorexia. As in subclinical mastitis, the milk yield is decreased, bacteria are present in the secretion, and the composition of the milk is changed [76]. Milk production is critically reduced and the character of the milk is apparently changed [77].

The most important parameters of milk for cheesemaking are good reactivity with rennet, a high degree of curd firming capacity, and good syneresis ability and whey expulsion [94]. The effects of mastitis on clotting and whey drainage as well as on cheese yield have been comprehensively described by a number of authors [60;61;69;92;95-97]. Studies comparing individual milk samples have shown that milk coagulation property (MCP) is affected by physical and chemical parameters such as titratable acidity [98], SCC [69], protein and casein contents, and calcium and phosphorus concentrations [99]. Several other factors influence MCP including casein content [100;101], κ-casein variants [102-106], titratable acidity [99], pH [107;108], and calcium content [109].

Nevertheless, the mechanism of rennet-induced coagulation is not completely explained and a detailed classification of milk from infected udder quarters regarding cheese-making properties is missing.

3.3.1.4 Method of measurement

Chemical procedures

In the course of the rennet-induced coagulation of milk κ-casein is split into para-κ-casein and macropeptide, which diffuses into the serum. One option to measure the coagulation is the quantification of the macropeptide in 8 % TCA [110], whereas the results depend on the solubility of the macropeptide fractions being dependant on the concentration of TCA [50]. In 8 % TCA the whey proteins are no longer soluble, which is positive for the analysis, but a part of the non-glycosylated macropetide denatures under these conditions and is precipitated with the whey proteins. Thus, a lower amount of CMP is determined.

LIESKE et al. (1996, 1996, and 1997) have developed a method which is able to detect the CMP being formed during rennet action [53;111;112]. They use the fact that GMP has its maximum solubility in 12 % TCA. The entire amount of CMP is quantitatively soluble in 6 % TCA, if the acid was conditioned hydrophobically with Na_2SO_4 before. The method is based on the selective solubility of CMP und GMP in 6 % TCA in 0.175 M sodium sulfate and in 12 % TCA, respectively, following their isolation from the TCA filtrate using analytical desalting columns (EconoPAK 10DG, BioRad) and, consecutively, the photometric measurement of the absorption at 217 nm and adjustment with the reagent blank value. N.-g. CMP is the calculated difference between the absorptions of CMP and GMP. The method can be used to obtain the kinetics [111] and also for end point analysis [113]. Results obtained correspond to results obtained with a chromatographic method (fast protein liquid chromatography equipped with a Mono S column) [53].

Another method for the determination of CMP is the high performance liquid chromatography [34] as well as the fast protein liquid chromatography [114].

LÉONIL and MOLLÉ (1991) used the cation-exchange fast protein liquid chromatography to determine the concentration of macropeptide in rennet whey and pH 4.6 filtrates [115]. From these investigations it became obvious that the TCA pretreatment in the CMP analysis is a very critical step because of the different sensitivity of CMP to TCA [115], thus leading to a modification of the buffer composition by LIESKE et al. (1996, 1996, and 1997) allowing a lossless quantification of CMP fractions with the spectrophotometric method [53;111;112]. In further works, the calculation of the results was improved by defining a correct factor for the molar extinction of CMP at 217 nm [113].

LÉONIL and MOLLÉ (2005) used liquid chromatography-electrospray coupled with mass spectrometry as well as liquid chromatography-electrospray coupled with tandem mass spectrometry for the determination of CMP in dairy products [116].

Physical procedures

The study of milk gelation during rennet-induced coagulation is of great interest due to economic reasons. FOX, GUINEE, COGAN, and MCSWEENEY (2000), LUCEY (2002), O'CALLAGHAN, O'DONNELL, and PAYNE (2000), THOMASOW and VOSS (1977), and VAN HOOYDONK and VAN DEN BERG (1988) give an overview of the instruments and techniques used to monitor coagulation [117-121].

Overall, the techniques can be classified into mechanical, vibrational, and ultrasonic systems, systems which measure the electrical conductivity, hot wire, and optical systems. Only some of these techniques are used in practice in a cheese factory.

LUCEY (2002) lists difficulties which occur in practice [118]. Some of the devices are difficult to clean-in-place and some of them have to be removed before cutting and stirring. The most crucial point is that the measuring system for the online monitoring of the rennet-induced coagulation should be non-destructive to gain information of the native gel without deformation.

Most widely, online monitoring of milk is done by optical probes such as NIR diffuse reflectance and NIR transmission types or probes which respond to rheological changes such as hot wire or torsional vibration. A selection of instruments which were reported to be in use and commercially available for online measurement of milk coagulation is given in Table 3-7.

Table 3-7: **Selection of instruments for the online measurement of milk coagulation [122]**

Instrument	Principle	References
Rheoswing	Torsional vibration	[123]
Nametre	Torsional vibration	[124;125]
Opti-set	Hot wire	[126]
CoaguLite	Fibre optic NIR diffuse reflectance	[127;128]
NIR Systems (offline)	Reflectance spectroscopy	[129]

3.3.2 Acid coagulation

3.3.2.1 Production technology

Generally, yoghurt is produced by fermentation of the lactose by means of lactic acid bacteria. Thermophilic fermentation is carried out at temperatures of 40…45 °C and time periods of 3…6 h. A process flow chart of set-style yoghurt is presented in Figure 3-5.
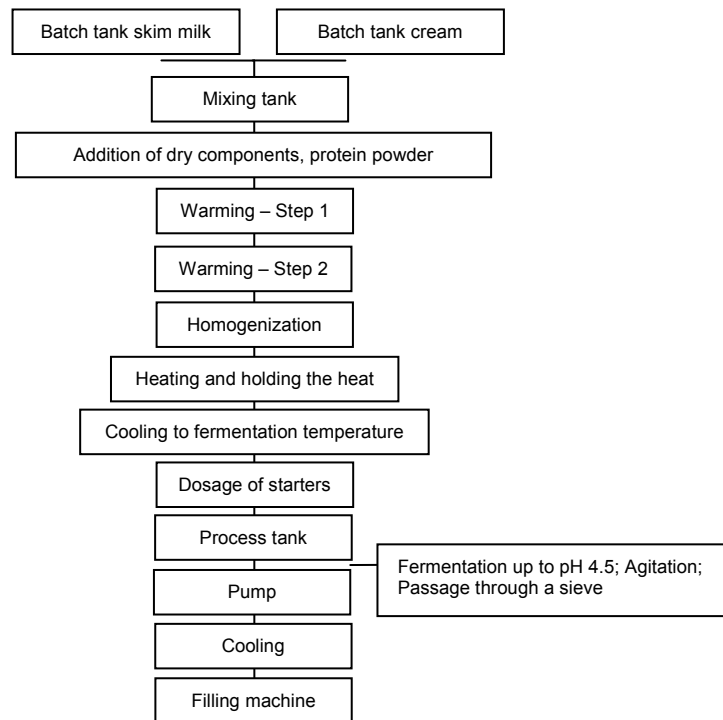
Figure 3-5: **Process flow chart of stirred yoghurt [48]**

During fermentation, lactic acid is produced, which leads to an acidification of the product. As a result, several physicochemical changes of the casein micelles occur. Originally, there is a high net negative charge in milk, which is reduced as the isoelectric point of casein is reached at pH 4.6. A reduction in surface charge (zeta potential) takes place. As an effect, casein micelles come closer and aggregate. The aggregates are connected through hydrophobic and electrostatic interactions [130].

Yoghurt can be divided into two types: set-style yoghurt which is fermented in retail packages and stirred yoghurt which is fermented in huge vats. In addition, drinking yoghurt exists, which is based on stirred yoghurt. At best, the structure of set-style yoghurt is destroyed not before consumption while the degradation of stirred yoghurt occurs during further manufacture.

Stirred yoghurt is described as micro-gel particle dispersion exhibiting a yield point and showing shear-thinning and time-dependent flow properties [131]. Consequently, the technology, especially after fermentation, has to be adapted to the special requirements of the product to maintain typical texture elements and to minimize the tendency for syneresis.

3.3.2.2 Rheological measurement of the acid coagulation

During yoghurt fermentation the NEWTONIAN fluid milk changes to a visco-elastic fluid—a gel. By use of the torsion oscillator an inline-online measurement of the viscosity becomes possible.

With the knowledge of viscosity and pH value both depending on time the conventional fermentation process is divided into four main sections [10;123;132]:

1. NEWTONIAN behavior of milk until coagulation

2. the flocculation step in which casein micelles are interconnected to agglomerates because of hydrophobic interactions on acidification conditions (structure viscosity). This period is characterized by an exponential increase of the process viscosity.

3. the gelation with constant structure formation velocity, and

4. sigmoidal increase of the complex viscosity.

Figure 3-6 displays the process viscosities of a conventional process with standard milk (casein/whey-protein-relation = 4.8:1). Additionally, the figure contains the pH value depending on time. The sample reaches a level of the process viscosity of 166 mPa·s which is in the range of the well-established level of 150-160 mPa·s for a conventional process.
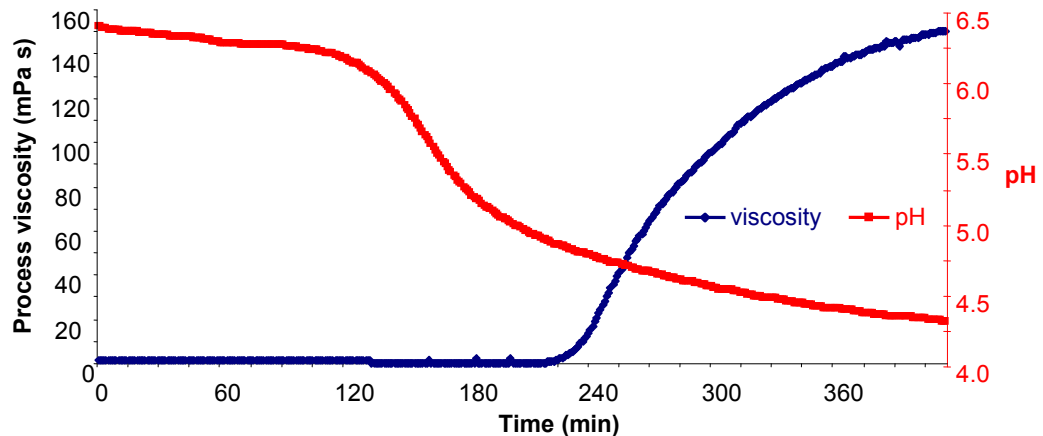
Figure 3-6:   **Process viscosity and pH curve of conventional acidification at 38 °C (Casein: whey protein = 4.8:1) [12]**

The start milk pH value was 6.41. Regarding the four main sections described above, the greatest differences in the structuring take place in the first (up to 210 min) and fourth (up to 415 min) section. The second (up to 240 min) and third (up to 250 min) section of the gel formation lie in the same time frame.

The first attachments of the casein micelles take place after 210 min at pH 4.96. Here, the limit of 10 mPa·s—stated by SENGE—is exceeded. After this section with exponential increase in viscosity the third section follows which is characterized by a linear increase. This section is—with 10 min—quiet short. Subsequently, the fourth section follows with a sigmoidal increase in viscosity. This section is the longest one and lasts nearly half of the processing time. Here, the most structures are formed.

The sigmoidal course of the viscosity can be explained by the hindered emplacement of the casein micelles into the gel network. In the section with constant structure formation velocity the network was intensified/packed by convective transport. This is now no longer possible. The dominating driving forces of the gel formation are now diffusion effects due to hydrophobic interactions.

The fermentation was done until a pH value of 4.42 after 415 min was reached to prevent further acidification of the product.

Figure 3-7 represents the process viscosities and the course of the pH value over time for an enriched content of whey proteins (casein/whey-protein-relation = 2.1:1).
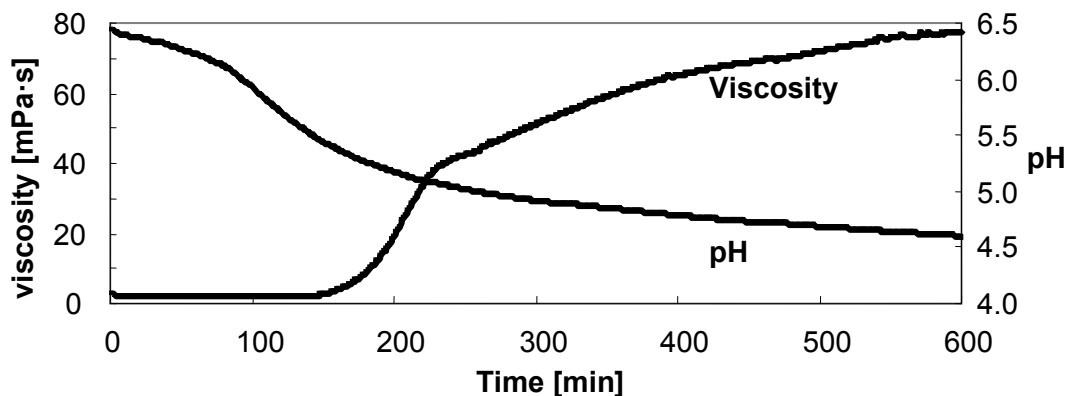
Figure 3-7:   **Process viscosity and pH curve of non-conventional acidification at 38 °C (Casein: whey protein = 2.1:1) [2;10]**

The addition of whey protein concentrate in sour milk products is advantageous because of economic and nutritional advantages. In this case the four sections of the conventional process have to be enlarged to six sections with formation of a particle gel.

A so-called "whey protein sharp bend/break" was observed which takes place immediately after the third gel formation section. And after that a second linear section was found [2;10].

The functionality of added whey proteins is discussed as a crucial parameter. Especially the processing of WPC 65 and WPC 35 can cause thermal induced changes in the protein functionality due to thermal processes during evaporation of the whey.

Additionally, a limit is known for the loading of the casein by β-Lg, as long as whey proteins are no structure forming agents in the wider sense; thus gel formation takes place at lower level of the complex viscosity [10].

3.3.3 Combined acid and rennet-induced coagulation

3.3.3.1 Production of quark

Quark is produced via combined acid and rennet-induced coagulation. The majority of quark in Germany is produced by the thermo process [133]. The flow chart of the quark production is presented in Figure 3-8.
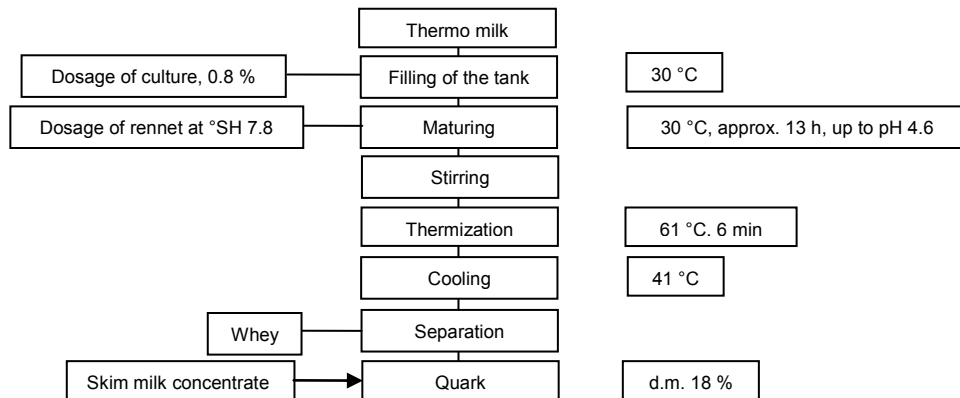
Figure 3-8: **Production of quark [134]**

For instance, the milk is thermized at 88 °C for 6 min. As a consequence the whey proteins β-Lg and α-La co-precipitate onto the caseins. Through a heat treatment at 61 °C for 6 min after fermentation the aggregation is enhanced resulting in an improved whey separation. Subsequently, the stirred curd is cooled to separation temperature [135-139]. From a material scientific view, quark can be described as a micro-gel particle dispersion.

3.3.3.2 Fermentation process

If the course of the process viscosity and the pH value over time are viewed during this process, Figure 3-9, six individual sections have been identified by SCHULZ (2000) [123].
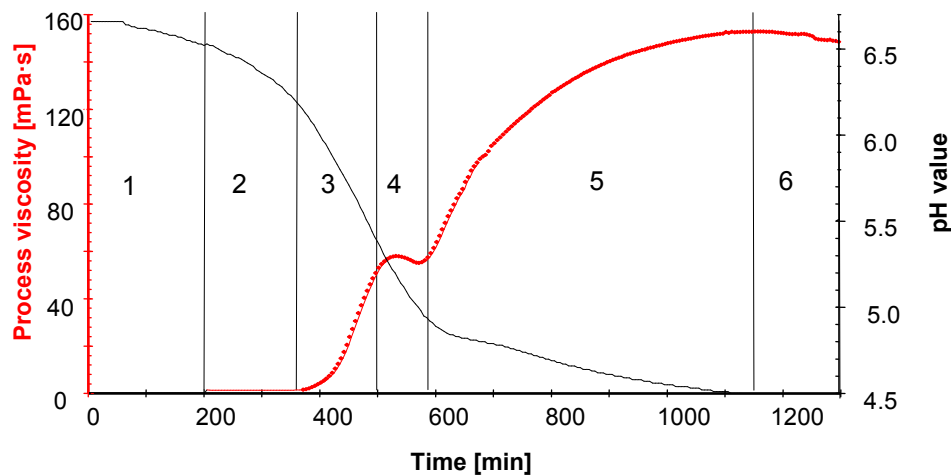
Figure 3-9: **Course of process viscosity and pH value during the combined acid and rennet-induced coagulation [123]**

During the individual sections the following processes occur [123]:

1. Adaptation of the culture and acidification until pH value is reached at which rennet-induced coagulation has started

2. Primary phase of the rennet-induced coagulation (enzymatic hydrolysis of the Phe_{105}-Met_{106} bond of κ-casein)

3. Secondary phase of the rennet-induced coagulation (flocculation, gel formation)

4. De-mineralization and collapse of the casein micelles, modification of the sour gel structure

5. Dominating acid action, acid coagulation, formation of the final rennet-acid-gel

6. Syneresis starting with micro-syneresis.

The local minimum of the process viscosity in section four results from two competing mechanisms. On the one hand, the viscosity increases due to rennet-induced coagulation. On the other hand, the viscosity decreases because of de-mineralization of the micelles (dissolution of calciumphosphate). This phenomenon causes a weakening of the bonds which is of a temporary nature only. Thus, in the course of fermentation the momentary loss of firmness is compensated.

3.4 Production of dairy powders

Various dairy powders exist which are mainly milk powder, skim milk powder, sodium caseinate, whey protein concentrate, and isolate powder. Dehydrated milk products like milk powder, mainly skim milk powder and whey protein concentrate powders are often used in yoghurt production to increase the non-fat solids content. The quality of these protein preparations strongly influence the production process and the quality of the final product. Quark powder is used mainly in the bakery industry for fillings, pastries, and long-life bakery products (convenience product for bakery) but also for ice cream, chocolate, sports foods, and desserts.

3.4.1 Milk powder

Powdered milk is a manufactured dairy product made by evaporating milk to a state of dryness. A water content less than 5 % ensures the storage stability. The most commonly produced milk powder is the skim milk powder. The powder is produced from pretreated milk (cleaning, standardization, and heat-treatment) which is at first condensed and subsequently dried [140].

3.4.2 Skim milk powder

Generally, skim milk powders are assessed according to the degree of denaturation indicated by the whey protein nitrogen index (WPNI). For medium heat skim milk powder the WPNI is in the range of 1-5.99 mg N g^{-1}. Low heat skim milk powder reveals a lower degree of denaturation with WPNI > 6.0 mg N g^{-1}.

Actually, powders with a high content of undenatured whey protein nitrogen result in qualities comparable to fresh milk [141]. Due to the low degree of denaturation the skim milk powders are easy to hydrate, show an improved solubility and a secured functionality.

Figure 3-10 displays the block diagram of a technological production scheme of skim milk powder.
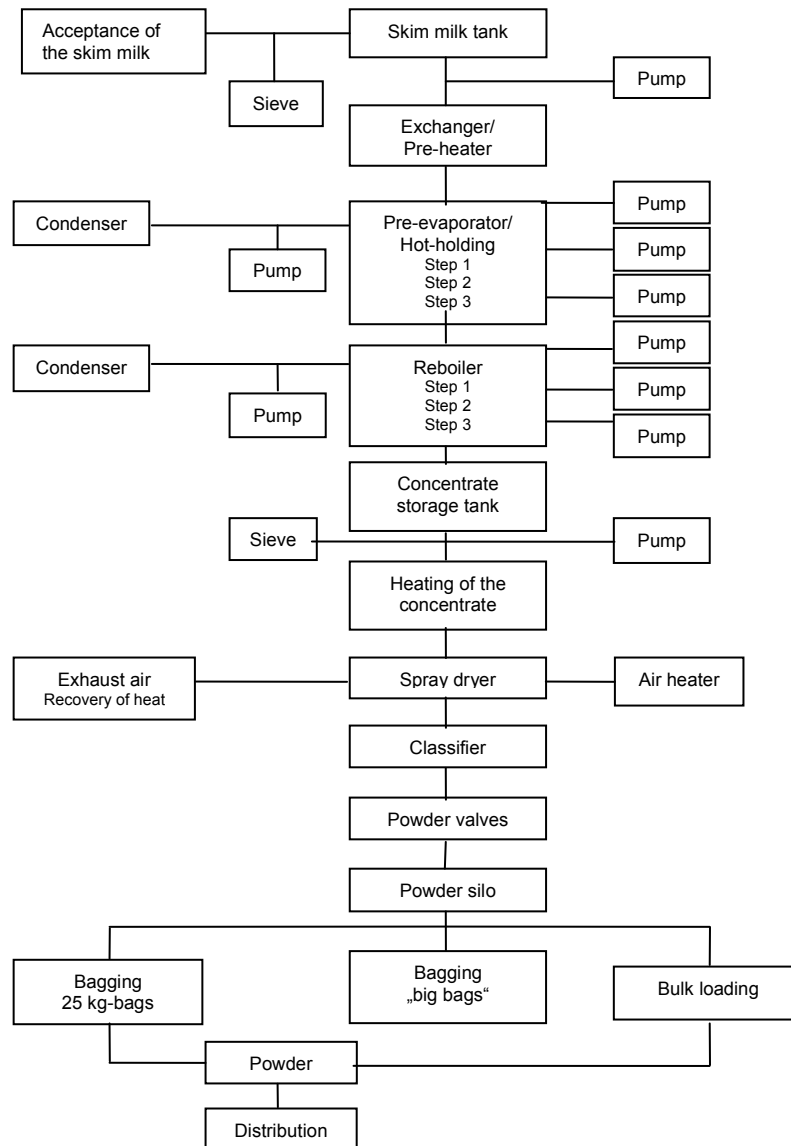
Figure 3-10: **Technological production scheme of skim milk powder [11]**

3.4.3 Whey protein powder

The raw material for the production of whey protein powder is acid whey from cottage cheese or casein manufacture (pH 4.6) and sweet whey or rennet whey from the manufacture of cheese products involving rennet treatment [142]. Sweet whey is produced under enzymatically induced casein coagulation and includes residual coagulating enzyme(s), casein proteolysis fragments (CMP), and smaller quantities of salts and minerals [15;16;142-145].

The manufacture, properties, and uses of whey proteins have been reviewed by DE WIT (1998), KINSELLA and WHITEHEAD (1989) and MORR and HA (1993) [146-148].

Two of the most important whey protein products are WPC (34-80 % protein) and WPI (> 90 % protein) [144;149-152]. Primarily, the whey proteins are concentrated. Thus, remaining casein particles and residual fat are removed by separators. Subsequently, the whey is pasteurized to prohibit microbiological growth [153].

Generally, the manufacture of WPC involves UF and/or DF at pH 3.0 (acid UF/DF WPC) or pH 6.5 (normal UF WPC and neutral UF/DF WPC) [142-144;150;152;154-159], removal of water by condensing (optional step), i.e., evaporation under vacuum or reverse osmosis [160], and spray drying.

WPI can be produced under two different conditions which are the membrane fractionation (MF,UF-DF) and spray drying, and the physical and chromatographic fractionation (IE) [150;160] coupled with concentration (evaporation or UF) and spray drying [142;149].

In WPI production all residual fat is removed by the MF membrane. During the MF/UF process all soluble whey proteins are concentrated, whereas in the IE process some proteins, e.g., glycomacropeptide (GMP), lactoferrin and small peptide fragments are not (usually) recovered [161]. Thus, there are nutritional and possibly functional differences between these two types of WPI.

A manufacturing scheme of WPC and WPI is given in Figure 3-11. The boxes highlighted in green represent a possible production line of WPC powder using UF and spray drying.

Figure 3-11: **Manufacturing scheme of WPC and WPI [48]**

A common method to produce WPC with 30-90 % protein involves a clarification step at 50 °C followed by UF (and perhaps DF depending on the final protein content) and spray drying (175-200 °C inlet, 80-90 °C outlet) [148].

Table 3-8 displays a selection of the composition of whey protein powders with about 35 % protein proposed by various authors.

Table 3-8: Composition of whey protein powders with about 35 % protein

Component	WPC35	WPC34		
[%]	[140;152]	[162]	[160]	[149]
Produced by	UF+SD	UF/DF+SD	UF+SD	UF+SD
Protein	29.7	34	35.5	33.8-36.4
Lactose	46.5	53	51.8	51.2-56.0
Ash	7.8	7	5.8	1.6-7.0
Fat	2.1	3	2.9	3.4-4.0
Moisture	4.6	3	4	2.6-4.0

Table 3-9 lists a selection of the composition of whey protein powders with a protein content > 35 % proposed by various authors.

Table 3-9: Composition of whey protein powders with > 35 % protein

Component	WPC65	WPC80	WPC80				WPC80
[%]	[140;152]	[162]	[162]	[163]	[160]	[149]	[164]
Produced by	UF+SD	UF+SD	UF/DF+SD	UF/DF+SD	UF+SD	UF+SD	-
Protein	59.4	75.0	80	72-77	75.8	73.2-80.5	74.3-77.5
Lactose	21.1	3.5	6	6.7-11.1	11.5	4.5-6.0	11.8-14.7
Ash	3.9	3.1	3	2.5-2.9	3.8	3.0-4.0	2.6-4.8
Fat	5.6	7.2	7	2.1-4.9	4.8	7.0-9.5	1.9-4.2
Moisture	4.2	4.0	4	1.8-6.7	4	4.0-5.0	3.4-4.9

Particle size of WPC 80: 53-382 µm [164]

The true protein content of UF-processed concentrates was reported to be in the range of 66-73 % [165;166]. A lower protein content can occur as a result of different milk types and a modified method of cheese making [165]. ONWULATA, KONSTANCE, and TOMASULA (2004) analyzed six WPC 80 which were purchased from commercial sources and found wide variations in composition [164]. The variations in functionality were minimized through sieving and using powders with a smaller particle size distribution range.

Several commercial WPC and WPI products have been analyzed for composition, functionality, protein aggregation, and physico-chemical properties [150;167-169]. The results showed that considerable variability in functionality and other properties existed between various commercial and laboratory WPC and WPI products.

3.4.4 Quark powder

The production of quark powder is done via spray drying of low fat quark after dilution to 16 % dry matter. The low fat quark can be described as a paste having high interaction between protein and water which is dried to 95 % dry matter. Even if the low fat quark is diluted it imparts a high potential of hesion which is characterized by interactions of cohesion and adhesion. This potential hinders the sufficient atomization prior to drying.

3.4.5 Spray drying

Spray drying allows the conversion of liquid substances into dry, free-flowing powders which eases the handling and allows the use in dry applications [153;170]. Here, the concentrated feed is atomized into the drying chamber by a pressure nozzle or centrifugal disc atomizer via rotating discs with a speed of 225 s^{-1} [171].

In the production of dairy powders the pressure nozzle atomizers are in discussion in order to produce powders with only small content of occluded air, high bulk densities, and good flowability. On the other hand, wheel atomizers were found to produce droplet sizes being insensitive to feed rate fluctuations and fluctuations in concentration (viscosity and feed rate); thus they are able to operate at higher feed viscosities. A great disadvantage is the occurrence of ballooning of the dried particles. The wheel atomizer acts as a fan pumping air through the vanes during wheel rotation [172].

A spray dryer is displayed in Figure 3-12.
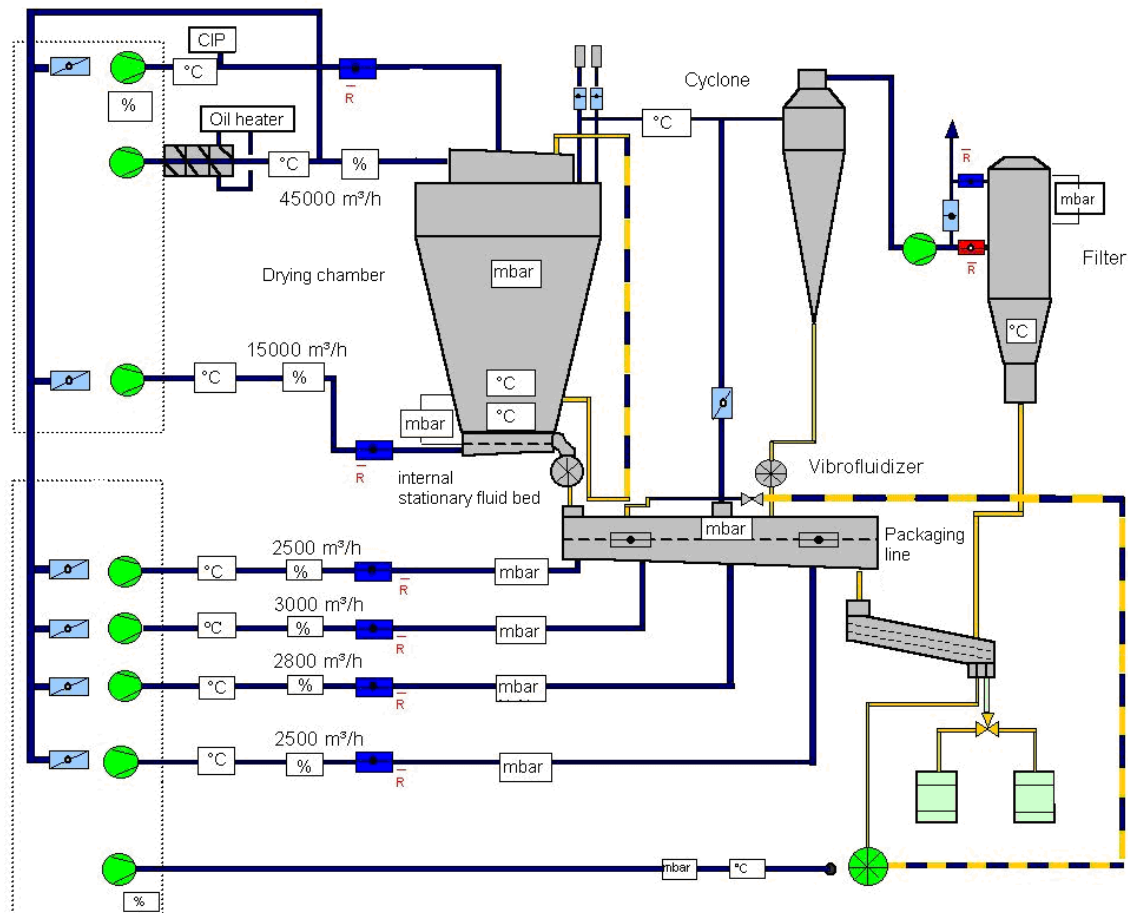
Figure 3-12:   Representation of a spray dryer [173]

Although spray drying has been used for several years, problems occur because it is difficult to effectively model the spray drying process. Three individual processes have to be taken into consideration: knowledge about the atomization process, description of the airflow within the dryer, and the drying kinetics of the individual droplets.

Usually, the spray drying process involves four basic steps [174]:

1. the atomization of the feed into the drying chamber containing circulating hot dry air

2. the dispersion of the droplets within the dry air

3. the drying itself

4. the separation of the dry particles—the powder—which is generally done via cyclone and filter systems.

The drying chamber contains circulating hot air with temperatures between 180 to 220 °C. Because of the high surface of the small droplets, the water evaporates at once. The protein particles and the air cool down which prevents an overheating of the powder [153]. The dried protein particles are separated with the cyclone and filter system.

The atomization process needs a closer consideration because atomization conditions were found to be central to the spray drying process. They define particle size, particle density, and bulk density [175]. Apart from the atomization the heating conditions and the feed characteristics determine particle size and bulk density [172].

Generally, the atomization of fluids is divided into primary atomization which occurs near the nozzle and secondary atomization which describes the break-up of drops further downstream [174]. The ambient conditions and the break-up of droplets can be described by the following dimensionless numbers:

- The REYNOLDS number describes the relation between inertial forces and viscous forces and characterizes the fluid flow. It depends on material characteristics, nozzle geometry, and spray velocity.

$$Re = \frac{\rho \cdot v \cdot d}{\eta}$$

Equation 3-1

- The WEBER number describes the relation between inertial forces and surface tension forces. Like the REYNOLDS number it depends on material characteristics, nozzle geometry, and spray velocity.

$$We = \frac{\rho \cdot v^2 \cdot d}{\sigma}$$

Equation 3-2

High values of both *Re* or *We* number promote more rapid and finer atomization.

- The OHNESORGE number describes the relation between viscous forces and surface tension forces. It depends on material characteristics and nozzle geometry.

$$Oh = \frac{\eta}{\sqrt{\sigma \cdot \rho \cdot d}}$$

Equation 3-3

By means of the OHNESORGE and REYNOLDS number the various mechanisms of jet break-up could be divided into different sections in a graph, Figure 3-13. Only at high *Re* numbers does a complete atomization occur [176].
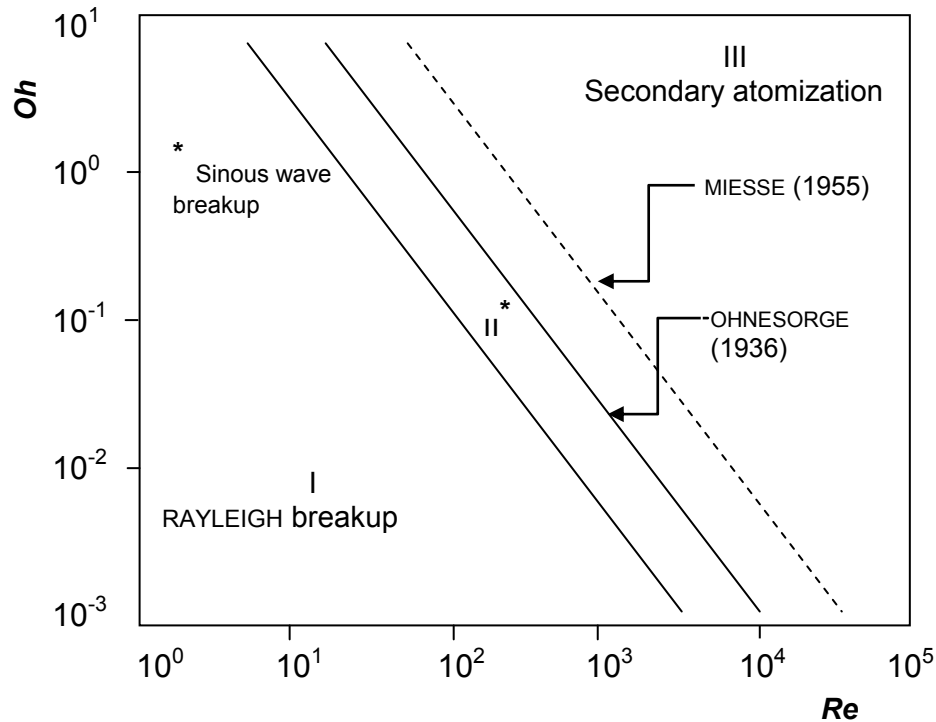
Figure 3-13:   Classification of models of disintegration [176]

Consequently, the atomization process, the viscosity, temperature, and concentration of the feed, and inlet temperature of the spray dryer were found to influence the powder properties to a great extent [177].

Several quality parameters of spray dried milk powders and the influencing factors have been summarized by WOODHAMS and MURRAY (1974), CARIĆ and MILANOVIĆ (2004), and AUGUSTIN, CLARKE, and CRAVEN (2003) [178-180].

3.5 Functional properties of dairy powders

3.5.1 General

Functional properties reflect the intrinsic physicochemical properties of the proteins, i.e., amino acid composition and disposition of amino acid residues, conformation, molecular size, shape, flexibility, net charge, molecular hydrophobicity, substituent chemical groups, and sulfhydryl groups [148]. The functional behavior of milk proteins in food products, however, is much more complicated [146]. The most important properties of powdered food products are handling aspects like the flow behavior or dust prevention but also instant properties wetting, dispersibility or solubility are determined by the micro-structure of the product [181].

In section 3.5.2 of this text the rehydration behavior is outlined in detail.

3.5.2 Rehydration behavior

The rehydration behavior of dairy powders is a very important quality parameter because a sufficient rehydration is necessary to obtain desired technological properties, e.g., stabilization of emulsions and formation of gels and foams. The rehydration of powdered foods involves the following steps (with partial overlapping) [181-185]:

Wettability: wetting of the powder bulk, wetting of the single agglomerates, desagglomeration

It is the property of a powder to imbibe a liquid under the influence of capillary forces. It was very often found to be the rate-controlling step [182;186].

If a fluid enters a cylindrical capillary with smooth and clean walls a wetting angle between the interface and the pore wall is formed. The wetting angle influences the strength of the capillary pressure p_c according to [184;187;188]:

$$p_c = \frac{2 \cdot \sigma \cdot \cos \delta(v)}{r_c}$$
<div align="right">**Equation 3-4**</div>

As a result of the capillary pressure the liquid is imbibed.

The capillary pressure is opposed by the pressure drop p_w in flow direction. The liquid enters the cylindrical capillary with a certain velocity v assuming that $p_c = p_w$ and the dynamic contact angle $\delta(v) = \delta = const.$ [184]:

$$v = \frac{\sigma_L \cdot r_c \cdot \cos \delta}{4 \cdot \eta_L \cdot y}$$
<div align="right">**Equation 3-5**</div>

Sinkability/Submerging

It is the ability of a particle to sink in water. The rate of descent (the settling velocity, v_S) is determined for Re < 1 (mass % < 5 %)/NEWTONIAN liquid according to STOKES for spheres, whereas the interactions between the sinking particles and the fluid are neglected [183;184;189]:

$$v_S = \frac{d_P^2 \cdot g}{18 \cdot \eta_L} \cdot (\rho_P - \rho_L)$$
<div align="right">**Equation 3-6**</div>

From equation 3-6 it can be derived that powders with small particles (particle average) or particles with low density due to entrapped air caused by spray drying remain on the fluid surface. Additionally, the sedimentation velocity increases with decreasing density of the fluid and viscosity.

Typically, an average particle size of ≥ 100 µm and a particle density of ~1500 kg·m^{-3} are enough for sufficient sinking [182].

Dispersibility of the primary particles and solubility (if soluble)

A particle can possess the property to disintegrate into fine or primary particles. Admittedly, the particles have to settle slowly enough so that the dispersion will remain stable and no sediment is formed.

3.5.3 Factors influencing the rehydration behavior

Several factors influence the rehydration behavior of food powders. In the following, selected, mostly intrinsic factors comprising compositional aspects but also processing technology are viewed in detail having an influence on the rehydration behavior of dairy powders.

Besides the intrinsic factors the rehydration conditions which are agitation, pH value, ionic strength, and temperature have a considerable influence on rehydration but these parameters were kept constant during analysis.

Degree of heating

Generally, the caseins are more heat stable than the whey proteins. In milk the caseins are originated as micelles which are highly hydrated (3.7 g water g^{-1} protein) [41]. In the course of the drying of milk powders water has to be replaced and the protein structure needs to reconfigure which might afford time [190].

The degree of denaturation is an important parameter of proteins as long denaturation leads to an unfolding of tertiary and secondary structures. Functional groups of the inside of the molecules are now free and can interact with each other or other protein molecules [14]. Thus, aggregates are formed. Due to the denaturation of whey proteins the functional properties are altered and the solubility is depleted [140]. HAVEA, SINGH, CREAMER, and CAMPANELLA (1998) heated WPC solutions at 75 °C and found the formation of aggregates consisting of β-Lg, α-La, BSA, caseins, and minor proteins [191]. The mechanisms involved were attributed to non-covalent interactions and disulphide cross-linking.

In the course of denaturation the protein structure can be irreversibly changed resulting in reduced protein solubility [192]. Because of its high content of disulfide and the free thiol group of β-Lg, whey proteins can be easily denatured and aggregate or gel if the temperature, pH, or ionic strength are changed [157;193;194].

Particle size

Food's micro-structure acts in most cases as a connection between product properties and processing conditions [181].

The most important parameters determining the micro-structure of a powder are the primary particle size, the agglomerate size, the porosity of agglomerates, the porosity of the powder bulk, and the binding forces between the particles [181].

Aside from the methods and conditions of atomization (disc or nozzle) the particle size is determined by the properties of the raw material, its dry matter/concentration and the drying conditions (drying temperature, feed temperature) [177].

In a study of HECHT and KING (2000) particle morphology was found to depend on surface tension of the spray dried material. Spray dried sucrose particles were found to exhibit a spherical shape compared to coffee particles because of the nearly doubled surface tension, which serves to minimize the overall interfacial area of the particles during drying [195].

Lactose

Several individual proteins have been spray dried and carbohydrates were found to be effective in stabilization of the proteins [196-198]. ALLISON, CHANG, RANDOLPH, and CARPENTER (1999) suggested hydrogen bonding between the carbohydrate and the protein to be the stabilizing mechanism [199]. From experience it is known that lactose inhibits the thermal induced aggregation of whey proteins [200;201].

SPIEGEL (1999) studied the aggregation of WPC by laser diffraction [202]. The properties of aggregates formed were closely related to the denaturation kinetics of β-Lg. Lactose was found to slow down the denaturation of β-Lg when WPC was heated at 80 °C which was also observed by BERNAL and JELEN (1985), GARRETT et al. (1988), JOU and HARPER (1996), and PLOCK, SPIEGEL, and KESSLER (1998) [201;203-205].

Lipids

The fat droplets of fresh milk are surrounded by a milk fat globule membrane (MFGM). The main constituents are phospholipids and proteins, i.e., lipoproteins, glycoproteins, and metalloproteins. According to TÖPEL (2004) the main proportion of the absolute protein fraction are the globular proteins [14]. WALSTRA and JENNESS (1984) stated an essential proportion of the enzymes xanthinoxidase and alcalic phosphatase [15].

Denatured whey proteins can attach to the milk fat globule membrane and can connect to the membrane substances. Thus, whey protein agglomerates can be formed which subsequently sediment [14]. Compared to WPI this happens more often for WPC and the proportion of remaining fat is much greater [149].

According to RATTRAY and JELEN (1995) lipids hinder thermal aggregation of whey protein powders [200].

Chapter 4: Materials and Methods

4.1 Materials

4.1.1 Milk

Cow milk

Raw cow milk was obtained from a controlled herd in Brandenburg consisting of 300 dairy cows (breed Holstein Schwarzbunt) of which 116 were lactating.

The raw bulk milk—a mixture of morning and evening milk—was kept in a tank at a temperature of 6 °C. Milk samples were analyzed within 24 h; additionally, milk was taken from infected udder quarters before and after medication with Benzylpenicillin-Procain 1 H_2O or Cefquinonsulfat. The waiting time for milk is six days after the last antibiotic injection.

Laser diffractometry was done on

- raw milk

- commercial milk with 1.5 % fat (pasteurized and homogenized) which was obtained from a local supermarket

- whey including thin whey, concentrated whey, and final mixed whey which were obtained from a company that provided samples taken during the production of whey-related products.

Goat milk

Raw goat milk was obtained from a controlled herd in Brandenburg consisting of 60 goats.

Milk preparation

The supplied milk samples were defatted by centrifugation in a Sigma 6K10 centrifuge (Sigma Laborzentrifugen GmbH, Osterode, Germany) at 3000 g and 6 °C for 30 min. The fat was replaced with a spatula and the defatted milk was filtered through a coarse filter to ensure complete separation of the fat. The pH value was measured at 20 °C with a CG 840 pH meter (Schott, Mainz, Germany). In the case of pH correction, HCl or NaOH were added.

For the chemical and rheological experiments the calcium content of the samples was increased by 2 mM $CaCl_2$ to adjust for deficiencies occurring due to cooling and centrifugation of the raw milk samples.

Subsequently, up to 700 ml milk were heated to 32 °C in a water bath and stirred for 45 min (R100CT manufactured by CAT Ingenieurbüro M. Zipperer GmbH, Staufen, Germany; blade agitator; d = 0.05 m, 16 blades, angle ~ 30°) prior to spectrophotometric analysis and rheological measurements.

4.1.2 Sweet whey, whey protein concentrate, and skim milk powder

Section I

22 WPC powders of different protein content (sweet whey powder, WPC 35, 60, 70, and 80) and one SMP were provided by several companies which are indicated in Table 4-1.

Table 4-1: Classification of the samples according to companies, section I

Sample	Company
Sweet whey powders: 13 1, 13 2, 13 3	A
WPC 35 1	B
WPC 35 2, 35 3, 60 1, 60 2, 80 5	C
WPC 35 4	D
WPC 35 5, 35 6, 35 7, 60 4, 60 5, 70 2, 80 2, 80 3, 80 4	E
WPC 60 3, SMP	F
WPC 70 1, 80 1	G

All WPC and the SMP were classified by the companies to be insufficient for use or to cause problems in sour milk technology.

Section II

Eleven WPC powders were provided by three different companies. Company H displayed specific production dates, see Table 4-2.

Table 4-2: Classification of the samples according to companies, section II

Sample	Company
WPC 30, WPC 35 8, 35 9, 35 10	B
WPC 35 11 (October 9, 2008), 35 12 (August 1, 2009), 35 13 (August 30, 2009), 35 14 (January 30, 2009), 60 6 (March 19, 2009), 60 7 (August 17, 2009)	H
WPC 80 6	G

Company H gave additional information on some of the WPC 35 which indicated specific properties. WPC 35 13 and WPC 60 6 were assigned the label "heat stable". The WPC 35 14 was assigned the label "high gel".

4.1.3 Low fat quark

The low fat quark was taken from the cheese dairy just before conducting the experiments. The dosage of skim milk concentrate and whey protein was stopped at the time of sampling. Thus, conditions were comparable to the production of the reference quark powder. The quark powders were produced on large and small scale in section I and II. In section II the quark powder was atomized via disc atomization (calculated shear rates 1,483,700 s^{-1} and 18,500 s^{-1}). In section I the quark powder was atomized via pressure nozzle (calculated shear rate 800 s^{-1}). The pilot plant used was dimensionized for a capacity of about 400 l h^{-1}. The equipment is described below in detail. The reference powder and competitor's products were obtained from different companies.

Pilot plant

1. Transport of the quark was carried out after preparation according to reference in an external cooled container, V = 1 m³. The quark was piped via hose connection to a mono pump (progressive cavity pump) with a frequency-controlled motor in order to maintain the flow rate/delivery rate control. The container was emptied under atmospheric pressure.

2. Progressive cavity pump: d = 100 mm, l = 1000 mm, $\dot{V}_{max}$ = 1700 l·h^{-1} restricted to ~1000 l h^{-1} water, flow rate quark = ~300…400 l·h^{-1}

3. The quark was piped via pressure tubing DN 65 from the bottom up into a Terlet scraped surface heat exchanger T2-4 (two concentric heat exchange surfaces). An efficient heat transfer was achieved by continuous scraping of the entire surface (32 scrapers with an offset of 90°). From a rheological and procedural view the scraped surface heat exchanger can be characterized as a mixer/blender and not as a shearing member with a shear gap. The warming of the product was done via hot water feeding. Calculated/empty volume = ~150 l, heated surface = 4.4 m², Interspace between scrapers $\rightarrow$ 0, Agitator speed = 61 min^{-1}, drive capacity = 7.5 kW·h^{-1}

4. Product outlet via steel tubing DN 50. Measurement of temperature and flow rate. Integration of the compressed air connection. Control of the compressed air input and display of the number of standard cubic meters. The tubing led to linkage No. 7.

5. From the linkage a hose line led to the lance with the nozzle which was actually dimensionized for the atomization of skim milk concentrate (large-scale atomization). The inlet of compressed air to the lance was done via pressure hose with previous reduction to 3.6…3.8 bar.

6. Drying in a Büchi dryer for comparison.

Scale-up: production of quark powder on large-scale dryer

The quark with a standardized dry mass was delivered to the dryer in a container, piped into a silo, and stored over night. The start-up operations of the scraped surface heat exchanger and pipes leading to the reservoir of the dryer were done with water. The quark was brought via tubes DN 50 of 60 m length into the reservoir. At this point, the temperature of the quark was 55 °C. A resting time of 30 min occurred at this temperature which cannot be positively assessed regarding graininess and wheying-off. The inlet air temperature of the dryer corresponded to the temperature in the small-scale dryer.

4.2 Chemical methods

4.2.1 Determination of the pH value

The milk samples were stirred at 35 °C for 30 min at 330 U·min^{-1}. After cooling of the milk to 20 °C, the pH value was measured by the pH meter CG 840 (Schott, Mainz, Germany). Before measurement the pH meter was standardized with a 7.0-pH and a 4.0-pH solution.

4.2.2 Determination of moisture

The moisture [g·kg^{-1}] and the d.m. [%], respectively, were determined according to DIN 10 321 "Determination of the water content of dried milk" by oven drying.

4.2.3 Determination of ash content

The ash content [%] was determined according to DIN 10477 "Determination of the total ash content of milk and milk products".

4.2.4 Determination of the total nitrogen content

The total nitrogen content was determined by the KJELDAHL method (IDF, international dairy: 20B, 1993). Total protein content was obtained using the conversion factor 6.38.

The NCN content was determined after fractionation of the milk samples with acetic acid and sodium acetate. 40 ml milk and 40 ml double-distilled water were warmed to 35 °C. 4 ml 10 % (v/v) acetic acid were added and after 10 min 4 ml 1 N sodium acetate was added. After cooling to 20 °C, the pH value reduced to 4.6 and the sample was filled up to 100 ml with double-distilled water. Subsequently, the whey was filtered from the casein. The filtrate was used for the determination of NCN.

4.2.5 Determination of the calcium content

The calcium content was determined by a complexometric method [206]. The principle of this method is the formation of complexes between calcium ions and ethylenediaminetetraacetic acid, sodium salt (Chelaplex III), during titration and a color change of the calcium sensitive indicator Calcein.

1 ml of full-fat raw milk were filled up to 100 g with double-distilled water, 4 ml of a 50 % (w/v) KOH solution and 100 µl of the indicator Calcein ($c = 0.1$ g in 25 ml Methanol) were added. Titration was carried out with 0.01 M Chelaplex III until the indicator changed its color. The calcium content in the sample was calculated from the consumption of Chelaplex III. The determination was done in triplicate. The calcium content $c_{Ca^{2+}}$ was calculated according to equation 4-1.

$$c_{Ca^{2+}} = \frac{b \cdot 0.4008 \cdot 100}{E} \cdot F$$

Equation 4-1

4.2.6 Determination of the lactose content

The lactose content was determined by an enzymatic method (lactose/D-galactose test, R-Biopharm AG, Darmstadt, Germany) using the UV-visible spectrophotometer CE 1020 manufactured by Cecil Instruments Ltd., Cambridge, England. Prior to analysis the samples were clarified with Carrez-I solution (Potassium-hexa-cyano-ferrate (I)) and Carrez-II solution (zinc sulfate).

4.2.7 Determination of the fat content

The fat content [%] of the milk powders was determined according to DIN EN ISO 1736 "*Bestimmung des Fettgehaltes, gravimetrisches Verfahren (Referenzverfahren) (ISO 1736:2000) für Milchpulver und Trockenmilcherzeugnisse*".

4.2.8 Determination of the rennet activity

The chymosin used is CHY-MAX^{TM} Plus (Chr. Hansen GmbH, Nienburg, Germany) which is a fluid product produced by fermentation of *Aspergillus niger* var*. Awamori.*

The rennet strength was determined with reconstituted low-heat skim milk powder (NILAC). To obtain reconstituted milk, 11 g low-heat skim milk powder (NIZO, Ede, The Netherlands) milk powder was dispersed in 100 g 0.02 M $CaCl_2$. Next, the milk was kept at 35 °C in a water bath for 1 h. It was stored overnight in the refrigerator at 6-8 °C. On the following day the pH value was adjusted to 6.45, the reconstituted milk was heated to 35 °C in a water bath and stirred for 45 min.

The chymosin was diluted 1:50 in 0.02 M $CaCl_2$. For the determination of the rennet strength 25 g and 50 g of reconstituted milk were clotted with the chymosin. The visual clotting time was measured.

4.2.9 Determination of the visual clotting time

The visual clotting time was determined simultaneous to rheological measurements. 50 ml of the milk to which chymosin was already added were separated into a beaker, and also tempered in a water bath to 32 °C. The visual clotting time is the time at which small coagulum occurred on a microscope slide.

4.2.10 Spectrophotometric analysis of CMP and GMP

The method is based on the selective solubility of CMP und GMP in 6 % TCA in 0.175 M sodium sulfate and in 12 % TCA, respectively, following their isolation from the TCA filtrate using analytical desalting columns EconoPAK 10DG (BioRad Laboratories GmbH, Munich, Germany), and consecutively, the photometric measurement of the absorption at 217 nm using the UV-visible spectrophotometer CE 1020 (Cecil Instruments Ltd., Cambridge, England) and adjustment with the reagent blank value. N.-g. CMP is the calculated difference between the absorptions of CMP and GMP. The method can be used to obtain the kinetics and also for standard analyses [113].

The spectrophotometric method requires two critical steps that have an immense influence on the coagulation of the serum proteins: first, the dosing of the TCA, and second, the maintenance of a constant rotational speed during dosing of the acid. Because of the appreciable influence these steps were adapted to the equipment used. The geometry and the run down speed of the pipette influence the determined amount of CMP. A volumetric and a graduated pipette were tested.

Pipette type

No differences were obtained for both pipette types, Table 4-3. The following experiments were carried out with a volumetric pipette.

Table 4-3: Influence of the pipette type on the CMP content

Pipette type	CMP content $g \cdot l^{-1}$
Volumetric pipette	1.235
Graduated pipette	1.235

Rotational speed

The maintenance of a constant rotational speed during the addition of the acid is important for gaining reproducible results. If the rotational speed changes during dosing, local imbalances can occur and lead to differences in the results. The optimal rotational speed was measured for the CMP because this is the parameter which is affected the most. Because of the high TCA concentration during analysis of GMP this is very stable. In the first experiment the rotational speed was varied between 1000, 1300 and 1500 U·min^{-1}. In a second experiment the interval of the rotational speed was shortened (1200, 1300, and 1400 U·min^{-1}). The determined CMP contents at different rotational speed are given in Table 4-4.

Table 4-4:   **CMP content depending on rotational speed**

Rotational speed given by the display U·min^{-1}	CMP content g·l^{-1}
1000	1.102
1300	1.264
1500	1.628

The analyzed milk sample had a protein content of 3.39 %. The casein content in milk is ~ 80 % of the whole protein [15]. Thus, the casein content in the raw milk sample can be calculated to 2.7 %. Milk contains 2-4 g κ-casein per liter on average [16] and CMP equals 40 % of the molecular weight of κ-casein. On average, 1 g casein contains 46 mg CMP. As a result, the calculated or theoretical amount of CMP in our experiment should be 1.242 g·l^{-1} milk. Comparing this theoretical value with the obtained results in Table 4-4, a rotational speed of 1300 U·min^{-1} seems to be optimal. In a second experiment the interval of the rotational speed was shortened using the same milk sample. The obtained CMP contents are given in Table 4-5.

Table 4-5:   **CMP content depending on rotational speed, repeated experiments**

Rotational speed given by the display U·min^{-1}	CMP content g·l^{-1}
1200	1.202
1300	1.245
1400	1.379

Results prove that a rotational speed of 1300 U·min^{-1} is optimal for the equipment used.

4.2.11 Development of a fast chemical method for the assessment of the protein solubility

The solubility of proteins is detrimental for the functional properties, as long as for example the ability to form gels, stabilize emulsions and foams depend on it. The most commonly used methods to determine solubility are the protein dispersibility coefficient, coefficients of soluble or dispersible nitrogen, and protein solubility profile [207].

The method developed here is based on the standard method ISO 15323 "Dried milk protein products—Determination of nitrogen solubility index" in which the sample is stirred for 2 h [208]. By deviating from the standard method an attempt is made to shorten this procedure and make it more applicable for rapid use.

The sample was precisely weighted (on 1 mg) into a beaker. The sample amount was calculated according to the individual protein content. About 1 g of protein was to be weighted in. 70 ml of double-distilled water was added. Via magnetic stirrer ($700 \: U \cdot min^{-1}$) the sample was dispersed for 5 min. Subsequently the pH value was adjusted to 7.0. The solution was then stirred for 1 h by the R100CT manufactured by CAT Ingenieurbüro M. Zipperer GmbH, Staufen, Germany and the protein content of this solution was determined.

Subsequently, a centrifugation step was done in the Sigma 6K10 centrifuge (Sigma Laborzentrifugen GmbH, Osterode, Germany) at 3000 g and 22 °C for 10 min. The supernatant was filtered and the protein content was determined via KJELDAHL. The protein solubility (*PS*) is calculated according to equation 4-2.

$$PS = \frac{P_{Supernatant}}{P_{Solution}}$$

Equation 4-2

The *PS* focuses on the solubility of the sample nitrogen. A higher *PS* points towards better solubility of the sample nitrogen at pH 7.0 and after 1 h dispersion time. The dispersion time was shortened to 1 h to make this method more rapid and practicable. The results obtained with this method will later be compared to the laser diffraction results.

4.2.12 Removal of lipids by chitosan

Chitosan is a cationic polyelectrolyte/polysaccharide (pKa~6.5) [209;210] derived from crustacean or fungal chitin and is soluble in aqueous acidic media due its basicity [209]. It has a high positive charge on $-NH3^{+}$-groups when dissolved enabling it to adhere or aggregate with negatively charged molecules either in solution or in colloidal state. Thus, flocculation is induced [209;211]. Chitosan is able to bind fatty acids via ionic binding [212] and it can interfere with neutral lipids via hydrophobic interactions [209]. Additionally, it is described to have interesting nutritional and physiological characteristics for example, hypocholesterolemic effect, reduction of lipid absorption, and enhancement of cholesterol elimination [213].

Chitosan interacts with surface-active material, e.g., phospholipids, small-molecule surfactants, bile acids [214], or proteins [214-216]. It has already been used to remove lipids form cheese whey [217] and for the reduction of cholesterol [212]. The chitosan-protein interaction was found to be of physical (electrostatic) or chemical (Maillard) origin [214]. In a study by HATTORI, NUMAMOTO, KOBAYASHI, and TAKAHASHI (2000) chitosan interacted with β-Lg via a Maillard type reaction [218].

HWANG and DAMODARAN (1995) precipitated MFGM fragments (lipids) from cheese whey by means of chitosan and found the optimum concentration of chitosan was 0.01 % [217]. This precipitation involves electrostatic interactions at pH 4.5 due to the extreme positive charging. The MFGM fragments are negatively charged. The main whey proteins in their native state α-La, β-Lg, lysozyme, and bovine serum albumin are either positively charged or electrically neutral at pH 4.5. Additionally, the whey proteins are highly soluble at their isoelectric pH and remain in solution at pH 4.5. Thus, the selective precipitation of the MFGM-chitosan complex is possible.

GUZEY and MCCLEMENTS (2006) studied the interaction of chitosan and β-Lg and found no interaction or the formation of soluble complexes at pH 3 and 4 because both molecules exhibited similar charges [214]. At pH 6 and 7 both molecules had opposite charges and formed insoluble complexes. CASAL et al. (2006) selectively precipitated β-Lg present in whey by chitosan and isolated the undenatured β-Lg to use it for food applications [219].

Chitosan was obtained from Carl Roth GmbH & Co. KG, Karlsruhe, Germany, CAS-number [9012-76-4], deacetylation 90.1 %.

The method was adopted from HWANG and DAMODARAN (1995) [217]. An aliquot of chitosan solution, c = 1 % (w/v) in 10 % acetic acid, was added to the rehydrated WPC solution, c = 1 % (w/v), at room temperature to an end chitosan concentration between 0.01 and 0.03 %. The pH was adjusted to 4.5 by adding 1 M HCl. After incubation time of 10 min the mix was centrifuged at 3000 g for 10 min at 10 °C in a Sigma 6K10 centrifuge (Sigma Laborzentrifugen GmbH, Osterode, Germany). The turbidity of the supernatant was measured at 500 nm and 660 nm using the UV-visible spectrophotometer CE 1020 manufactured by Cecil Instruments Ltd., Cambridge, England. A control, containing no added chitosan, was performed under identical conditions.

4.2.13 High-Performance Size Exclusion Chromatography (HPSEC)

HPSEC was performed at room temperature using the HPLC system ÄKTAbasic™ 10, Amersham Biosciences, Uppsala, Sweden, consisting of a separation unit (pump P-900, UV-monitor UV-900 operating at 280, 256 and 214 nm), UV-flow cell (10 mm), injection valve INV-907, mixer M-925 and flow restrictor FR-904) and a personal computer running UNICORN™ control system version 5.01, Amersham Biosciences, Uppsala, Sweden.

The chromatographic column was Tricorn Superose 12 HR 10/30, Amersham Biosciences, Uppsala, Sweden, with an exclusion limit of ~2000 kDa and a void volume of 7.00 ml.

Prior to HPSEC all buffers were filtered and degassed with the mobile phase conditioner M-3522, BioRad Laboratories GmbH, Munich, Germany. The samples were filtered through 0.20 μm filters, Minisart®, Sartorius AG, Göttingen, Germany. The flow rate of the mobile phase was 0.500 ml·min^{-1}. A sample volume of 0.1 μl was injected.

β-Lg from bovine milk (lyophilized powder, CAS-Nr. 9045-23-2) and α-La from bovine milk (lyophilized powder, 9051-29-0) were obtained from Sigma-Aldrich Chemie GmbH, Munich, Germany. BSA was obtained from Pierce, Illinois, USA (c = 2 mg·ml^{-1} in a 0.9 % aqueous NaCl solution containing sodium azide). γ-Globulin (bovine, lyophilized, MW ~ 150 000) was purchased from Serva Feinbiochemica GmbH & Co. KG, Heidelberg, Germany.

The amounts of the main whey proteins α-La and β-Lg were calculated from the regression lines; refer to Figure 12-1 in the Appendix.

Separation of proteins—Native protein profile

The appropriate amount of WPC to make a 0.2 % (w/v) protein solution was dispersed in 0.15 M NaCl, 0.05 M Sodiumdihydrogenphosphate pH 7.2, stirred for 2 h with a magnetic stirrer, and left overnight in the refrigerator at 6 °C for complete rehydration. Prior to chromatography the sample was tempered to room temperature. A filtration of the samples through a 0.20 μm filter Minisart®, Sartorius AG, Göttingen, Germany was omitted. All analyses were made in duplicate.

Separation of proteins—Protein fractionation at pH 4.6

The appropriate amount of WPC to make a 2 % (w/v) protein solution was dispersed in double-distilled water. The pH value was adjusted to 4.6. Next, the solution was centrifuged in a Sigma 6K10 centrifuge (Sigma Laborzentrifugen GmbH, Osterode, Germany) at 3000 g and 10 °C for 10 min. The supernatant was taken for analysis. Prior to analysis it was diluted 1:10 in 0.15 M NaCl, 0.05 M Sodiumdihydrogenphosphate pH 7.2.

Separation of proteins—Chitosan-treated sample

The appropriate amount of WPC to make a 1 % (w/v) protein solution was dispersed in double-distilled water. The pH value was adjusted to 4.5. After addition of the chitosan concentration leading to the lowest turbidity, the solution was centrifuged in a Sigma 6K10 centrifuge (Sigma Laborzentrifugen GmbH, Osterode, Germany) at 3000 g and 10 °C for 10 min. The supernatant was taken for analysis. Prior to analysis it was diluted 1:5 in 0.15 M NaCl, 0.05 M Sodiumdihydrogenphosphate pH 7.2.

4.2.14 Hydrophobic Interaction Chromatography (HIC)

Several methods exist for the separation of caseins by liquid chromatography including diverse sample preparations as well as the application of various chromatographic columns. Well established methods for the separation of the caseins are ion-exchange chromatography [220-224] and hydrophobic interaction chromatography [225;226]. Recently, LIESKE and VALBUENA (2008) fractionated casein by hydrophobic interaction chromatography using the sample preparation of BRAMANTI et al. (2003) and the Source 15PHE PE 4.6/100 column, Amersham Biosciences, Uppsala, Sweden [227]. This method was found to be very practical for the separation of isolated casein as well as of casein in whole milk samples. Therefore, this method was employed.

HIC was performed at room temperature using the HPLC system ÄKTAbasic™ 10, Amersham Biosciences, Uppsala, Sweden, consisting of a separation unit (pump P-900, UV-monitor UV-900 operating at 280, 256 and 214 nm), UV-flow cell (10 mm), injection valve INV-907, mixer M-925 and flow restrictor FR-904) and a personal computer running UNICORN™ control system version 5.01, Amersham Biosciences, Uppsala, Sweden. A Source™ 15PHE PE 4.6/100 column, Amersham Biosciences, Uppsala, Sweden, was used for all experiments.

Prior to HIC all buffers were filtered and degassed with the mobile phase conditioner M-3522, BioRad Laboratories GmbH, Munich, Germany. The samples were filtered through 0.20 μm filters Minisart®, Sartorius AG, Göttingen, Germany and were applied to the column by manual injection.

Commercial caseins were obtained from Fluka Chemie AG, Buchs, Switzerland: β-casein from bovine milk (≥ 80 %, product no. 22086), α-casein from bovine milk (≥ 70 %, product no. 22084) and κ-casein (≥ 90 %, product no. 22087). Table 4-6 displays the chromatographic conditions.

Table 4-6: **Chromatographic conditions of the HIC analysis**

Flow rate	0.500 ml·min^{-1}
Sample injection	
- sample amount:	500 µl
Linear gradient:	5-20 ml (from 100 % high salt to 100 % low salt buffer)
Absorbance measurements performed at:	280 nm

The appropriate sample amount (protein concentration: 7 mg·ml^{-1}) was dispersed in a sample buffer and left overnight at 6°C for complete solvation of the proteins. Prior to HIC, samples were diluted in a high salt buffer to a final protein concentration of 0.5 mg in 500 µl.

Figure 4-1 represents the chromatograms of the commercial α-, β-, and κ-casein.
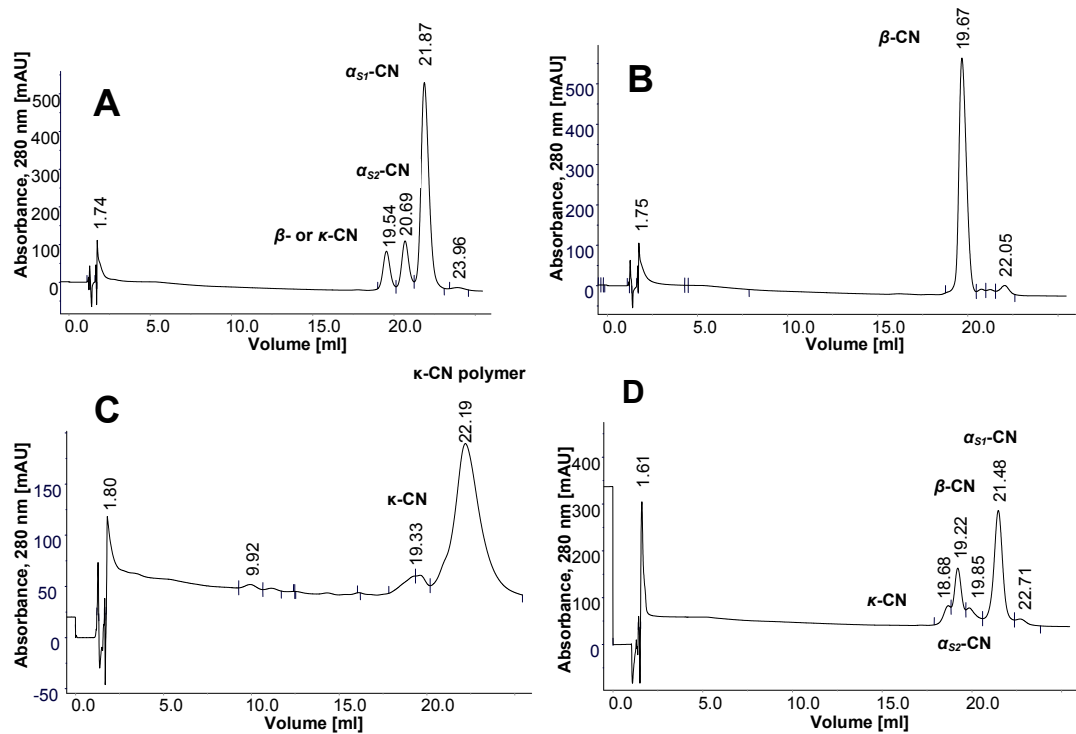
Figure 4-1: **Chromatograms of the commercial caseins**

A : α-**CN with retention times 21.87 min (α_{S1}-CN) and 20.69 min (α_{S2}-CN)**

B: β-**CN with retention time of the main peak 19.67 min**

C: κ-**CN with two peaks κ-CN (retention time: 19.33 min) and κ-CN-polymers (retention time: 22.19 min)**

D: **New Zealand casein with κ-CN (18.98 min), β-CN (19.52 min), α_{S2}-CN (19.86 min), and α_{S1}-CN (21.48 min)**

α-casein separates in three peaks, one attributed to α_{S1}-casein (retention time: 21.87 min) and one attributed to α_{S2}-casein (retention time: 20.69 min). The third peak has not been identified yet [228]. According to the retention times of the β-casein and κ-commercial-casein it can be assumed that this peak corresponds to either β-casein or κ-casein or a mixture of both.

β-casein is eluted in one main peak (19.67 min). The minor peaks have not been identified yet. It could be a contamination with κ-casein polymers or γ-caseins derived from hydrolysis of β-casein by indigenous plasmin [228]. κ-casein is separated with two peaks: κ-casein (retention time: 19.33 min) and κ-casein-polymers (retention time: 22.19 min).

The chromatogram of the New Zealand casein represents a typical casein profile obtained by the Source™ 15PHE PE 4.6/100 column: κ-casein (18.68 min; consisting of the glycosylated variants and the major part of the non-glycosylated κ-casein [227]), β-casein (19.22 min), α_{S2}-casein (19.86 min), and α_{S1}-casein (21.48 min).

According to LIESKE and VALBUENA (2008) the peak at 22.71 min can be attributed to non-glycosylated κ-casein in polymerized form being the most hydrophobic protein in the chromatogram [227]. This corresponds to the chromatogram of the commercial κ-casein which had a peak consisting of polymers around 22.19 min. LIESKE and VALBUENA (2008) found this second κ-casein peak to be typical for processed casein products [227]. Consequently, this peak is missing in chromatograms of caseins separated from raw milk, see Figure 5-11.

4.2.15 SDS-Page

Electrophoresis was done using the mini-vertical gel electrophoresis unit SE 250, Hoefer Inc., Holliston, USA, according to the method of SCHÄGGER and VON JAGOW (1987) [229]. The method used allows a separation of proteins in the range from 1 to 100 kDa. The gels were cast in the dual gel caster SE 245, Hoefer Inc., Holliston, USA. The composition of the stock solutions and the acrylamide/bisacrylamide mixture can be read from Table 4-7 and Table 4-8. PAGE was performed under dissociating and reducing (SDS-PAGE) conditions which allow the separation of proteins by molecular weight.

Table 4-7:   **Stock solutions for alkaline SDS-Page**

Buffer	Tris [M]	Tricine [M]	pH value	SDS [%]
Anode buffer	0.2	-	8.9[1]	-
Cathode buffer	0.1	0.1	8.25[2]	0.1
Gel buffer	3	-	8.45[1]	0.3

[1] Adjusted with concentrated HCl   [2] No correction of pH

Table 4-8:   **Composition of the acrylamide/bisacrylamide mixture**

Acrylamide/bisacrylamide mixture	Acrylamide [w/v]	Bisacrylamide [w/v]
49.5 % T, 3 % C	48 g in 100 ml	1.5 g in 100 ml

The composition of the stacking and the separating gel is given in Table 4-9.

Table 4-9: Composition of the stacking and separating gel

	Stacking gel [4% T, 3 % C]	Separating gel [10% T, 3 % C]
Acrylamide/bisacrylamide mixture	1 ml	3.05 ml
Gel buffer	3.1 ml	5 ml
Glycerol	-	2 g
Double-distilled water	8.4 ml	5 ml
10 % ammonium persulfate	100 µl	80 µl
TEMED	10 µl	8 µl

The constituents were mixed and polymerized without degassing by addition of 8 µl TEMED and 80 µl 10 % ammonium persulfate solution. After polymerization for 30 min the stacking gel was prepared. The components were mixed and the gel was polymerized with the addition of 10 µl TEMED and 100 µl 10 % ammonium persulfate solution. The separating gel was overlaid with the stacking gel (3 cm).

Electrophoresis was performed at room temperature for 30 min, 30 V, and 30 mA. After the protein bands had reached the separating gel the electrophoresis unit was put into the refrigerator. The electrophoresis was carried out at 50 mA and 200 V_{max} for 1.5 h until the blue lines had reached the bottom of the gels.

Fixing was carried out for 30 min using a solution of 50 % methanol and 10 % acetic acid. The gels were stained in 0.025 % Serva blue R in 10 % acetic acid overnight. Destaining was achieved with 10 % acetic acid for 2 h. The destaining solution was renewed every 30 min.

Figure 4-2 displays the molecular weight standard for comparison. On the left side the molecular weight of the standard bands are given. The main whey proteins are assigned on the right side [191;230;231].
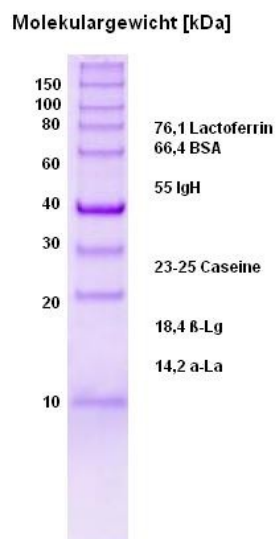
Figure 4-2: Molecular weight standard Roti®-Mark

Sample preparation

For the protein profiles 500 µl of a 1 % protein solution (WPC with 35 % protein) and 250 µl of a 1 % protein solution (WPC with 60, 70, and 80 % protein), respectively, are diluted in 1 ml sample buffer. Samples were incubated for 2 h at 40 °C in the sample buffer which consists of 4 % SDS, 20 % glycerol (w/v), 50 mM Tris, 2 % Mercaptoethanol (v/v), 0,01 % Serva blue R. The sample buffer was adjusted with HCl to pH 6.8. 7 µl of the samples and 8-10 µl of the standard Roti®-Mark 10-150 manufactured by the company Carl Roth GmbH & Co KG, Karlsruhe, Germany, were placed under the cathode buffer using a microliter syringe.

4.3 Physical methods

4.3.1 Rheological measurements during the rennet-induced coagulation

Rheological measurements were carried out with a Rheoswing RSD 1-1 device from Physica Messtechnik GmbH, Stuttgart, Germany. The viscosity is recorded using the UDS–200 software (Physica Messtechnik GmbH, Stuttgart, Germany). The measuring error of the Rheoswing is 0.03 % of the full scale value. The measuring range is 1 to 100 mPa·s.

The defatted milk samples were tempered to 32 °C for 45 min at 330 U·min^{-1}. The chymosin was diluted 1:50 in 0.02 M CaCl$_2$. In the case of bovine milk 5.4 ml chymosin solution and in the case of caprine milk 3.5 ml chymosin solution were added to 600 ml milk.

The measuring system used in this study enables the expansion of three phases [117;232] to five sections: 1. NEWTONIAN behavior, 2. Structure-viscosity (Non-NEWTONIAN), 3. Viscoelasticity (section with constant gel formation velocity), 4. Viscoelasticity (sigmoid course of the gel formation velocity), and 5. Viscoelasticity (syneresis), Figure 4-3.
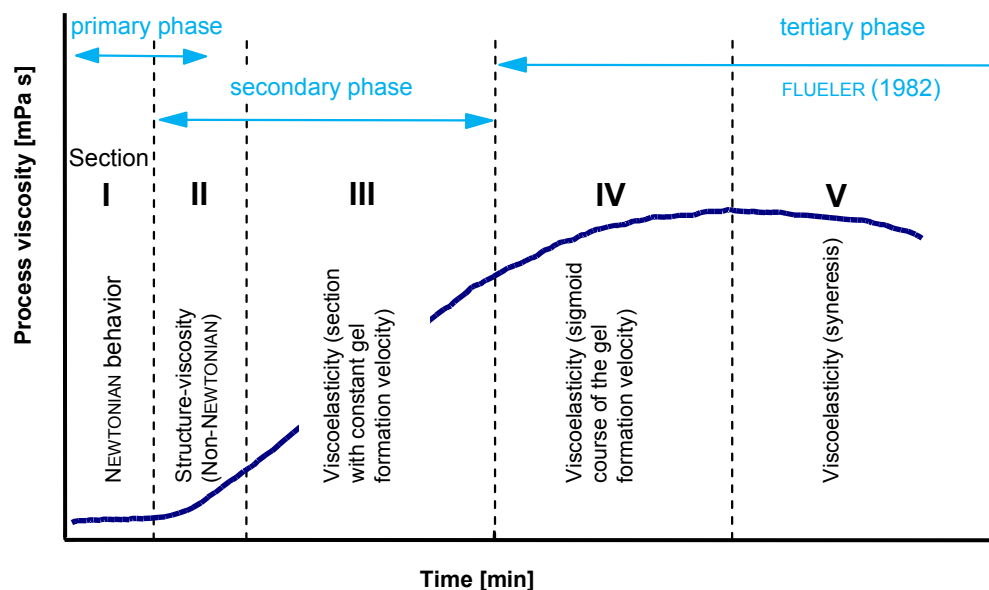
Figure 4-3:   **Schematic diagram of the rennet-induced coagulation of raw milk [123]**

Section I of the curve (Figure 4-3) displays the primary phase and sections II and III of the curve (Figure 4-3) display the secondary phase of the rennet-induced coagulation according to FLUELER (1982) [49].

The primary phase and the secondary phase can be divided into three sections which are relevant for the structure formation [233] and are discussed in detail. Furthermore, the curve progression gives information about the rennetability of milk [122;123].

The method of sectioning is described in [122;123]. The borders of the sections are determined by the saltus function determined by the differential quotient DQ_i, equation 4-3, according to the method developed by SCHULZ (2000) [123].

$$DQ_i = \frac{\eta(t_i) - \eta(t_{i-1})}{t_i - t_{i-1}} = \frac{\eta(t_i) - \eta(t_{i-1})}{1\,\text{min}}$$

Equation 4-3

Additionally, measurements were carried out to determine the precision (repeatability) of the rheological method in the case of rennet-induced coagulation. The precision is a measure for the scattering of the individual values around the mean value. Precision provides an indication of random errors. The standard deviation s describes the performance of the precision [234-236]. The standard deviation s is calculated according to equation 4-4.

$$s = \sqrt{\frac{\sum (x_i - \bar{x})^2}{N - 1}}$$

Equation 4-4

To assess the repeatability, the rennet-induced coagulation of a milk sample (commercial milk, fat 1.5 %, homogenized, and pasteurized) was measured over time with the Rheoswing RSD 1-1 device under same conditions for three different times. The standard deviation was calculated.

Results show that the standard deviation is small but increases slightly during the process of rennet-induced coagulation; Figure 12-3 in the Appendix.

4.3.2 Rheological measurements of quark and quark powder

Rheological measurements were done by the rheometer MC 120, Physica Messtechnik GmbH, Stuttgart, Germany, equipped with a Z3 DIN rotational cylinder ($\dot{\gamma}_{max}$ = 1054 s^{-1}).

The flow behavior of the low fat quark and the rehydrated quark samples was determined by controlled stress rheometry/shear rate (CSR).

According to calculations the shear rates during atomization via pressure nozzle were calculated to be 800 s^{-1}. Therefore, the rheological measurements were carried out at $\dot{\gamma}_{max}$ = 100, 500, and 1000 s^{-1}.

The regression of the rheological data was mainly done according to the HERSCHEL-BULKLEY model. At high temperatures the OSTWALD-DE WAELE model became valid for application. The properties of selected rheological models are listed in Table 4-10.

Table 4-10: **Selected rheological models**

Model	Constitutive equation Pa	Dynamic, effective, and process viscosity Pa·s	Number of model parameters	
NEWTON	$\tau = f(\dot{\gamma}) = \eta \cdot \dot{\gamma}$	$\eta = f(\dot{\gamma}) = \dfrac{\tau}{\dot{\gamma}}$	1	**Equation 4-5**
OSTWALD-DE WAELE	$\tau = K \cdot \dot{\gamma}^n$	$\eta_{eff} = K \cdot \dot{\gamma}^{n-1}$	2 structure viscosity	**Equation 4-6**
HERSCHEL-BULKLEY	$\tau = \tau_0 + K \cdot \dot{\gamma}^n$	$\eta_{eff}(\dot{\gamma}) = \dfrac{\tau_0}{\dot{\gamma}} + K \cdot \dot{\gamma}^{n-1}$	3 non-linear, plastic	**Equation 4-7**

The consistency index K stands synonymously for the viscosity (inner friction). The flow index n can be used to assess the structure stability of the product. If n increases $n \rightarrow 1$ a shearing of the sample is indicated, pointing at structure instability. If n decreases or remains constant a solidification of the structure and a preservation of the structure, respectively, are indicated. The yield point τ_0 is an indicator for the structuring elements in the product. The thixotropic area A_{Th} characterizes the dependence of the structure stability at constant shear rate. It is an easy-to-measure parameter pointing to rheodynamic behavior. The thixotropic area correlates with the structure deformation work. The higher the thixotropic area, the higher the structure instability of the product and its susceptibility for the influence of mechanical energy [237-240].

Figure 4-4 displays a measuring profile of the controlled shear rate measurements. Five measuring sections and the preset deformation velocity are displayed. The fifth section is regressed according to the models listed in Table 4-10.
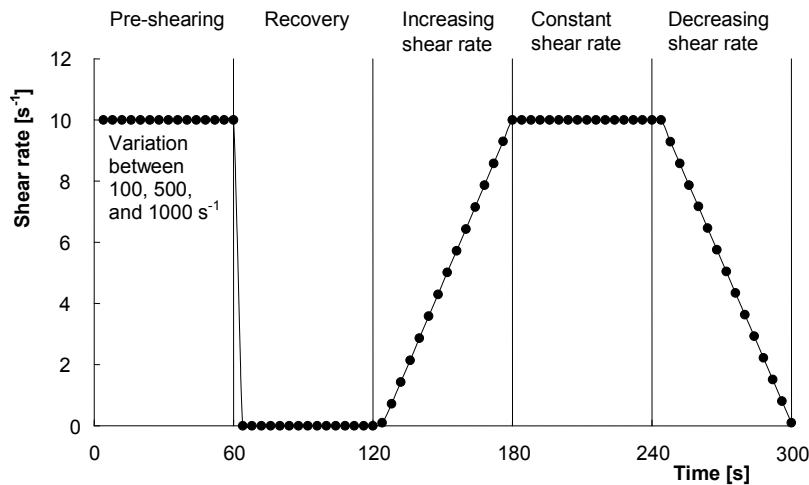
Figure 4-4: **Measuring profile of the controlled shear rate measurements exemplarily for $\dot{\gamma}_{max}$ = 100 s^{-1}**

Scale-up: production of quark powder on a pilot plant and small-scale dryer

The scale-up was accompanied by rheological measurements of the raw material low fat quark (10 °C, $\dot{\gamma}_{max}$ = 100, 500, and 1000 s^{-1}) and during processing of the raw material quark (MS1), the warmed quark after passage of scraped surface heat exchanger (MS3), the quark after passage of the nozzle without supply of air, variant I (MS4), and the quark after passage of the nozzle with supply of air, variant II (MS5). Sampling (MS2) after the pump was not undertaken. All rheological measurements were done at $\dot{\gamma}_{max}$ = 1000 s^{-1}. Instructions by the customer required that the supporting temperature points were fixed at 10 °C, 35 °C, 45 °C, 55 °C, and 65 °C. The powder functionality was assessed via water retention after 1 h of rehydration. The rehydration was done according to standard procedure (two-step dispersion).

Scale-up: production of quark powder on large-scale dryer

Rheological measurements during production were taken of the product following the scraped surface heat exchanger and after the tube inlet. The raw material quark was not measured because the sampling was not undertaken. The rehydrated powders obtained from large-scale production were not measured because of the insufficient water binding capacity.

Determination of the properties of the raw material low fat quark

Rheological measurements of the low fat quark with 18 % dry matter were done at 10 °C on different production dates to compare the properties of the incoming product before processing (Preparation I). Additionally, the quark was diluted to 16 % dry matter and dispersed by the hand-held blender 2005-12 ESGE, Unold AG Hockenheim, Germany for 3 min to determine the mechanically-induced structure deformation (Preparation II).

The third preparation procedure started with the warming of the quark (16 % dry matter) in the water bath to 35 °C under slow mechanical agitation by a means of wire wisk and a subsequent shearing of the quark with the hand-held blender 2005-12 ESGE, Unold AG, Hockenheim, Germany, for 3 min.

Influence of thermal and mechanical parameters on the low fat quark matrix

Rheological measurements for the determination of the influence of temperature and shear rate on low fat quark were done in the temperature range 0 to 70 °C with ΔT = 10 K at $\dot{\gamma}_{max}$ = 100, 500, and 1000 s^{-1}. The results were aimed to give information whether thermal or mechanical influences dominate the de-structuring of the low fat quark.

Rheological investigations into the rehydration kinetics

Firstly, the functionality of quark powder was assessed exemplarily for the examination of the water retention. Measurements were done after rehydration of 10, 15, and 20 min to assess the water uptake exemplarily for the change in rheological parameters. Rehydrated quark powders were dried on small (7.1, 7.2, and 7.3) and large scale.

4.3.3 Static laser light scattering

4.3.3.1 Principle

The interaction of light with particles can be described by reflection of light at the particle's surface, diffraction of light at the particle's contour (FRAUNHOFER diffraction), refraction of light at the surface of particle and medium, and absorption of light inside the particle. As a consequence, these interactions cause interference phenomena which give rise to a characteristic scattering pattern with characteristic minima and maxima.

Laser diffraction is based on the principle that particles scatter laser light in a certain diffraction pattern in every direction. In the pattern, the scattered light intensities at different angles depending on size, shape, and optical properties of the particle. In the case of particles in the micron area, diffraction is the main principle which causes the light scattering [241;242].

Following assumptions have been made in order to fully describe scattering patterns: the particles are optically homogeneous and spherical, and are present in a dilute random argument (independent, incoherent scattering) [241;242].

In general, the scattering intensity of unpolarized light by a single spherical particle can be written as [241]:

$$I(\theta) = \frac{I_0}{2k^2a^2}\left\{[S_1(\theta)]^2 + [S_2(\theta)]^2\right\}$$

Equation 4-8

Practically, the scattering pattern is deconvoluted based on FRAUNHOFER or MIE. The fundamental theory of light scattering by homogeneous and isotropic spherical particles was described by MIE (1908) [243]. It accounts for all types of light interactions.

The scattering theory according to MIE is necessary for analysis in which optical effects resulting from reflecting or transparent spherical particles and from polarization effects appear.

As a consequence, this theory requires the knowledge of various optical parameters which are the complex refractive index (ratio of the refractive index of particle to that of medium) comprising a real part representing the refractive properties of particle and medium and an imaginary part representing the light absorption properties of the particle [241].

$$m = \frac{(n_{RP} - k_{IP} \cdot i)}{n_m}$$

Equation 4-9

Disadvantages of the MIE theory are problems in assessment of the real optical properties. They depend on crystal structure, impurities, wavelength of the light, non-sphericity, and surface roughness [241].

However, the FRAUNHOFER diffraction theory requires no previous knowledge of optical parameters and is useful for analysis of nonspherical particles. But the application of this theory is limited for opaque materials, particles are considered to be circular, two-dimensional disks, only the interaction of light at the contour of the particle is taken into consideration, and the scattering is considered in the near-forward direction (θ is small). Additionally, it yields biased results for (ultra)fine transparent particles [241].

As indicated above, for the different theories various advantages and disadvantages exist. All instruments use the assumption of spherical particles. FRAUNHOFER can be used for particles > 50 µm. MIE theory is used for transparent particles in the range 1-50 µm. For particles in this size range, that are reasonably opaque (k_{IP} > 0.5) and/or

$\dfrac{n_{RP}}{n_m}$ > 1.1, FRAUNHOFER or MIE theory can be used [241].

The schematic configuration of a laser diffractometer is given in Figure 4-5. The laser light irradiates each particle which causes a scattering pattern depending on size and shape [244].
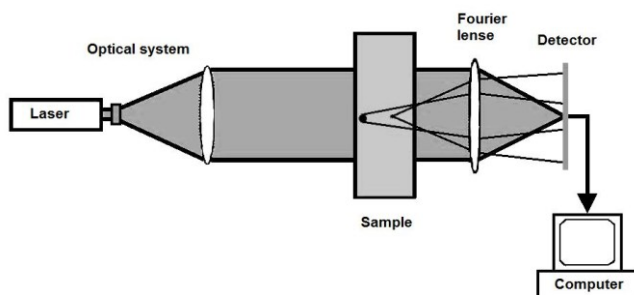
Figure 4-5: **Schematic configuration of a laser diffractometer [244]**

To date, laser diffraction or static light scattering is a common method in dairy science to measure the size of fat globules [245], lactose crystals [246], casein micelles [247] and in complex media skim milk [248], and whole milk [249;250].

The rehydration of powders was already studied by different methods: viscosity [251-253], ultrasonic spectrometry [254], NMR spectroscopy [255;256], light microscopy [253] and static light scattering [253;257;258]. In the study of MIMOUNI et al. (2009) for the first time the size distribution was not only characterized by one mean diameter [257]. Here, the volume concentration of particles was viewed over time of rehydration.

Nevertheless, most of the literature focuses on the rehydration of casein-based powders [186;251;253-259] and less information is available about the rehydration of whey protein based powders [186]. There is still the industrial need of a rapid method for the quality control of dairy powders.

The particle size distributions were measured by static laser light scattering with the Horiba LA-950 analyzer manufactured by the company Retsch Technology, Haan, Germany operating with two laser sources at 405 and 655 nm. The LA-950 features a circulation system for wet measurements. For dry measurements the dispersion unit PowderJet was used.

4.3.3.2 Wet measurements

Protein fractionation at pH 4.6

The appropriate amount of WPC to make a 2 % (w/v) protein solution was dispersed in double-distilled water. The pH value was adjusted to 4.6. Next, the solution was centrifuged in a Sigma 6K10 centrifuge (Sigma Laborzentrifugen GmbH, Osterode, Germany) at 3000 g and 10 °C for 10 min. The supernatant was taken for analysis.

Chitosan-treated samples

The appropriate amount of WPC to make a 1 % (w/v) protein solution was dispersed in double-distilled water. The pH value was adjusted to 4.5. After addition of the chitosan concentration leading to the lowest turbidity, Table 12-9, the solution was centrifuged in a Sigma 6K10 centrifuge (Sigma Laborzentrifugen GmbH, Osterode, Germany) at 3000 g and 10 °C for 10 min. The supernatant was taken for analysis.

Kinetics—Characterization of the rehydration behavior

Section I: A concentration of 10 % (w/v) WPC was produced by weighting the powder into a beaker and wetting it with a rubber spatula after addition of a small amount of double-distilled water. The residual water amount was added and mixed on the magnetic stirrer at room temperature. The rotational speed was kept constant. The measurement was started immediately. Further measurements were done after 5, 10, 15, 20, 30, and 60 min as well as after 4 and 24 h. During the first 20 min, the sample was continuously stirred on the magnetic stirrer. For further measurements, the sample was stirred 10 min before measurement to produce a homogenous mixture.

From the sample beakers an aliquot was taken and pipetted into the fluid measuring cell of the unit until a correct obscuration was reached. A "medium" fluid level was chosen.

For some samples the actual amount of sample inserted into the laser diffractometer was measured by a graduated pipette because the laser diffractometer is not able to count the number of particles. The distribution is only a relative volume distribution.

Section II: The powder was directly added to the fluid measuring cell at medium fluid level. The exact amount was weighted. The circulating pump was set to level 2 which equals 466 U·min^{-1} and the integrated stirrer was set to level 10 which equals 3350 U·min^{-1} for 1 min. Then, the stirrer was switched off. The measurement of the particle size distribution was done after 1, 5, 10, 15, 20, 30, and 60 min.

In parallel, a concentration of 10 % (w/v) WPC was produced by weighting the powder into a beaker and adding double-distilled water. The sample was stirred at 500 U·min^{-1} for 10 min with the stirrer R100CT manufactured by CAT Ingenieurbüro M. Zipperer GmbH, Staufen, Germany. The sample was then stored in the refrigerator. Before measurement after 4 and 24 h the sample was stirred 5 min at 200 U·min^{-1} to produce a homogenous mixture.

All measurements were done at least in triplicate.

Quark powders

Samples of quark powder were wetted with a rubber spatula after addition of a small amount of double-distilled water. The residual water amount was added (18 % dry mass) and mixed on the magnetic stirrer at room temperature. The rotational speed was kept constant. After 2 h of rehydration the samples were measured by laser diffraction at a refractive index of 1.52 for the protein and 1.333 for the water.

4.3.3.3 Dry measurements

The dry measurements were carried out with the PowderJet unit. The vibratory feeder of the dispersion unit was filled with powder. During measurement the whole sample amount was fed into the analysis unit to prevent possible demixing processes which might alter or slide the particle size spectrum. The number of iterations was fixed to 15. The PowderJet unit allows the application of different dispersing pressure to separate the powder particles which are only vacuum, 0.1 MPa, and 0.3 MPa.

4.3.3.4 Refractive indices

The FRAUNHOFER theory is used as a measuring principle in the case of dry measurements.

The LA-950 uses the MIE Scattering Theory according to ISO 13320 as a measuring principle for particle sizes similar or smaller than the wavelength of the incident light [260]. In this case, the light is increasingly scattered with large angles to the side and the reverse. Here, the required complex refractive index is made up of two parts—the real part, which is a physical property of a material, and an imaginary part, which accounts for the absorption of light during the interaction with the particle [244].

The refractive indices used in the case of wet measurements were 1.333 for the double-distilled water and 1.52 for the real part and 0 for the imaginary part of the protein with exception of WPC 80 3. Here, the particle size after rehydration was very large so that FRAUNHOFER theory was used as measuring principle.

The data were analyzed by the software LA-950 version 5.20, Retsch Technology, Haan, Germany. The LA-950 allows the variation of the distribution. The base volume was chosen for the analysis. In the case of the basis volume, the frequency distribution shows the proportion of the total volume of the particles of a specific size to the total volume of all particles by setting the total volume of all particles to 100 %.

4.3.3.5 Mathematical fundamentals

The following values are calculated from the distributions by the software:

1. D_{50}: Particle diameter for cumulative distribution value 50%.
2. Diameter on cumulative %: Particle diameter that correspond to the accumulated distribution values. The D_{10} represents the size of the small particles and the D_{90} represents the large particles.
3. Specific surface: Total surface area (cm^2) per unit volume (1 cm^3). In general, the value calculated using particle size distribution data is different from the surface area calculated using other measurement principles.
4. Standard deviation of the distribution depending on the arithmetic mean diameter.

4.3.4 Particle size distribution analysis—quark powder

The particle size distribution analysis was done by the laser particle sizer Analysette 22, Fritsch GmbH, Idar-Oberstein, Germany. The quark powders were fluidized in isobutanol (apolar). Interactions with the protein spectrum as well as swelling were omitted. The frequency and the cumulative frequency distribution were obtained. The software calculates the following parameters: arithmetic mean of the average value in µm, standard deviation in µm, variance in µm², D_{10}, D_{50}, and D_{90}-value in µm, and the specific surface in m²·g^{-1}.

4.3.5 Scanning electron microscopy

SEM was done at the Zentralinstitut für Elektronenmikroskopie ZELMI, TU Berlin, by the S-2700 scanning electron microscope, Hitachi, Tokyo, Japan. The dry powders were spread on small sample glasses. Additionally, WPC samples were hydrated (c = 0.1 % (w/v)) for two hours on the magnetic stirrer. 7 µl were then pipetted on the small sample glass which was hydrophylized by soap solution before and dried in an exsiccator at room temperature for 24 h. In preparation for SEM all samples were gold-sputtered (thickness: 15 nm) in a high-vacuum evaporator SCD 030, Balzers, Wiesbaden-Nordenstadt, Germany.

The micrographs were obtained at different magnification.

The size of the particles being detected via SEM was determined by digital image analysis using the software analySIS FIVE, Olympus, Hamburg, Germany.

4.4 Statistical analysis

4.4.1 Quality investigations of dairy powders

Statistic analysis was done according to BORTZ, LIENERT, and BOEHNKE (2000) and KUBINGER (1986) [261;262]. A non-parametric method was chosen for data analysis which uses the ranking-after-alignment principle. In the case of the dry measurements only small differences between the measurements exsist. Therefore, averages of three replicated measurements were analyzed by the two-step analysis of variance using the program mKVA [263]. Two independent variables (pressure with the level only vacuum, 0.1 MPa and 0.3 MPa and the protein content with the levels 13, 35, 60, 70, and 80 %) and one dependent variable (the D_{10}, D_{50}, D_{90}, specific surface or standard deviation) were analyzed.

Additionally, the influence of the protein content on the volume concentration of peak 1 and 2 after complete rehydration was analyzed with this method. The dependent variable were the volume concentration of peak 1 and peak 2, respectively. The independent variable was the protein content with the levels 13, 35, 60, 70, and 80.

For the wet measurements, differences between the three measurements per sample were to some extent very high, so statistical analysis was done by a two-factorial design with repeated measurements using data alignment. Two independent variables (the rehydration time with the levels 1 min (start), 10 min, and 24 h (rehydrated) and the protein content with the levels 13, 35, 60, 70, and 80 %) and one dependent variable (the D_{10}, D_{50}, D_{90} or specific surface) were analyzed.

The distribuiton of the wet measurements is in most cases a bimodal distribution in some cases multimodal. The analysis was done for the parameters of peak 1 and peak 2. Because only few powders had a third peak; no statistical analysis was done for it.

Contrast analysis was done according to SCHAICH and HAMERLE (1984) for comparison of all h samples and according to WILCOXON and WILCOX (1964) for comparison of a sample with the remaining h-1 samples [264;265].

Additional to the analysis made for all WPC the WPCs of section II were chosen to determine the exact influence of the rehydration time. Therefore, statistical analysis was done by a two-factorial design with repeated measurements using data alignment. One independent variable, the rehydration time with the levels start, 10 , 30, 60, 240 min, and 24 h, and one dependent variable, the D_{50} of peak 1 and 2, were analyzed. Contrast analysis was done according to SCHAICH and HAMERLE (1984) for comparison of all h samples [265].

4.4.2 Rennet-induced coagulation

Statistic analysis was done according to BORTZ, LIENERT, and BOEHNKE (2000) and KUBINGER (1986) [261;262]. A non-parametric method was chosen for data analysis which uses the ranking-after-alignment principle. Only the results of the individual cows were viewed. Thus, the results of cows A, B, and G were omitted because they were viewed over time and individual values of each cow were interdependent. The data were analyzed by the two-step analysis of variance using the program mKVA [263].

Differences in the composition (CMP, GMP content, and relation GMP/CMP) and the process viscosity (start, 12, 16, 22, 26, 60, and 100 min) due to the health status of the cow were determined by setting the health status as the independent variable.

Chapter 5: Rennet-induced coagulation of cow milk

The structure formation during renneting of normal cow bulk milk and milk from infected udder quarters will be compared in this chapter.

Until now, only the physical changes of milk from healthy cows during rennet-induced coagulation have been published [1-5]. Here, a connection between physical and biochemical parameters is presented and the biochemical parameters are related to the coagulation parameters. Additionally, the process viscosity will be presented as an objective parameter for the pre-calculation of the optimal cutting time.

Chapter 5 starts with the connection of the biochemical and rheological results. Later on, the results of the chemical analysis and the rheological measurements are discussed in detail.

5.1 Release of CMP and GMP in the course of the rennet-induced coagulation

5.1.1 Normal raw bulk cow milk

Figure 5-1 displays the release of CMP and GMP measured in absorption at 217 nm during the course of the rennet-induced coagulation for two raw milk samples. Furthermore, the rheological results are given. The point of visual clotting is indicated by an arrow.
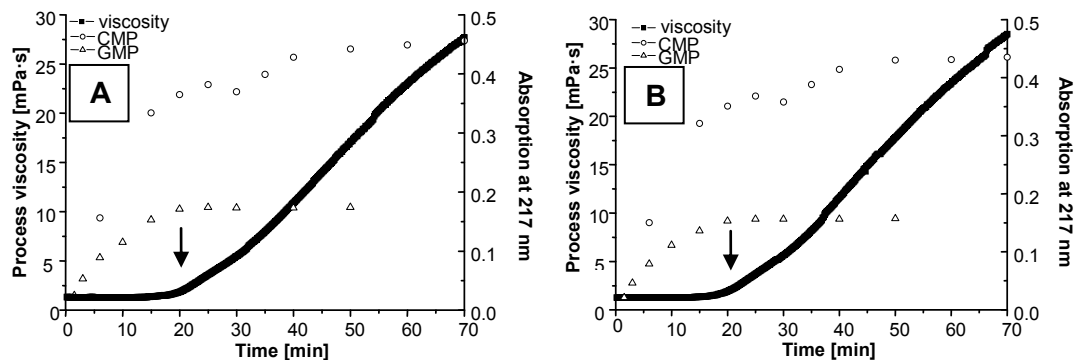
Figure 5-1:   **Release of CMP and GMP and process viscosity over time of two samples of normal milk**

After the addition of chymosin until the visual clotting point which was observed at 20 min the curve of CMP has a very steep course because both macropeptide variants are split in parallel. Subsequently, the curve reaches a constant level. At this point nearly 98 % of GMP is split from the κ-casein which is in agreement to the findings of LIESKE, FABER, and KONRAD (1996) [111]. The splitting of n.-g. CMP is still continuing. The reason for the decelerated splitting of n.-g. CMP might be the limited accessibility of the chymosin-sensitive bond. N.-g. CMP is expected to be located in the inside of the casein micelle. As a fact, the enzyme has to cover a longer distance until it can split the bond. GMP, as it is located on the outside of the micelle, can be split faster [3-5]. After its release the size of the micelle is reduced and the distance for the enzyme to the n.-g. CMP is becoming smaller. Hence, chymosin-sensitive peptide bonds inside the micelle can be split.

After the point of visual clotting, which was in case of normal milk approximately 20 min, the curves of CMP and GMP have a bend. Because the amount of CMP and GMP cannot be reduced the reason might be the restricted analytical availability. This phase is the main section of structure formation.

The development of viscosity in the chronological sequence of the process steps during the rennet-induced coagulation can be read from Table 5-1. The values are means of 15 measurements. The measuring system used in this study enables the expansion of three phases [117;232] to five sections. The first three sections are relevant for the structure formation [233] and are discussed in detail. The fourth section starts after 60 min. Section 1 and 2 are time-demanding but the resulting structure is low. Section 1 is characterized by the dominating enzymatic reaction which means the splitting of κ-casein and the loss of hydration. The characteristic structure formation takes place in section 3 with a constant structure formation velocity.

Table 5-1: **Results of the rheological measurements contrasted to the biochemical results**

Sec-tion	\multicolumn{6}{c}{Rheological results}	\multicolumn{2}{c}{Biochemical results}
	t	Δ t	η	Δ η	Structure formation velocity	State of structure	CMP	GMP
	min	min	mPa·s	mPa·s	mPa·s·min^{-1}		%	%
1	12	12	1.4 ± 0.09	→ 0	→ 0	Fluid milk/NEWTON	35 (6 min)	71 (10 min)
2	26	14	3.9 ± 0.62	2.5	0.18	Structure viscosity Intersection between 1 and 3		
2.1	16	4	1.53 ± 0.12	→ 0	→ 0	Fluid milk/NEWTON	75 (15 min)	87 (15 min)
2.2	22	6	2.61 ± 0.50	1.09	0.18	Structure viscosity/chains	82 (20 min)	98 (20 min)
2.3	26	4	3.9 ± 0.62	1.29	0.32	Viscoelastic gel	86 (25 min)	100 (25 min)
3	60	34	20.01 ± 2.7	16.11	0.47	Viscoelastic gel	96 (40 min)	100 (-)
Technological relevance: up to 30 min

5.1.2 Cow milk from infected udder quarters

Figure 5-2 represents the release of CMP and GMP measured in absorption at 217 nm during the course of the rennet-induced coagulation for two raw milk samples from infected udder quarters. Furthermore, the rheological results are given.
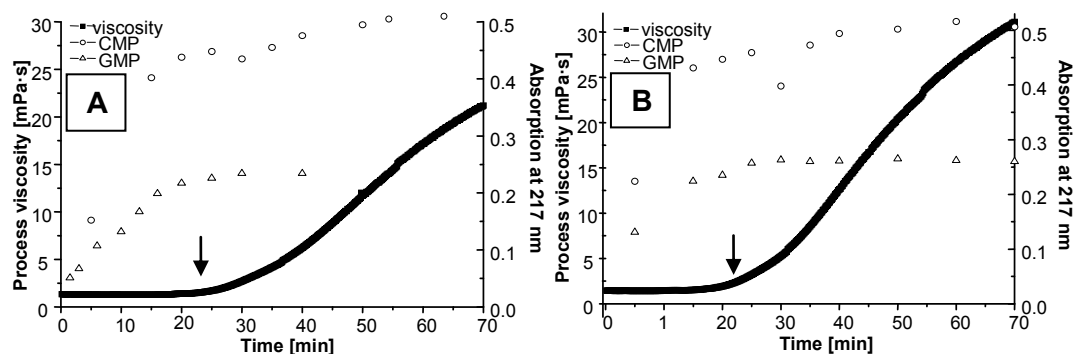
Figure 5-2: **Release of CMP and GMP and the process viscosity over time of two samples of milk from infected udder quarters**

Compared to normal raw milk, the point of visual clotting was observed 3 min later after 23 min and is indicated by an arrow.

The course of the CMP and GMP release of milk from infected udder quarters is nearly identical to the observations made for milk from healthy cows, Figure 5-1.

Table 5-2 lists the amount CMP and GMP released during the rennet-induced coagulation of normal raw bulk milk and milk from infected udder quarters.

Table 5-2: **Comparison between the release of GMP and CMP of normal raw milk and milk from infected udder quarters**

Time	Normal raw milk		Milk from infected udder quarters	
min	GMP %	CMP %	GMP %	CMP %
10	71	n. b.	56	n. b.
15	87	75	85	84
20	98	82	93	89
25	100	86	100	91
40	100	96	100	98

The amount of GMP in milk from infected udder quarters is a bit smaller compared to normal raw milk. The reason might be the later point of visual clotting. The milk from infected udder quarters coagulates a few minutes later so that splitting rates cannot be exactly compared. The amount of CMP in milk from infected udder quarters was found to be higher.

Presumably, in milk from the infected udder part a higher proportion of CMP is glycosylated or substances are present which behave very similar to GMP (e.g., peptides). Reasons for that might be a different casein spectrum, the changed availability of the rennet-sensitive bond, and changed enzyme status.

WEDHOLM (2008) reported a higher concentration and number of peptides with increasing SCC because of more protease types present at higher SCC [266].

5.2 Chemical analysis

5.2.1 Rennet activity

The rennet activity of the chymosin solution used for the coagulation of milk is determined to eliminate losses in activity during storage. The rennet activity was 1:10659 $g \cdot g^{-1}$.

5.2.2 Raw bulk cow milk

Overall 14 normal bulk milk samples were analyzed. The results of the spectrophotometric analysis which are the CMP, GMP, n.-g. CMP content in $g \cdot l^{-1}$, the relation of GMP/CMP, the protein content in %, and the $pH_{32 °C}$ are presented in Table 5-3. Furthermore, the average value and the standard deviation of 14 bulk milk samples for each chemical parameter are given in Table 5-3.

Table 5-3: **Results of the spectrophotometric analysis, protein content, and pH $_{32 °C}$ of 14 normal bulk milk samples**

No	CMP $g \cdot l^{-1}$	GMP $g \cdot l^{-1}$	n.-g. CMP $g \cdot l^{-1}$	GMP / CMP	Protein %	pH $_{32 °C}$
1	1.288	0.478	0.810	0.37	3.24	6.51
2	1.305	0.482	0.823	0.37	3.29	6.51
3	1.375	0.551	0.824	0.40	3.31	6.45
4	1.214	0.425	0.789	0.35	3.17	6.51
5	1.252	0.491	0.761	0.39	3.30	6.55
6	1.283	0.468	0.815	0.36	3.39	6.52
7	1.299	0.545	0.754	0.42	3.41	6.51
8	1.321	0.520	0.801	0.39	3.43	6.45
9	1.120	0.403	0.717	0.36	3.44	6.47
10	1.240	0.445	0.759	036	3.34	6.54
11	1.273	0.456	0.817	0.36	3.40	6.51
12	1.102	0.402	0.700	0.37	3.35	6.53
13	1.210	0.448	0.762	0.37	3.13	6.51
14	1.126	0.416	0.710	0.37	3.28	6.54
$\bar{x}$	1.243	0.466	0.774	0.375	3.32	6.51
$\pm s$	0.078	0.047	0.042	0.020	0.09	0.03

On average, raw bulk milk from healthy cows contained 1.243 $g \cdot l^{-1}$ CMP from which 37.5 % was glycosylated and 62.5 % was not. These findings correspond to former CMP analysis of bulk milk samples from the north of Brandenburg [111]. FERRON-BAUMY et al. (1992) used a chromatographic method according to LÈONIL and MOLLÈ (1991) and found 42 % GMP of CMP [115;267].

The concentration of macropeptide in rennet whey corresponds to the casein content of milk [3-5]. Accordingly, spectrophotometric analysis should be correlated to the protein content. Milk contains 2-4 g κ-casein l^{-1} on average [16]. The CMP is identical to 40 % of the molecular mass of κ-casein. In terms of theoretical calculation, 1 g casein contains 46 mg CMP on average [3-5]. This means a theoretical CMP content of 1.205 $g \cdot l^{-1}$ if the casein content is 2.62 %. This theoretical value agrees well with the average value of 1.243 $g \cdot l^{-1}$ of 14 bulk raw milk samples.

The pH$_{32\,°C}$ (temperature of rennet coagulation) of the bulk milk samples lies in the range 6.45–6.55 with an arithmetic mean of 6.51. OKIGBO et al. (1985) found a mean pH of milk from normal quarters close to 6.6; abnormal milk samples with an SCC > 500,000 ml^{-1} were significantly higher (6.74) [268].

Table 5-4 presents the non-casein nitrogen (NCN) in %, the casein content in %, the casein number, and the calcium content in mg Ca^{2+}·100 ml^{-1} of six normal bulk milk samples.

Table 5-4: NCN, casein content, casein number, and calcium content of six normal bulk milk samples

No.	NCN %	Casein %	Caseinnumber Casein·100/protein	Calcium mg Ca^{2+}·100 ml^{-1}
9	0.98	2.46	71.51	125.6
10	0.63	2.71	81.14	125.6
11	0.69	2.78	81.76	125.62
12	0.67	2.68	80.0	124.8
13	0.63	2.50	79.87	123.7
14	0.67	2.61	79.57	123.6
$\bar{x}$	0.71	2.62	79.14	124.8
$\pm s$	0.13	0.12	3.75	0.9

The results of the protein content (3.32 ± 0.09 %), the casein content (2.62 ± 0.12 %), and the NCN (0.71 ± 0.13 %) are in the range reported by NG-KWAI-HANG et al. (1984) who found 3.314 ± 0.002 % protein, 2.694 ± 0.001% casein, and 0.699 ± 0.001 % serum protein [58].

The casein number represents the relation of casein content to total protein in milk (casein as a percentage of crude protein). On average, the bulk milk samples contain 79.14 ± 3.75 % casein and about 20 % whey protein from the total protein. This value is in the normal range. According to WALSTRA and JENNESS (1984) the share of casein in total protein is 80 % [15]. NG-KWAI-HANG et al. (1984) reported a casein number of 79.35 ± 0.01 [58]. WALSTRA and JENNESS (1984) stated a value of 3.25 % for the protein content of normal milk [15].

The calcium content of the bulk milk samples is 124.8 mg Ca^{2+}·100ml^{-1} on average. This is an optimal value for raw milk [269].

Table 5-5 displays the fat content in % and the SCC in 1000 ml^{-1} of six normal bulk milk samples. The analysis was done by the Landeskontrollverband (LKV) Waldsieversdorf.

Table 5-5: Fat content and SCC of normal bulk cow milk

No.	Fat %	SCC 1000 ml^{-1}
9	4.13	212
10	4.24	335
11	3.98	324
12	3.90	150
13	3.90	150
14	4.18	160
$\bar{x}$	4.05	
$\pm s$	0.147	

The somatic cell counts of bulk milk samples 9, 12, 13, and 14 are below 300,000 ml^{-1}. The somatic cell count of bulk milk samples 10 and 11 with > 300,000 ml^{-1} is increased, Table 5-5. The Regulation No. 853/2004 of the European Parliament and the Council of 29.04.2004 and the *Milchverordnung* define a maximum SCC of 400,000 ml^{-1} for bulk milk [270-272]. According to the guidelines on normal and abnormal raw milk SMITH, HILLERTON, and HARMON (2001) and HILLERTON (1999) udder quarters are assessed to be infected with subclinical mastitis if a limit of 200,000 ml^{-1} is exceeded for one udder quarter [273;274].

5.2.3 Cow milk from infected udder quarters

Overall 29 samples of milk from selected cows experiencing intramammary infection were analyzed of which the first 13 samples were taken from single cows. The samples remaining were taken from three different cows during udder infection and medication with antibiotics. The results of the spectrophotometric analysis which are the CMP, GMP, and n.-g. CMP content in g·l^{-1}, the relation of GMP/CMP, the protein content in % and the pH $_{32\,°C}$ are presented in Table 5-6.

Table 5-6: **Results of the spectrophotometric analysis and pH $_{32\,°C}$ of milk from infected udder quarters**

No		CMP g·l^{-1}	GMP g·l^{-1}	n.-g. CMP g·l^{-1}	GMP / CMP	pH $_{32\,°C}$
1		1.615	0.785	0.830	0.48	6.54
2		1.568	0.714	0.854	0.45	5.63
3		1.439	0.595	0.844	0.41	6.52
4		1.533	0.723	0.810	0.47	6.17
5		1.428	0.635	0.793	0.44	6.55
6		1.549	0.786	0.763	0.50	6.52*
7		1.426	0.676	0.750	0.47	6.51*
8		1.436	0.682	0.754	0.47	6.56*
9		1.087	0.753	0.335	0.69	6.51*
10		1.165	0.771	0.396	0.60	6.51*
11		1.519	0.743	0.776	0.49	6.51*
12		1.102	0.621	0.481	0.56	6.51*
13		0.828	0.504	0.324	0.60	6.48*
$\bar{x}$		1.361	0.691	0.670	0.510	6.43
$\pm\,s$		0.238	0.084	0.204	0.079	0.26
A1	Cow A	-	-	-	-	6.86
A2		0.889	0.432	0.457	0.49	6.42
A3		-	-	-	-	6.58
B1	Cow B	-	-	-	-	6.69
B2		1.192	0.601	0.591	0.50	6.21
B3		1.06	0.813	0.247	0.76	6.49*
B4		1.219	0.822	0.397	0.67	6.51*
B5		1.198	0.63	0.573	0.52	6.45*
B6		1.311	0.693	0.618	0.53	6.47*
G1	Cow G	0.811	0.702	0.109	0.86	6.51*
G2		0.913	0.516	0.397	0.56	6.51*
G3		0.986	0.557	0.411	0.57	6.48*
G4		-	-	-	-	6.50*
G5		0.918	0.450	0.468	0.49	6.44*
G6		1.042	0.645	0.397	0.62	6.51*
G7		1.186	0.57	0.616	0.48	6.44*

* pH value corrected

On average, raw milk from infected udder quarters contains 1.361 ± 0.238 g·l^{-1} CMP from which 51.0 % was glycosylated and 49.0 % was not. The high standard deviation indicates the broad fluctuation range. The average concentration of GMP with 0.691 ± 0.084 g·l^{-1} is increased compared to milk from healthy cows and the average concentration of n.-g. CMP with 0.670 ± 0.204 g·l^{-1} is decreased. These findings are in accordance with the latest study of LIESKE and VALBUENA (2008) [275].

Presumably, in milk from the infected udder part substances are present which behave very similar to GMP (e.g., peptides ≥ 6 kDa) under the conditions of the spectrophotometric method used. Reasons for that might be a different casein spectrum, the changed availability of the rennet-sensitive bond, and changed enzyme status.

WEDHOLM (2008) reported a higher concentration and number of peptides with increasing SCC because of more protease types present at higher SCC [266]. URECH, PUHAN, and SCHALLIBAUM (1999) found a clear relationship between health status and the occurrence of the protease for milk from cows suffering from subclinical mastitis [81]. LIESKE and VALBUENA (2008) reported that peptides resulting from enzymatic splitting of milk, cellular, and blood constituents would behave similar to GMP under the experimental conditions [275;276].

The hypothesis stated by LIESKE and VALBUENA (2008), that antibiotics are UV-active and lead to a higher absorption because they might be bound to GMP, can be disproved because samples B3, B6, 9, G1, G7, and 13 were taken before medication and the GMP content had already increased [275].

The pH value at 32 °C (temperature of rennet coagulation) is 6.43 on average. The pH value was adjusted to enhance the comparability of the rheological results. KLEI et al. (1998) and MUNRO, GRIEVE, and KITCHEN (1984) reported a higher pH of the skim milk with high SCC than that of the skim milk with low SCC [61;97]. Higher levels of citrate and bicarbonate found due to udder inflammation may be responsible for elevated pH levels [76].

Table 5-7 presents the protein content in %, the non-casein nitrogen (NCN) in %, the casein content in %, the casein number and the calcium content in mg $Ca^{2+} \cdot 100$ ml^{-1} of 21 milk samples from infected udder quarters.

Table 5-7: **Protein, NCN, casein, calcium content and casein number of 21 milk samples from infected udder quarters**

No.	Protein %	NCN %	Casein %	Caseinnumber Casein·100/ protein	Calcium mg $Ca^{2+} \cdot 100$ ml^{-1}
9	3.57	1.08	2.49	69.75	95.44
10	4.08	0.76	3.32	81.37	155.65
11	3.81	0.69	3.30	86.61	126.49
12	2.98	0.74	2.24	75.16	88.88
13	3.02	1.22	1.80	59.60	133.46
A1	2.88	1.58	1.30	45.13	124.95
A2	2.48	1.01	1.47	59.27	123.62
A3	2.66	0.49	2.17	81.59	108.86
B1	2.91	0.97	1.94	66.66	102.09
B2	3.27	0.70	2.57	78.59	98.10
B3	3.26	0.95	2.30	70.55	111.53
B4	3.30	0.65	2.65	80.30	111.53
B5	3.27	0.65	2.62	80.12	106.00
B6	3.60	0.75	2.85	79.17	104.83
G1	3.21	0.81	2.40	74.53	119.54
G2	3.15	0.90	2.25	71.43	119.90
G3	3.09	0.92	2.17	70.23	118.70
G4	3.16	0.97	2.19	69.30	119.00
G5	3.18	0.60	2.58	81.13	118.60
G6	3.17	0.97	2.20	69.40	116.10
G7	3.29	0.71	2.58	78.42	117.70

A calcium content of 136 mg $Ca^{2+} \cdot 100$ ml^{-1} was reported to be an average value for normal milk [15;86]. An infectious udder inflammation leads to a decreased calcium content [85]. This statement can be proved by samples B2, 9, 12, and 13. In contrast, the calcium content of sample 10 is with 155 mg·100 ml^{-1} increased. In addition, sample 10 has the highest protein and casein content. OGOLA, SHITANDI, and NANUA (2007) reported a significant effect of SCC status on the mineral composition. Milk with a SCC smaller 250,000 ml^{-1} had a calcium concentration of 119.5 mg·100 g^{-1}; milk with a SCC > 750,000 ml^{-1} contained 97.8 mg·100 g^{-1} [277]. These findings did not correspond to other studies [75;278] but to the present one as long as sample 10 has a very low SCC of 79,000 ml^{-1}, Table 5-8. As in most milk Ca is associated with casein; reduced casein concentrations reported in the study could explain the lowered calcium levels in infected quarters. It can be expected that this effect was the reason for the increased Ca content of sample 10.

The protein content for milk from infected udder quarters is recorded to be between 2.48 % and 4.08 %. An average protein content of 3.32 ± 0.09 % (Table 5-3) of milk from healthy cows was determined in the present study. Compared to milk from healthy cows larger variations exist for milk from infected udder quarters, Table 5-7. DANG et al. (2008) examined the raw milk composition in the course of mastitis and found protein contents on day 1 of 3.44 % and 3.49 % on day 9 [279]. KLEI et al. (1998) found higher protein, casein, and pH for milk with high SCC than for milk with low SCC [97]. No clear trend was observed for the present results, Table 5-7.

The casein number of healthy milk was found to be 79.14 % on average, Table 5-4. According to WENDT (1998), cows suffering from an infectious udder inflammation synthesize less casein and more whey proteins [85]. Samples A1, A2, B1, 9, G4, G6, and 13 have a casein number smaller than 70 %. Milk samples A3, B4, B5, 10, 11, and G5 have a casein number larger than 80 %.

KLEI et al. (1998) reported that the percentages of total nitrogen and casein were higher for the high SCC skim milk, but the casein as a percentage of crude protein was lower for the milk with high SCC than the milk with low SCC [97]. This was also reported previously [61;96;280]. This could not be confirmed with the present results. A problem which has to be considered is the relatively long time between the SCC measurement and the further chemical/rheological analysis. For the milk of the single cows only an overall value of the SCC was determined.

Table 12-1 lists the allocation of the sample number and the cow type, the medication with antibiotics, and the length of medication.

Table 5-8 displays the fat content in % and the SCC in 1000 ml^{-1} of 21 milk samples from infected udder quarters. The analyses were done by the LKV Waldsieversdorf (LKV). The SCC was analyzed at the beginning of the udder infection and after medication.

Table 5-8: **Fat content and SCC of 21 milk samples from infected udder quarters**
Results were obtained from the LKV Waldsieversdorf

No.	Fat %	SCC 1000 ml^{-1}
9	4.08	247
10	5.28	79
11	4.85	516
12	3.64	622
13	3.68	132
A1	3.83	105
A2	3.83	105
A3	3.35	105
B1	3.82	967
B2	3.82	967
B3	3.61	762
B4	3.61	762
B5	3.61	762
B6	3.61	762
G1	4.02	1004
G2	4.02	1004
G3	4.02	1004
G4	4.02	1004
G5	4.02	1004
G6	3.84	59
G7	3.84	59

The SCC of samples B1, B6, 11, 12, and G1-G5 with 500,000-1,004,000 ml^{-1} show an increase. An increased amount of somatic cells indicates an infectious udder inflammation. The other milk samples have a SCC between 59,000-132,000 ml^{-1} and are therefore in the range of normal milk [273;274]. Before analysis the milk samples were skimmed so that the fat content should have had no influence on the rheological results.

5.3 Rheological measurements of raw bulk cow milk

For scientific reasons the coagulation was observed far beyond the practical cutting time of the curd which is usually 25 min in cheese production [49;55;153].

A sigmoidal curve which is typical for the rennet-induced coagulation was obtained representing a continuous transition from fluid milk to structure viscosity (flocculation) and finally leading to the formation of a visco-elastic gel.

5.3.1 Characterization of the overall process [1-5]

Figure 5-3 displays the mean value of the process viscosity (N = 15) during the rennet-induced coagulation in relation to time up to 60 min for raw bulk milk.

The equations are regression results of the individual sections. The error bars represent the standard deviation.

The plotted regression equations in the figure are:

Section 2.1: $\eta(t) = 0.031t + 1.006$, $R^2 = 0.929$

Section 2.2: $\eta(t) = 0.338e^{0.092t}$, $R^2 = 0.984$

Section 2.3: $\eta(t) = 0.323t - 4.494$, $R^2 = 0.999$

Section 3: $\eta(t) = 0.500t - 9.855$, $R^2 = 0.998$
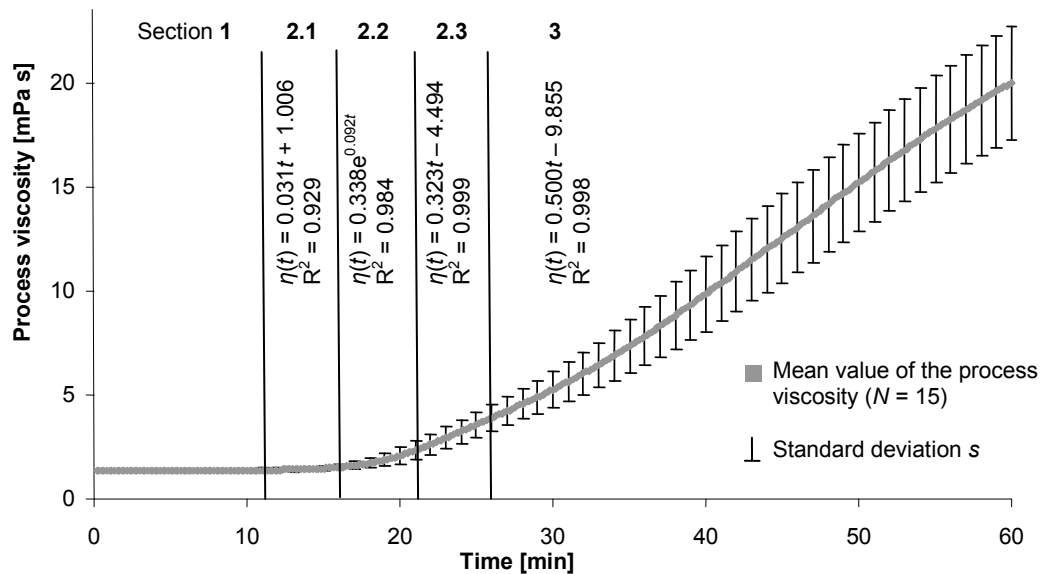
Figure 5-3: **Process viscosity of raw bulk milk during rennet-induced coagulation**

The entire process is divided into three sections relevant for structure formation, whereas section 2 is divided into three sub-sections.

The sub-sections are important as long as the regression results of the whole section 2 (12 to 26 min) leads only to a R² of 0.9521 with a regression line of $\eta(t) = 0.4477e^{0.0802 \cdot t}$. This can be improved by dividing section 2 into three subsections.

Because differences between the structural developments of raw bulk milk were found to be very small, the process viscosity can be drawn as a mean of fifteen samples.

With the use of this method the end viscosities can be calculated as soon as the process reaches the linear function of section 3. This new method enables a prediction of the cheese-making process and is more reliable compared to visual observations.

5.3.2 Allocation into sections

In the following, a structural discussion is done for the average course of the process viscosity and the whole process is divided into sections until section 3, as shown in Figure 5-3.

Section 1 [1 min ≤ t ≤ 12 min] with dominating enzymatic reactions: Figure 5-4 presents section 1 of the overall process ($N = 15$) which starts immediately after addition of rennet with an adaptation. This section is dominated by the enzymatic splitting of κ-casein resulting in the loss of hydration of the casein micelles.
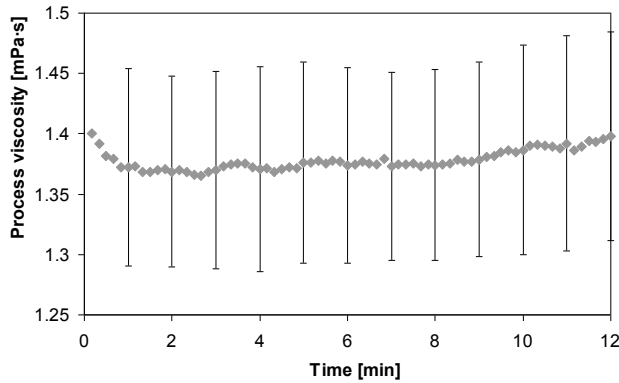
Figure 5-4:   **Section 1 of raw bulk milk**

Section 2 [12 min ≤ t ≤ 26 min], transfer from enzymatic reactions to flocculation: Figure 5-5 displays the whole section 2 and the three subsections. This phase is important for the structure development of the curd. The whole section is displayed in Figure 5-5 A.
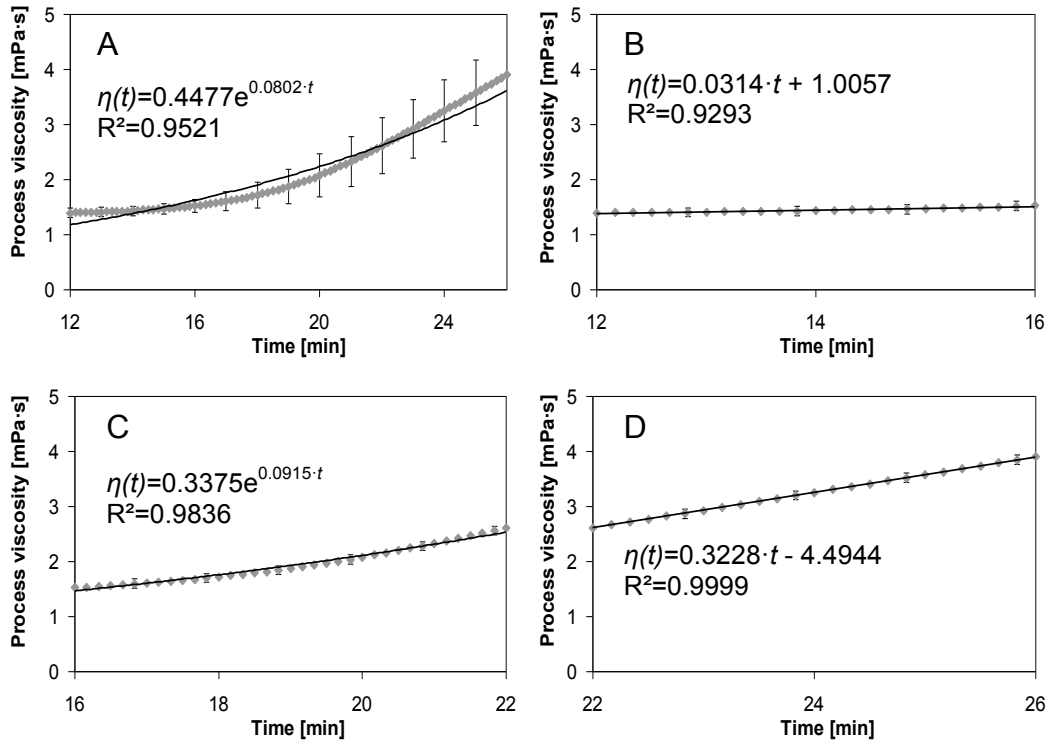
Figure 5-5:   **Section 2 of raw bulk milk**
A: whole section, B: section 2.1, C: section 2.2, D: section 2.3

Section 2 is divided into three subsections:

Section 2.1 takes from 12 to 16 min, Figure 5-5 B. It starts with the viscosity minimum and ends at the point of critical hydrolysis coinciding with initial molecular interactions and aggregation between the casein micelles. Until the end of this section the micelles are equally dispersed without structure and have less contact [2]. The change in viscosity in section 2.1 is very small.

Section 2.2 is the main part of the structure formation and takes from 16 to 22 min, Figure 5-5 C. In section 2.2 the increase in viscosity is nonlinear. In this phase the change in structure takes place and chains are formed. Section 2.2 describes the continuous change from the enzymatic phase to the flocculation step. The rheological investigations correspond to the biochemical investigations. If a share of 87 % (15 min) of GMP is split, flocculation starts resulting in steady changes in viscosity. The formation of chains is dominating up to a viscosity of 2.61 ± 0.50 mPa·s after 22 min is reached, Table 5-1.

In section 2.3 (22 to 26 min) the viscosity can be described by a linear function, Figure 5-5 D. It can be concluded that the micelle chains reach a critical chain length and chain concentration.

Sections 2.1 and 2.3 are described by a linear function and section 2.2 is described by an exponential function.

Section 3 [26 min ≤ t ≤ 60 min], gel formation: The three-dimensional casein network is hardened due to formation of calcium bridges. Section 3 is characterized by the highest level of structure formation velocity; Table 5-1. Section 3 can be described by a linear function, Figure 5-6. Now, a pre-calculation of the optimal end-viscosity of the curd becomes possible. Section 3 is important for cheese production because the curd is cut with respect to time or firmness of the curd.

Subsequent to section 3 section 4 starts.

The graph shows a plot with x-axis labeled "Time [min]" ranging from 26 to 58, and y-axis labeled "Process viscosity [mPa·s]" ranging from 0 to 25. The fitted equation shown is $\eta(t)=0.4995 \cdot t - 9.8549$ with $R^2=0.9977$.

Figure 5-6: **Section 3 of raw bulk milk**

Table 12-2 in the Appendix lists the regression results of the sections for each milk sample. The time up to 30 min is very informative for cheese processing because until that point the curd has been cut and cheese processing is already proceeding.

It has to be admitted here that the biochemical processes proceed prior to the rheological processes. The biochemical processes are time-demanding. The transition from physicochemical processes to flocculation represents a transition from a time-demanding process to a process which is more time-independent. The gel formation describes only a physical state of order and is therefore independent from the time factor.

Table 5-9 lists the mean value of the process viscosity of the 15 raw bulk milk samples at different times of coagulation ± *s* and the structure.

Table 5-9: **Process viscosity of raw bulk milk samples after different coagulation times**

Time min	Process viscosity mPa·s	*s* (*N* = 15)	Structure
0	1.4	0.10	NEWTON
12	1.4	0.09	
16	1.5	0.12	Structure viscosity
22	2.6	0.50	
26	3.9	0.62	Complex viscosity
60	20.0	2.71	gel

The scattering of the process viscosity is relatively small especially at coagulation times below 20 min. Coagulation times up to 30 min are of considerable significance for the cutting of the curd on industrial scale.

5.4 Rheological measurements of cow milk from infected udder quarters

5.4.1 Characterization of the overall process

The coagulation behavior of twenty-seven samples of milk from infected udder quarters was examined. Substantial differences were found for the coagulation behavior of milk from infected udder quarters. The course of the curves of the process viscosity over time is very divergent so that it is very difficult to make an over-all statement about the coagulation behavior validity of all milk samples from infected udder quarters. It is therefore more applicable to differentiate between results of the milk samples and to characterize them according to selected parameters. The process viscosity after 60 min is the parameter employed to divide the milk samples into four classes.

Class I comprises milk samples with a process viscosity after 60 min of > 40 mPa·s (43.4 ± 3.87 mPa·s on average after 60 min) which is increased compared to normal milk with 20.01 ± 2.714 mPa·s on average after 60 min, Table 12-3.

Class II is composed of milk samples with a process viscosity after 60 min ≥ 20 mPa·s and < 40 mPa·s (27.91 ± 4.08 mPa·s on average after 60 min), Table 12-4.

Class III contains the milk samples with a process viscosity after 60 min between 10 and 20 mPa·s (15.7 ± 3.53 mPa·s on average after 60 min) and characterizes the milk samples with a slightly lower process viscosity after 60 min (2.10 ± 0.85 mPa·s on average after 60 min) compared to normal milk, Table 12-5.

The fourth class comprises milk samples which show no or poor coagulation with a process viscosity after 60 min which does not differ appreciably from the value of the starting viscosity, Table 12-6.

Class I contains $N = 4$ (14.8 % of the whole sample amount), class II $N = 8$ (29.6 % of the whole sample amount), class III $N = 10$ (37 % of the whole sample amount), and class IV $N = 5$ milk samples (18.5 % of the whole sample amount).

The structural development of raw milk from infected udder quarters during rennet-induced coagulation up to 60 min is shown in Figure 5-7 for the four classes. It is an attempt to transfer data obtained in the sections found for raw bulk milk to milk from infected udder quarters. The standard deviation is given for every class.
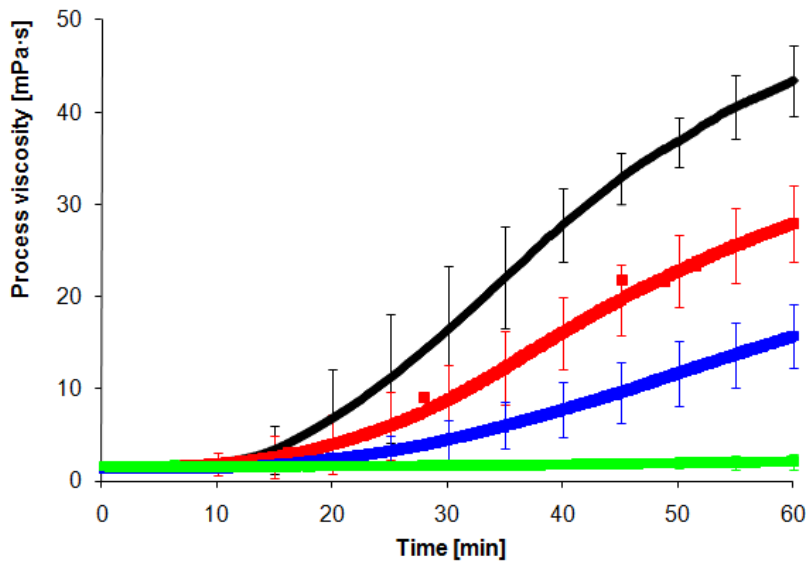
Figure 5-7: **Process viscosity of milk from infected udder quarters**
Values are means, ■ class I ($N = 4$), ■ class II ($N = 8$), ■ class III ($N = 10$), ■ class IV ($N = 5$)

Table 5-10 and Table 5-11 display the average chemical composition of the class I to IV milks. For comparison the average composition of milk from healthy cows taken from Table 5-3 and Table 5-4 is displayed. Additionally, the line named 'intersection' indicates whether the results of the milk from healthy cows and milk from individual classes overlap or not. If no intersection occurs, the milk composition is very much altered due to udder inflammation.

Table 5-10: **Average chemical composition of class I to IV milk and milk from healthy cows for comparison**
Protein, NCN, CN, Ca content, and pH value at 32 °C, values are means

	Protein	NCN	CN	CN-No.	Ca	pH $_{32\,°C}$
	%	%	%	-	mg·100 ml^{-1}	
Class I	3.61 ± 0.41	0.70 ± 0.05	2.95 ± 0.41	81.67 ± 3.48	121.56 ± 25.68	6.42 ± 0.14
Class II	3.28 ± 0.21	0.83 ± 0.21	2.46 ± 0.19	74.88 ± 5.76	112.61 ± 11.46	6.50 ± 0.04
Class III	3,08 ± 0.25	0.91 ± 0.17	2.17 ± 0.34	69.95 ± 6.89	115.95 ± 12.12	6.50 ± 0.03
Class IV	3.01 ± 0.41	0.95 ± 0.47	2.07 ± 0.64	68.14 ± 16.68	110.18 ± 10.23	6.63 ± 0.15
Healthy cows	3.32 ± 0.09	0.71 ± 0.13	2.62 ± 0.12	79.14 ± 3.75	124.8 ± 0.959	6.51 ± 0.03
Intersection	yes	yes	yes	yes	yes	yes

Table 5-11: **Average chemical composition of class I to IV milk and milk from healthy cows for comparison**

CMP, GMP, n.-g. CMP, the relation GMP/CMP, and $\eta_{60\,min}$, values are means

	CMP $g \cdot l^{-1}$	GMP $g \cdot l^{-1}$	n.-g. CMP $g \cdot l^{-1}$	GMP / CMP	$\eta_{60\,min}$ mPa·s
Class I	1.269 ± 0.168	0.686 ± 0.083	0.584 ± 0.155	0.528 ± 0.050	43.4 ± 3.87
Class II	1.252 ± 0.239	0.628 ± 0.110	0.623 ± 0.105	0.506 ± 0.088	27.91 ± 4.08
Class III	1.033 ± 0.203	0.637 ± 0.135	0.396 ± 0.176	0.621 ± 0.126	15.7 ± 3.53
Class IV	1.463 ± 0.215	0.739 ± 0.065	0.724 ± 0.150	0.505 ± 0.035	2.10 ± 0.85
Healthy cows	1.243 ± 0.078	0.466 ± 0.047	0.774 ± 0.042	0.375 ± 0.02	20.01 ± 2.71
Intersection	yes	no	yes	no	yes

It was found by statistical analysis that the contents of CMP, GMP, and n.g.-CMP have no significant influence (α = 0.01) on the process viscosities after different times of coagulation even if only the milk from healthy cows was taken into consideration.

The most important differences occur for the protein, NCN, CN content, and the casein number, Table 5-10. The class I milks have a very high protein and casein content on average which is even higher than the contents of milk from healthy cows. This might be the reason for the high process viscosity after 60 min, Table 5-11. Studies comparing individual milk samples have shown that milk coagulation property (MCP) is affected by physical and chemical parameters such as protein and casein contents, and calcium and phosphorus concentrations [99].

Additionally, the pH value is slightly lower for class I milk. In other studies a desirable MCP correlated with a low pH value [107;108;281].

At this time the higher protein/casein content of class I and II milks seems to be very desirable because for milk from healthy cows higher concentration of casein [282;283] and individual caseins [65;284;285] resulted in higher cheese yields.

Additionally, a significant correlation between casein number and curd firmness was found [286], which in turn positively corresponded with higher cheese yield [287]. But what is noticeable is the increased GMP content and the altered relation of GMP/CMP compared to milk from healthy cows, which indicates casein hydrolysis due to a changed enzyme status, thus verifying the udder inflammation.

Class IV milks reveal very high contents of NCN indicating that the content of bovine serum albumin and immunoglobulins is increased due to leakage from the blood [82]. On the other hand, the casein content is reduced, leading to lower process viscosities after 60 min. In literature, low casein to true protein ratios as a result of increasing somatic cell count and milk proteolysis have been related to decreasing cheese yield [96].

Differences in the composition due to the health status of the cow were determined by statistical analysis. It was found that the GMP content and the relation GMP/CMP were significantly higher (α = 0.01) for ill cows.

If the CMP content is viewed in comparison to milk from healthy cows, it is increased in the case of class I and II milks, Table 5-11. Because of the high standard deviation this increase is not significant. Within the group of the milks from ill cows it is reduced due to the decreasing casein content from class I to class III milks. In addition, the relation GMP/CMP deviates from that of milk from healthy cows indicating that not only the casein content influences the CMP content. The n.-g. CMP is decreased compared to milk from healthy cows for class I to III milks. Within the group of the ill cows the content decreases from class I to III milks which was also reported by LIESKE and VALBUENA (2008) [275]. They stated that the enzymatic availability of the Phe_{105}-Met_{106} bond of the sugar-free variant of CMP was affected by structural changes in casein micelles for poor coagulating ($\eta_{60\,min}$ = 11 mPa·s) milks.

For class IV milks the CMP (GMP and n.-g. CMP) content increases despite of the very low casein content in these milks. Here, the enzyme status might have undergone an immense change. There is an increased activation of plasmin from plasminogen in mastitic milk [87-89]. It has been shown that there is elevated plasmin activity in mastitic milk, which causes increased casein hydrolysis [76;90;91]. The increased casein hydrolysis results in small peptides which behave very similar to GMP and n.-g. CMP under the experimental conditions and cause the higher contents which are consequently not only related to CMP but also to the hydrolysis products.

The results of the spectrophotometric analysis indicate that the caseins in milk of class IV have undergone further changes compared to the caseins present in the other milk samples of infected udder quarters. Those immense changes are reflected in the poor coagulation properties ($\eta_{60\,min}$ = 2.10 ± 0.85 mPa·s). For this purpose, the HIC analysis was done to gain further information on the changed casein profile.

5.4.2 Allocation into sections

Figure 5-8 displays section 1 for milk from infected udder quarters. For milk from healthy udders this section starts immediately after addition of rennet. As can be seen from Figure 5-8 the relationships are different for class I and II milk. Here, the increase in viscosity starts earlier after about 8 min.
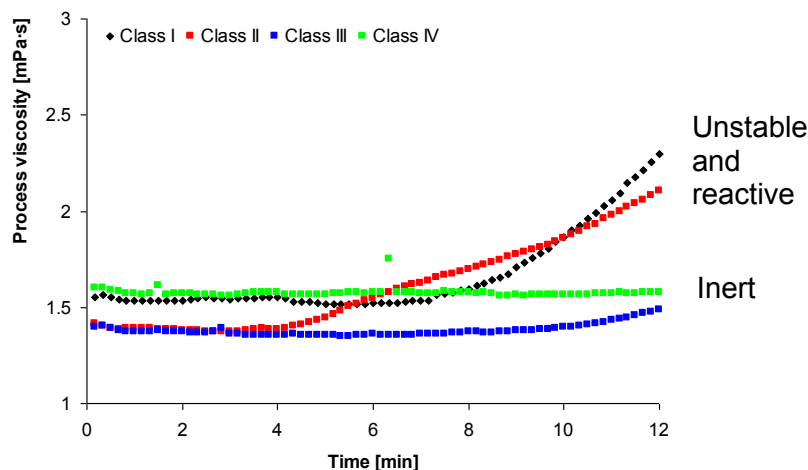
Figure 5-8: **Section 1 of milk from infected udder quarters**

Section 2 [12 min ≤ t ≤ 26 min], which characterizes the transfer from enzymatic reactions to flocculation, is displayed in Figure 5-9. Part A displays the whole section.
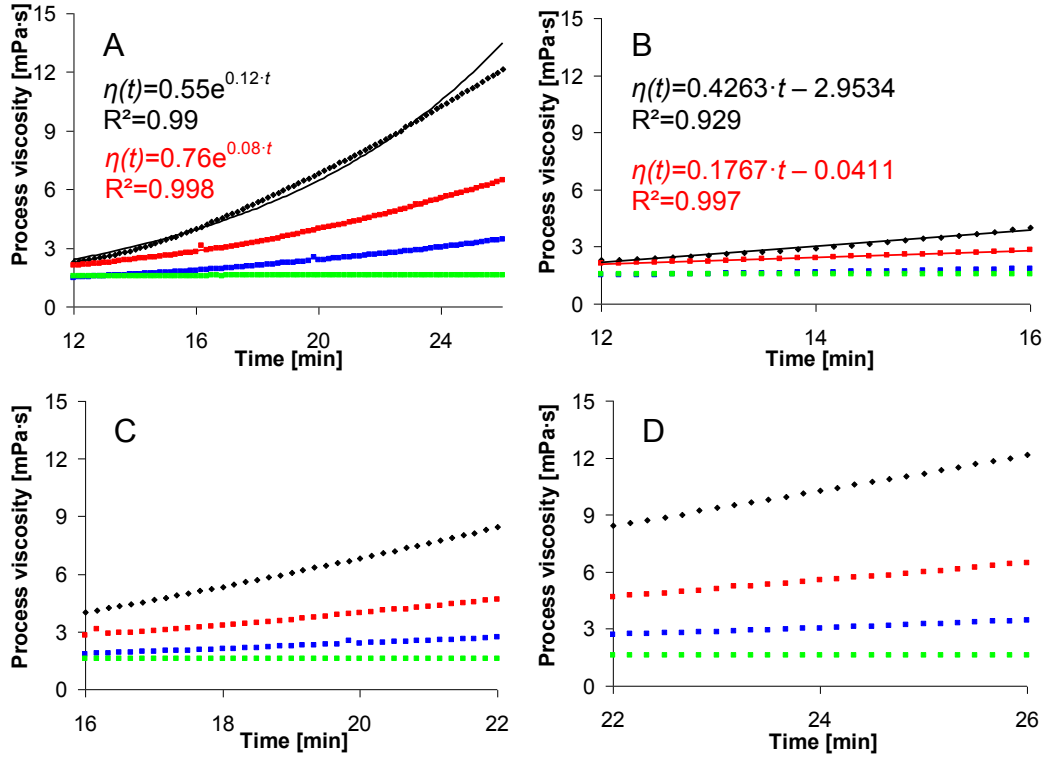
Figure 5-9: **Section 2 of milk from infected udder quarters**
A: whole section, B: section 2.1, C: section 2.2, D: section 2.3 ,
Class I ■, II ■, III ■, IV ■

Section 2.1 is shown in Figure 5-9 B. It starts with the viscosity minimum and ends at the point of critical hydrolysis coinciding with initial molecular interactions and aggregation between the casein micelles. Until the end of this section the micelles are equally dispersed without structure and ha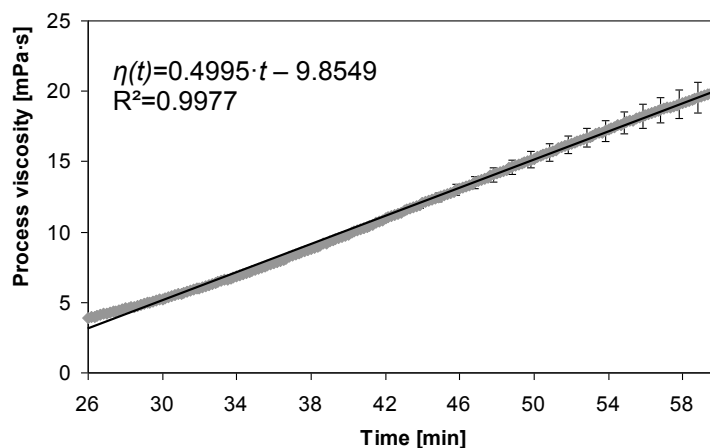ve less contact. The change in viscosity in section 2.1 is minimal in the case of healthy cows. In the case of class I and II milk the increase in viscosity is relatively high which might be related to an altered/a deficit micelle structure and a better availability of the rennet-sensitive bond.

Section 2.2 represents the main part of the structure formation and takes from 16 to 22 min for healthy milk, and the increase in viscosity is nonlinear. This is not the case for milk from infected udder quarters, Figure 5-9 C. Here, the increase is linear. For normal milk in this section a change in structure takes place and casein micelle chains are formed. Section 2.2 describes the continuous change from the enzymatic phase to the flocculation step with a more or less linear function.

In section 2.3 (22 to 26 min) the viscosity can be described by a linear function for milk from healthy cows as well as for milk from infected udder quarters, Figure 5-9 D. (Class I: $\eta(t) = 0.933 \cdot t - 12.103$ $R^2 = 0.9993$, Class II: $\eta(t) = 0.442 \cdot t - 5.0531$ $R^2 = 0.9989$, Class III: $\eta(t) = 0.1889 \cdot t - 1.4834$ $R^2 = 0.9968$, Class IV: $\eta(t) = 0.0036 \cdot t - 1.501$ $R^2 = 0.6945$.

It can be concluded that the micelle chains reach a critical chain length and chain concentration and the dynamic of the chain formation is disrupted.

Sections 2.1, 2.2, and 2.3 are described by a linear function for milk from infected udder quarters.

Section 3 [26 min ≤ t ≤ 60 min], gel formation: Section 3 is characterized by the highest level of structure formation velocity in the case of milk from healthy cows, Figure 5-6. This section is important for cheese production because the curd is cut with respect to time or firmness of the curd. Significant differences between milk from infected udder quarters and healthy cows occur in section 3 in the phase of the gel formation; Figure 5-10.
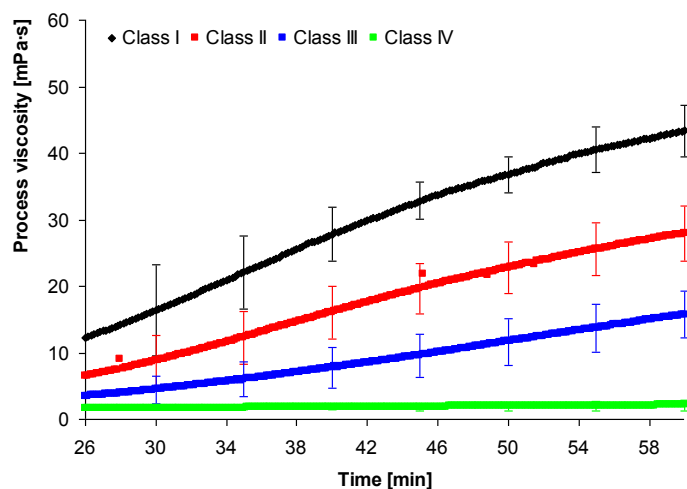
Figure 5-10: **Section 3 of milk from infected udder quarters**

The viscosity can no longer be described by a linear function in the case of class I and II milk; a plateau has been reached. In the case of class III milk the process viscosity can be described by a linear function but the level of viscosity after 60 min is only 15.70 ± 3.53 mPa·s compared to 20.00 ± 2.71 mPa·s for normal milk. In the case of class IV milk no coagulation can be observed which means that no gel is formed.

Table 5-12 contains the process viscosity of the 27 milk samples from infected udder quarters at different times of coagulation and for the four classes.

The scattering of the process viscosity of milk from healthy cows was found to be relatively small especially at coagulation times below 60 min, Table 5-9. In the case of milk from infected udder quarters the scattering is very high and differences exist between the classes. For practical relevance, coagulation times up to 30 min are interesting. But even here a high scattering exists.

Table 5-12: **Process viscosity of the four classes after different time of coagulation**

	Time [min]						Class
	0	**12**	**16**	**22**	**26**	**60**	
Process viscosity [mPa·s]	1.55	2.30	4.00	8.44	12.17	43.40	**I**
	1.41	2.11	2.81	4.68	6.47	27.91	**II**
	1.40	1.49	1.85	2.69	3.42	15.70	**III**
	1.60	1.57	1.57	1.61	1.66	2.10	**IV**

Following conclusions can be drawn:

- Section 1: for class I and II milks this section takes a shorter time. Here, an increase of the process viscosity starts already after 8 min instead of 12 min for milk from healthy cows and points at an altered micelle structure.

- Section 2.1: class I and class II milk have a relatively high increase in process viscosity (slope: 0.43 and 0.18) indicating an altered/disturbed micellar system, whereas the change in viscosity for milk from healthy cows is very small in this section (slope 0.0314).

- Section 3: The process viscosity cannot be described by a linear function in the case of class I and II milk; a plateau has been reached. In the case of class III milk the process viscosity can be described by a linear function but the level of viscosity after 60 min is only 15.70 ± 3.53 mPa·s compared to 20.00 ± 2.71 mPa·s for normal milk. In the case of class IV milk no coagulation can be observed which means that no gel is formed.

- The rapid renneting of class I and II milk indicates an altered/a disturbed micelle structure which is also proved by the altered GMP/CMP relation that is actually undesirable for cheese making.

The structural differences or deviating kinetics of change in viscosity between normal milk and milk from infected cows might be founded in the altered casein content and/or in a limited functionality of the caseins due to hydrolysis. As a result, a coagulum is built up that is very instable and not able to incorporate the whey into the casein network.

5.5 Connection of the rheological results to the casein profile analyzed by HIC

The results of the spectrophotometric analysis indicated that the caseins in milk of class IV had undergone further changes compared to the caseins present in the other milk samples of infected udder quarters. The HIC analysis was done to gain further information on the changed casein profile.

5.5.1 Normal raw cow milk

Figure 5-11 is a typical profile of the hydrophobic interaction chromatography of casein obtained from raw unprocessed cow milk without udder inflammation.
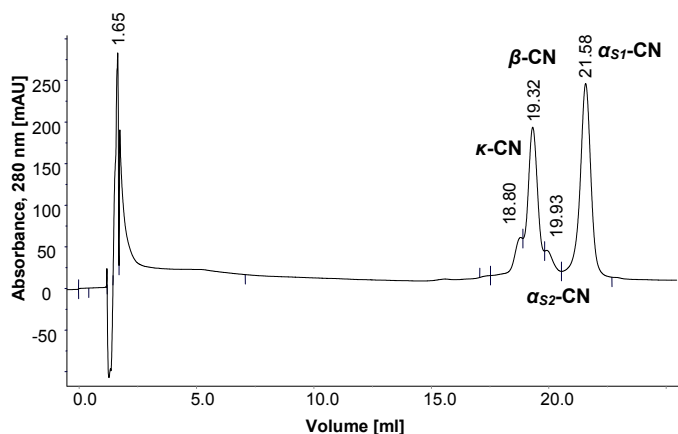
Figure 5-11:   HIC chromatogram of casein obtained from raw unprocessed cow milk

The first peak after 1.65 min represents the exclusion limit. Here, sample components are separated that are not hydrophobic which are all the whey proteins and peptides [227]. The caseins are separated according to their hydrophobicity in the following order: $\kappa < \beta < \alpha_{S2} < \alpha_{S1}$. LIESKE and VALBUENA (2008) calculated the amounts of the individual caseins and found the percentage of α_{S2}-casein undervalued due to interference with β-casein [227]. It can be assumed that this happened here too.

5.5.2 Infected udder quarters, cow A

Figure 5-12 displays the HIC chromatogram of the casein from sample 1 of cow A (Class IV milk) and the process viscosity over time during rennet-induced coagulation.
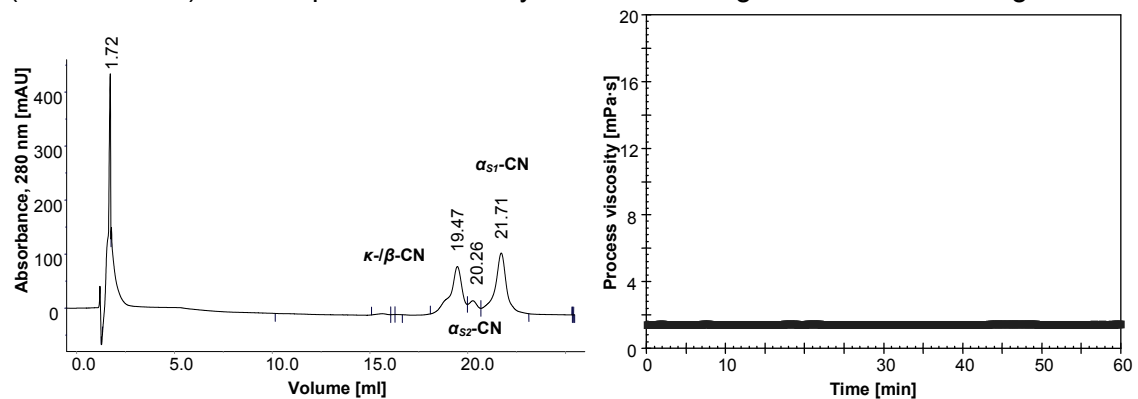
Figure 5-12:   **Chromatogram (left) and process viscosity during rennet-induced coagulation over time (right) of sample 1 (A1)**

Sample 1 was obtained from the infected udder part of cow A before medication. It had a high pH value of 6.86 at 32 °C. CMP and GMP were not measured. The protein content was 2.88 % and casein was 1.30 %. The amount of casein was found to be very low.

Coagulation of the milk was not observed within 60 min pointing on large changes in milk composition. Regarding the casein profile it becomes clear that κ-casein is not separated as a single peak indicating molecular-structural changes—a polymerization with β-casein—and inherent changes of hydrophobicity [227]. If κ-casein was polymerized with β-casein, it could be difficult for the enzyme to split the bonding between the amino acid 105 and 106. This might be the reason why no coagulation was possible.

LIESKE and VALBUENA (2008) proposed the formation of κ-casein multimers to be the reason of the different resolution (separation as a single peak) [227].

In another paper LIESKE and VALBUENA (2008) proved their statement and found a changed surface of non-renneting micelles with cross-linked κ-casein molecules due to oxidation of their free SH group [275]. The lack of free, "reactive" SH groups results in insufficient gel formation because they no longer contribute to the stabilization of the rennet gel network. Additionally, the formation of SS-linked κ-casein multimers would result in reduced enzymatic availability of the Phe_{105}-Met_{106} bond inside the casein micelles.

Sample 2 (Class III milk) was taken from the infected udder part of cow A after five days of medication with Benzylpenicillin-Procain. Sample 2 had a lower pH value of 6.42 at 32 °C. It had 0.889 $g \cdot l^{-1}$ CMP, 0.432 $g \cdot l^{-1}$ GMP, 0.457 $g \cdot l^{-1}$ n.-g. CMP and the relation of GMP to CMP was 0.49.

Figure 5-13 displays the HIC chromatogram of the casein from cow A after five days of medication and the process viscosity over time during rennet-induced coagulation. Coagulation of the milk was observed within 60 min. The visual point of clotting occurred after 14 min. Now, κ-casein is separated as a single peak.
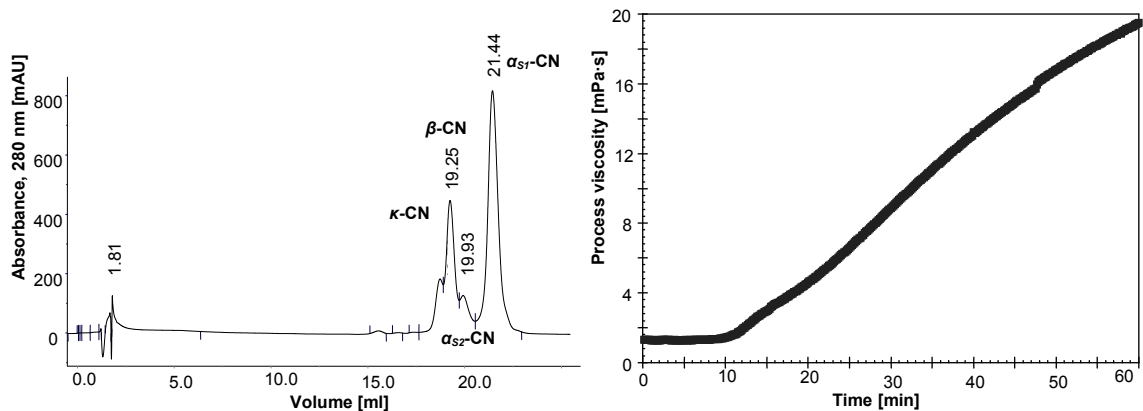
Figure 5-13: **Chromatogram (left) and process viscosity during rennet-induced coagulation over time (right) of sample 2 (A2)**

5.5.3 Infected udder quarters, cow B

Sample 4 (B1; Class IV milk) was taken from an infected cow which was medicated with Benzylpenicillin-Procain. The milk sample was taken two days after the start of the medication. The pH value was 6.69 at 32 °C. Rheological results showed no coagulation. The chromatogram, Figure 5-14, shows no separation of κ-casein.
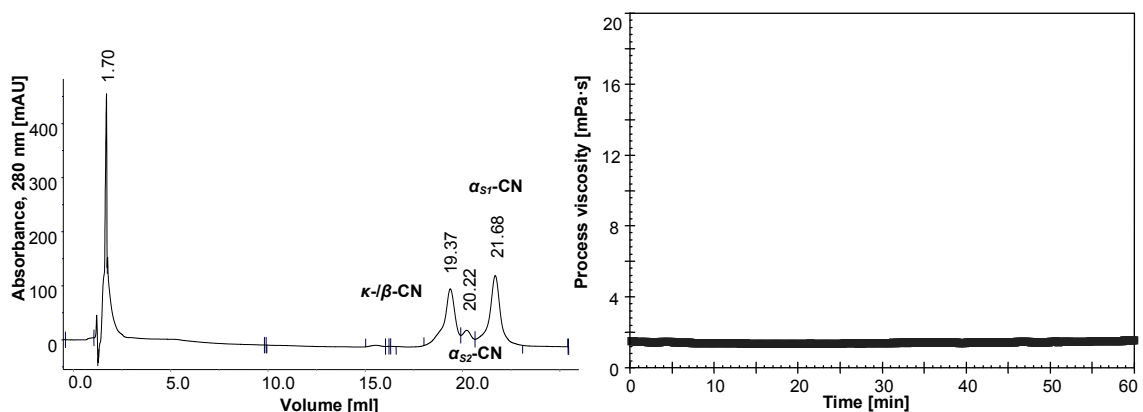
Figure 5-14: **Chromatogram (left) and process viscosity during rennet-induced coagulation over time (right) of sample 4**

Sample 6 (B3; Class II milk) was taken from cow B after medication. It had a visual clotting time of 30.3 min. The casein number was in the area 70.55. The casein content of 2.30 % was found to be too low. The chromatogram shows the single fraction of κ-casein again, Figure 5-15. Additionally, the process viscosity after 60 min is with ~12 mPa·s on a low level (~20 mPa·s after 60 min for healthy cows).
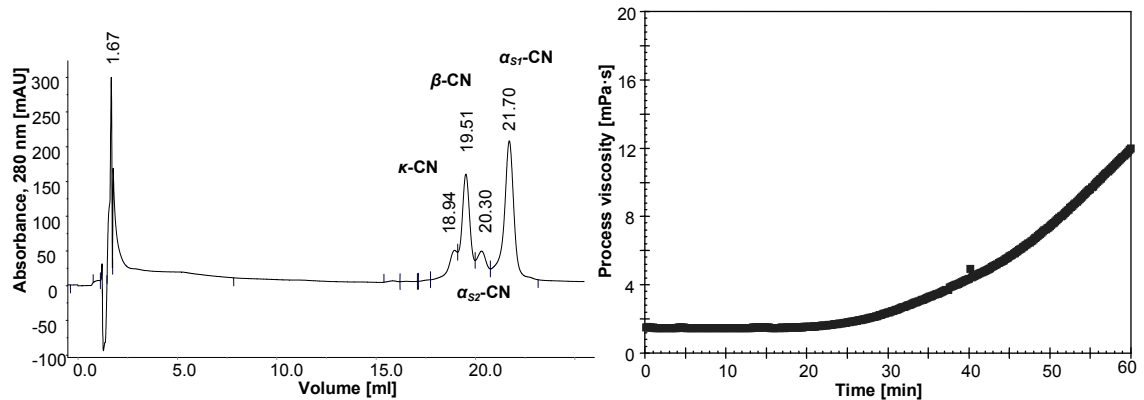
Figure 5-15: **Chromatogram (left) and process viscosity during rennet-induced coagulation over time (right) of sample 6**

The casein profile of sample A1 and B1 (Class IV milks) was analyzed, Figure 5-12 and Figure 5-14. For both samples the casein profile changed dramatically; the κ-casein was not eluted as a single peak, which proves the statement made on the basis of the spectrophotometric analysis that the protein status of non-coagulating milk had undergone immense changes.

Poor coagulation properties (long coagulation time, low curd firmness) in comparison to cleavage of caseins have been reported before [102;268]. WEDHOLM (2008) found a significantly lower concentration of κ-casein in relation to total casein in poorly and non-coagulating milk [266].

5.6 Selected results from cow G after medication with antibiotics

Cow G suffered from an udder inflammation with a high SCC of 1004·1000 ml^{-1}. The first milk sample G1 was taken from the infected udder part before intramammary medication with Benzylpenicillin-Procain. The following milk samples were taken every day. On day two a second medication with antibiotics was done. Sample G4 was taken after the second medication. The sample G7 was taken after the end of medication.

The $pH_{32\ °C}$ of the milk samples of cow G can be viewed in Table 5-6. The chemical parameters protein content in %, casein content in %, non-casein nitrogen in %, casein number (casein content 100/protein), and the calcium content in mg Ca^{2+}·100 ml^{-1} are shown in Table 5-7. The days of medication are displayed in Table 12-1 and the SCC in 1000 ml^{-1} in Table 5-8.

The development of the CMP, GMP, and n.-g. CMP contents in the course of the udder inflammation and antibiotic therapy can be seen in Figure 5-16. Sample G1 does not contain any antibiotic substances. The proportion of GMP in the whole CMP of 86 % compared to milk from uninfected cows with 36.4 % is far too high.

The hypothesis stated by LIESKE and VALBUENA (2008), that antibiotics are UV active and lead to a higher absorption because they might be bound to GMP, can be disproved [275]. Presumably, in milk from the infected udder part a higher proportion of CMP is glycosylated or substances are present which behave very similar to GMP (e.g., peptides). Reasons for that might be a different casein spectrum, the changed availability of the rennet-sensitive bond, and changed enzyme status.

Sample G2 was taken one day after the first application of Benzylpenicillin-Procain 1 H_2O. The GMP content decreased to 56 %. Sample G7 was taken after the end of medication. Here, the CMP, GMP, and n.-g. CMP contents are at a normal level again. On average, raw bulk milk from healthy cows contained 1.243 $g \cdot l^{-1}$ CMP from which 37.5 % was glycosylated and 62.5 % was not.
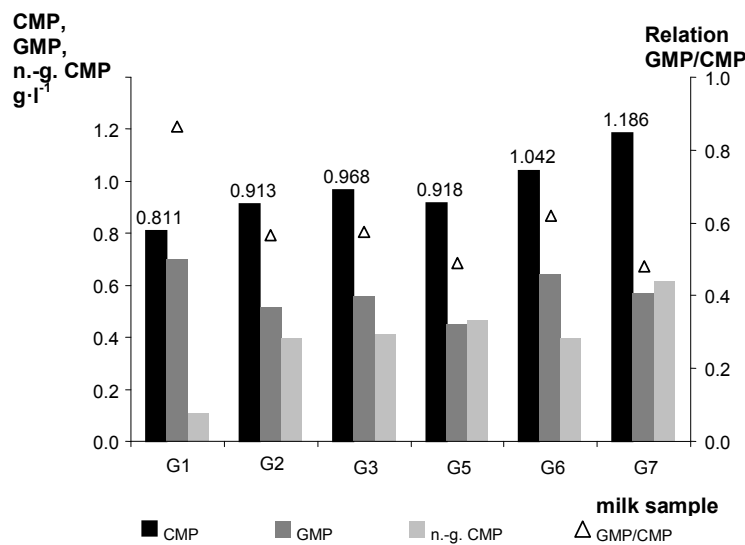
Figure 5-16: Contents of CMP, GMP, n.-g. CMP and relation GMP/CMP in the course of the udder inflammation and medication of cow G

Figure 5-17 displays the process during coagulation over time. For the sake of clarity only four of the seven milk samples taken from cow G during udder inflammation and medication are shown.

No.	$\eta_{60\ min}$ mPa·s	CN No.
G1	10.4	74.53
G2	12.9	71.43
G5	24	81.13
G7	27.2	78.42
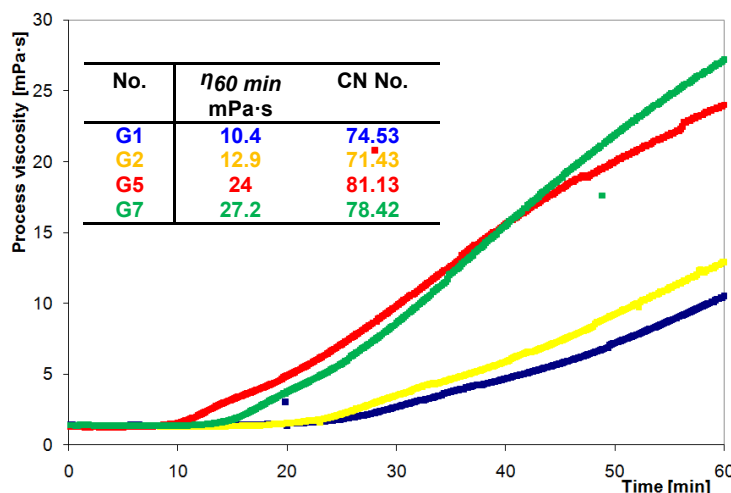
Figure 5-17: Selected process viscosities during udder inflammation and medication of cow G

It is obvious that only sample G7 shows a "normal" coagulation behavior with a process viscosity of 27.2 mPa·s after 60 min. The other samples have a process viscosity after 60 min at a lower level and a weaker structure. Only sample G7 shows a further increase of the process viscosity and therefore a stable gel. Here, the casein number is at a normal level with 78.42. After medication the composition of the milk satisfies the characteristics of a healthy cow with a good technological suitability.

5.7 Summary of the chapter

Experiments were carried out to gain more scientifically-based information on biochemical changes of κ-casein and the mechanism of structuring during rennet induced-coagulation of bulk raw milk and milk from infected udder quarters of cows. The main focus of the research was the time-dependent coupling between the biochemical reaction of the casein and the structural change from the fluid milk to the rennet gel by inline-online detection of the process viscosity. The rheological method allowed a grading of the process into five sections, whereas the first three sections were discussed in detail. The process of rennet-induced coagulation was assessed from a material scientific point of view. With the use of the torsion oscillator measurements the resulting structuring mechanisms can be examined. The process viscosity is presented as an objective parameter for the pre-calculation of the optimal cutting time. The rheological model represents a technological tool which can be used as an early warning and control system.

Huge differences were found for the coagulation behavior of milk from infected udder quarters. The course of the curves of the process viscosity over time was found to be very divergent. Thus, an over-all statement about the coagulation behavior, valid for all milk samples from infected udder quarters, can not be made and a differentiation according to the process viscosity after 60 min of coagulation was necessary. In combination with chemical analysis and HIC profiles the altered casein profile was detected. For the first time an attempt is made to differentiate between milk from infected udder quarters regarding cheese-making parameters. Thus, a connection between modification of the milk protein and the rheological investigations, the development of structure, was accomplished. These findings may help to optimize cheese production.

Chapter 6: Rennet-induced coagulation of goat milk

Chapter 6 deals with the structure formation during renneting of goat milk. The transferability of the rheological measurements and the spectrophotometric analysis from cow to goat milk will be assessed.

More information regarding the correlation between chemical changes—release of CMP—and rheological parameters—process viscosity, development of the structure— will be obtained as long as divergent findings exist about the caprine casein micelle size.

The micelle size of caprine milk was reported by ONO and CREAMER (1986) to be larger than that of bovine milk [44]. REMEUF and LENOIR (1986) stated that the caprine micelles were smaller [46].

6.1 Release of CMP and GMP in the course of the rennet-induced coagulation of goat milk

Figure 6-1 displays the release of CMP and GMP measured in absorption at 217 nm during the course of the rennet-induced coagulation for the three goat milk samples 1, 2, and 4. Furthermore, the rheological results are given. The magnitude of the CMP and GMP release is very similar to that of raw cow milk.

In the case of sample 4 the CMP content increases after 45 min. This can be attributed to a second proteolysis step.
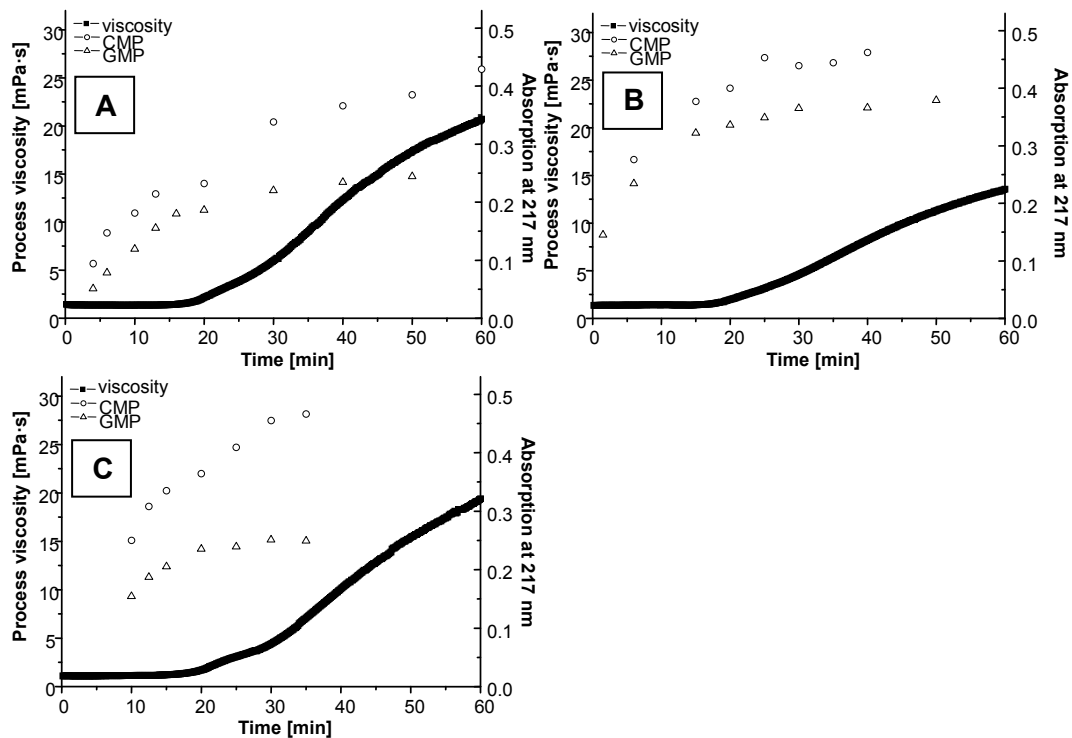
Figure 6-1:   Release of CMP and GMP and process viscosity over time of sample 1 (A), sample 2 (B), and sample 4 (C) (goat milk)

The development of viscosity in the chronological sequence of the process steps during the rennet-induced coagulation of goat milk 1 can be taken from Table 6-1.

Section 1 and 2 are time-demanding but the resulting structure is low. Section 1 is characterized by the dominating enzymatic reaction which indicates the splitting of κ-casein and the loss of hydration. For goat milk, section 2.3 was found to have a high structure formation velocity. The characteristic structure formation starts in section 2.3 which takes place earlier compared to cow milk and carries on to section 3 with a constant structure formation velocity.

Table 6-1: **Results of the rheological measurements of goat milk sample 1 contrasted to the biochemical results**

Sec- tions	Rheological results					Biochemical results	
	t	Δ t	η	Δ η	Structure formation velocity	CMP	GMP
	min	min	mPa·s	mPa·s	mPa·s·min^{-1}	%	%
1	12	12	1.36 ± 0.01	→ 0	→ 0	33.3 (10 min)	48.8 (10 min)
2	26	14	4.18 ± 0.05	2.82	0.20		
2.1	16	4	1.45 ± 0.02	→ 0	→ 0	42.8 (15 min)	73.8 (15 min)
2.2	22	6	2.83 ± 0.06	1.38	0.23	42.8 (20 min)	76.2 (20 min)
2.3	26	4	4.18 ± 0.05	1.89	0.47	62.4 (30 min)	76.6 (25 min)
3	60	34	20.7 ± 0.9	16.52	0.49	71.0 (50 min)	95.9 (40 min)

The release of CMP and GMP of goat milk micelles was found to be slower compared to cow milk from healthy cows. The release of GMP is completed after 25 min whereas in the case of goat milk this lasts up to 50 min. Goat milk was found to contain more κ-casein [15;43] than cow milk. Nevertheless, RICHARDSON, CREAMER, and MUNFORD (1973) reported that the composition of caprine κ-casein was very similar to that of bovine milk indicating that the rennet sensitive bond should be available [45]. Diverging information about caprine micelle size exist. The present results indicate that caprine casein micelles are smaller leading to decelerated splitting rates of GMP due to increased distances which have to be covered by the enzyme.

6.2 Chemical analysis

Table 6-2 displays the chemical composition especially the CMP, GMP, and n.-g. CMP in g·l^{-1}, the pH value at 32 °C, and the calcium content in mg·100 ml^{-1} of the four goat bulk milk samples.

Table 6-2: **Chemical analysis of the four goat milk samples**

Sample	CMP g·l^{-1}	GMP g·l^{-1}	n.-g. CMP g·l^{-1}	GMP/CMP	pH$_{32\,°C}$	Calcium mg·100 ml^{-1}
1	1.015	0.661	0.354	65.1	6.67	119.4
2	0.85	0.619	0.231	72.8	6.62	122.2
3	1.127	0.657	0.47	58.3	6.62	102.6
4	1.169	0.686	0.484	58.6	6.65	106.6

The results of Table 6-2 show differences compared to the results obtained for raw bulk cow milk. On average, raw bulk milk from healthy cows contained 1.243 g·l^{-1} CMP, Table 5-3, from which 37.5 % was glycosylated and 62.5 % was not. In the case of raw bulk goat milk less CMP was found which was at maximum 1.169 g·l^{-1} from which 58.6 % was glycosylated. The low CMP content was not expected in so as far as literature data indicate a higher degree of κ-casein of 10-24 % [15;43] compared to 10-13 % [15]. But even here, large fluctuation margins exist.

Additionally, the high amount of 58.6 % glycosylated macropeptide contradicts results of other studies. MORENO et al. (2001) reported that approximately 36 % of caprine κ-casein was glycosylated [288]. ADDEO et al. (1978) and RECIO et al. (1997) found at least five caprine κ-casein forms in milk protein electrophoresis assays, the main one being non glycosylated [289;290]. Nevertheless, the amount of data in the literature on this question is limited and further research in this area is needed.

Differences in the calcium content between bovine and caprine milk were found to be small. The pH value of goat milk with 6.6 is a slightly higher than that of cow milk with 6.52 on average.

6.3 Rheological measurements of raw bulk goat milk

6.3.1 Characterization of the overall process

Figure 6-2 displays the process viscosity during the rennet-induced coagulation of four bulk goat milk samples and one sample of commercial goat cheese production up to 60 min.
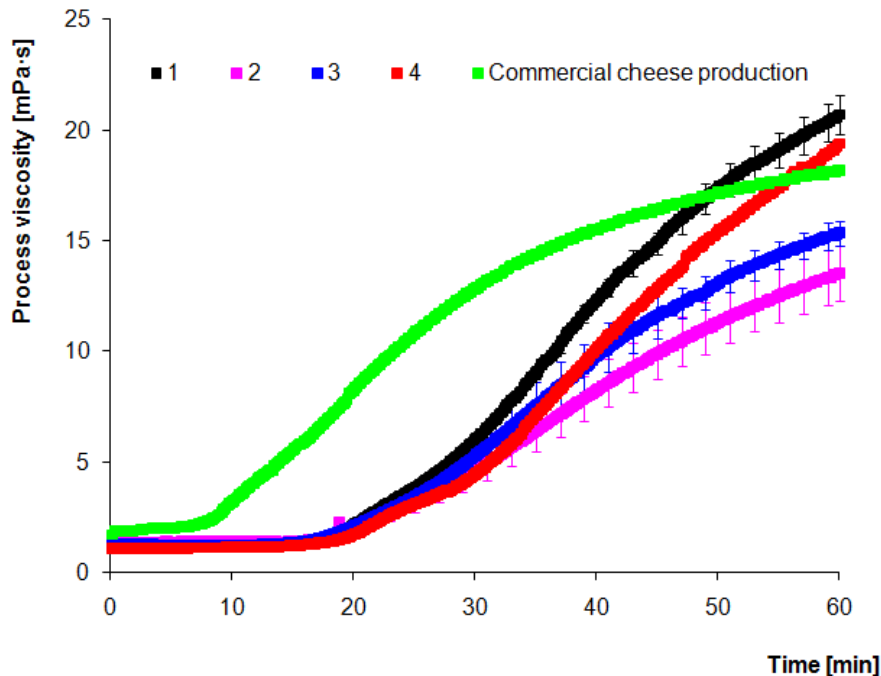
Figure 6-2: **Process viscosity of raw bulk goat milk during rennet-induced coagulation Sample 1 ■, sample 2 ■, sample 3 ■, sample 4 ■ and commercial cheese production ■. Values are averages ± _s_**

6.3.2 Allocation into sections

In the following, the entire process is divided into sections as shown in Figure 5-3 for milk from healthy cows. Figure 6-3 displays section 1 for three goat milk samples.
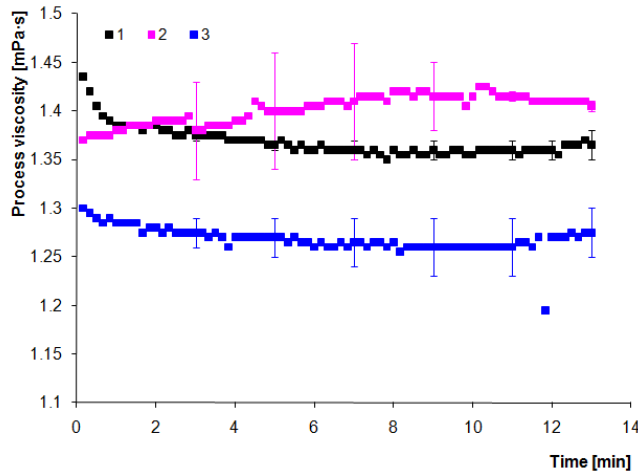
Figure 6-3: **Section 1 of three goat milk samples**

For milk from healthy cows section 1 starts immediately after addition of rennet. As can be seen from Figure 6-3 the relations are different for goat milk. Here, the viscosity increases one minute later after about 13 min.

Section 2 which lasts from 12 min to 26 min for cow milk and from 13 min to 26 min for goat milk characterizes the transfer from enzymatic reactions to flocculation and is displayed in Figure 6-4.
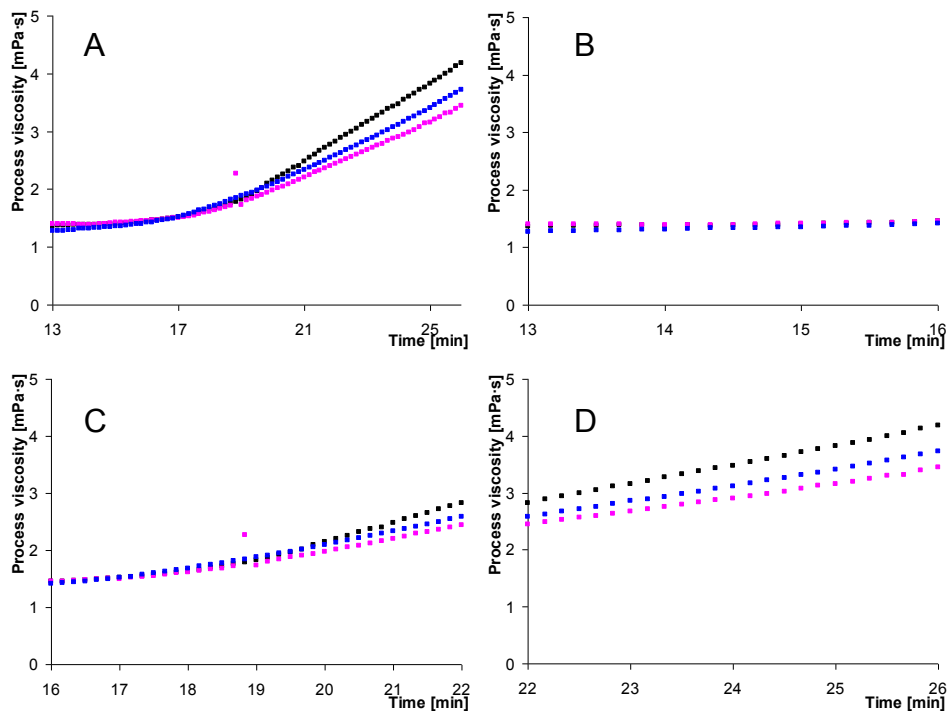
Figure 6-4: **Section 2 of three goat milk samples**
Sample 1 ■, sample 2 ■, sample 3 ■
A: whole section, B: section 2.1, C: section 2.2, D: section 2.3

Section 2 is important for the structure development of the curd. The regression results of the three samples are: sample 1 $\eta(t) = 0.3122\ e^{0.0987 \cdot t}$ R² = 0.9597, sample 2 $\eta(t) = 0.4328\ e^{0.0781 \cdot t}$ R² = 0.9576, sample 3 $\eta(t) = 0.3476\ e^{0.0906 \cdot t}$ R² = 0.9854. Section 2 can be divided into three subsections.

Section 2.1 starts with the viscosity minimum and ends at the point of critical hydrolysis coinciding with initial molecular interactions and aggregation between the casein micelles. The change in viscosity in section 2.1 is relatively small in the case of healthy cows as well as for goat milk, Figure 6-4 B.

Here, the slope is at the same level (goat milk 0.017-0.0459; cow milk: 0.031, Figure 5-3). The regression results of the samples are: sample 1 $\eta(t) = 0.0255 \cdot t + 1.0278$ R² = 0.9199, sample 2 $\eta(t) = 0.017 \cdot t + 1.1651$ R² = 0.6309, sample 3 $\eta(t) = 0.0459 \cdot t + 0.6724$ R² = 0.9833.

Section 2.2 is the main part of the structure formation and takes from 16 to 22 min for healthy milk and for goat milk as well, Figure 6-4 C. Here, the increase in viscosity is nonlinear and can be described by an exponential function (sample 1 $\eta(t) = 0.1984\ e^{0.11937 \cdot t}$ R² = 0.9738, sample 2 $\eta(t) = 0.3203\ e^{0.0916 \cdot t}$ R² = 0.9309, sample 3 $\eta(t) = 0.2593\ e^{0.01044 \cdot t}$ R² = 0.9982). In this phase the change in structure takes place and chains are formed. Section 2.2 describes the continuous change from the enzymatic phase to the flocculation step.

In section 2.3 (22 to 26 min) the viscosity can be described by a linear function for milk from healthy cows as well as for goat milk, Figure 6-4 D (sample 1 $\eta(t) = 0.334 \cdot t - 4.5222$ R² = 0.9996, sample 2 $\eta(t) = 0.2832 \cdot t - 3.6644$ R² = 0.9987, sample 3 $\eta(t) = 0.2449 \cdot t - 2.9581$ R² = 0.9977). It can be concluded that the micelle chains reach a critical chain length and chain concentration.

For goat milk, sections 2.1 and 2.3 are described by a linear function and section 2.2 is described by an exponential function.

Section 3 is characterized by the highest level of structure formation velocity in the case of milk from healthy cows, Figure 5-6. This section is important for cheese production because the curd is cut with respect to time or firmness of the curd. After 60 min section 4 would start.
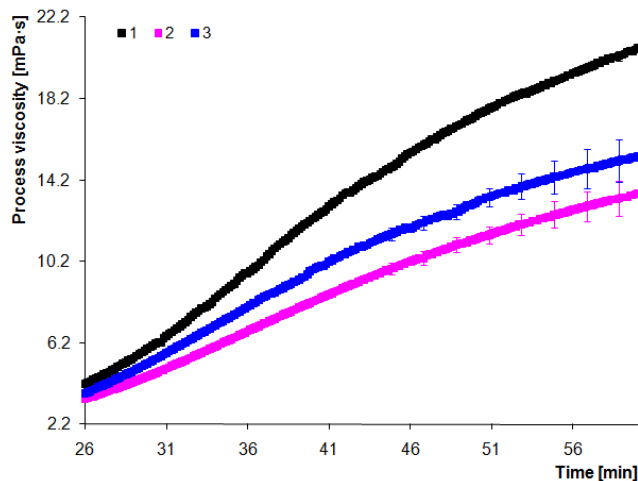
Figure 6-5:   **Section 3 of three goat milk samples**

The level of viscosity after 60 min is 20.7 ± 0.9 mPa·s of goat milk sample 1 which is at the same level as cow milk 20.00 ± 2.71 mPa·s. Goat milk samples 2 and 3 reach only a level of 13.35 ± 1.25 mPa·s and 15.35 ± 0.55 mPa·s, respectively. Significant differences between milk from healthy cows and goat milk occur in section 3 in the phase of the gel formation, Figure 6-5. The viscosity cannot be described by a linear function in the case of goat milk; a plateau has been reached. This implies that the goat casein network has a weaker structure and is not as stable as the cow casein network. As a consequence, during cheese manufacture of goat milk this has to be taken into consideration.

6.3.3 Commercial goat cheese production

Figure 6-6 displays the sections of coagulation of a sample of commercial goat cheese production. Here, goat milk was clotted by rennet but was also acidified by starter cultures.

In panel B: $y = 0.8722e^{0.1285x}$, $R^2 = 0.971$
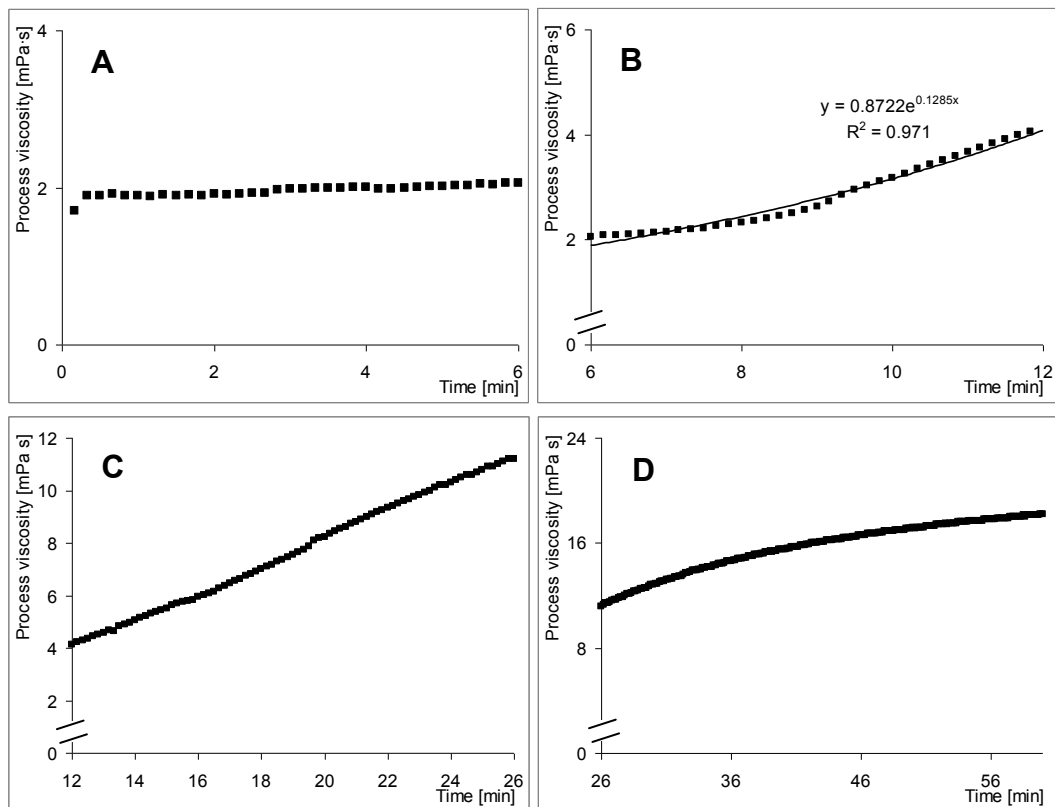
Figure 6-6: **Coagulation of goat milk during commercial goat cheese production**
A: Section 1, B: Section 2.2, C: Section 2.3, D: Section 3

In comparison to goat milk which was only clotted by rennet, the coagulation differs for goat milk under the conditions of conventional cheese production.

Section 1 (A in Figure 6-6), which starts immediately after addition of rennet, is with 6 min very short. For cow milk and goat milk clotted by rennet, section 2 was subdivided into three sub-sections. This is no longer possible in the case of milk during the production of goat cheese.

Section 2.1, which ends at the point of critical hydrolysis coinciding with initial molecular interactions and aggregation between the casein micelles, was not detected here. Assumable, the time was too short because the milk used for commercial goat milk production was acidified by lactic acid bacteria before rennet-induced coagulation.

Immediately after section 1 the viscosity increases exponentially (B in Figure 6-6). This section lasts from 6 min to 12 min and is described as section 2.2. Here, the main part of the structure formation takes place. This section is very early.

Section 2.2 lasts from 16-22 min in the case of cow and goat milk under the conditions of rennet-induced coagulation.

In section 2.3 (C in Figure 6-6) the viscosity is described by a linear function. It takes until 26 min in the case of goat milk under the conditions of commercial cheese production which is comparable to the results obtained for cow and goat milk above.

Section 3 (D in Figure 6-6), which was in the case of cow and goat milk described by a linear function, cannot be described as a linear function for goat milk under the conditions of commercial cheese production. Here, the viscosity reaches a constant level after 60 min of 18.2 mPa·s which is on a same level with cow milk 20.00 ± 2.71 mPa·s.

6.4 Summary of the chapter

Experiments were carried out to gain more scientifically-based information on biochemical changes of κ-casein and the mechanism of structuring during rennet-induced coagulation of raw goat milk. The main focus of the research was the time-dependent coupling between the biochemical reaction of the casein and the structural change from the fluid milk to the rennet gel by inline-online detection of the process viscosity. The results suggest that the rheological measurements and the spectrophotometric analysis can be transferred to goat milk. The rheological method allowed a grading of the process into five sections, whereas the first three sections were discussed in detail. Significant differences during rennet-induced coagulation of milk from healthy cows and goat milk occurred in section 3 in the phase of the gel formation. The viscosity cannot be described by a linear function in the case of goat milk; a plateau has been reached. However, with the use of the rheological method the end viscosities can be calculated as soon as the process reaches the linear function of section 3. This method enables a prediction of the cheese-making process and is more reliable compared to visual observations.

Chapter 7: Quality investigations of dairy powders

The production of a high quality yoghurt with respect to taste, smell, consistency, and appearance which is stable over a long time period without whey separation (syneresis) is of utmost importance to get consumer acceptance. Thus, a detailed description of the reactions occurring during structure formation and structure kinetic during acidification of milk is needed.

Common methods used to prevent syneresis of stirred yoghurt are the increase of the dry matter, the homogenization of milk, the thermal modification of the milk protein, the choice of culture, and the reduction of mechanical stress [6;291].

In the course of the production of yoghurt several critical influencing factors exist that determine its structure. Chapter 7 focuses on the addition of powder to standardize the non-fat solid contents of the milk.

Here, a rapid method is developed which can be used for the characterization and assessment of the powder quality and functionality. In detail, the particle size of the dairy powders is measured during rehydration. The rehydration behavior (detection of kinetics) and the final particle size obtained from the PSDs are used to assess the powders. The presence of large particles in the PSDs indicates the presence of heat-denatured protein aggregates being a result of the processing history.

Generally, the manufacture of WPC involves UF and/or DF [142-144;150;152;154-159], removal of water by condensing, i.e., evaporation [160], and spray drying. A prolonged exposure to high temperatures is more likely a result of the evaporation process than of the spray drying. However, in a study of DE LA FUENTE et. al (2002) evaporation and subsequent spray drying of ultrafiltered retentates caused no significant changes in any of whey protein components for a well run WPC manufacturing process. They related the different functionality of WPC products to modifications of proteins and other components caused by the processes that are used in cheese or casein manufacture rather than to the WPC manufacturing process [292].

7.1 Artifacts—defects in whey protein functionality

It is of immense importance that the proteins used to increase the dry matter are in their native state as long as the study of SCHORSCH, WILKINS, JONES, and NORTON (2001) indicates that if pre-denatured whey proteins are present in the yoghurt milk large aggregates exist, which are not able to interact with the casein micelle surface during heat treatment [9]. Those aggregates could act as a destructive filler or structure breaker in acid milk gels leading to the formation of an inhomogeneous particle gel possessing indifferent structures. As a result two main problems can be identified, when whey proteins with altered/disturbed functionality are used: Firstly, the existence of large whey protein aggregates (excess of whey proteins and existence of denatured whey proteins) which cannot be integrated into the casein network. Secondly, the hindrance of co-precipitation between whey proteins and caseins because whey proteins are already denatured.

As a consequence of an excess of whey proteins, particles of β-Lg and α-La are formed. Additionally, denatured proteins bind to each other and form larger aggregates.

After the coagulation and the formation of an initial gel in form of a visco-elastic fluid the whey protein aggregates possess a larger size than the gaps in the gel network formed by the casein molecules, thus a continuous integration is not possible. The particle gel lacks in stability, is grainy, and tends to syneresis after treatment. This has an immense influence on the further processing, for example the use of sieves is necessary.

Fermentations have been observed using whey proteins with defective functionality [10-13]. Here, an inhomogeneous particle gel with indifferent structural properties was formed. Figure 7-2 and Figure 7-1 display the structure formation during fermentation with altered/disturbed whey protein functionality.
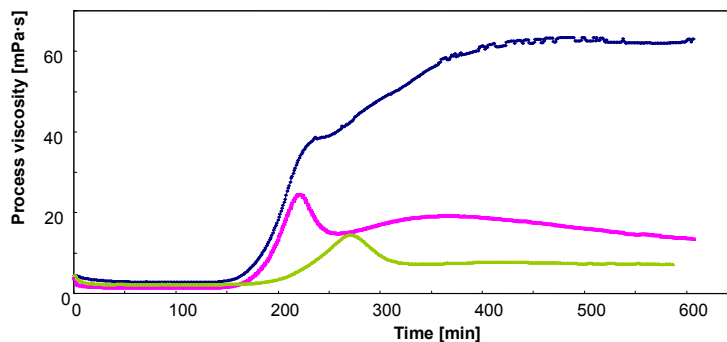
Figure 7-1: **Process viscosity during fermentation with altered whey protein functionality [10;11]**
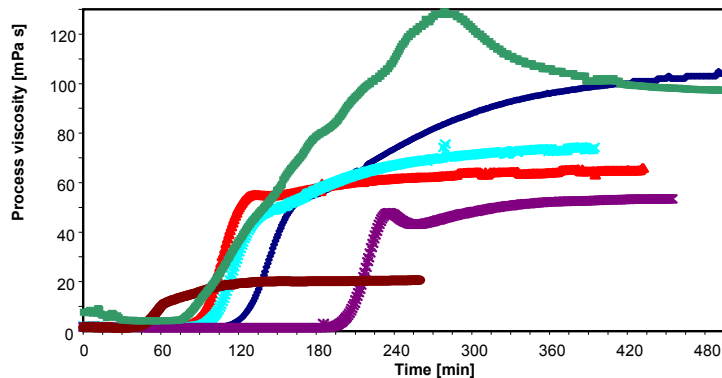
Figure 7-2: **Process viscosity during fermentation with altered whey protein functionality [12]**

The intensity of the disturbance of the conventional formation of the acid milk gel can be attributed to the charge and amount of whey protein as well as the processing technology of the added whey proteins [12;13]. For powders already containing denatured whey proteins the formation of complexes due to co-precipitation between whey proteins and caseins during hot-holding is prevented. But this formation of complexes is crucial for the gel formation mechanism as well as for the gel firmness during fermentation. If this mechanism is disordered particle gels are formed with lower viscosity as compared to conventional acid milk gels. It can also be described to be an inhomogeneous structure of a gel on the one hand and micro-particle dispersion on the other hand in spite of an acid milk gel.

The results clearly prove the major influence of the powder properties determined by physical parameters on the structure elements of the yoghurt gel. In the production flow a share of 15 % defective fermentation can be predicted. Generally, the use of concentrates (30 % dry matter)—in spite of powders—has been discussed to be advantageous because thermal treatment was avoided partially or in total.

SPIEGEL (1999) recommended a particle size of aggregates in WPC < 1 µm for use in fermented products because larger aggregates cannot be easily integrated into the casein network [202]. These particles break up the gel structure and lead to a grainy texture [15]. Although these aggregates should be minimized to below 1 µm due to the use of a homogenization step [291;293], a reaggregation due to the thiol/disulfide interchange reaction can subsequently occur during heat treatment. This influence becomes stronger with increasing content of amino acids containing sulphur [294]. Additionally, aggregates detected in the native rehydrated WPC powders point at heating regimes which caused denaturation.

7.2 Chemical analysis

7.2.1 Chemical analysis—Section I

Table 7-1 displays the results of the chemical analysis of the sweet whey powders having 13 % protein, the SMP, and the WPC powders with 35 and 60 % protein. The chemical parameters ash, water, protein, fat, lactose, and galactose content (%) were determined. The standard deviation for each parameter is given.

Table 7-1: Results of the chemical analysis of the SWP, SMP, WPC 35, and the WPC 60 in %, section I

Sample	Pro-tein	s	Protein in d.m., calculated	Ash	s	Wat-er	s	Fat	s	Lac-tose	s	Ga-lac-tose
SWP 13 1	13.51	0.29	13.83	7.64	0.02	2.29	0.02	0.50	0.01	75.79	0.16	0.35
SWP 13 2	13.49	0.20	13.84	7.54	0.06	2.56	0.14	0.68	0.05	75.45	0.35	1.24
SWP 13 3	13.16	0.24	13.57	7.34	0.00	3.00	0.01	0.90	0.12	71.41	0.32	0.29
SMP	34.77	0.28	36.18	7.74	0.00	3.89	0.09	0.96	0.16	50.42	0.29	0.10
WPC 35 1	32.40	0.04	33.75	7.68	0.01	3.99	0.02	2.81	0.02	50.41	0.50	0.46
WPC 35 2	35.77	0.21	37.39	4.00	0.00	4.32	0.06	2.89	0.02	47.86	0.20	0.21
WPC 35 3	33.29	0.07	35.20	6.07	0.03	5.44	0.10	2.08	0.01	50.29	0.05	0.73
WPC 35 4	34.78	0.12	36.35	7.15	0.01	4.33	0.01	2.94	0.13	47.06	0.49	0.86
WPC 35 5	33.17	0.13	34.31	7.79	0.04	3.33	0.05	4.26	0.18	48.05	0.12	0.59
WPC 35 6	34.49	0.02	35.94	5.93	0.04	4.03	0.08	2.21	0.06	47.34	0.13	0.36
WPC 35 7	33.45	0.29	35.34	6.13	0.01	5.33	0.02	2.95	0.08	42.23	0.30	0.58
WPC 60 1	60.39	0.14	62.29	6.16	0.03	3.05	0.03	4.71	0.06	20.66	0.23	5.75
WPC 60 2	59.08	0.31	60.96	3.98	0.03	3.09	0.01	4.09	0.24	20.93	0.38	5.61
WPC 60 3	62.03	0.23	64.49	4.08	0.03	3.81	0.05	3.72	0.19	20.42	0.24	0.09
WPC 60 4	59.55	0.16	61.52	3.88	0.07	3.20	0.02	5.05	0.22	20.44	0.52	0.01
WPC 60 5	58.57	0.08	61.41	5.97	0.00	4.62	0.08	6.45	0.12	17.05	0.24	0.39

The analyzed fat content of the SWP corresponds to results found by BANAVARA, ANUPAMA, and RANKIN (2003) [295]. Here, the lipid content ranged between 0.03-2.0 %. The fat content of the whey was found to depend on process parameters such as coagulum firmness at cutting, mechanism of cutting, size of the curd, and time allowed for skin formation on curd particles [296].

The results of the chemical analysis of the WPC 35 are in agreement with the results of WANG and LUCEY (2003) who analyzed WPC which were produced by ultrafiltration [149].

Table 7-2 displays the results of the chemical analysis of the WPC powders with 70 and 80 % protein. The standard deviation for each parameter is given.

Table 7-2: **Results of the chemical analysis of the WPC 70 and 80 in %, section I**

Sample	Pro-tein	s	Protein in d.m., calculated	Ash	s	Wa-ter	s	Fat	s	Lac-tose	s	Ga-lac-tose
WPC701	68.49	0.52	70.98	7.56	0.02	3.51	0.04	3.18	0.13	11.86	0.66	0.08
WPC702	70.20	0.23	72.86	7.74	0.01	3.65	0.12	2.88	0.18	9.13	0.26	0.18
WPC801	77.04	0.34	80.84	4.04	0.03	4.70	0.07	6.30	0.19	0.34	0.13	0.00
WPC802	74.74	0.35	79.56	3.90	0.08	6.05	0.16	2.19	0.16	4.01	0.27	0.05
WPC803	77.19	0.40	80.34	3.91	0.00	3.92	0.20	0.89	0.19	8.90	0.32	0.25
WPC804	74.90	0.04	79.16	2.93	0.01	5.13	0.11	5.20	0.03	4.21	0.43	0.02
WPC805	77.53	0.30	82.25	2.93	0.09	3.88	0.09	3.59	0.01	4.72	0.02	2.21

The results of the WPC 60 and WPC 70 correspond to results obtained by ZADOW (1986) for WPC 65, unless the ash and fat content were smaller in the case of the WPC 60 and lactose and fat content were lower and ash content was higher in the case of WPC 70 [152]. The chemical composition of the WPC 80 is in agreement with previous studies by MORR and FOEGEDING (1990) and WANG and LUCEY (2003) [149;150].

7.2.2 Chemical analysis—Section II

Table 7-3 displays the results of the chemical analysis of eleven WPC powders. The chemical parameters ash, water, protein, protein in d.m., fat, and lactose content (%) were determined. The standard deviation for each parameter is given.

Table 7-3: **Results of the chemical analysis of the WPC in %, section II**

Sample	Pro-tein	s	Pro-tein[A]	Ash	s	Wat-er	s	Fat	s	Lac-tose	s	NSI[B]	s
WPC30	28.96	0.14	30.12	7.90	0.01	3.84	0.01	1.70	0.00	50.1	0.02	65.7	0.57
WPC358	32.47	0.01	33.76	7.83	0.01	3.82	0.04	2.40	0.10	43.66	0.37	64.4	0.06
WPC359	33.39	0.21	35.45	9.08	0.05	5.66	0.30	2.50	0.00	41.45	0.42	86.8	1.68
WPC3510	33.60	0.18	35.72	8.26	0.02	5.94	0.34	3.45	0.05	45.34	0.55	93.9	0.24
WPC3511	33.04	0.08	34.45	6.03	0.02	4.09	0.05	2.25	0.25	47.83	0.07	94.0	2.70
WPC3512	33.56	0.14	34.9	6.57	0.00	3.85	0.07	1.88	0.13	46.72	0.24	88.9	0.16
WPC3513	33.54	0.42	35.04	6.68	0.00	4.29	0.00	2.25	0.00	47.86	0.16	97.4	1.04
WPC3514	32.99	0.02	34.81	6.85	0.00	5.24	0.03	1.60	0.00	46.3	0.18	95.7	0.94
WPC606	57.34	0.06	60.14	6.07	0.01	4.66	0.02	2.63	0.13	22.57	0.31	94.3	2.60
WPC607	57.02	0.01	59.68	4.86	0.00	4.45	0.02	3.75	0.05	20.68	0.14	85.9	1.16
WPC806	77.52	0.11	81.33	4.43	0.02	4.68	0.01	6.00	0.00	1.92	0.24	89.9	0.05

[A]**in d.m., calculated**
[B] **parameter in accordance to NSI**

The results of the WPC 35 are in agreement with the results of WANG and LUCEY (2003) who analyzed WPC which were produced by ultrafiltration [149]. The results obtained for the WPC 60 and the WPC 80 correspond to literature data [149;150;152].

Additionally, to the results obtained in section I in section II a parameter was measured according to the NSI. The results are listed in Table 7-3.

In general, a high NSI parameter points to an acceptable solubility of the powder's nitrogen. Overall, the solubility of the powders is very good with NSI parameter in the range between 85.9 and 97.4 %. Only two powders reveal a very low NSI which are the WPC 30 of 65.7 % and the WPC 35 8 of 64.4 %. This low NSI might be related to production-related changes assumable for a higher degree of protein denaturation which will be discussed later in detail.

7.2.3 Chitosan treatment

Selected WPCs were treated with chitosan to remove aggregate matters. For this purpose, the optimal chitosan concentration was determined for each WPC to achieve maximum removal of fat. Table 7-4, Table 12-7, and Table 12-8 in the Appendix display the amount of chitosan added to the sample in %, the extinction measured at 500 and 660 nm, and the percent of the initial turbidity for each WPC. A reduction of the turbidity measured at 500 and 660 nm indicates the removal of fat and also protein aggregates.

Table 7-4:   Results of the chitosan treatment of WPC 70 1

Chitosan (%)	$E_{500\ nm}$	% of initial turbidity	$E_{660\ nm}$	% of initial turbidity
0	0.027	100	0.021	100
0.01	0.029	107.41	0.022	104.76
0.012	0.036	133.33	0.026	123.81
0.016	0.338	1251.85	0.204	971.43
0.018	1.573	5825.92	1.141	5433.33
0.02	1.625	6018.52	1.206	5742.86

The following statements can be made on the basis of information given in Table 7-4, Table 12-7, and Table 12-8:

- Most of the WPC show a reduction of extinction at 500 and 660 nm with increasing amount of chitosan until a nearly constant level of extinction is reached.

- WPC 35 1 has a very low extinction at 500 nm and 660 nm and even a very small amount of added chitosan reduces the extinction to a low level which is not further reduced by a higher amount of added chitosan.

- WPC 80 1 and WPC 80 5 seem to reach a minimum of extinction at 500 and 660 nm. A higher amount of added chitosan leads to an increase in extinction. This is a common, well-described phenomenon in literature [216;219;297;298]. Due to a overdosing of the polymer a restabilization of coagulated solids can happen resulting in an increase of turbidity.

- WPC 70 has a relatively small extinction without chitosan Table 7-4. After the addition of even a small chitosan concentration the turbidity increases dramatically. It might be an overdosing but BOUGH and LANDES [216] reported a decreased turbidity after a further increase of the chitosan concentration. In the case of WPC 70 1 this did not happen.

From these findings different amounts of chitosan were added to the appropriate WPC before HPLC analysis, see Table 12-9 in the Appendix.

7.2.4 Results of the high-performance size exclusion chromatography (HPSEC)

Size-exclusion chromatography has been extensively used to study heat-induced aggregation of whey proteins [157;299;300].

Figure 7-3 displays a chromatogram of a native WPC 30. The first peak of all chromatograms which eluted after 7 ml corresponds to the exclusion limit, i.e., aggregates [231], residual lipid fraction (e.g., phospholipids) [149] or lipo-proteins, and denatured-aggregated proteins [150].
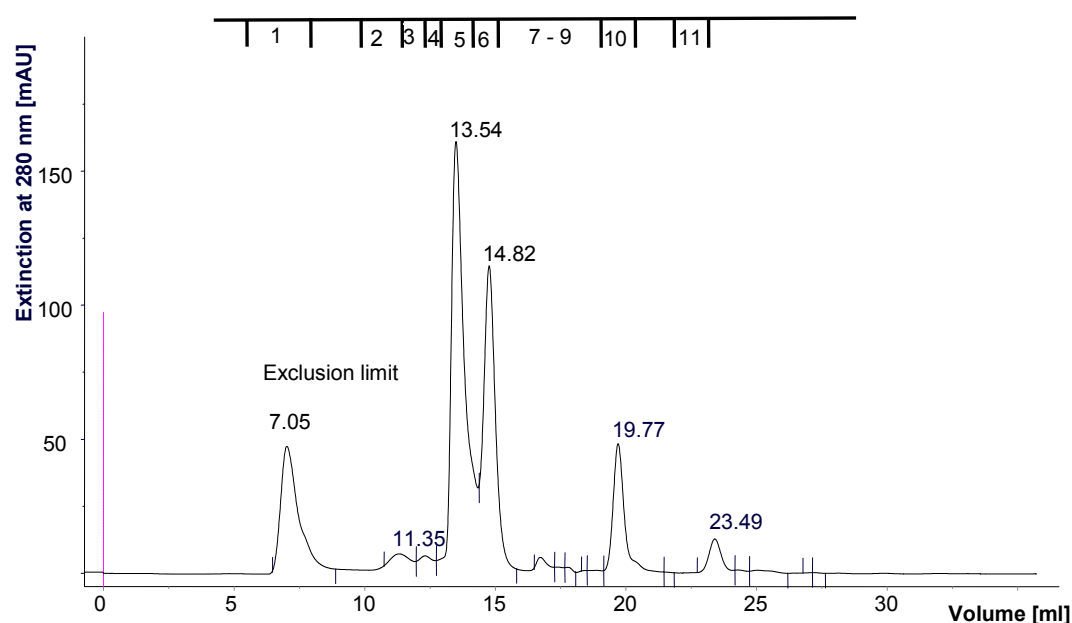
Figure 7-3: Chromatogram of a WPC 30 (c = 0.0693 g·10 ml^{-1})

The second peak after ~11.3 ml might be IgG and the third peak after ~ 12.3 ml might be BSA or combinations of both. Looking at the elution profiles of the BSA and IgG standards in Figure 12-2 in the Appendix it becomes obvious that there is an overlapping of the peaks; there is no clear separation.

β-Lg elutes in the fifth peak after ~ 13.6-13.7 ml. The sixth peak after ~ 14.7-14.8 ml corresponds to α-La in all chromatograms. These results correspond to WANG and LUCEY (2003), DE LA FUENTE et al. (2002), and LAW et al. (1993) [149;292;301].

Peaks 7 to 9 have not been identified yet. They correspond to minor components, e.g., lactose, peptides [149;301]. These minor components were found to be present at higher concentration in the low protein content WPC (< 34%, wt/wt, protein).

According to ANDREWS, TAYLOR, and OWEN (1985) who used the same column to separate native whey proteins, the peak around 19.7 ml—which is here peak 10— corresponds to orotic acid and another further peak, which eluted near the total column volume 23-24 ml and is here peak 11, corresponds to UV-active salts and/or vitamins [302].

The results of the HPLC analysis of selected WPCs of section I which are the relation of β-Lg/α-La, the β-Lg content as proportion of the protein content in % and the α-La content as proportion of the protein content in % are displayed in Table 7-5 and Table 7-6.

HPLC analysis was done of the native samples without any treatment, of the samples after protein fractionation at pH 4.6, and after clarification with chitosan. The protein fractionation at pH 4.6 was done to determine the influence of the pH (and perhaps the influence of a centrifugation step) on the occurrence of aggregate matter in comparison to the chitosan clarification. This allows the identification of the effect of chitosan alone because during clarification with chitosan the pH is reduced to 4.6 and a centrifugation step is done. HPLC analysis was undertaken to check whether the main whey proteins were influenced by chitosan clarification and/or pH 4.6.

Table 7-5: **HPSEC results of selected native WPC, section I**

	β-Lg/α-La -	β-Lg content, proportion of the protein content %	α-La content, proportion of the protein content %
WPC 35 1, native	1.95 ± 0.01	22.55 ± 0.04	11.59 ± 0.03
WPC 35 2, native	2.54 ± 0.02	37.62 ± 0.24	14.71 ± 0.00
WPC 35 3, native	2.87 ± 0.01	39.32 ± 0.23	13.72 ± 0.03
WPC 60 1, native	2.44 ± 0.01	34.70 ± 0.05	14.32 ± 0.07
WPC 60 2, native	2.61 ± 0.00	33.15 ± 0.16	12.69 ± 0.08
WPC 70 1, native	2.54 ± 0.02	44.28 ± 0.46	17.44 ± 0.29
WPC 80 1, native	3.73 ± 0.03	43.62 ± 0.35	11.69 ± 0.01
WPC 80 5, native	3.28 ± 0.02	40.15 ± 0.55	12.29 ± 0.22

Table 7-6: **HPSEC results of selected WPC after pH 4.6 and chitosan treatment, section I**

	β-Lg/α-La -	β-Lg content, proportion of the protein content %	α-La content, proportion of the protein content %
pH 4.6			
WPC 35 1, pH 4.6	1.98	21.56	10.91
WPC 35 2, pH 4.6	2.57	36.87	14.37
WPC 35 3, pH 4.6	3.06	43.57	14.23
WPC 60 1, pH 4.6	2.63	36.05	13.73
WPC 60 2, pH 4.6	2.76	34.65	12.55
WPC 70 1, pH 4.6	2.76	42.06	15.24
WPC 80 1, pH 4.6	4.05	39.76	9.82
WPC 80 5, pH 4.6	3.46	40.27	11.64
Chitosan treatment			
WPC 35 1, chitosan	1.91	21.06	11.05
WPC 35 2, chitosan	2.56	35.59	13.93
WPC 35 3, chitosan	2.91	43.99	15.1
WPC 60 1, chitosan	2.65	34.98	13.22
WPC 60 2, chitosan	2.73	34.32	12.57
WPC 70 1, chitosan	2.78	37.61	13.54
WPC 80 1, chitosan	4.16	44.58	10.72
WPC 80 5, chitosan	3.43	42.32	12.34

The concentration of the main whey proteins α-La and β-Lg is not very much effected by either pH 4.6 fractionation or chitosan treatment, Table 7-5 and Table 7-6. This result is in agreement with WANG and LUCEY (2003) [149]. These findings suggest that the HPSEC is able to detect the native whey proteins which are really solved and not part of aggregated matter.

The amounts of the main whey proteins of the WPC with high protein contents correspond to the data from literature. WANG and LUCEY (2003) stated an amount of β-Lg between 48-73 % and 15-21 % α-La for native WPI samples calculated from the total peak area [149]. The same results were reported by MORR and FOEGEDING (1990) [150]. They investigated WPCs with a protein content >70 % and found 40-76 % β-Lg and 14-24 % α-La.

The results of the HPLC analysis of native WPCs of section II which are the relation of β-Lg/α-La, the β-Lg content as proportion of the protein content in % and the α-La content as proportion of the protein content in % are displayed in Table 7-7. Additionally, the parameter in accordance with the NSI is listed.

Table 7-7:   **HPSEC results of WPC, section II**

Sample	β-Lg/α-La	β-Lg content, proportion of the protein content	α-La content, proportion of the protein content	NSI parameter	s
	-	%	%	%	%
WPC 30	1.64	19.92 ± 0.30	12.12 ± 0.13	65.7	0.57
WPC 35 8	2.01	24.60 ± 0.09	12.22 ± 0.43	64.4	0.06
WPC 35 9	3.46	42.60 ± 0.29	12.33 ± 0.17	86.8	1.68
WPC 35 10	2.9	41.06 ± 0.17	14.14 ± 0.09	93.86	0.24
WPC 35 11	2.9	42.05 ± 0.11	14.48 ± 0.04	94.0	2.70
WPC 35 12	2.47	36.37 ± 0.21	14.71 ± 0.28	88.9	0.16
WPC 35 13	2.49	37.34 ± 0.25	14.97 ± 0.17	97.4	1.04
WPC 35 14	2.69	41.09 ± 0.50	15.27 ± 0.19	95.7	0.94
WPC 60 6	2.58	37.25 ± 0.04	14.41 ± 0.06	94.29	2.60
WPC 60 7	2.41	37.30 ± 0.31	15.49 ± 0.24	85.9	1.16
WPC 80 6	3.26	43.93 ± 0.54	13.46 ± 0.12	89.9	0.05

The statement made on the parameter in accordance to the NSI in Table 7-3 that WPC 30 and WPC 35 8 have undergone serious changes during production (high degree of denaturation) is confirmed by the results of the HPSEC in Table 7-7 (highlighted in red). Here, especially the amount of β-Lg is reduced to about 20 % which is nearly the half of the content determined for the rest of the WPC.

If the results of section I are viewed, it can be assumed that WPC 35 1, which has also a very low content of the main whey proteins, would have also had a very low NSI. It can be assumed that those three powders have undergone critical changes during production. The connection to the results of the laser diffraction will be discussed below.

Figure 7-4 and Figure 7-5 display the chromatograms of two WPCs of the native sample, the sample treated with pH 4.6, and the chitosan treated sample.

E280 nm

Volume [ml]
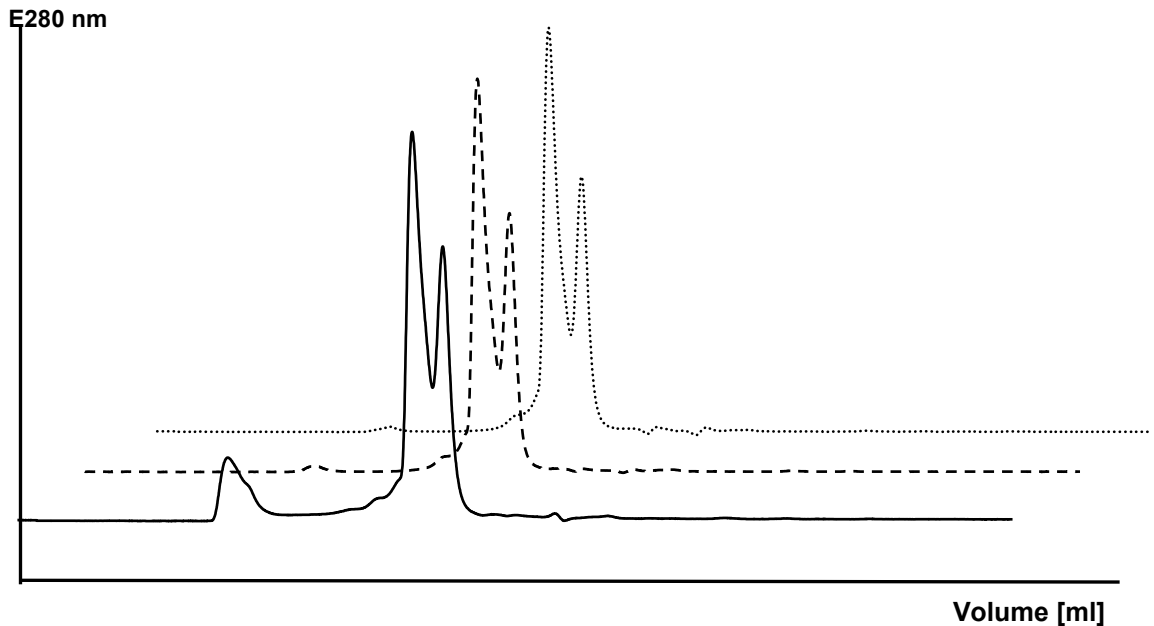
Figure 7-4:   **Chromatogram of WPC 80 1**
(_____) native, (- - - -) pH 4.6, (.......) chitosan treated

E280 nm

Volume [ml]
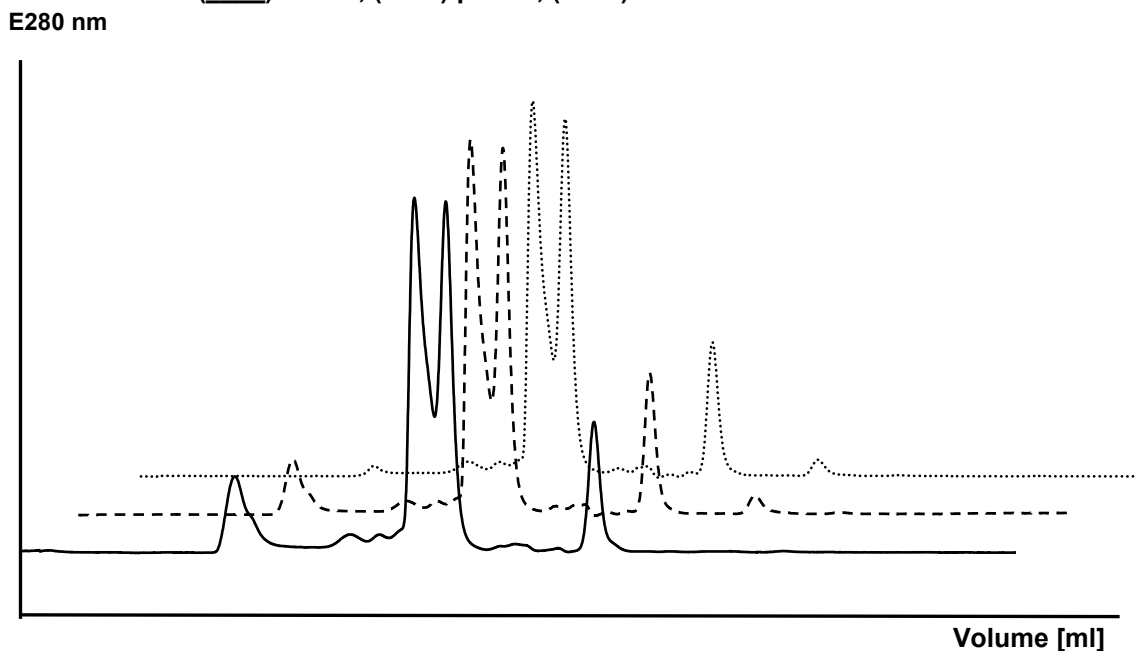
Figure 7-5:   **Chromatogram of WPC 35 1**
(_____) native, (- - - -) pH 4.6, (.......) chitosan treated

In the case of WPC 80 1 the exclusion limit became smaller due to pH 4.6 treatment. But no more reduction was achieved by means of chitosan treatment. In case of WPC 35 1 the exclusion limit became smaller due to pH 4.6 treatment. A high reduction was achieved by chitosan treatment. WANG and LUCEY (2003) also used chitosan clarification before multi-angle laser light scattering and size-exclusion chromatography [149].

These findings mention a nearly complete disappearance of peak 1 after chitosan treatment, which indicates that this peak consists of residual lipids which were mainly negatively charged, e.g., phospholipids. These lipids formed a complex with chitosan [149]. In the present study the information on the change of the exclusion limit during treatment of the samples may not be overrated because it was found that the HPLC column has a filtration effect itself, so that some fractions did not enter the column and did not become part of the analysis.

Overall, the area of the first peak was reduced by pH 4.6 treatment and chitosan treatment to a different degree. This effect was found for the selected WPCs except for WPC 35 1 and WPC 35 3. The area of the first peak of WPC 35 1 and WPC 35 3 was not effected by pH 4.6 treatment but decreased due to chitosan clarification. As long as denatured whey proteins are insoluble at pH 4.6 [148] a decrease in the exclusion limit might suggest a precipitation of denatured whey proteins.

HWANG and DAMODARAN (1995) analyzed the supernatant of chitosan treated whey by HPLC and found an identical profile in terms of number of peaks and peak area, except for a peak at the void volume of the column in the case of the untreated sample [217]. This high molecular weight species might be the result of the presence of smaller than 0.2 µm milk fat globule membrane (MFGM) fragments in the filtrate. It can be assumed that no soluble protein was lost during precipitation by chitosan. After the chitosan treatment some protein was lost (5 %)—determined by KJELDAHL—of the untreated whey and the supernatant. Lost protein might be lipoproteins associated with the MFGM fragments.

FERNANDEZ and FOX (1997) added chitosan to fractionate cheese whey and analyzed the supernatant and precipitate by Urea-PAGE, gel filtration chromatography, and HPLC [211]. With the help of chitosan (c = 0.01 %) it was possible to fractionate water-soluble peptides in cheese whey especially at pH 4.0. The amount of low-molecular weight peptides was higher in the supernatant, and high-molecular weight peptides were more present in the precipitate, proving the effect that chitosan is able to separate the aggregates from the WPC.

Figure 7-6 displays the chromatogram of the WPC 80 3 which—in comparison with the standards—contains only β-Lg.
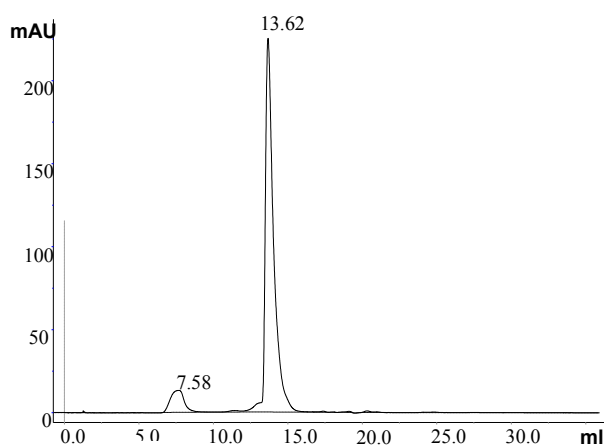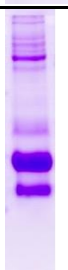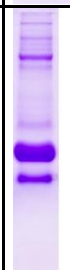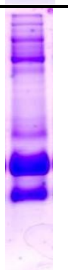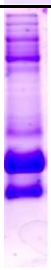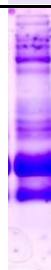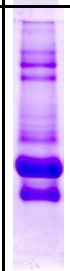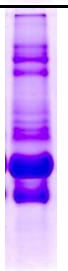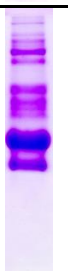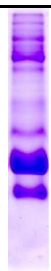
Figure 7-6:   Chromatogram of WPC 80 3

7.2.5 Protein profiles determined by SDS-PAGE
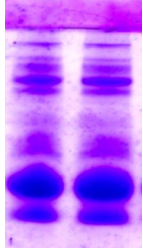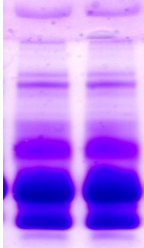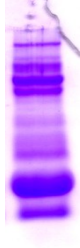
Table 7-8 displays the SDS-PAGE profiles of the analyzed whey protein powders. According to the molecular weight standard (Figure 4-2), the lower bands represent the β-Lg und α-La. Most of the WPC contain residual casein. The WPC 80 3 shows a diverging behavior. The strongest band can be attributed to β-Lg [191;303].

Table 7-8: SDS-PAGE profiles of the analyzed powders

In Table 7-9, Table 12-10, and Table 12-11 in the Appendix the SDS-PAGE profiles of selected samples are given. They were analyzed in native state, after adjustment to pH 4.6, and after treatment with chitosan. Here, the sediment and the supernatant after centrifugation were analyzed.

Table 7-9: SDS-PAGE profiles of WPC 35 1 after different pre-treatment

Sample	Native	pH 4.6	Chitosan Supernatant	Chitosan Sediment	
WPC 35 1					BSA Caseins β-Lg α-La

Especially for WPC 35 1, 35 2, 80 5, 60 1, and 60 2 it can be seen that after pH 4.6 treatment the amount of particles/proteins/bands in the range of large molecular weight are diminished. After chitosan treatment the supernatant nearly consists of α-La and β-Lg and BSA. It can be assumed that these proteins are dissolved because of the results from HPLC and laser diffractometry. The sediment contains the separated proteins, mainly high molecular weight proteins but also higher amounts of α-La and β-Lg. Our results prove that chitosan separates the lipids and additional proteins (even α-La and β-Lg). Those correspond to the larger aggregates because after chitosan treatment no undissolved particles were detected by laser diffractometry. But HPLC showed a constant native protein content, Table 7-5 and Table 7-6.

7.3 Physical analysis

7.3.1 Rheological measurements

The rheological method described here was not found to be very useful for the examination of the rehydration behavior of the protein powders. The analyzed powder concentrations of 2, 5, and 10 % are too small to detect huge differences during rehydration with the use of the torsion oscillator measurements. Although the rheological method was found to be efficient to detect deficits in fermentation processes it was not found to be sensitive enough to detect differences of the functional properties and the quality of the powders at an earlier stage, meaning prior to use. Results were therefore omitted.

7.3.2 Static laser light scattering

7.3.2.1 Optimization of the measuring method—dry measurements

Dry measurements were done under three different conditions: only vacuum, 0.1 MPa, and 0.3 MPa (air compression: high) to optimize the measurement method. It was assumed that the pressure used for the dispersion of particles may influence the particle spectrum leading to a better separation/isolation of the powder particles due to a needed input of energy. The impact of pressure on the particle size is described by statistical analysis of the D_{10}, D_{50}, D_{90}, the specific surface, and the standard deviation taken from the distribution function.

The D_{10}, D_{50}, D_{90}, the specific surface, and the standard deviation taken from the distribution based on volume are given in Table 12-12 (only vacuum), Table 12-13 (0.1 MPa), and Table 12-14 (0.3 MPa) in the Appendix. The values are averages of three replicates. The standard deviation for each parameter is given.

The statistical analysis regarding the influence of pressure on the parameter of the PSD leads to the conclusion that the pressure used to disperse the particles only has a significant effect on the D_{10}. This implies an influence of the pressure on the small particles (the left side) in the distribution function. With increasing pressure, the D_{10} decreases, leading to finer particles. The results of the statistical analysis are given in Table 12-15. The level of significance is α = 0.01; exceptions are indicated.

Because of the relatively small effect of the pressure on the parameter of the PSD it was set to 0.1 MPa during the following experiments.

7.3.2.2 Results of the dry measurements—Section I

In the case of dry measurements in section I a unimodal distribution is obtained for all analyzed protein powders. Table 7-10 displays the average values of the D_{10}, D_{50}, D_{90}, the specific surface and the standard deviation of the protein classes of section I.

Table 7-10: Average values of the D_{10}, D_{50}, D_{90} (µm), the specific surface (cm²·cm^{-3}), and the standard deviation (µm) of the WPC classes

	D_{10}	D_{50}	D_{90}	Spec. surf.	Std. dev.
only vacuum					
SWP 13	53.91	125.38	259.21	692.80	87.12
WPC 35	32.29	85.59	208.28	999.52	74.44
WPC 60	26.30	58.90	130.44	1309.37	44.67
WPC 70	22.99	48.78	92.95	1488.25	32.82
WPC 80	32.67	85.19	164.63	1127.16	55.71
	(27.58)	(57.90)	(115.25)	(1280.39)	(38.79)
0.1 MPa					
SWP 13	52.86	126.20	257.95	733.50	87.08
WPC 35	29.36	86.52	212.28	1065.19	76.70
WPC 60	23.08	55.01	127.93	1447.43	44.92
WPC 70	18.98	43.31	89.16	1733.25	32.88
WPC 80	28.68	83.08	165.37	1245.91	57.26
	(23.54)	(54.05)	(115.50)	(1422.14)	(40.53)
0.3 MPa					
SWP 13	52.14	128.55	264.32	916.50	89.44
WPC 35	28.27	86.93	209.92	1034.13	75.69
WPC 60	21.15	53.56	126.63	1531.80	44.65
WPC 70	17.75	42.32	90.43	1811.42	34.01
WPC 80	27.01	81.68	164.18	1303.20	57.09
	(21.92)	(52.58)	(115.11)	(1488.13)	(40.65)

Values in brackets are calculated without WPC 80 2

The results of the statistical analysis are given in Table 12-15 in the Appendix. The level of significance is α = 0.01; exceptions are indicated.

The influence of the protein content on the parameter taken from the PSD was found to be significant in the case of the D_{10}, D_{50}, D_{90}, specific surface, and standard deviation. The following statements can be made about the protein classes:

- On average, the D_{10}, D_{50}, D_{90}, and the standard deviation decrease with increasing protein content in the order: 13 > 35 > (80) > 60 > 70 (Table 7-10).

- On average, the specific surface increases with increasing protein content in the order: 13 > 35 > (80) > 60 > 70 (Table 7-10). The group of the WPC 80 behaves differently because of sample WPC 80 2. The powder WPC 80 2 differs in all values (Table 7-10), but rehydration behavior was found to be good, see below.

- If the contrast analysis is viewed in Table 7-11, which shows the significant differences (α = 0.01) in the D_{10}, D_{50}, D_{90}, specific surface, and standard deviation between each protein group, differences are significant between the lower protein contents 13 and 35, each compared with the higher protein contents. The differences between the higher protein contents are insignificant, thus indicating that the particle sizes of the powders with higher protein contents are very similar to each other.

Table 7-11: **Results of the contrast analysis regarding the protein content, section I**

	D_{10} μm	D_{50} μm	D_{90} μm	Spec. surf. $cm^2 \cdot cm^{-3}$	Std. dev. μm
SWP13/35	sig.	sig.	not sig.	sig.	not sig.
SWP13/60	sig.	sig.	sig.	sig.	sig.
SWP13/70	sig.	sig.	sig.	sig.	sig.
SWP13/80	sig.	sig.	sig.	sig.	sig.
35/60	sig.	sig.	sig.	sig.	sig.
35/70	sig.	sig.	sig.	sig.	sig.
35/80	not sig.	not sig.	not sig.	not sig.	sig.
60/70	not sig.	not sig.	not sig.	not sig.	not sig.
60/80	not sig.	not sig.	not sig.	not sig.	not sig.
70/80	sig.	sig.	not sig.	sig.	not sig.

No significant influence exists for the interactions of the protein content and the pressure, indicating that for each WPC between a group the influence of pressure acts in the same way.

7.3.2.3 Results of the dry measurements—Section II

During section II dry measurements were done from eleven more WPC with protein contents between 30 and 80 % at 0.1 MPa. Because of the small amount of WPC with a protein content of 60 % (N = 2) and 80 % (N = 1) the WPC of the first section were supplemented by the WPC of section II and a statistical analysis was conducted for the whole group. The results will be discussed below.

The D_{10}, D_{50}, D_{90}, the specific surface, and the standard deviation taken from the distribution based on volume are displayed in Table 12-16 in the Appendix. The values are averages of three replicates. The standard deviation for each parameter is given.

From these results it becomes clear that company B (WPC 30, 35 8-10) produces powders with a very uniform size. The size variations of the powders produced by company H (WPC 35 11-14, 60 6 and 7) are much larger and might indicate processing problems.

Most PSD were found to be unimodal with the exception of WPC 35 11, 13, 14, and 60 7. Here, bimodal distribution functions were detected, red curves in Figure 12-6 and Figure 12-7 in the Appendix.

If the WPC of section II are added to those of section I, the statistical analysis results in following statements: the protein content with the classes 13, 35, 60, 70, and 80 % is found to have a significant influence on the D_{50}, the D_{10}, and the specific surface (α = 0.05).

Overall, the D_{50} increases in the order 70 < 60 < 80 < 35 < 13; the D_{10} increases in the order 70 < 60 < 35 < 80 < 13 and the specific surface increases in the order 13 < 35 < 80 < 60 < 70. Thus, the same trend as in section I was found.

Table 7-12 lists the results of the contrast analysis. Here, the most significant differences (α = 0.01) are present between the low protein WPC and those with higher protein content. The particle sizes of the WPC having higher protein contents (60-80 %) show no significant differences.

Table 7-12: **Results of the contrast analysis regarding the protein content, section II**

| | D_{10} | D_{50} | Spec. surf. |
	µm	µm	cm²·cm⁻³
SWP13/35	sig	not sig.	not sig.
SWP13/60	sig	sig	sig
SWP13/70	sig	sig	sig
SWP13/80	sig	sig	sig
35/60	not sig.	not sig.	not sig.
35/70	sig	sig	sig
35/80	not sig.	not sig.	not sig.
60/70	not sig.	not sig.	not sig.
60/80	not sig.	not sig.	not sig.
70/80	sig	not sig.	not sig.

7.3.2.4 Optimization of the measuring method—wet measurements

Measurement of raw materials

Static laser light scattering measurements were done on raw milk, commercial milk, and whey to obtain more information about the raw materials. Figure 7-7 displays the PSD of raw milk and contains the parameters D_{10}, D_{50}, D_{90}, and specific surface taken from the PSD with a refractive index of 1.52/0.

	D_{50} µm	D_{10} µm	D_{90} µm	specific surface cm²·cm⁻³
$\bar{x}$	3.822	2.491	6.003	16678
$\pm$	0.500	0.234	1.081	2024
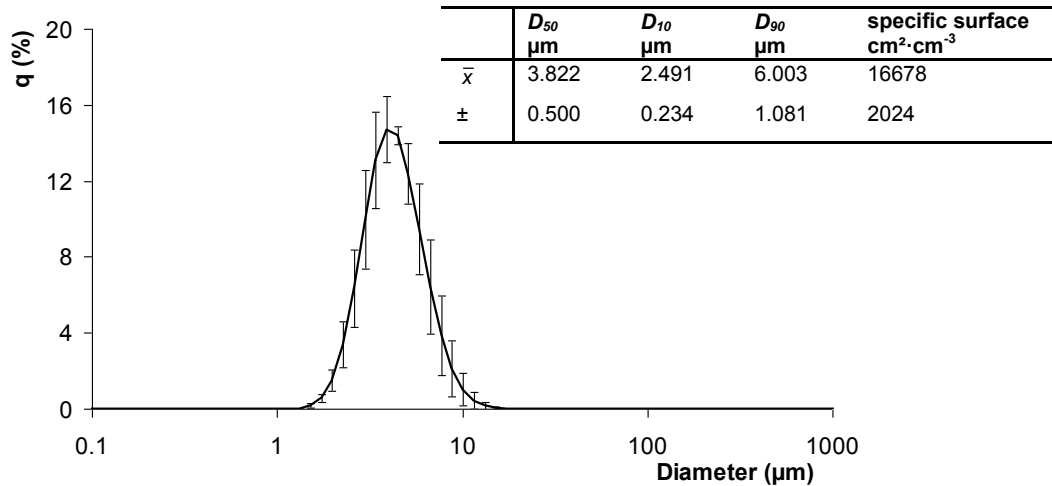
Figure 7-7:   **PSD and parameter calculated from the PSD of raw milk with fat (N = 3)**

On average of three replicated measurements the milk fat globules of unprocessed raw milk have a D_{50} of 3.8 ± 0.5 µm and a D_{90} of 6.0 ± 1.1 µm which corresponds to literature data [14;304].

The unimodal size distribution contradicts the results obtained by SAVEYN et al. (2006) [249]. They analyzed the particle size distribution of raw milk by laser diffraction and time-of-transition using a refractive index of 1.472. The laser diffraction revealed a bimodal distribution with modal diameters of 0.28 µm and 3.95 µm which were attributed to casein micelles and fat, respectively. The time-of-transition principle resulted in a unimodal distribution with a modal diameter of 4.47 µm. SAVEYN et al. (2006) [249] stated that time-of-transition was not able to detect the submicron casein micelles but laser diffraction was. The present results—even if the scatter patterns are deconvoluted using 1.472 instead of 1.52—show only a unimodal size distribution. This difference might be related to the larger size of the fat droplets in the present study which might have been dominating the PSD.

Figure 7-8 displays the PSD and parameter calculated from the PSD of commercial milk (1.5 % fat, homogenized, pasteurized; N = 3) which has a bimodal shape in comparison with raw milk, Figure 7-7. The obtained PSD of pasteurized milk corresponds to PSD of UHT milk [305]. The first peak which has a D_{50} of 0.16 µm can be related to casein micelles [249]. According to TÖPEL (2004) homogenization reduces the size of the fat droplets below 2 µm [14]. Therefore, peak 2 with a D_{50} of 0.94 µm can be very likely attributed to homogenized milk fat droplets.

	D_{10} µm	D_{50} µm	D_{90} µm
$\bar{x}$ Peak 1	0.09	0.16	0.30
±	0.00	0.00	0.02
$\bar{x}$ Peak 2	0.66	0.94	1.42
±	0.00	0.01	0.02
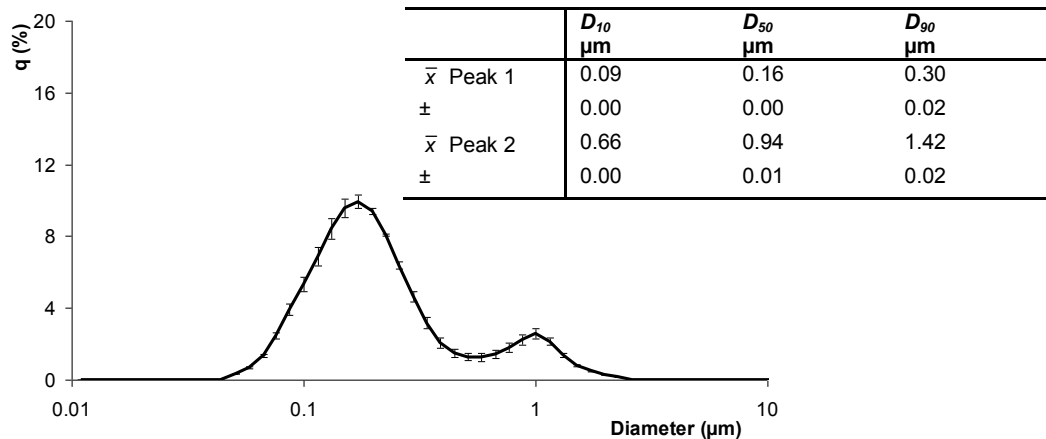
Figure 7-8: **PSD and parameter calculated from the PSD of commercial milk**

Figure 7-9 displays the PSD of thin whey, whey concentrate, and final mixed whey for the production of whey products. Values are means of $N = 2$, 4, and 2 replicates.
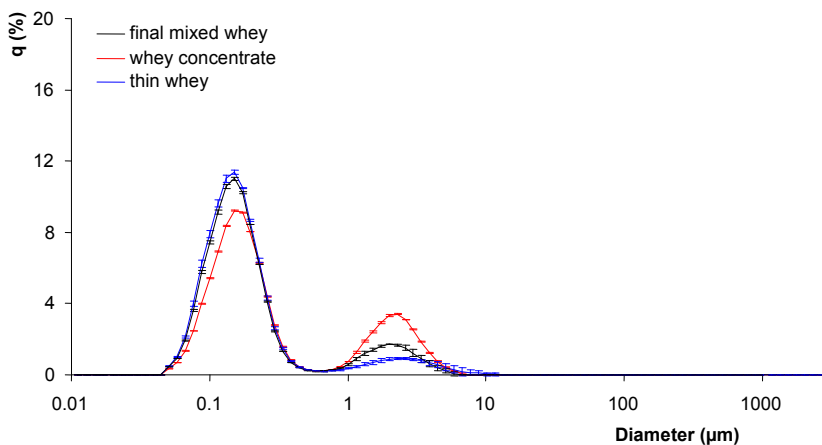
Figure 7-9: **PSD of thin whey, whey concentrate, and final mixed whey**

It can be concluded from Figure 7-9 that the volume concentration of the second peak increases with thermal treatment which is also proved by the share of the first peak taken from Table 12-17 in the Appendix. Here, the share of the first peak is 85.23 % for the thin whey which decreases to 72.95 % for the whey concentrate. This result proves the hypothesis that the volume concentration of peak 2 is detrimental in assessing the solubility/thermal treatment/denaturation of dairy powders because it increases in the course of thermal treatment.

The PSD of the thin whey can be used for comparison of the PSD of dairy powders after rehydration because a change points at processing-related influences for example heat treatment. Furthermore, D_{90} values larger than 3.4 µm can be attributed to severe heat treatment, Table 12-17.

Table 12-18 in the Appendix displays the measurement results of the final mixed whey after different periods of time which gives an indication of the fluctuations in particle size of the whey. It can be seen that the largest fluctuations occur for the D_{90} of the second peak.

pH 4.6 treatment

DE WIT (1998) attributed a reduced solubility (determined at pH 4.6) to whey protein denaturation, which was usually a result of evaporation and drying of whey protein products [146]. As a consequence it might be possible to remove denatured whey proteins and caseins by means of pH 4.6 treatment to gain further information about peak composition/classification.

Table 7-13 displays the D_{10}, D_{50}, and the D_{90} of peak 1 and 2 after the adjustment of the sample to 4.6, centrifugation and re-adjustment of the pH to 7.0.

Table 7-13: *D_{10}, D_{50}, and D_{90} (µm) of peak 1 and 2 after pH 4.6 treatment*

	Peak 1			Peak 2		
	D_{10}	D_{50}	D_{90}	D_{10}	D_{50}	D_{90}
SMP	0.132	0.212	0.315	-	-	-
	0.130	0.206	0.304	2.635	3.899	5.754
WPC351	0.080	0.146	0.277	0.830	1.520	3.032
	0.078	0.139	0.264	0.648	1.073	1.981
WPC352	0.077	0.127	0.207	1.131	1.784	2.818
	0.072	0.119	0.207	0.697	1.097	1.875
WPC353	0.084	0.145	0.246	0.869	1.470	2.557
	0.077	0.128	0.216	0.785	1.225	1.946
WPC601	0.073	0.121	0.213	0.638	0.966	1.484
	0.073	0.124	0.222	0.660	1.038	1.762
WPC602	0.087	0.157	0.274	1.229	2.170	3.785
	0.080	0.145	0.271	0.791	1.227	2.039
WPC603	0.086	0.150	0.253	0.918	1.712	3.376
	0.087	0.151	0.254	0.874	1.632	3.241
WPC701	0.087	0.142	0.219	2.355	3.945	6.661
	0.086	0.142	0.224	1.860	3.005	4.831
WPC801	0.152	0.251	0.365	2.726	4.372	6.789
	0.147	0.238	0.345	2.523	3.959	6.071
WPC805	0.116	0.301	0.639			
	0.135	0.227	0.361	0.804	1.241	2.189

In comparison to the untreated, native samples (Table 12-19, Table 12-20, Table 12-21, and Table 12-22) the following changes occur due to pH 4.6 treatment: no very large particles are detectable and in most cases D_{10}, D_{50}, and D_{90} of peak 1 and 2 are smaller after pH 4.6 treatment. If the results are compared to the native whey (Figure 7-9 and Table 12-17) the results of the dairy powders after pH 4.6 treatment (Table 7-13) are very similar to those of the native whey indicating the removal of larger aggregates. This hypothesis becomes particularly clear when Figure 7-10 is viewed.
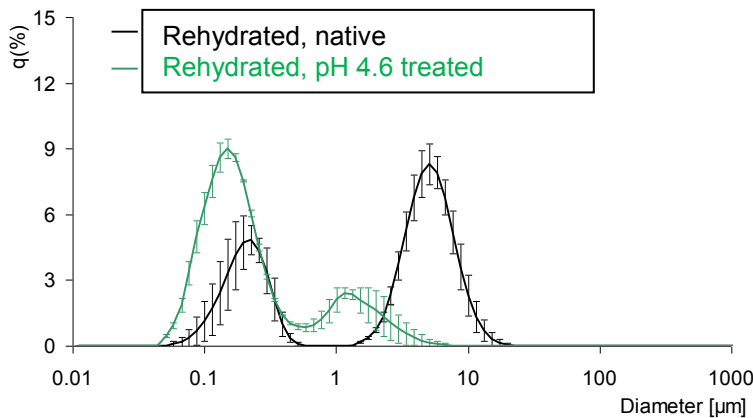
Figure 7-10: **PSD of native and pH 4.6 treated WPC 35 1**

Figure 7-10 displays the PSDs of the native WPC 35 1 and after pH 4.6 treatment. WPC 35 1 is one powder which has a high volume concentration of peak 2 and a reduced concentration of β-Lg (Table 7-5) and is therefore assessed to have a reduced functionality. The shift of the PSD due to pH 4.6 treatment to smaller particle sizes and the simultaneous reduction of the volume concentration of peak 2 point at the removal of large aggregates.

Figure 7-11 displays the volume distributions of the native, rehydrated WPC 60 3, WPC 70 1, and the SMP and the sediment and supernatant after pH 4.6 treatment, respectively.
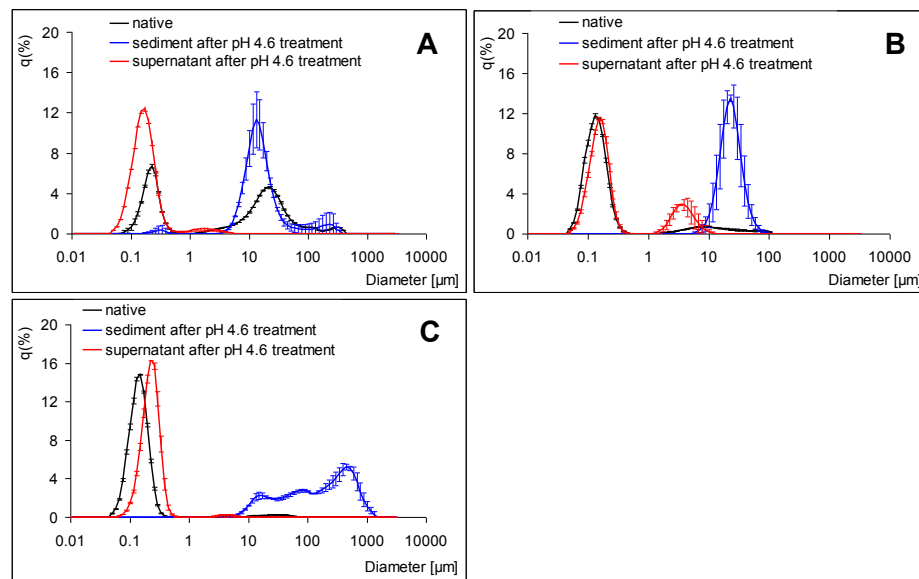
Figure 7-11: **PSD of the native, rehydrated sample, sediment and supernatant after pH 4.6 treatment; A: WPC 60 3, B: WPC 70 1, C: SMP**

For samples WPC 60 3 and SMP the volume distribution of the supernatant after pH 4.6 treatment looks very similar to those of native whey (Figure 7-9) with its bimodal shape and a very large peak in the area of small particle sizes around 0.1 µm and a smaller peak around 2-4 µm. Even the values of D_{10}, D_{50}, and D_{90} of peak 1 and peak 2 are very similar for the different WPCs and the SMP, see Table 7-13. After pH 4.6 treatment a more uniform volume distribution is obtained and particle sizes > 10 µm are no longer present. The sediment after pH 4.6 treatment contains larger aggregates and caseins. The figures display a peak in the area of larger particle sizes (> 10 µm).

Verification of the refractive index used

A problem which has to be discussed and solved before taking measurements is the choice of the refractive index, especially if submicron particles are present in the sample. The scattering patterns of the wet measurements are deconvoluted according to MIE. The MIE theory requires the knowledge of various optical parameters which are the complex refractive index comprising a real part representing the refractive properties of particle and medium and an imaginary part.

For the dairy powders, especially for those containing whey proteins as the dominating protein fraction, it is very difficult to determine the precise refractive index because of the variability of the composition.

There are whey proteins, remaining caseins/casein micelles, fat droplets, and aggregates of proteins which might be present in different degrees. Additionally, no exact published data exist. Generally, the following sizes of the main milk proteins were reported: casein micelles with a mean diameter of 100 nm, radius of the whey proteins: α-La 1.8 nm, diad-axis of β-Lg (occurring as a dimer) 3.5 nm, radius of BSA 4 nm, and tetrad axis of IgG 6 nm [306-309].

Additional to the considerations made above, the LA-950 software provides two different calculations—χ^2 and R—to quantify both the quality of the raw data and the calculation of the reported particle size distribution using the chosen real and imaginary parts of the refractive index. These calculations compare the measured raw data in each channel (i.e., detector) to the amount of light scattering predicted for the reported PSD. A lower value for either χ^2 or R parameters indicates a more appropriate fit of the raw data to the calculated PSD [310].

$$\chi^2 = \sum \left\{ \frac{1}{s_i^2} \left[z_i - z(x_i) \right]^2 \right\} \qquad \qquad \textbf{Equation 7-1}$$

$$R = \frac{1}{N} \sum_{i=1}^{N} \left\{ \frac{1}{z(x_i)} \left| z_i - z(x_i) \right| \right\} \qquad \qquad \textbf{Equation 7-2}$$

χ^2 and R indicate the degree of similarity between the refractive index used to produce the particle size distribution calculation result and the actual scattering data measured at each channel of the detector. The closer to "0", the greater the similarity.

In combination with the calculations provided by the software and the SEM imaging method the real and imaginary part of the refractive index were optimized and resulted in a real part of the refractive index of 1.52 and 0 for the imaginary part of the refractive index. The cumulative PSD obtained from the SEM micrographs and that of the laser diffraction using 1.52 as a real and 0 as an imaginary part of the refractive index of WPC 35 12 are displayed in Figure 7-12.
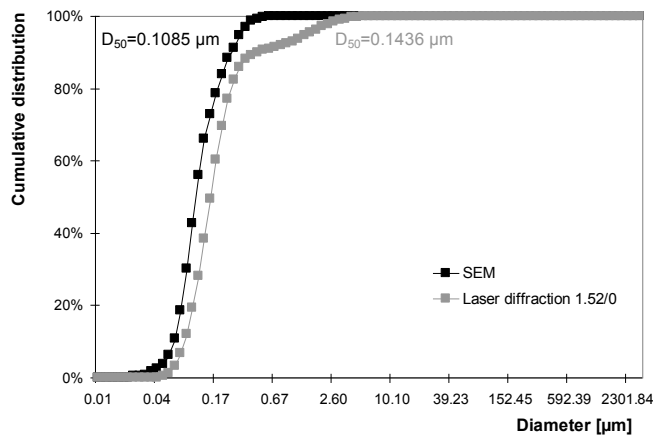
Figure 7-12: Cumulative PSD obtained by SEM micrographs and laser diffraction; WPC 35 12

Differences in the cumulative PSD between the both methods—SEM and laser diffraction—are visible. The D_{50} is 0.1085 µm in the case of SEM and 0.1436 µm in the case of laser diffraction using 1.52 and 0 as real and imaginary part of the refractive index, respectively.

The most important difference between both methods is the fact that the results of the SEM are based on particle number whereas the results of laser diffraction are volume based. As a consequence the PSD is bimodal in the case of laser diffraction, Figure 7-13 B. Peak 2 has a D_{50} of about 1.6 µm.

Figure 7-13 displays the SEM micrograph of the rehydrated and dried WPC 35 12 (A) and the PSDs of the dry sample and the sample after the start of rehydration (1 min) and the end of rehydration (24 h) (B).
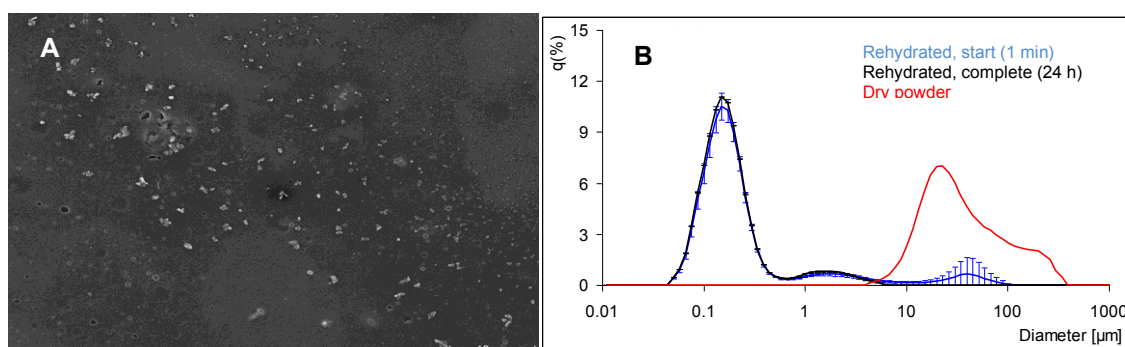
Figure 7-13:   SEM micrograph of WPC 35 12 (A) and PSDs during rehydration (B)

SEM was chosen to verify the results of the laser diffractometry.

From the micrograph in Figure 7-13 A it becomes obvious that WPC 35 12 contains not only small particles. Some particles with a size of about 2 µm are visible but they are present in small number. If the number-based PSD is calculated, only particles of high number contribute to the PSD.

Additionally, the sample preparation for the SEM requires a drying of the rehydrated samples plus a sputtering under vacuum which might have caused shrinkage of the particles. The protein particles in a wet state measured with laser diffraction might have a higher volume due to hydration. Furthermore, the sample preparation, in particular the dosage of the small sample amount (7 µl) with a plunger lift pipette for the SEM, might have caused shearing and therefore smaller protein particles.

POSTE and MOSS (1972) proposed a refractive index between 1.3-1.6 for proteins based on ellipsometry measurements of protein film [311]. Those values correspond to the results of VOROS (2004) [312].

The refractive index used to deconvolute the scattering patterns contradicts results obtained by KENNEL (1994) who investigated the size and structure of whey protein aggregates by laser diffraction (LS130 by the company Coulter Electronics GmbH) with a measuring range of 0.1-1000 µm and SEM [313]. It was found that for large aggregates a refractive index of 1.45 was suitable and for small aggregates a refractive index of 1.37 was used for the calculation of the PSD. Nevertheless, the laser diffraction apparatus used was only able to detect particles >100 nm. The measuring range of the new apparatus is much lower.

Additionally, KENNEL (1994) did not take into consideration that the SEM distributions are based on number and the laser diffraction results are based on volume [313]. They chose the refractive index which fitted the data best, but still huge differences occurred in the distributions.

Figure 7-14 displays the SEM results of WPC 30 and WPC 35 8 which were both characterized by a high volume concentration of peak 2 in the PSD (Table 12-26). In comparison to Figure 7-13 larger aggregates are present in the samples. These results qualify the statements made on the basis of laser diffraction analysis.
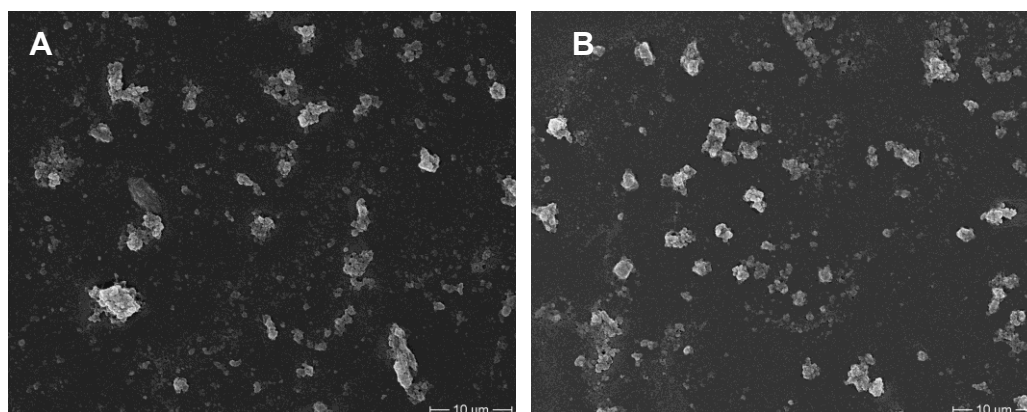
Figure 7-14: **SEM micrographs**
A: WPC 30; B: WPC 35 8

Sample amount used to measure the particle spectrum

Due to the specifications of the instrument used, the amount of the particles analyzed within a measurement cannot be counted. Therefore, in section I the amount of sample (10 % powder in double-distilled water) was measured by a graduated pipette which was necessary to obtain the optimal transmission of the laser. In section II the powders were directly dosed into the wet measurement unit and the exact powder amount was weighted. The data are given in Table 7-14 for section I and in Table 7-15 for section II.

Table 7-14: **Sample amount and fat content of selected powders of section I**

Sample	131	SMP	80 3	80 2	35 1	70 1	60 3	60 1	80 1
Average of the sample amount (c = 10 %)(ml)	16	1.5	7.5	3	2.5	6.5	2.0	0.75	1.5
Fat content (%)	0.5	0.96	0.89	2.19	2.81	3.18	3.72	4.71	6.30

Table 7-15: **Sample amount and fat content of powders of section II**

Sample	Average of the sample amount g	Fat content %
WPC 30	0.076 ± 0.014	1.7
WPC 35 8	0.057 ± 0.008	2.4
WPC 35 9	0.200 ± 0.005	2.5
WPC 35 10	0.146 ± 0.022	3.45
WPC 35 11	0.358 ± 0.043	2.25
WPC 35 12	0.298 ± 0.026	1.88
WPC 35 13	0.306 ± 0.058	2.25
WPC 35 14	0.348 ± 0.005	1.6
WPC 60 7	0.132 ± 0.010	3.75
WPC 60 6	0.164 ± 0.009	2.63
WPC 80 6	0.084 ± 0.004	6.00

It can be clearly seen that for SWP 13 1 nearly the twentyfold amount of sample has to be inserted compared to WPC 60 1.

In section I the amount of sample decreased with increasing fat content. The samples WPC 60 1 and 70 1 behaved somewhat differently. For WPC 70 1 more sample had to be inserted and for WPC 60 1 a lesser amount had to be inserted than expected from the fat content. It can be assumed that other factors—perhaps the number of aggregate particles—would have had an additional influence on the sample amount. For example, WPC 70 1 has a third peak and WPC 60 1 does not.

Moreover, the SMP behaves differently. Here, a lesser amount of sample had to be inserted than expected from the very low fat content. But SMP differs in composition from the other WPC. It contains more casein which might have an additional effect on the sample amount used.

When the results of section II are viewed in Table 7-15 it becomes clear that the amount of dosed sample is not dependent on the fat content which is due to the relatively low differences in fat content between the samples, with the exception of WPC 80 6. Samples WPC 30 and 35 8 attract—in turn—attention by the very low amount of dosed sample, thus proving the hypothesis that these are powders with reduced functionality.

7.3.2.5 Results of the wet measurements

The investigation of the rehydration behavior and the determination of the particle size of the rehydrated dairy powders was of main interest in the present work. Here, the PSD of the dairy powders was analyzed after different times of rehydration.

In contrast to the mainly unimodal PSD of the dry powders after rehydration—in most cases—a bimodal or multimodal distribution resulted. The LA-950 software allows the immediate examination of the individual peak on the basis of the multi modal report. In the following, the peak with the smaller particle size is called peak 1 and the peaks in the area of larger particles are called peak 2 and peak 3, respectively.

Influence of rehydration time and protein content on the parameters taken from the PSD

The impact of the rehydration time and the protein content on the particle size is described by statistical analysis of the D_{10}, D_{50}, D_{90} of peaks 1 and 2 taken from the samples which were analyzed immediately, after 10 min, and after complete rehydration. It was hypothesized that rehydration of the powders is a time-dependent process and that the production of dairy powders with higher protein content would involve an increased heat treatment leading to larger particle sizes due to heat denaturation.

The D_{10}, D_{50}, and the D_{90} of the distribution are given in Table 12-19 and Table 12-20 for Peak 1, in Table 12-21 and Table 12-22 for Peak 2, and in Table 12-23 for Peak 3 in the Appendix.

The particle spectra of nearly all powders are altered during rehydration especially in the area of particles with larger diameter. Most of the powders were found to have rehydration kinetics showing immense changes in the frequency of the single peaks. The powders with rehydration kinetics have a multimodal distribution.

The results of the statistical analysis which point at the influence of the rehydration time and protein content on the parameter taken from the PSD are given in Table 7-16 (α = 0.01).

Table 7-16:   Results of the statistical analysis

	Rehydration time	**Protein content**	**Interaction**
D_{10} Peak 1	Sig.	Sig.	Not sig.
D_{50} Peak 1	Sig.	Sig.	Not sig.
D_{90} Peak 1	Sig.	Sig.	Not sig.
D_{10} Peak 2	Sig.	Sig.	Sig.
D_{50} Peak 2	Sig.	Sig.	Sig.
D_{90} Peak 2	Sig.	Sig.	Sig.

The following statements can be made on the basis of the statistical analysis for the distribution based on volume:

The rehydration time has a significant influence on all dependent variables of the first and second peak (α = 0.01), thus pointing to the very diverging progress of the rehydration and supporting the hypothesis that rehydration of dairy powders is a time-dependent process. Contrast analysis was done to detect differences within the steps of rehydration. For this purpose, the parameters of the distribution curves are compared between the start of rehydration and 10 min of rehydration, between the start of rehydration and full rehydration, and between 10 min of rehydration and full rehydration. The results are displayed in Table 12-24 in the Appendix. Most of the differences are significant for α = 0.01 indicating that huge changes occur during rehydration. The powders have not reached a solvation balance/a constant particle size after 10 min. The progress of rehydration is continuous.

The protein content has a significant influence on all dependent variables of the first and second peak (α = 0.01), indicating that the distributions and the particle parameter are characteristic for the protein content. Overall, after complete rehydration the D_{10}, D_{50}, and the D_{90} of peak 1 increase in the order 70 < (80 without WPC 80 3) < SWP < 35 < 60 < 80 and the D_{10}, D_{50}, and the D_{90} of peak 2 increase in the order 80 < 70 < SWP < 35 < 60. The significant differences between the protein classes were analyzed by contrast analysis and are displayed in Table 12-25 in the Appendix. Most of the pairwise comparisons are significant (α = 0.01). Nevertheless, there is no definite trend that the particle size after rehydration increases with increasing protein content. The hypothesis that a higher protein content is—by all means—accompanied by a high degree of denaturation has to be disproved.

Variations in protein content and protein solubility were attributed to several processing parameters such as heat treatments (multiple pasteurizations, hot well holding, evaporation, spray dryer chamber), increases in osmotic strength during concentration, pH changes, and contributions from different cheese cultures and manufacturing procedures [295].

As a consequence, a positive correlation between protein content and protein solubility was found for SWP but also several samples with a high protein content exhibited low protein solubility.

The interaction between the protein content and the rehydration time is significant in the case of peak 2 (α = 0.01), indicating that the rehydration behavior exemplarily for the development of the particle size in peak 2 is linked to the protein content.

Influence of the protein content on the volume concentration

During rehydration the volume concentration [V.c.] (%) of peak 1, peak 2, and peak 3 change. Table 12-26 in the Appendix displays the development of the volume concentration of the peaks after different times of rehydration. However, it has to be taken into consideration that because of the percentage distribution of the PSDs frequency data have to be handled with care. Nevertheless, an attempt is made to assess the solubility and the degree of denaturation of the powders on the basis of the V.c. of the individual peaks.

In section 'Influence of rehydration time and protein content on the parameters taken from the PSD' the hypothesis that a higher protein content is—by all means— accompanied by a high degree of denaturation was disproved. Thus, the hypothesis has to be stated that independently of the protein content a high degree of denaturation causes a high volume concentration of the second peak in the PSDs.

Volume concentrations of the second peak larger than 60 % were found to be critical especially if they persist over the rehydration time. Those powders have to be assessed to possess a low solubility and a high degree of denaturation.

The following statements can be made on the development of the volume concentration of the individual peaks during rehydration:

1. The volume concentration of peak 1 increases.

2. The volume concentration of the peak 2 and 3 decreases.

This proves the assumption that the primary powder particles (peak 3) are dissolved and peak 1 and peak 2 are formed.

Statistical analysis was done to identify the influence of the protein content on the volume concentration of peak 1 and 2 after the start of rehydration and full rehydration. It was found that the protein content significantly influences the volume concentration of peak 1 (α = 0.01) and peak 2 (α = 0.05) at the beginning of the rehydration (1 min). The influence did not become significant after rehydration for the volume concentrations of both peaks.

Contrast analysis showed a significant difference of the volume concentration of peak 1 between the protein contents 60/70, 13(SWP)/70, and 13(SWP)/80 (α = 0.01) and 13(SWP)/35, 35/70, and 60/80 (α = 0.05). Contrast analysis showed a significant difference of the volume concentration of peak 2 between the protein contents 60/70, 13(SWP)/70 (α = 0.01) and 13(SWP)/35, 13(SWP)/80 (α = 0.05).

Average values of the volume concentration of peak 1, at the start are 18.8 % for SWP 13, 58.1 % for WPC 35, 43.0 % for WPC 60, 83.0 % for WPC 70, and 74.4 % for WPC 80. Average values of the volume concentration of peak 2, at the start are 65.7 % for SWP 13, 31.0 % for WPC 35, 48.2 % for WPC 60, 8.5 % for WPC 70, and 23.7 % for WPC 80.

Although contrast analysis is not statistically significant between all protein contents, the results suggest that volume concentration of peak 1 becomes smaller for lower protein contents and the volume concentration of peak 2 increases with decreasing protein content.

Considering the hypothesis that low soluble protein powders possess a high volume concentration at peak 2, it can be concluded that powders with lower protein content have on average a lower solubility after 1 min. This statement should be relativized due to the fact that this influence is only statistically significant for the initial stages of rehydration. After a long period of rehydration (24 h) the influence of the protein content on the volume concentration of peak 1 and 2 is not significant. Here, the volume concentration is no longer influenced by the protein content. Now, the effect of the differing solubilities and the degree of denaturation becomes the driving force.

On the basis of the volume concentrations after 10 min of rehydration in Table 12-26 it becomes obvious that the results are comparable to the results obtained after 24 h. This substantiates the statement that the laser diffraction method can be used as a rapid control method giving information about the solubility and the degree of denaturation after a short time period.

Determination of state of equilibrium during hydration

In the section 'Influence of rehydration time and protein content on the parameters taken from the PSD' the hypothesis that rehydration of dairy powders is a time-dependent process was proven. Here, the exact time is determined which is necessary to reach a state of equilibrium during rehydration.

The D_{50} of the WPC of section II in the course of rehydration after start, 10, 30, 60, 240 min, and 24 h of peaks 1 and 2 was statistically analyzed for the determination of significant differences. The rehydration time was found to have significant influence (α = 0.01) on the D_{50} of both peak 1 and peak 2. The results of the contrast analysis can be taken from Table 7-17. Here, a pairwise comparison of the D_{50} after different rehydration time was made. Because the differences are significant between 30 min and 24 h and 60 min and 24 h for both peaks, it can be assumed that the rehydration process has not been completed and continues. Only the difference of the D_{50} after 240 min and 24 h is not significant, indicating that state of equilibrium regarding the rehydration has been reached after 240 min.

It is also striking to observe that in the case of peak 1 significant differences occur for longer rehydration time but not between the start and 10 min, 30 min, and 60 min, indicating that changes of peak 1 take place in a time-delayed manner.

Table 7-17: **Results of the contrast analysis regarding the rehydration time, section II**

Pairwise comparison	$D_{50,\ Peak\ 1}$ µm	$D_{50,\ Peak\ 2}$ µm
Start_10	not sig.	sig.
Start_30	not sig.	sig.
Start_60	sig. (α =0.05)	sig.
Start_240	sig.	sig.
Start_24	sig. (α =0.05)	sig.
10_30	not sig.	not sig.
10_60	not sig.	not sig.
10_240	sig.	not sig.
10_24	sig.	not sig.
30_60	not sig.	not sig.
30_240	sig.	not sig.
30_24	sig.	sig.
60_240	sig.	not sig.
60_24	sig.	sig.
240_24	not sig.	not sig.

Skim milk powder (SMP)

From the protein content the SMP was classified to the WPC 35 group. But differences exist. It has to be considered that the protein composition of the SMP is totally different and consists mainly of caseins. The PSDs of SMP after the start and at complete rehydration ($N = 3 \pm s$) are displayed in Figure 7-15. The distribution of the dry powder is given in red.
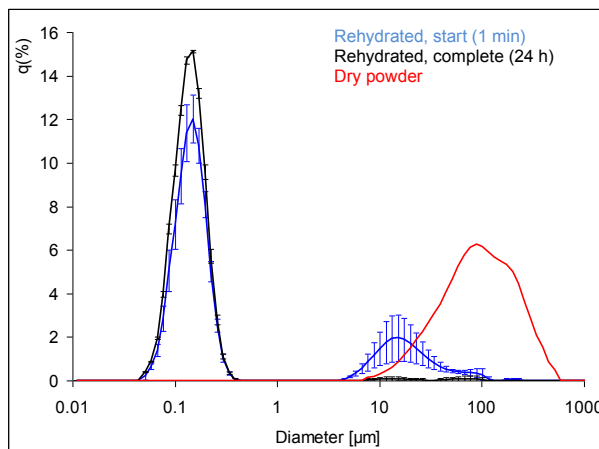
Figure 7-15: **PSD of the SMP after the start and complete rehydration ($N = 3 \pm s$); the distribution of the dry powder is given in red**

Contradictory to our results no submicron peak was observed in the recently published study of MIMOUNI et al. (2009) [257]. In this study the rehydration behavior of spray-dried milk protein concentrate containing at least 70 % casein was investigated by laser diffraction using a refractive index of 1.57. A bimodal size distribution with sizes from 60-500 µm after 10 min of rehydration at 24 °C was detected. The smaller peak was attributed to primary powder particles (30-37 µm) produced by atomization in the spray dryer and the larger peak was due to agglomerated powder particles.

In the present study a submicron peak was detected plus two further peaks at the beginning of rehydration, one being in the size range of the dry powder particles, intersection in Figure 7-15.

The third peak was attributed to primary powder particles which dissolve during rehydration. This was also observed by MIMOUNI et al. (2009) [257]. In the case of SMP after rehydration only a small volume concentration remained for the third and second peak, Table 12-26, and peak 1 reached nearly 100 %.

The third peak has a volume concentration of about 2.4 % after 10 min and disappears after 15 min. After 60 min the volume concentration of peak 2 reaches a constant level of about 3-4 % which remains constant up to 24 h. MIMOUNI et al. (2009) reported that 5 % of undissolved material was still present after 480 min rehydration time but the dissolution was considered to be complete because no further changes occurred [257]. On this basis the dissolution of the SMP was completed after 60 min which is much shorter compared to the studies of MIMOUNI et al. (2009) and GAIANI et al. (2007) who found that dissolution took up to 807 min [186;257].

7.4 Discussion of the results of the chemical and physical analysis

7.4.1 Rehydration behavior of dairy powders

Generally, the rehydration time was found to have a significant influence on the particle size of all WPC and the SMP of the present study. This indicates that the state of equilibrium was not reached immediately after rehydration but took up to 24 h in some cases. Statistical analysis of the WPC of section II proved that rehydration was completed by 240 min because the difference between the D_{50} of peak 1 and 2 was no longer significant. In the literature no data were found for rehydration times of WPC powders. Only some data exist for the dissolution of casein-based powders. MIMOUNI et al. (2009) and GAIANI et al. (2007) reported that dissolution took up to 807 min (~13 h) for casein-based powders [186;257]. Under production conditions, rehydration takes place within 3 to 8 h in the mixing tank or size reduction is achieved via high pressure homogenization.

In line with the results of the laser diffraction a grading of the dairy powders thus becomes possible. The dairy powders can be classified into six different groups regarding the solubility behavior. An overlapping between the groups is possible. All in all, group 1 and 2 characterize dairy powders with poor/reduced functionality.

The figures display the PSDs of the powders immediately after rehydration and after complete rehydration (24 h). Nevertheless, particle size was measured after 1, 5, 10, 15, 20, 30, 60 min, 4, and 24 h.

1.   The volume concentration of the second peak dominates which is the case for WPC 30, 35 1, 35 5, 35 6, 35 8, and 60 4 (poor rehydration)

Figure 7-16 displays the PSD of WPC 30 in the course of rehydration and the distribution of the dry powder (red curve). The curves are results of three replicated measurements. The error bars indicate the standard deviation. Immediately after hydration the PSD of WPC 30 is bimodal with only a minimal overlapping between the PSD of the dry powder and the rehydrated powder. The volume concentration of both peaks—if observed visually—undergoes only small changes during rehydration. Attention should be paid to the high frequency of peak 2 characterizing particles > 1 μm.
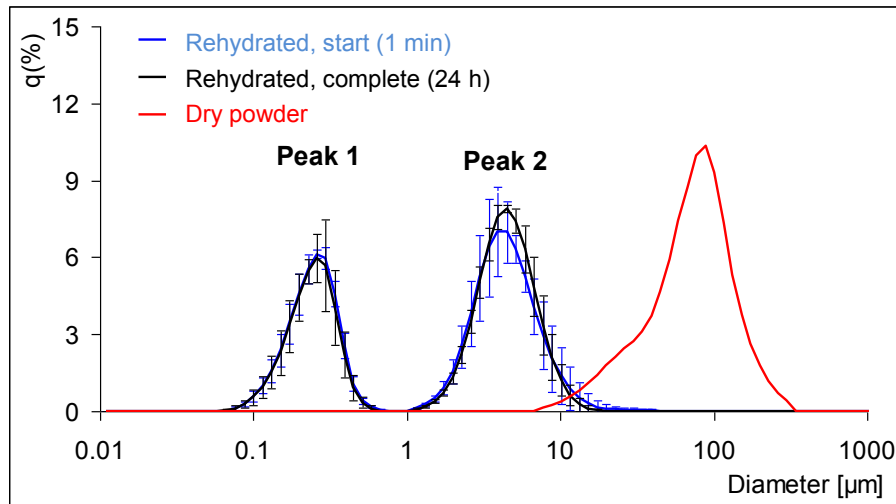
Figure 7-16:   **PSD of WPC 30 in the course of rehydration and the dry powder**

2.   The volume concentration of the second peak dominates plus a kinetic is detected (WPC 60 3) (poor rehydration)

Figure 7-17 displays the volume distribution functions of WPC 60 3 during rehydration and the distribution of the dry powder (red curve). The curves are results of three replicated measurements. The error bars indicate the standard deviation.
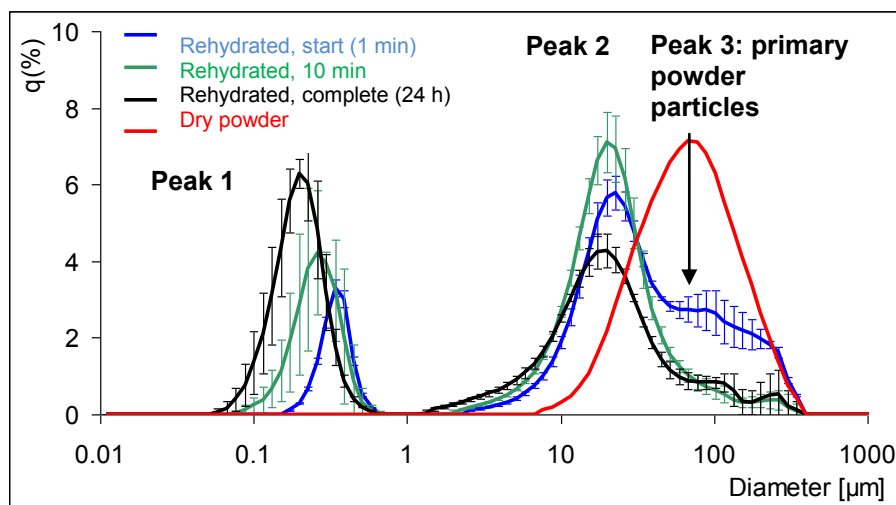
Figure 7-17:   **PSD of WPC 60 3 in the course of rehydration and the dry powder**

It can be clearly seen that in the course of rehydration the first peak increases and the second decreases. A third peak can be detected at the beginning of rehydration in the range of the dry powder particles. From these results it becomes obvious that a third peak represents primary powder particles produced by atomization in the spray dryer which decompose into two peaks (aggregate matter) in the course of rehydration.

This statement is in contradiction to MIMOUNI et al. (2009) who attributed the smaller peak to primary powder particles (30-37 µm) produced by atomization in the spray dryer and the larger peak to agglomerated powder particles but did not identify any submicron peak [257].

3.   The volume concentration of peak one dominates (WPC 35 2 35 4, 60 1, 60 2, 60 5, 80 1, and 80 4). Figure 7-18 displays the PSD of WPC 80 4 as an example for this group. The curves are results of three replicated measurements. The error bars indicate the standard deviation.
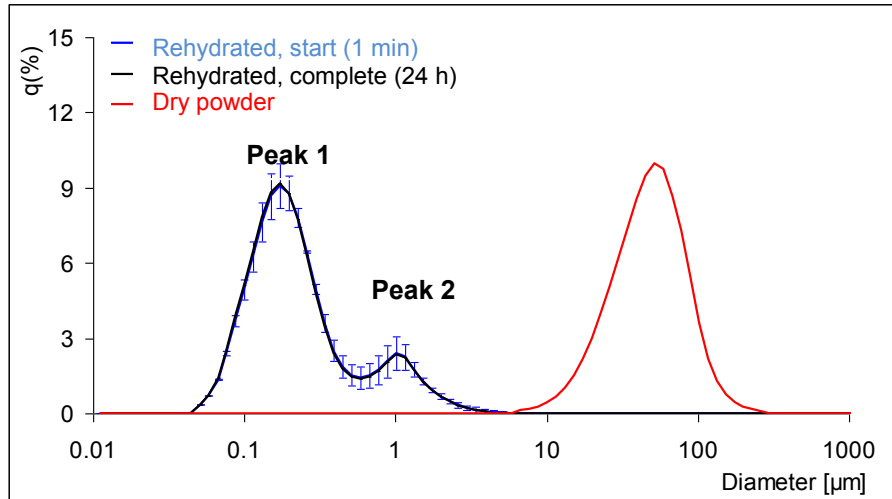
Figure 7-18:   **PSD of WPC 80 4 in the course of rehydration and the dry powder**

Figure 7-18 displays the PSD of WPC 80 4 in the course of rehydration and the distribution of the dry powder (red curve). Immediately after hydration the PSD of WPC 80 4 is bimodal without an overlapping between the PSD of the dry powder and the rehydrated powder. The volume concentration of both peaks undergoes only minimal changes during rehydration. Attention should be paid to the very low frequency of peak 2 characterizing particles > 1 µm.

4.   The volume concentration of peak one dominates plus a kinetic is detected (WPC 35 3, 35 7, 35 9-14, SMP, 60 6, 60 7, 80 2, 80 5, and 80 6). Figure 7-19 displays the PSD of WPC 60 6 as an example for this group. The curves are results of three replicated measurements. The error bars indicate the standard deviation.
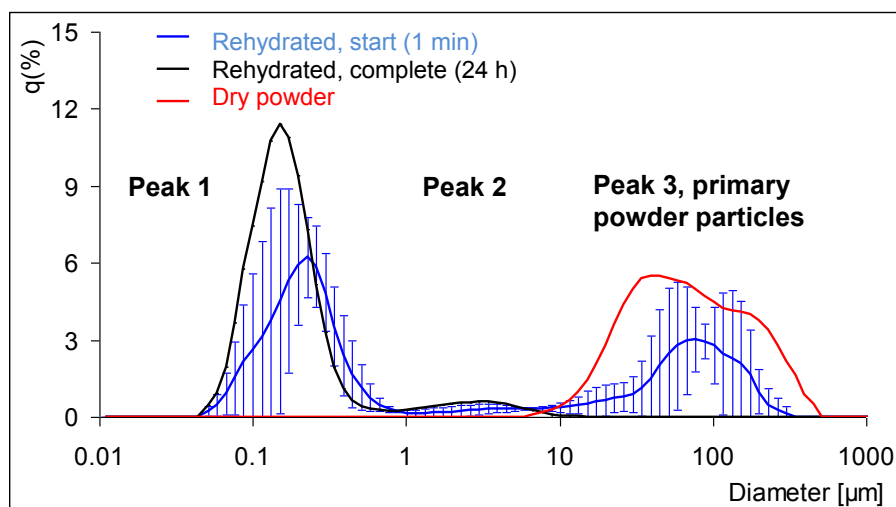
Figure 7-19:   **PSD of WPC 60 6 in the course of rehydration and the dry powder**

Figure 7-19 displays the PSD of WPC 60 6 in the course of rehydration and the distribution of the dry powder (red curve). Immediately after hydration, the PSD of WPC 60 6 is multimodal with a remarkable overlapping between the PSD of the dry powder and the rehydrated powder which characterizes the dissolution of dry powder particles.

The volume concentration of the peaks undergoes immense changes during rehydration which means that kinetics were detected. Nevertheless, attention should be paid to the very low frequency of peak 2 which characterizes particles > 1 µm after rehydration.

5.   A third peak is present (SWP 13 1-13 3, WPC 70 1 and 70 2). Figure 7-20 displays the PSD of WPC 70 1 as an example for this group.
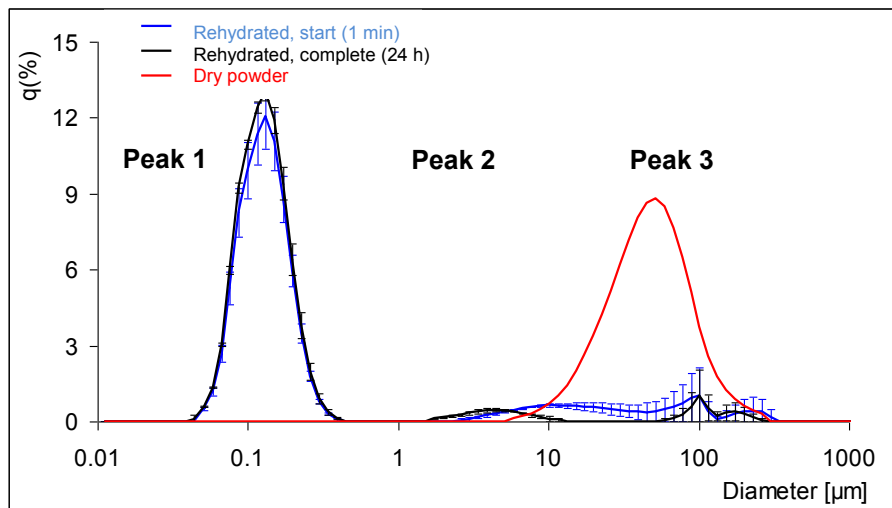
Figure 7-20:   PSD of WPC 70 1 in the course of rehydration and the dry powder

Figure 7-20 displays the PSD of WPC 70 1 in the course of rehydration and the distribution of the dry powder (red curve). The curves are results of three replicated measurements. The error bars indicate the standard deviation. Immediately after hydration the PSD of WPC 70 1 is trimodal with an overlapping between the PSD of the dry powder and the rehydrated powder.

The volume concentration of the peaks undergoes changes during rehydration and at the end of the rehydration (24 h) a third peak is still detectable. What is remarkable is the very low frequency of peak 2 and peak 3 which characterize particles > 1 µm.

6. Detection of swelling, WPC 80 3

Figure 7-21 displays the volume distribution of WPC 80 3 during rehydration and of the dry measurements (red curve). The curves are results of three replicated measurements. The error bars indicate the standard deviation. No small particles are present in the distribution.
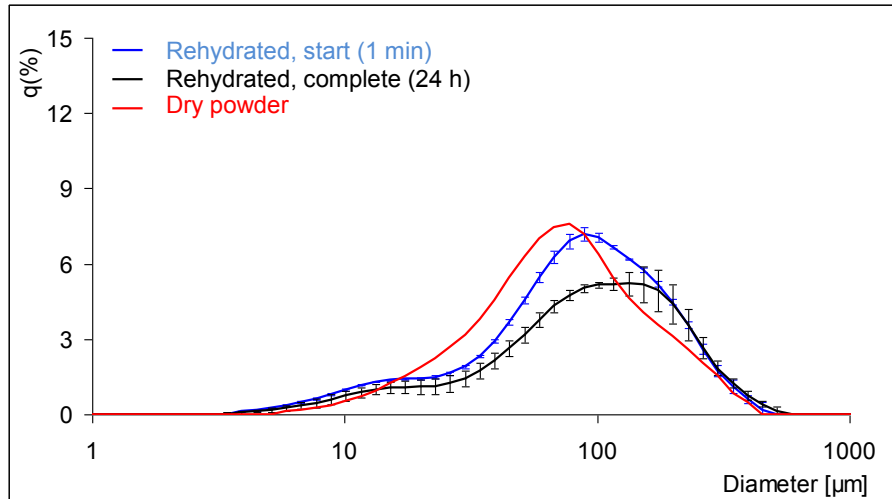
Figure 7-21: **PSD of WPC 80 3 in the course of rehydration and the dry powder**

The protein content of WPC 80 3 nearly consists solely of β-Lg, Figure 7-6, indicating that a fractionation was done during the production of WPC 80 3. Usually, two different conditions are involved in whey protein isolate production which are the membrane fractionation (MF,UF-DF) and spray drying, and the physical and chromatographic fractionation (IE) [150;160] coupled with concentration (evaporation or UF) and spray drying [142;149]. During the ion-exchange adsorption process the β-Lg can be eluted from the column by 0.1 M HCl indicating that during the fractionation or isolation of whey proteins serious changes not only in the pH but also in mineral composition or the heating regime are involved.

The behavior of WPC 80 3 is very different from all other WPC in the course of rehydration. The development of the particle size points to a swelling (D_{50} dry: 66 µm, D_{50} rehydrated: 83 µm), Figure 7-21. The WPC 80 3 is the only powder that still has a unimodal distribution after rehydration. The D_{90} increased from ~ 200 µm to ~ 230 µm. It has to be admitted that the visual assessment of the rehydrated WPC 80 3 lead to the result that the particles were swollen and not dissolved because they were still present.

In most of the cases no swelling of particles was detected for WPC powders. This finding is in agreement with the literature [186]. Whey protein powders contain mainly globular proteins which do not bind much water as is the case with casein micelles [314-316]. Thus, no swelling occurs or the swelling is limited for WPCs. However, DYBING and SMITH (1991) mentioned that denatured whey proteins can bind large amounts of water [160].

The visual assessment of the rehydrated WPC 80 3 and the results of the laser diffraction measurements suggest that the β-Lg is not soluble due to denaturation. Variations of whey protein content, solubility, and degree of denaturation of WPC depending on processing history (membrane processes, ionic exchange techniques, and specific defatting, desugaring, and desalting processes) have also been observed by DE WIT, KLARENBEEK, and ADAMSE (1986) [317].

7.4.2 Peak classification

The assignment of the peaks to individual whey constituents is very difficult. In milk the peaks were attributed to casein micelles and fat, respectively [249;305]. In whey the amount of casein and fat droplets should be quite small. Additionally, an increase of peak 2 due to heat treatment was detected (Figure 7-9), thus pointing to different compounds building up the peaks of whey and dairy powders compared to milk. As a consequence, especially the second peak has to be attributed to aggregate matter and/or MFGM fragments which are soluble after pH 4.6 treatment.

Because the protein content of WPC 80 3 nearly consists solely of β-Lg and no small particles are present in the distributions it can be concluded that the smaller particles of other distributions consist of other whey proteins, or more likely—on the basis of the SDS-PAGE results, Table 7-9—of interactions of other whey proteins with the β-Lg or remaining fat. However, the production technology of WPC 80 3 differs compared to the other WPC powders.

It was found in the present study that after chitosan treatment no peak was detectable by static light scattering but HPSEC results proved an unchanged concentration of the main whey proteins (Table 7-5 and Table 7-6).

SDS-PAGE profiles were analyzed of selected samples (Table 7-9, Table 12-10, and Table 12-11) of the native state, after adjustment to pH 4.6, and after treatment with chitosan. Here, the sediment and the supernatant after centrifugation were analyzed. It can be seen that after pH 4.6 treatment the thickness of the bands in the area of large molecular weight are diminished.

After chitosan treatment the supernatant nearly consists of α-La and β-Lg and BSA. It can be assumed that these proteins are dissolved because of the results from HPSEC and static light scattering. The sediment contains the separated proteins—mainly high molecular weight proteins—but also higher amounts of α-La and β-Lg. Giving evidence that peaks 1 and 2 are made up of those protein aggregates. Additionally, chitosan was found to interact with surface-active material e.g., phospholipids, small-molecule surfactants, bile acids [214], or proteins [214-216].

It has already been used to remove lipids from cheese whey [217]. There are additional compounds which have been removed and might have caused the peaks. The present results prove chitosan separates the lipids and additionally protein aggregates (even α-La and β-Lg) from rehydrated WPC.

7.4.3 Assessment of the solubility of the powders

The present study was done to obtain an algorithm for the assessment of the solubility exemplarily for the functionality of the dairy powders using the laser diffraction method. In connection with the results of the HPSEC (β-Lg content characterizing the amount of native protein in the sample) and the parameter in accordance to the NSI, this procedure is a viable one. The volume-related concentration of peak 2 (particle size > 1 µm) is the important parameter for the assessment of solubility. Values higher than 50 % characterize critical functionality. Additionally, the size of the particles of the second peak is important.

It can be concluded that the solubility decreases with increasing particle size. Especially samples WPC 30 and WPC 35 8 with low NSI (Table 7-3) and low concentration of β-Lg (Table 7-7) and the WPC 35 1 with a low concentration of β-Lg (Table 7-5) are characterized by a high volume concentration > 60 % of the second peak (D_{50} = 4-6 µm), Table 12-26. For the WPC 35 1 it is more than 90 %, Table 12-26. Powders that possess a good solubility regarding NSI and HPSEC have a volume concentration of peak 2 smaller than 20 %, Table 12-26. From these observations it can be concluded that the powders WPC 35 1, 35 5, 35 6, 35 8, 60 3, 60 4, and 30 also possess a low solubility.

It was discussed above that large aggregates cannot be integrated into the casein network during sour milk fermentation. From the examples discussed here the D_{90} of the second peak taken from the volume distribution was > 10 µm in the case of SWP 13 3, WPC 35 6, 35 8, 60 3, 80 1, 80 6, and SMP after full rehydration, Table 12-21 and Table 12-22.

Actually, the third peak which was attributed to primary powder particles, persisted in some cases—for example for the WPC35 6 and SWP13 2, Table 12-23—over a long time period of rehydration. Further research is needed to assess the effect of those WPC in sour milk products as long as the parameter in accordance to the NSI is only a measure for the nitrogen solubility—and with respect to this parameter, to the HPSEC results, and the volume concentration of the second peak—the SWP 13 3, WPC 80 1, and 80 6 were not assessed to have a reduced functionality.

Of the 34 analyzed samples 19 were found to have a third peak. In Table 12-23 in the Appendix the D_{10}, D_{50}, and the D_{90} of the third peak are displayed after the steps of rehydration. Sometimes only one or two values occur in the Table which is the case when only one or two of the three analyzed samples showed a peak after rehydration. Nevertheless, most of the powders have no third peak at the end of rehydration. Additionally, the LA-950 provides a volume-based PSD which means that a third peak represents particles with high volume but small number. From the present study it can be concluded that the occurrence of a third peak in the PSD does not necessarily point to a low solubility unless the main proportion of particles is located in the first peak.

Actually, the measuring principle of the LA-950 leads to an overestimation of the particles forming the third peak. The volume-based PSD particles or aggregates larger in size are displayed with a large peak but their number might be very small.

The number of those large aggregates located in the third peak—from several micrometers upwards, > 20 µm—present in all analyzed samples, is too low to dominate the functionality.

The occurrence of solubility kinetics, which can only be detected by laser diffraction but not by NSI or HPSEC, is a further characteristic property determining the functionality. A powder possessing a kinetic value has to be negatively assessed if the kinetics require an immense time investment and if the volume concentration of peak 2 is very high.

7.4.4 Comparison of the results of the dry and wet measurements

In the present study no connection was found between the particle size of the dry powders and the rehydration behavior, which means the particle size of the individual peaks after rehydration in detail. It was assumed on the basis of a study of ONWULATA, KONSTANCE, and TOMASULA (2004) and ONWULATA and TOMASULA (2006) [164;318] that large particles in dry state are more denatured and consequently more insoluble. The most soluble fractions had particle dimensions of less than 100 microns

The powders which are assessed to have poor solubility (WPC 30, 35 1, 35 5, 35 6, 35 8, 60 3, and 60 4) have totally unnoticeable particle sizes in dry state. They are neither very large nor very small, Table 12-13 and Table 12-16. Even the powders that show a third peak after rehydration which are exemplarily SWP 13 1 (D_{50} = 114.52 ± 1.03 µm) and WPC 70 1 (D_{50} = 44.37 ± 0.62 µm) have diverging particle sizes in dry state so that a rating of the powders regarding the solubility only on the basis of the results of the dry measurements is not possible.

7.4.5 Particle size and composition

During the production of WPC powders the variation in particle size can be attributed to multiple effects caused by the processing conditions or equipment design (several methods of water removal such as falling film evaporation followed by spray drying, control of the residual moisture content in the final product by filtermattype dryers or fluidized bed dryers, some smaller plants try to achieve complete drying in the spray dryer itself by reducing nozzle pressure (lower feed rates) and increasing inlet air temperature, atomization conditions such as high-pressure nozzle or a rotary disk atomizer) and also to the source and composition of the liquid whey [295]. As a result, particle size of commercial WPC 80 was reported to vary between 53 and 382 µm [164] and particle size of SWP obtained from several dairy processing plant varied between 92 and 234 µm [295].

For the present results it was found that the protein/lactose content significantly determines the particulation. The higher the protein content of the powders, the smaller the particles in dry state. On average, the SWP have a D_{50} of 128.55 µm, the WPC 35 of 86.93 µm, the WPC 60 of 53.56 µm, the WPC 70 of 42.32 µm, and the WPC 80 of 81.68 µm (WPC 80 2 included).

The finding that the particle size decreases with increasing protein content is against all expectations as long as it was reported that an increasing viscosity would increase the final particle size of the dried powder [179;319].

ADHIKARI, HOWES, SHRESTHA, and BHANDARI (2007) reported the viscosity of a 5 % WPI solution to be twice as high as the viscosity of a 5 % lactose solution (2.03 ± 0.11 mPa·s compared to 1.01 ± 0.01 mPa·s). Additionally, differences in the surface tension exist. The surface tension of a WPI solution (5 %) is with 40 mN·m^{-1} much lower compared to a surface tension of 65 mN·m^{-1} of a lactose solution (5 %) indicating that WPI is surface-active [320].

In a study of EL-SAYED, WALLACK, and KING (1990) drops of sucrose collapsed during drying and formed smooth, solid particles [319], which was also reported by HECHT and KING (2000) [195]. Besides this, coffee drops were dried. Coffee like WPI has a much lower surface tension and the viscosity of concentrated coffee solution like WPI is higher than that for sucrose, owing to the presence of high-molecular weight components. Dried coffee drops were found to be hollow because the high viscosity resists surface tension forces acting to shrink a ruptured shell geometry and also resists implosion after the particle cool [195]. A similar behavior was reported for dried skim milk (53 % lactose, 37 % caseinate) drops which kept expanded due to the rigid surface [319].

The studies described above have suggested that an increasing protein content in whey protein concentrate/lactose solution would result in larger final particle sizes after drying. It is therefore more likely that the decreasing particle size with increasing protein content does not result from compositional variations, but rather from deviating processing conditions like higher feed temperature, higher atomization pressure in order to systematically decrease final particle size of dairy powders with high protein content.

No correlation exists between the particle size and the ash, fat, and moisture content.

ONWULATA, KONSTANCE, and TOMASULA (2004) found that whey protein powders with greater particle size possess a significantly higher fat content [164]. In the present study this connection was not found.

7.4.6 Particle size and results of the HPSEC

As a result of the laser diffraction particle sizes were found to be > 20 μm and in some cases around 200-300 μm for the third peak of the rehydrated samples, Table 12-21, Table 12-22, and Table 12-23.

The area of the first peak of the HPSEC profiles for the native samples was found to be high for WPC 35 9, 12, 13, and 60 6 compared to the other selected samples, highlighted in red in Table 7-18. But according to the present results these WPC can not be attributed to have the most aggregated proteins which was presented in the literature [231;292].

The results of the laser diffractometry, Table 7-18, show that these WPCs have small particle sizes at peak 1. WPCs with a small exclusion limit have larger particles. If the volume concentrations of peak 1 are viewed after rehydration in Table 7-18 it is remarkable that the powders which are assessed to have a poor/reduced solubility (WPC 30, 35 1, 35 8) and have a small volume concentration at peak 1, highlighted in green in Table 7-18, reveal low exclusion limits in HPSEC.

Table 7-18: Exclusion limit, fat content, V.c. of peak 1, and D_{50} of peak 1 after complete rehydration of selected WPCs

Sample	Exclusion limit		Fat content	D_{50} peak 1, rehydrated	V.c. peak 1, rehydrated
	1	**2**			
	Area (mAU·ml)		%	µm	%
WPC 30	9.20	9.45	1.70	0.222	38.6
WPC 35 1	9.5	8.7	2.81	0.14	35.9
WPC 35 2	15.2	22.0	2.89	0.22	74.3
WPC 35 3	19.8	21.8	2.08	0.16	71.7
WPC 35 8	13.25	10.15	2.40	0.246	25.3
WPC 35 9	52.27	54.31	2.50	0.166	81.2
WPC 35 10	25.26	23.93	3.45	0.200	78.8
WPC 35 11	43.90	35.73	2.25	0.145	90.4
WPC 35 12	57.27	58.86	1.88	0.144	91.3
WPC 35 13	57.92	55.70	2.25	0.143	90.2
WPC 35 14	42.96	41.66	1.60	0.146	83.1
WPC 60 1	11.6	14.5	4.71	0.22	57.5
WPC 60 2	9.5	9.7	4.09	0.22	67.7
WPC 60 6	59.70	55.72	2.63	0.141	92.7
WPC 60 7	43.94	44.34	3.75	0.150	90.8
WPC 70 1	48.9	44.4	3.18	0.10	91.7
WPC 80 1	18.9	22.9	6.30	0.2	78.2
WPC 80 5	19.3	25.4	3.59	0.13	92.3
WPC 80 6	27.46	42.74	6.00	0.155	75.0

The HPSEC results indicate that the column itself acts as a filter. Only the very small particles pass the column and bigger particles are retained so that WPC containing more small particles have a higher exclusion volume in HPSEC. Therefore, the area of the exclusion limit obtained by HPSEC measurements is not a useful tool to study the degree of aggregation of WPCs. The static light scattering method is found to be more suitable for this purpose because all aggregates are detected. HPSEC would lead to false results because the small particles/aggregates are overestimated and the bigger particles/aggregates do not become part of the analysis.

WPC 30 for example has only a volume concentration of 38.6 % at peak 1 which means that peak 2 has a high volume concentration. Therefore, HPSEC experiments resulted in a very low exclusion limit. This result would be misleading if this was attributed to a low content of aggregates. It is only a low concentration of small particles and the parameter according to the NSI proved that the solubility of WPC 30 was low, Table 7-3.

In former studies by ROUFIK, PAQUIN, and BRITTEN (2005) and DE LA FUENTE et al. (2002) the peak of the exclusion limit was attributed to aggregated material [231;292]. ROUFIK, PAQUIN, and BRITTEN (2005) used two columns for HPSEC which were the TSK Gel G-4000 PW XL (separation range: 10-1500 kDa) and the TSK Gel G-3000 PW XL (separation range: 0.5-800 kDa) [231]. They stated that HPSEC is a useful tool to study protein aggregation in WPC and to employ this for a quality control of the WPCs before application.

DE LA FUENTE et al. (2002) followed the processing of WPC and analyzed samples after each processing step by SEC-MALLS using two columns: Superose 6 HR 10/30 (separation range: 5-5000 kDa) and Superdex 75 HR 10/30 (separation range: 3-70 kDa) [292].

Cheese whey and acid whey were investigated after clarification, retentate mid-way through ultrafiltration/diafiltration, retentate after diafiltration, concentrate after evaporation, WPC after spray drying. Before SEC measurements all samples were ultracentrifuged and filtered (0.22 µm). The aggregates which eluted near the void volume using the Superose column were found to have molecular weights between 2000-150 kDa for cheese whey and 2000, 650, and 220 kDa for acid whey. From these results it can be assumed that even after ultracentrifugation and filtration large aggregates remained in the sample. DE LA FUENTE et al. (2002) calculated the proportions of the individual whey proteins and the "soluble" aggregates from the SEC profiles and stated that there were more aggregates present in cheese whey than in acid whey [292].

In the present study a Tricorn Superose 12 HR 10/30 with an exclusion limit of globular proteins of ~ 2000 kDa and an optimal separation range of 1–300 kDa was chosen. In combination with laser diffraction the attribution of the size/area of the exclusion limit to aggregated material and therefore an assessment of the WPC quality has to be undertaken with caution, even if the separation range of the column is higher ([292]: max 5000 kDa) because the column itself was found to act as a filter.

Nevertheless, HPSEC results provide information about the content of native whey proteins, which are the content of α-La and β-Lg in detail. In combination with NSI and laser diffraction it was shown that powders having a low concentration of β-Lg are also characterized by a high volume concentration >60 % of the second peak and a low NSI. Please refer to section 7.4.2 for detailed information. These data imply that not the exclusion limit but the β-Lg obtained by HPSEC analysis provide information about heat denaturation of the whey proteins in dairy powders.

7.5 Summary of the chapter

Commonly, dairy powders are used to increase the dry matter of the yoghurt milk for the production of stirred yoghurt. It was found that in the production flow a share of 15 % defective fermentation might occur. To date the functionality (degree of denaturation) of the whey proteins used cannot be assessed by means of common/routine laboratory analytics in the dairy. A rapid method is needed. Chapter 7 deals with the method development of such a rapid method using the principle of laser diffraction. In combination with the chemical analysis, HPLC, and a parameter in accordance to the nitrogen solubility index the results have been verified. The laser diffraction method allows a grading of the dairy powders prior to application in the process milk allowing a rejection of dairy powders with reduced solubility. This method delivers reliable results regarding powder functionality at an very early stage. If the results of the volume concentration are viewed, the method enables a grading of the solubility after 10 min. It can be used before measurements of the fermentation with a torsion oscillator on laboratory scale and increases the production reliability.

The results of the statistical analysis have shown that a solubility equilibrium of the WPC powders is reached within 240 min because changes in particles sizes between 240 min and 24 h are no longer significant.

The protein content was found to have a significant influence on the particle size in dry state as well as on particle size in rehydrated state which indicates the important influence of type of production technology on particle size. However, the final particle size of WPC powders has to be related to multiple effects caused by the processing conditions or equipment design and also to the source and composition of the liquid whey [295].

Nevertheless, the volume concentration of the individual peaks which was chosen as important parameter for the assessment of the powder functionality is independent at protein content except for the very early beginning of rehydration suggesting that the production technology overall has no influence but functionality which means the degree of denaturation in detail does play a significant role.

The practical benefit of these findings is that a small final particle size of the dry SWP/WPC powder is not by all means necessary to obtain a good rehydration behavior because the powders particle size was not found to provide significant evidence for the degree of denaturation.

Chapter 8: Production of quark powder

An enormous industrial need exists for the modeling and optimization of the spray drying process, especially the atomization of viscous, highly-structured products particularly if the functional properties of the powdered material are to be preserved. On rehydration quark powder should reveal a smooth, paste-like structure as the original quark without sedimentation but with sufficient water retention.

The processing technology of quark powder will be investigated. The attempt is made to atomize the quark by a nozzle atomizer instead of the commonly used disc atomizer for the drying of highly-structured feed material.

The functionality of quark powder is assessed exemplarily for the examination of the water retention. For this purpose, rheological measurements can be done after different times of rehydration to assess the water uptake exemplarily for the change in rheological parameters. Market samples—produced on large-scale dryer—were measured for comparison.

In order to optimize the spray drying process the attempt is made to primarily characterize the influence of thermal and mechanical parameters on the low fat quark matrix (material characteristics) and to obtain results for the atomization process. A dispersing step might be indispensable for a good powder quality because the dispersing results in smaller quark particles before atomization. When quark powder is produced by spray drying, insufficient atomization can cause quality problems of the powder after rehydration. Those quality problems are normally related to separation of very large particles from the atomizer. The time of exposure of the very large particles in the dryer might be too short to result in complete drying. Hence, only the surface is dried. Because of long diffusion path of the water and water vapor to the interface no cooling effect takes place and a crustification occurs at the surface of the quark particles. Additionally, this crustification inhibits a complete drying of the inner part of the particles which very likely negatively influences the wetting of the particles and therefore the functionality. It is therefore hypothesized that a de-structuring of the quark matrix before atomization would lead to a favorable atomization which means smaller droplets in detail.

8.1 Investigations into the production technology

8.1.1 Production of quark powder on a pilot plant and small-scale dryer (pressure nozzle atomizer)

Rheological measurements were done during processing of the raw material quark (MS1), the warmed quark after passage of scraped surface heat exchanger (MS3), the quark after passage of the nozzle without supply of air, variant I (MS4), and the quark after passage of the nozzle with supply of air, variant II (MS5).

8.1.1.1 Rheological measurements

The efficiency of the atomization was observed via visual assessment of the atomized quark. The parameters of the experiments are listed in Table 12-27, see Appendix. It is necessary to mention that the nozzle geometry was dimensionized for the atomization of skim milk concentrate (200 µm).

Figure 8-1 displays the processing with incorporation of air into the warmed quark.
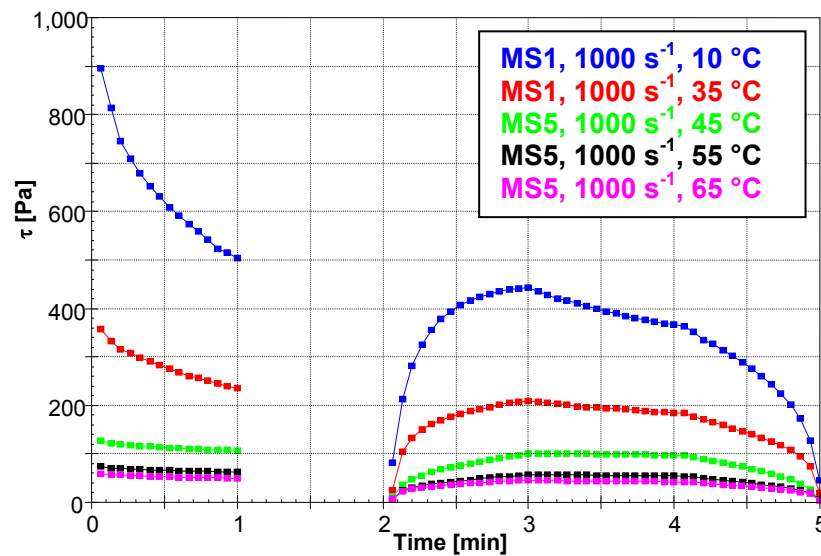
Figure 8-1: **Processing of the quark after warming with supply of air**

Table 8-1 lists the regression results.

Table 8-1: **Rheological parameters**

T	τ_0	K	n	r	s	A_{TH}	$\dot{\gamma}_{max}$	Comments
°C	Pa	Pa·s^n	-	-	Pa	Pa·s^{-1}	s^{-1}	
10°	72.33	17.85	0.634	0.999	2.57	6991	100	
10°	27.54	23.59	0.415	0.999	1.89	43434	500	16 % d.m./10°C
10°	20.48	24.22	0.426	0.995	2.82	56027	1000	
35°	29.18	6.94	0.676	0.998	2.3	1768	100	16 % d.m./35°C
35°	2.62	16.06	0.347	0.999	2.62	37000	1000	
35°	1.14	3.46	0.486	0.999	1.24	23504	1000	MS3
35°	2.04	2.05	0.519	0.999	0.273	7228	1000	MS4
35°	3.08	2.73	0.556	0.999	0.34	16801	1000	MS5 Air
45°	-2.74	20.04	0.299	0.999	0.88	20623	1000	MS1
45°	3.07	2.72	0.472	0.999	0.78	19362	1000	MS3
45°	1.68	1.86	0.483	0.999	0.49	4454	1000	MS4
45°	3	2.8	0.508	0.99	0.43	6,999	1000	MS5 Air
55°	-2.51	13.53	0.286	0.998	1.47	9043	1000	MS1
55°	0.47	1.02	0.488	0.997	0.62	5683	1000	MS3
55°	-0.11	1.69	0.389	0.994	0.71	1819	1000	MS4
55°	2.47	2.52	0.435	0.999	0.47	4636	1000	MS5 Air
65°	-3.39	6.98	0.242	0.997	1.06	7114	1000	MS1
65°	2.17	1.17	0.451	0.996	0.65	6360	1000	MS3
65°	-0.98	3.59	0.279	0.988	0.99	3189	1000	MS4
65°	-0.83	4.57	0.32	0.998	0.8	5599	1000	MS5 Air
10°	67.07	10.07	0.769	0.999	4.54	7468	100	Rehydration standard
10°	65.75	7.73	0.801	0.999	3.83	3442	100	V122

MS1: raw material quark
MS3: warmed quark after passage of scraped SHE
MS4: quark after passage of the nozzle without supply of air, variant I
MS5: quark after passage of the nozzle with supply of air, variant II

The rheological measurements were now done at temperatures up to 65 °C with ΔT = 10 °K because of the measured temperatures of the quark during processing, Table 12-27 in the Appendix.

The regulatory behavior of the scraped heat exchanger had been defined with water. Due to changes in the fluid dynamics and thermo-caloric parameters and the reduced throughput of the quark its temperature rose to 65 °C.

On the basis of the obtained rheological data in Table 8-1 in combination with the results displayed in Figure 8-1 the incorporation of air cannot be positively assessed according to the effect on de-structuring of the quark matrix. A reason of this is the insufficient homogeneous incorporation of the air in the warmed matrix; a high yield point is detected.

At temperatures > 45 °C a complete reduction of the yield point was detected—except variant MS5—indicating a reduced particle size of the quark matrix which is necessary for a sufficient atomization into the drying chamber. Additionally, an immense influence of the process equipment on the necessary de-structuring of the matrix of the raw material quark was determined.

8.1.1.2 Assessment of the powder functionality

Figure 8-2 displays the water retention after 1 h of rehydration as an example for the functionality of the powders dried on a small-scale dryer using the pressure nozzle atomizer in comparison to raw material quark (10 °C, $\dot{\gamma}_{max}$ = 100 s^{-1}, 16 % d.m.). The rehydration was done according to standard procedure (two-step dispersion at 10 °C and 35 °C).
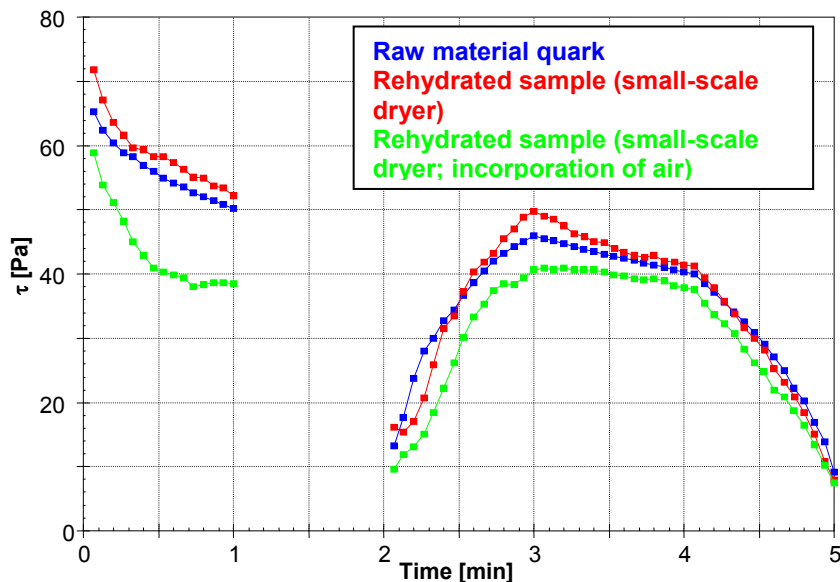
Figure 8-2:   Comparison of rehydrated quark (small scale) with original quark

Good water retention of the powder was already detected during rehydration. After 1 h resting time a slight syneresis occurred; this was removed by means of mechanical agitation.

The rheological results show that the curd structure without incorporation of air (standard) is more or less identical to that of the raw material. In general, the change in the warming regime (now 65 °C instead of 35 °C) was not found to be negative. Due to stronger thermal de-aggregation an acceptable atomization was achieved and the resulting product showed good water retention. In comparison to the reference powder the resulting powder was whiter and had a neutral smell/odor.

The atomization of the quark was continuously archived without buffer vessels. A resting at higher temperatures (55…65…70 °C) would result in higher graininess and wheying-off.

The production of quark on the small-scale dryer using the pressure nozzle atomizer resulted in good powder quality regarding the functionality: white color, odorless, easy to dry (on small scale), good rehydration with almost equal water retention compared to the raw material.

8.1.2 Production of quark powder on large-scale dryer, Section I

Rheological measurements during production were taken of the product following the scraped surface heat exchanger and after the tube inlet.

8.1.2.1 Rheological measurements

The data obtained from the quark warming are listed in Table 12-28 in the Appendix. Table 8-2 displays the regression results.

Table 8-2: Rheological parameters, scale-up; section I

T	τ_0	K	n	r	s	A_{TH}	Comments
°C	Pa	Pa·s^n	-	-	Pa	Pa·s^{-1}	
10	59.21	27.80	0.502	0.999	3.54	7537	After scraped SHE
10	29.46	11.57	0.579	0.999	2.10	4349	After tube inlet
10	25.13	6.78	0.69	0.999	0.90	4076	Product dried by small-scale dryer

The rehydrated powders obtained from large-scale production were not measured because of the insufficient water binding capacity.

8.1.2.2 Particle size analysis

The particle sizes were measured by laser diffraction. Results obtained for the reference powder are listed for comparison, see Table 8-3.

Table 8-3: Parameters of the laser diffraction measurements

	Large scale, Section I	Reference powder
Arithmetic mean of the average value (µm)	77.26	52.24
Variance (µm^2)	2507	3239
$D10$ (µm)	18.08	11.82
$D50$ (µm)	69.81	34.54
$D90$ (µm)	150.50	111.85
Specific surface (m^2·g^{-1})	0.2396	0.4316

The rehydration behavior of the quark powder produced by large-scale production in section I has to be assessed as inadequate. The D_{50} of the powder produced on large-scale is nearly twice as high as the D_{50} of the reference quark powder.

8.1.2.3 SEM results

Figure 8-3 represents the SEM micrographs of the powder produced in section I obtained at different magnification.
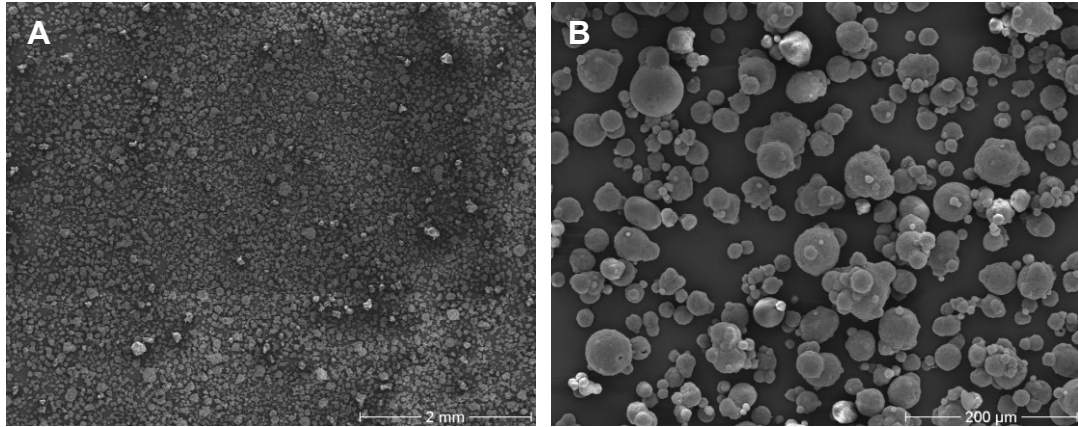
Figure 8-3: **SEM micrographs of the quark powder; Section I, large scale, pressure nozzle atomizer**

A: 20-fold magnification, B: 200-fold magnification

The reason for the insufficient wetting and structure formation behavior of the quark powder becomes clear from the SEM micrographs. Only very few small particles are visible. Most particles have agglomerated to larger clusters. Despite the arithmetic mean of the average value of 77.26 µm, 10 % of the particles are larger than 150.5 µm.

8.1.2.4 HIC analysis

Table 8-4 displays the results of the HIC analysis which are the α_{S1}-, α_{S2}-, and the κ-/β-casein content explained as a percentage of the overall casein content of the powder produced on large scale in section I.

Table 8-4: **Casein profile of the quark powder, large scale, section I**

Sample	α_{S1} %	α_{S2} %	κ/β %
Quark powder, section I, large scale	53.23	11.11	35.66

8.2 Material characteristics

Material characteristics obtained on the basis of the development of the rheological parameters of the low fat quark were determined by variation of temperature and method of dispersing (energy input before atomization).

8.2.1 Determination of the properties of the low fat quark

The material characteristics of the low fat quark and the influence of different treatments on the low fat quark matrix which are the variation of temperature and the method of dispersing were determined by rheological measurements.

Preparation I is the raw material with 18 % dry mass; preparation II includes a dilution step to 16 % dry mass and dispersion by the hand-held blender at 10 °C; preparation III involves a shearing by means of a wire wisk and dispersion by the hand-held blender at 35 °C.

Figure 8-4 displays the measuring curve of the raw material low fat quark as well as the influence of dilution from 18 % to 16 % and dispersing at 10 °C at $\dot{\gamma}_{max}$ = 100 s^{-1}, 500 s^{-1}, and 1000 s^{-1}. If the measured curves of the low fat quark at $\dot{\gamma}_{max}$ = 500 s^{-1} and 1000 s^{-1} with 18 % dry mass are viewed in Figure 8-4 a wall slip can be clearly identified. No wall slip is detected in the case of the diluted samples.
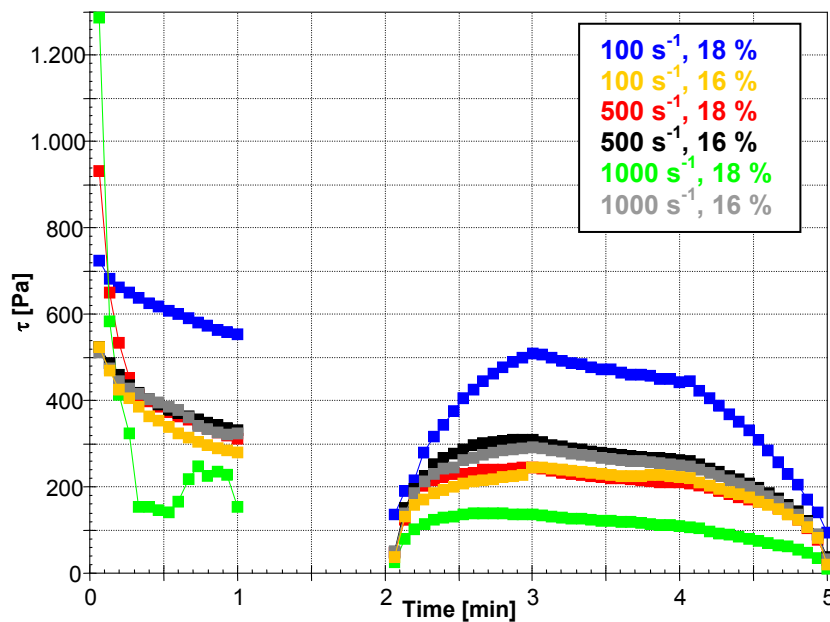
Figure 8-4: **Influence of dilution and dispersing at 10 °C on quark matrix**

The influence of dilution on the course of the curves at $\dot{\gamma}_{max}$ = 100 s^{-1} is logical because the curve after dilution runs below the curve of the original quark.

At $\dot{\gamma}_{max}$ = 500 s^{-1} the measuring curves before and after dilution are nearly identical which has to originate from wall slip and structure development due to the formation of foam after the first dispersing step.

Actually, the curve after dilution runs above that before dilution at $\dot{\gamma}_{max}$ = 1000 s^{-1} which has to be related to the wall slip which occurred for the original quark sample with 18 % dry mass.

Figure 8-5 displays the measuring curve of the low fat quark after the first dispersing step (preparation II), warming to 35 °C and a second dispersing step of 3 min (preparation III).
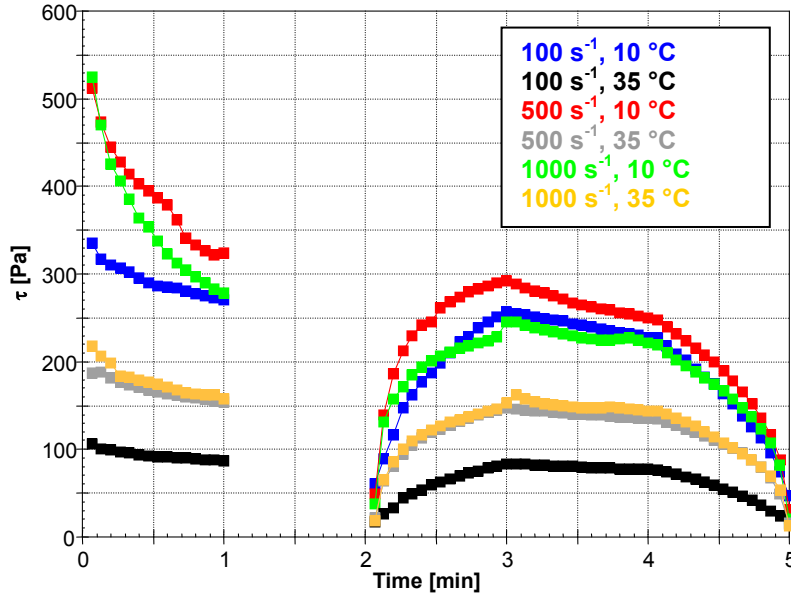
Figure 8-5: **Influence of dispersing at 10 and 35 °C on quark matrix, 16 % d.m.**

Overall, the higher temperature causes a de-structuring of the samples. Thus, the curves run on a lower level compared to the samples dispersed at 10 °C. After warming and the second dispersing step at 35 °C (preparation III) the brake torque was found to be higher for the higher shear rates compared to $\dot{\gamma}_{max}$ = 100 s^{-1}. This is only explainable by structure formation/development as a result of shearing due to incorporation of air.

Table 8-5 displays the average values of the rheological parameters obtained from five different experiments to obtain an overview of the input quality of the quark before spray drying. The standard deviation of each parameter is given.

Table 8-5: **Rheological parameters of low fat quark**

τ_0	K	n	r	s	A_{TH}	$\dot{\gamma}_{max}$	η_{eff}
Pa	Pa·s^n	-	-	Pa	Pa·s^{-1}	s^{-1}	Pa·s
Preparation I (18 %/10 °C)							
82.4±5.2	16.1±2.6	0.7±0	1.0±0	2.5±0.7	7552.4±809.7	100	4.5±0.2
(15.7±5.1)	24.2±11.6	0.4±0	1.0±0	3.5±0.6	42300.4±16357.5	500	(0.6±0.2)*
(4.5±3.0)	12.3±8.1	0.4±0	1.0±0	2.4±0.5	65969.4±32245.1	1000	(0.1±0.1)*
Preparation II (16 %/10 °C)							
40.3±10.4	14.0±2.0	0.6±0	1.0±0	2.1±1.2	3220.8±1380.1	100	2.9±0.8
12.5±2.4	18.8±5.8	0.4±0	1.0±0	1.8±0.5	32720.8±11584.4	500	0.7±0.5
7.3±1.9	14.3±2.3	0.4±0	1.0±0	2.6±1.1	64300.8±15969.1	1000	0.2±0.0
Preparation III (16 %/35 °C)							
18.1±9.5	5.5±3.8	0.6±0	1.0±0	1.3±0.4	1166.8±924.2	100	1.2±0.5
6.1±3.0	12.9±1.9	0.4±0	1.0±0	1.8±0.3	13223.6±10221.6	500	0.3±0.1
2.3±1.1	12.9±2.4	0.4±0	1.0±0	1.5±0.8	23755.0±16357.2	1000	0.2±0.0

* wall slip effects

The following statements can be made on the basis of the rheological parameters:

1. With increasing shear rate the yield point τ_0 decreases due to desaggregation/disintegration of curd particles.

2. A dispersing step causes a reduction of the yield point which is equal to a reduction of the particle size in quark.

3. The consistency factor K which increases at a shear rate of 500 s^{-1} behaves indifferently. An increase of K points to a hardening of the structure due to an increase of the inner friction because of an enhancement of the homogeneity.

4. The flow behavior index n is reduced from 0.7 to 0.4 which expresses the shear-related structural changes. Additionally, this points at an enhancement of the homogeneity due to desaggregation/disintegration of curd particles via mechanical forces.

5. The thixotropic area A_{Th} increases with increasing shear rate and acts as an indicator for the applied work to destroy the structure.

6. Each dispersing step causes a reduction of the thixotropic area which is equal to a reduction of the required work to destroy the structure for the subsequent atomization.

7. Even the first dispersing step at a low temperature causes a reduction of the effective viscosity which is necessary for the particulation.

8. The dispersing step is indispensable for a good powder quality because the dispersing results in smaller quark particles before atomization.

The preparation was found to have an immense effect on the original curd structure. In addition to the dilution from 18 % to 16 % dry matter the mechanical agitation via hand-held blender influences the rheological parameters. After preparation II the incorporation of air can be assumed to occur. During preparation III the incorporation of air definitely takes place. At higher shear rates the incorporation of air into the quark matrix results in a development of structure due to foam formation.

8.2.2 Influence of thermal and mechanical parameters on the low fat quark

The influence of thermal and mechanical parameters on the low fat quark matrix (18 % dry matter) was determined to obtain more information about the behavior of the quark during atomization. Figure 12-10 to Figure 12-15 display the viscosity and shear stress behavior in the temperature range from 0 to 70 °C at different $\dot{\gamma}_{max}$. Table 8-6 lists the parameters of the rheological analysis at $\dot{\gamma}_{max}$ = 100 s^{-1} in the temperature range from 0 to 70 °C, Table 8-7 at $\dot{\gamma}_{max}$ = 500 s^{-1}, and Table 8-8 at $\dot{\gamma}_{max}$ = 1000 s^{-1}.

Table 8-6: Regression results; *HB* model, $\dot{\gamma}_{max}$ = 100 s^{-1}

Temperature in °C	τ_0 Pa	K Pa·s^n	n -	r -	s Pa	A_{TH} Pa s^{-1}	η_{eff} (100 s^{-1}) Pa·s
0	91.14	23.30	0.622	0.9996	2.98	11150	5.00
10	73.16	20.97	0.590	0.9995	3.89	6933	3.91
15	65.85	18.47	0.596	0.9993	1.68	7059	3.53
20	57.91	14.84	0.574	0.9990	1.75	5167	2.67
30	33.76	12.06	0.567	0.9990	1.64	2568	1.98
40	20.04	7.89	0.552	0.9969	2.49	1171	1.20
50	16.09	6.78	0.545	0.9956	2.01	569	0.99
60	9.21	6.05	0.453	0.9970	0.80	262	0.58
70	5.03	2.66	0.427	0.9980	0.32	256	0.24

Table 8-7: Regression results, $\dot{\gamma}_{max}$ = 500 s^{-1}

Temperature in °C	τ_0 Pa	K Pa·s^n	n -	r -	s Pa	A_{TH} Pa s^{-1}	η_{eff} (500 s^{-1}) Pa·s
0	27.51	29.19	0.412	0.9996	2.79	76543	(2.22) *
10	21.00	33.27	0.408	0.9995	3.89	56817	2.38
15	18.75	25.69	0.404	0.9993	2.23	53812	1.84
20	14.98	20.11	0.395	0.9990	2.41	48339	1.39
30	9.88	19.29	0.384	0.9990	1.32	24245	1.24
40	0.18	23.10	0.324	0.9998	0.78	12271	1.03
50	-2.96	20.11	0.293	0.9956	0.55	7230	
	OW	17.41	0.314	0.9995	0.85		0.75
60	0.17	16.30	0.281	0.9996	0.55	4033	
	OW	16.45	0.280	0.9996	0.80		0.60
70	-1.47	9.79	0.238	0.9951	0.90	4409	
	OW	8.42	0.258	0.995	0.85		0.28

* incorrect due to wall slip

Table 8-8: Regression results, $\dot{\gamma}_{max}$ = 1000 s^{-1}

Temperature in °C	τ_0 Pa	K Pa·s^n	n -	r -	s Pa	A_{TH} Pa s^{-1}	η_{eff} (1000 s^{-1}) Pa·s
0 [500 s^{-1}]	27.51	29.19	0.412	0.9996	2.79	76543	(2.22)*
10	3.27	28.36	0.393	0.9995	2.59	84464	1.76
15	7.96	19.95	0.386	0.9993	1.16	95530	1.26
20	5.69	18.09	0.380	0.9990	3.26	107368	1.10
30	5.88	16.87	0.372	0.9990	1.91	69607	0.99
40	-2.27	20.87	0.313	0.9993	2.34	32253	
	OW	18.79	0.328	0.9998	0.77		0.85
50	-0.86	18.10	0.306	0.9956	1.64	21360	
	OW	17.41	0.314	0.9995	0.85		0.74
60	-1.45	14.98	0.287	0.9984	1.35	10529	
	OW	13.66	0.299	0.9990	1.25		0.54
70	-1.17	8.14	0.269	0.9932	1.31	13568	
	OW	7.06	0.288	0.9941	1.25		0.27

* Incorrect due to wall slip

Results highlighted in yellow are taken from the measurements done at $\dot{\gamma}_{max}$ = 500 s^{-1}

The regression of the rheological data obtained at $\dot{\gamma}_{max}$ = 100 s^{-1} was done according to the HERSCHEL-BULKLEY model. The deformation model fits the data very well which is proved by the high coefficient of correlation. The de-structuring of the low fat quark (18 % dry matter) is found to be dependant on temperature. At low temperatures (0, 10, 15, and 20 °C) the de-structuring is dominated by mechanical shear forces. The temperatures 15, 20, as well as 30 °C are the transition region in which shear forces and temperature are relevant. Above temperatures of 40 °C the temperature effect seems to dominate.

The lines in Table 8-7 and Table 8-8 highlighted in grey represent the transition of plastic flow behavior (yield point, HERSCHEL-BULKLEY model) to flow (structure viscosity, Non-NEWTONIAN fluid, OSTWALD-DE WAELE model).

At temperatures above 40 °C at $\dot{\gamma}_{max}$ = 500 s^{-1} and 1000 s^{-1} negative yield points are regressed with the HERSCHEL-BULKLEY model. From rheological view the model according to OSTWALD-DE WAELE applies to this case.

The rate of structure deformation increases with decreasing temperature. The thixotropic behavior which is an irreversible structure deformation due to the applied work to destroy the structure of the low fat quark was identified. In section 8.2.3 'Detection of interactions between mechanical energy and temperature' this effect will be explained more precisely.

8.2.3 Detection of interactions between mechanical energy and temperature

The following investigations deal with the influence of the temperature and shear force on the de-structuring of the quark matrix and extend the results made in section 8.2.2 'Influence of thermal and mechanical parameters on the low fat quark matrix'. For this reason the shear stress and the viscosity at different temperatures are displayed, Figure 12-16 to Figure 12-24 in the Appendix.

At 0, 10, 15, and 20 °C de-structuring is dominated by the influence of shear. An intersection of the pre-shearing curves occurs. Above temperatures of 30 °C no intersections occur due to dependence on shear. A higher shearing causes a stronger degradation of the effective viscosity. A transition section is determined. Now, the temperature becomes the more dominating influence on de-structuring. At a temperature ≥ 40 °C the temperature effect on the de-structuring dominates. Nevertheless, a low structure level exists; the quark is described as a non-NEWTONIAN fluid.

The results show that the quark matrix is degraded due to the dominating influence of the temperature that should be employed for the optimization of the production technology.

8.3 Assessment of the powder functionality (wheel atomizer), Section II

8.3.1 Rheological measurements

The functionality of quark powder has been assessed, which was done exemplarily for the examination of the water retention. Figure 8-6 displays the rehydration of the reference quark powder.
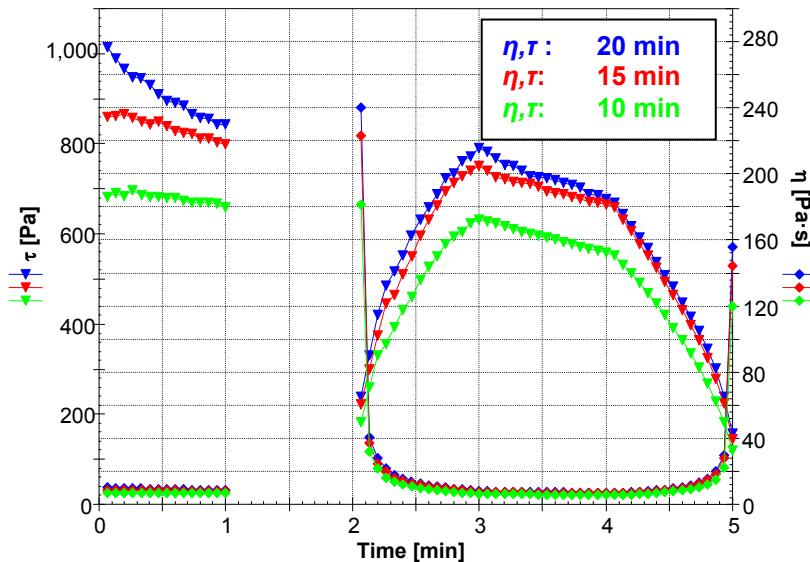
Figure 8-6: Kinetics of the rehydration of reference quark powder

After wetting, the water uptake and the restructuring strongly depend on time. A reason for that might be the convective transport into capillaries and the diffusive water transport into micro-capillaries smaller than 10^{-7} nm, respectively, after swelling and displacement of air from the capillary system which resulted from the drying.

Table 8-9 displays the regression results of the rheological data of rehydrated quark powder samples according to the HERSCHEL-BULKLEY model. Measurements were done at 20 °C.

Table 8-9: Regression results of quark powder samples in the course of rehydration

Sample	τ_0 Pa	K Pa·s^n	n -	r -	s Pa	A_{TH} Pa·s^{-1}	η_{eff} (100 s^{-1}) Pa·s
Reference							
10 min	97.94	21.35	0.667	0.9996	2.62	9448	5.59
15 min	115.69	28.69	0.637	0.9997	1.41	11541	6.55
20 min	120.90	34.96	0.596	0.9998	2.74	13328	6.65
Large-scale dryer Section II							
10 min	0.061	0.010	1.507	0.991	0.76	24	1.03
15 min	0.384	0.028	1.275	0.992	0.30	198	1.03
20 min	0.288	0.070	1.068	0.993	0.36	206	0.99
Small-scale dryer Section II							
7.1 20 min	126.33	20.74	0.681	0.9996	3.75	11242	6.03
7.2 20 min	123.44	20.43	0.687	0.9995	4.20	9102	6.06
7.3 20 min	123.16	15.88	0.731	0.9999	2.07	9443	5.83
Raw material low fat quark	96.66	14.83	0.690	0.999	1.92	9850	4.52

The measurement of a rehydration kinetic of the quark powder obtained from the small-scale dryer was not possible due to shortage of sample amount.

Exemplarily for the reference quark powder the flow curve after 20 min of rehydration runs on a higher level compared to native quark, which points to the very good functionality of the quark powder but also to differences in the dry matter. The yield point (indicator for the particle size) and the consistency index (indicator for the inner friction, intensive interaction between the permanent dipole water and milk protein) increase over time. As a consequence the flow behavior index n decreases and signalizes increasing structure stability. The thixotropic area point to an increasing applied work required to destroy the structure in the course of rehydration. The effective viscosity of the reconstituted quark increases. The phase of structure development appears to have been completed by 15 min.

The differences in the rheological data especially in the η_{eff} between the standard quark powder and quark powder produced on large scale are significant, Table 8-9. Due to the flow behavior index which is > 1 in the case of quark powder produced in a large-scale dryer a shear thickening flow behavior can be assumed. The shear thickening flow behavior becomes weaker with increasing rehydration time because interactions between proteins and water occur time-delayed. The yield point as an indicator for a paste is determined in the range of the measuring error.

The parameters determined after 20 min conform to the visual assessment which indicated de-mixing and immobilization of water. A flow behavior index > 1 signalizes the formation of a hydrate layer on the surface without strong interaction between water and protein. Similar rheological data were obtained during measurement of sand. The hypothesis of crustification of the surface of the casein particles which results in deficient water solubility is supported by the results and persists.

The quark powder produced on small scale shows an analog structure behavior to the standard plus a higher consistency exemplarily for the measured shear stress. Additionally, the rehydrated quark powders (reference powder and powders produced on small scale) reveal higher consistency compared to the original low fat quark with 18 % dry matter.

8.3.2 Particle size analysis

Table 8-10 displays the results of the particle size distribution analysis.

Table 8-10: Results of the particle size distribution analysis (section II)

Product	Reference material	Large scale	Small scale 7.1	Small scale 7.2	Small scale 7.3
Arithmetic mean of the average value (µm)	52.24	211.61	23.12	13.32	12.54
Variance (µm^2)	3239	28877	329	146	142
D_{10} (µm)	11.82	40.64	4.08	2.26	2.43
D_{50} (µm)	34.54	165.70	19.54	10.75	10.20
D_{90} (µm)	111.85	448.15	44.00	24.82	21.62
Specific surface (m$^2 \cdot$g^{-1})	0.4316	0.1237	0.7249	1.1304	1.1621

As anticipated, the dryer operations were found to determine the particle spectrum (separation of particles from the disc). The reference material has an arithmetic mean of the average value of 52.24 μm which is about a quarter of the particles size of the powder obtained from the large-scale dryer highlighted in red in Table 8-10. Additionally, the particles have a high specific surface resulting from a successful drying. The powder particles produced on small scale with the Büchi dryer are of smaller dimensions compared to the reference material. Hence, the functionality is equal and superior, respectively. The positive properties regarding the water retention (formation of structure) of the products was also determined. A reproduction of these parameters on a technical and production scale would result in superior quark powder qualities. At this time, the results for the production on large scale cannot be positively assessed because of the very large particle sizes.

8.3.3 SEM results

Figure 8-7 displays the 300- and 1500-fold magnification of the reference powder.
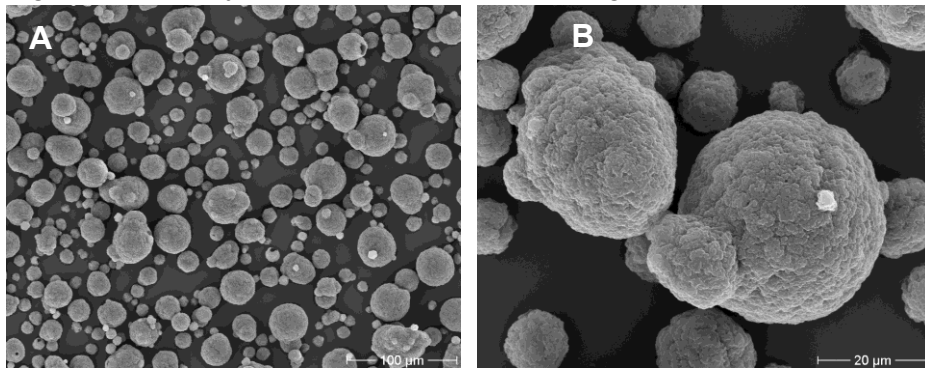
Figure 8-7: **SEM micrographs of the reference quark powder**
A: 300-fold magnification B: 1500-fold magnification

In comparison to the powder obtained on large scale a relatively homogeneous particle distribution is determined. Additionally, the contour of the particles seems to depend on the size of the particle. Small particles seem to be circular whereas larger particles become more ellipsoidal. The nature of the surface can be seen from Figure 8-7 part B. The surface appears to be fissured and indicates a porous, capillary structure.

Figure 8-8 displays the SEM micrographs of the quark powder produced on the large-scale dryer in section II.
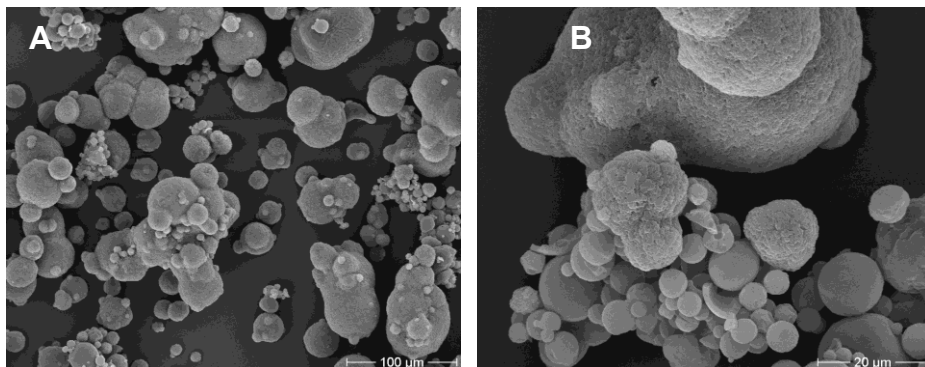
Figure 8-8: **SEM micrographs of the quark powder, large-scale dryer**
A: 300-fold magnification B: 1500-fold magnification

The 1500-fold magnification indicates a more inhomogeneous particle spectrum. The existing particle clusters are noticeable because larger particles have a smaller specific surface and are more difficult to dry which points at problems with the separation of the quark particles from the disc.

Figure 8-9 displays the SEM micrographs (300- and 1500-fold magnification) of the quark powder obtained on small scale, sample 7.1 in section II.
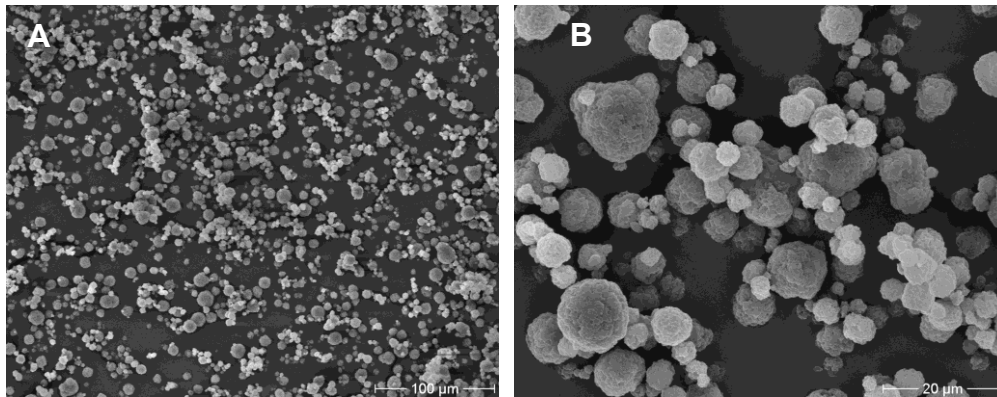
Figure 8-9: **SEM micrographs of the quark powder obtained by the small-scale dryer (7.1)**
A: 300-fold magnification B: 1500-fold magnification

A very homogeneous particle spectrum is achieved. The 1500-fold magnification shows the dominating proportion of the fine grain. The drying in the Büchi dryer can be classified to be superior compared to the large-scale production.

8.4 Assessment of the powder functionality of competitor's products

Additional to the experiments above, quark powder produced by another company was analyzed.

8.4.1 Rheological measurements

Table 8-11 displays the regression results (HERSCHEL-BULKLEY) of the rheological data.

Table 8-11: **Regression results of competitor's products**

Sample	τ_0 Pa	K Pa·s^n	n -	r -	s Pa	A_{TH} Pa·s^{-1}	η_{eff} (100 s^{-1}) Pa·s
Sample 1, 2 h	0.33	0.0003	1.973	0.625	0.11	12	0.008
Sample 2, 2 h	0.44	0.011	1.319	0.945	0.42	39	0.048
Sample 3, 2 h	12.97	10.46	0.557	0.999	1.25	1371	1.49

Compared to the reference powder and raw material low fat quark, Table 8-9, the competitor's products reveal a lower structural level. In the case of sample 1 only the 8-fold of water viscosity is achieved. Sample 3 can be assessed to be favorable compared to the other samples although the structure behavior is not as good as it is in the case of the reference powder.

Figure 8-10 displays the tendency for sedimentation of the samples (18 % d.m.) after 2 h of rehydration. Only sample 3 was stable after 2 h.

Figure 8-10: Sedimentation of competitor's quark powders after 2 h stand-by

On rehydration, the quark powders should reveal a smooth and paste-like structure with good water retention like original quark. Especially samples 1 and 2 show poor water retention with a strong sedimentation tendency. Thus, no stable product is obtained after rehydration.

8.4.2 Particle size analysis

The results of the particle size analysis of the powders measured in dry state are displayed in Table 8-12.

Table 8-12: Results of the particle size analysis of the dry powders (µm), $N = 3$

Material	D_{50}	Mode	D_{10}	D_{90}
Sample 1, average value	32.00	36.62	13.85	73.13
$\pm s$	0.17	0.01	0.08	0.85
Sample 2, average value	20.32	16.32	9.90	50.80
$\pm s$	0.02	0.00	0.04	0.70
Sample 3, average value	32.80	41.91	13.66	76.53
$\pm s$	0.12	0.01	0.02	0.72

The powder sample 2 has the smallest particle size with a D_{50} of 20.32 ± 0.02 µm. The other samples possess nearly identical particle sizes with a D_{50} of sample 1: 32.00 ± 0.17 µm and sample 3: 32.80 ± 0.12 µm. Only the D_{90} has a larger difference of about 3 µm. Here, the sample 3 has the largest particle size.

The results of the particle size analysis of the rehydrated powders are displayed in Table 8-13. The values are averages of three replicated measurements.

Table 8-13: Results of the particle size analysis of the rehydrated powders (µm), $N = 3$

Material	D_{50}	Mode	D_{10}	D_{90}
Sample 1	46.86	54.78	20.66	90.99
$\pm s$	0.00	0.00	0.06	0.65
Sample 2	33.57	42.07	13.12	73.31
$\pm s$	0.91	0.06	0.25	1.14
Sample 3, peak 1	10.88	12.20	5.56	21.43
$\pm s$	0.12	0.11	0.14	0.08
Sample 3, peak 2	63.06	71.66	36.47	115.59
$\pm s$	0.13	0.48	0.05	1.25

In the case of samples 1 and 2 unimodal distributions were obtained. In comparison to the dry measurements the differences were very small.

In the case of sample 2 the D_{50} increased from 20.32 ± 0.02 µm to 33.57 ± 0.91 µm on rehydration. In the case of sample 1 the D_{50} increased from 32.00 ± 0.17 µm to 46.86 ± 0 µm on rehydration. The slight increase of about 10 µm—indicating swelling— is minimal and substantiates the findings of the rheological results regarding the very poor water retention.

The particle size distribution of sample 3 was found to be multimodal. Table 8-13 displays the particle sizes for each peak individually. In comparison to the dry powder with a D_{50} of 32.80 ± 0.12 µm on rehydration one powder fraction has become smaller (D_{50}: 10.88 ± 0.12 µm) and one fraction is now larger (D_{50}: 63.06 ± 0.13 µm). These results suggest that simultaneously a swelling and dispersion of the powder particles occurred. In combination with the rheological results (Table 8-11) this sample has a higher technological quality.

8.4.3 HIC analysis

Table 8-14 displays the results of the HIC analysis which are the α_{S1}-, α_{S2}-, and the κ-/β-casein content explained as a percentage of the overall casein content.

Table 8-14: **Casein profile of the competitor's products**

Sample	α_{S1} %	α_{S2} %	κ/β %
Sample 1	53.18± 0.13	12.34 ± 0.33	34.49 ± 0.19
Sample 2	51.46 ± 0.49	12.48 ± 0.2	36.07 ± 0.69
Sample 3	41.995 ± 0.28	7.97 ± 0.13	50.03 ± 0.41

The casein profile of sample 3 deviates from that of sample 1 and 2. The determined casein relation $\alpha_{S1}:\alpha_{S2}:\beta$ and κ-casein is in accordance to the well-established relation of a native sample which is 40:10:35:15; here 42:8:50. On the contrary, the casein profile of samples 1 and 2 show a reduced content of the β- and κ-casein which can be related to the technological processes during fermentation.

The casein profile of the quark powder produced on large scale in section I (Table 8-4) can be compared to the profile obtained from competitor's products samples 1 and 2 which also showed an insufficient water binding capacity in contradiction to sample 3.

At this point the casein profile seems to be an indicator for the rehydration properties and functionality of the quark powders.

8.5 General remarks

To optimize the spray drying process in the present study the attempt was made to primarily characterize the influence of thermal and mechanical parameters on the low fat quark matrix and to obtain results for the atomization process.

The rheological results led to the conclusion that above 40 °C the temperature effect dominates. Here, the transition of plastic flow behavior (yield point, HERSCHEL-BULKLEY model) to flow (structure viscosity, Non-NEWTONIAN fluid, OSTWALD-DE WAELE model) occurs. The production of quark powder in a pilot plant and small-scale dryer resulted in good water retention of the powder on rehydration. A pressure nozzle atomizer was used.

The rheological results showed that the curd structure of the rehydrated powder without incorporation of air (standard) is equivalent to that of the raw material. In general, the change in the warming regime (now 65 °C instead of 35 °C) could be positively assessed. The stronger thermal de-aggregation resulted in an acceptable atomization with good water retention of the final product which had been suggested by the preliminary experiments. This effect had also been anticipated on the basis of a study by MULHELM, FRITSCHING, SCHULTE, and BAUCKHAGE (2003) [321]. They reported that the droplet diameter increased with increasing viscosity of the liquid—which happened during experiments when the temperature was decreased—because more energy was needed to separate the solid particles from each other.

The production of quark powder in the large-scale dryer using a pressure nozzle atomizer in section I resulted in a product which showed insufficient water-binding capacity. After rehydration large particles were visually detected. The drying/atomization conditions of the large-scale dryer have to be responsible for the poor functionality as long as previous results from the small-scale dryer and market products showed good powder properties, Figure 8-2 (small-scale dryer), Table 8-9 (reference powder) and Table 8-11 (sample 3). The visual assessment resulted in smaller particulation, particle interactions, and formation of dust (actually undesirable) of the product dried on small scale. These findings correspond to statements made by HECHT and BAYLY (2009) who observed that smaller dryers create smaller particles [322]. Furthermore, they pointed out that only very basic mass and energy balances are scaleable but the most processes undergo critical, unpredictable changes during scale-up.

In comparison to results obtained in section II using a wheel atomizer the particle sizes of the quark powder produced on large scale using a pressure nozzle atomizer were smaller, Table 8-3, but the water retention was poorer. No rheological measurements had been made in section I due to the deficient water retention. Additionally, the SEM micrographs of the powder produced on large scale using a pressure nozzle atomizer showed that most particles were agglomerated to larger clusters. Despite the arithmetic mean of the average value of 77.26 µm, 10 % of the particles were larger than 150.5 µm.

As a result, these findings correspond to general statements made on the advantages and disadvantages of atomizers. Wheel atomizers are in discussion to be favorable compared to pressure nozzle atomizers because the resulting droplet size is insensitive to feed rate fluctuations and fluctuations in concentration in combination with changed viscosity and feed rate and it is possible to operate with higher feed viscosities [172]. Additionally, the fact has to be taken into consideration that the nozzle geometry used was designed especially for the drying of skim milk concentrate which could have caused drying/atomization problems.

To date, data in the literature for the determination of the influence of the particle size on the rehydration of quark powder are not available. In our study quark powders with small particle sizes < 50 µm, Table 8-10, were found to have a favorable structure behavior plus a high consistency exemplarily for the measured shear stress, Table 8-9.

Investigations into competitor's products showed that a small particle size alone cannot be mandatory for a good rehydration behavior (Table 8-11 and Table 8-12). Other characteristics have to be responsible for this phenomenon.

The following critical statement has to be made: The pressure nozzle geometry used for the atomization of the quark was originally dimensionized for the drying of skim milk concentrate. Here, the nozzle geometry aims to produce particle sizes of about 200 µm. For a good quality quark powder a particle size of 20 µm is required. Preliminary experiments in section II showed that the functionality, especially the water retention, of quark powder particles was favorable for particles in that range. The use of correct nozzle geometry is a basic requirement for obtaining results with particles created of a size of 20 µm.

8.6 Summary of the chapter

Recently, the industrial need of investigations into the spray drying, especially the atomization of viscous liquids, was presented by HECHT and BAYLY (2009) [322]. They mentioned that most research was done on low-viscous liquids but typically the feeds are concentrated, viscous, and non-NEWTONIAN. The experiments carried out here were done to optimize the processing technology of quark powder. Admittedly, the pressure nozzle geometry used for the atomization of the quark was originally dimensionized for the drying of skim milk concentrate. Nevertheless, quark powder was produced which showed satisfactory water retention and showed comparable particle sizes compared to market products which were produced on large-scale.

Chapter 9: Recommendations

Although several replicated experiments were carried out regarding the structure formation during processing of dairy products and, derived therefrom, the development of methods that are able to control the quality of the raw material milk itself and its quality for the rennet-induced coagulation as well as further dairy additives like WPC and quark powders some proposals for further research can be made.

During rennet-induced coagulation of milk from infected udder parts it was found that these milk samples behaved very inconsistently. Large variations exist on structural levels and chemical composition. A classification was made on the basis of the process viscosity after 60 min. The obtained results suggest the importance of the analysis of the milk protein composition in milk grading.

The development of a HPLC method is needed to clarify the reason for the increased GMP content of milk from infected udder quarters compared to normal bulk milk. Furthermore, bacteriological examinations of the milk samples should be done to identify the specified microorganism establishing the infection which would enlarge the information obtained by chemical analysis. The results suggest that there might be a correlation of SCC and process viscosity $\eta(t)$ during rennet-induced coagulation which should be continually pursued.

The rennet-induced coagulation of goat milk was only investigated for very few samples. Here, an enlargement of the sample number is needed to prove the obtained results. Nevertheless, the obtained results suggest that the rheological measurements and the spectrophotometric analysis can be transferred to goat milk.

The method developed here to study the rehydration of whey protein concentrate powders was found to be useful as a rapid method to assess the powders regarding their solubility. Unfortunately, no fermentations were performed using the investigated powders under real production conditions. This would help to ensure the obtained results and to set limit values regarding the size and the volume concentration of peak 2 in the PSDs of the laser diffraction method. Additional to the laser diffraction method, a method should be used which delivers quantitative results providing the exact amount of particles in each size group.

During the experiments dealing with the investigation of the production of quark powders material characteristics were obtained which can be used for further optimization of the process. Nevertheless, more detailed research would be needed in the atomization and the scale-up during spray drying of highly structured products such as quark.

Chapter 10: Conclusions

The processes of the acid and rennet-induced coagulation and the drying technology—taking the production of quark powder as an example—were viewed in detail.

A spectrophotometric method was used to determine the released CMP and GMP during and at the end point of the rennet-induced coagulation of raw bovine bulk milk from healthy cows and cows suffering from an udder inflammation. Additionally, the characteristics of the renneting process were recorded with an RSD-1-1 torsion oscillator. This enabled the grading of the process into five sections, whereas the first three sections were discussed in detail. The course of the process viscosity of 15 raw bulk milk samples was measured to obtain a standard curve. With the use of the torsion oscillator measurements the resulting structuring mechanisms during rennet-induced coagulation can be examined. The process viscosity is found to be an objective parameter for the pre-calculation of the optimal cutting time. The rheological model represents a technological tool which can be used as an early warning and control system.

In comparison to milk from healthy cows the coagulation behavior of twenty seven samples of milk from infected udder quarters was examined. Huge differences were found for the coagulation behavior of milk from infected udder quarters. The course of the curves of the process viscosity over time was found to be very divergent. Thus, an overall statement about the coagulation behavior being valid for all milk samples from infected udder quarters cannot be made. It is therefore more applicable to differentiate between the milk samples and to characterize them according to selected parameters. The process viscosity after 60 min of coagulation was found to be a good parameter to divide the milk samples into four classes. For the first time an attempt is made to differentiate between milk from healthy cows and that from cows having infected udder quarters regarding cheese-making parameters.

The four classes behaved very differently. In combination with the results of the chemical analysis it was found that high process viscosities after 60 min depended on the increased protein content. A rapid renneting was attributed to an altered or disturbed micelle structure due to udder inflammation. The most detrimental changes occurred for non-coagulating milk samples. Here, hydrolysis of the casein was suggested by the results of the spectrophotometric analysis and the HIC profiles. For non-coagulating milks the CMP (GMP and n.-g. CMP) content increases despite of the very low casein content in these milks. Here, the enzyme status was discussed to have undergone an immense change due to increased activation of plasmin. The increased casein hydrolysis results in small peptides which behave very similar to GMP and n.-g. CMP under the experimental conditions and cause the higher contents which are consequently not only related to CMP but also to the hydrolysis products.

Viewing the rennet-induced coagulation of goat milk a high amount of glycosylated macropeptide was determined which is in contradiction to literature data. Nevertheless, the amount of literature data on this question is manageable and further research in this area is needed.

The results suggest that the rheological measurements and the spectrophotometric analysis can be transferred to goat milk. The rheological method allowed a grading of the process into five sections, whereas the first three sections were discussed in detail. Significant differences during rennet-induced coagulation of milk from healthy cows and goat milk occurred in section 3 in the phase of the gel formation. The viscosity cannot be described by a linear function in the case of goat milk due to the fact that a plateau has been reached.

Common methods used to prevent syneresis of stirred yoghurt are the increase of the dry matter, the homogenization of milk, the thermal modification of the milk protein, the choice of culture, and the reduction of mechanical stress [6;291]. The present work focuses the quality assessment of the powders which are added to yoghurt milk for the standardization of the non-fat solid contents of the milk. The rehydration behavior of dairy powders was investigated with a novel approach using laser diffraction. Here, a rapid method is developed which can be used for the characterization and assessment of the powder quality and functionality. In detail, the particle size of the dairy powders is measured during rehydration.

Rehydration was found to be accompanied with the reduction of the particle size of about three times ten. From the mostly unimodal distributions obtained for the dry measurements in most cases a bimodal or multimodal distribution resulted for the wet measurements based on volume. As a result of the differentiation into dissolved and poorly or incompletely dissolved particles between the single peaks, fields existed in which no undissolved particles were detected.

The investigations significantly proved the influence of the protein content on the particle size in dry and rehydrated state. During the production of WPC powders the variation in particle size can be attributed to multiple effects caused by the processing conditions or equipment design (methods of water removal or atomization conditions) and also to the source and composition of the liquid whey.

Additionally, an attempt was made to characterize the individual peaks occurring in the PSD obtained by static laser light scattering. It has been shown that for whey the frequency of the second peak increases with increasing thermal treatment.

Chitosan treatment of the samples demonstrated that it was possible to remove all undissolved material from the samples (no peaks were detected by static laser light scattering) whereas the protein content of the dissolved whey proteins remained nearly constant.

SDS-PAGE showed that Chitosan removed not only fat but also protein, assumably the larger aggregates.

The presence of large particles in the PSDs indicates the presence of heat-denatured protein aggregates being a result of the processing history. The results of the static laser light scattering in combination with the results of the HPSEC (content of native whey protein) and the parameter in accordance to the NSI showed that it is possible to assess powders according to their functionality which means the solubility in detail.

The volume concentration taken from the PSD obtained by laser diffraction enables a rapid grading of the powders because after only 10 min of rehydration a high or low volume concentration can be detected. Additionally, it was found that the HPSEC—especially the exclusion limit—is not an applicable tool to determine dairy powder functionality which was done in literature earlier.

In Chapter 8 the production technology of quark powder was examined. The attempt is made to atomize the quark by a nozzle atomizer instead of the commonly used disc atomizer for the drying of highly-structured feed material.

Material characteristics, the influence of thermal and mechanical parameters, of low fat quark were determined to obtain results for the atomization process. A dispersing step was found indispensable for a good powder quality because the dispersing results in smaller quark particles before atomization. The structure-weakening influence of the temperature can be used for the optimization of the production technology. When quark powder is produced by spray drying, insufficient atomization can cause quality problems of the powder after rehydration. Those quality problems are normally related to separation of very large particles from the atomizer leading to incomplete drying and the formation of a crust outside the particle which inhibits a complete drying of the inner part which very likely negatively influences the wetting and therefore the functionality. A de-structuring of the quark matrix before atomization is therefore necessary to produce smaller droplets.

The powder quality was assessed according to consistency and functional properties such as water retention after rehydration. On rehydration quark powder should reveal a smooth, paste-like structure as the original quark without sedimentation but with sufficient water retention. Market samples produced on large scale have shown that a small particle size is favorable to obtain sufficient water retention after rehydration.

Chapter 11: References

1. Brückner M, Senge B (2007) Milchwiss. 62:245-249.
2. Senge B (2008) Chemie Ingenieur Technik Special Issue: Neue Wege in der Lebensmittelverfahrenstechnik 80 (8):1125-1136.
3. Lieske B, Senge B (2006) Deutsche Molkereizeitung 127 (5).
4. Lieske B, Senge B (2006) Deutsche Molkereizeitung 127 (6):30-34.
5. Lieske B, Senge B (2006) Deutsche Molkereizeitung 127 (7):32-34.
6. Sodini I, Remeuf F, Haddad S, Corrieu G (2004) Critical Reviews in Food Science and Nutrition 44 (2):113-137.
7. Sodini I, Montella J, Tong PS (2005) Journal of the Science of Food and Agriculture 85 (5):853-859.
8. Mottar J, Bassier A, Joniau M, Baert J (1989) J. Dairy Sci. 72 (9):2247-2256.
9. Schorsch C, Wilkins DK, Jones MG, Norton IT (2001) J. Dairy Res. 68 (3):471-481.
10. Senge B, Tabel U, Blochwitz R, Lieske B (2005) Deutsche Molkereizeitung 126 20-27.
11. Senge B, Blochwitz R, Schulz S, Zywietz C (2003) Strukturstabilität von Rührjoghurt im Processing II. Technische Universität Berlin, Berlin
12. Petzold S (2004) Strukturstabilität von Rührjoghurt im Processing. Diploma Thesis, Technische Universität Berlin, Berlin
13. Liebenow A (2006) Strukturstabilität von Rührjoghurt im Processing Diploma Thesis, Technische Universität Berlin, Berlin
14. Töpel A (2004) Chemie und Physik der Milch vol 1. . Behr's, Hamburg.
15. Walstra P, Jenness R (1984) Dairy Chemistry and Physics. Wiley, New York.
16. Farrell HM, Jr., Jimenez-Flores R, Bleck GT, Brown EM, Butler JE, Creamer LK, Hicks CL, Hollar CM, Ng-Kwai-Hang KF, Swaisgood HE (2004) J. Dairy Sci. 87 (6):1641-1674.
17. Swaisgood HE (1982) Chemistry of milk proteins. In: Fox PF (ed) Developments in Dairy chemistry-1. Proteins. Appl. Sci. Publ., New York, NY, pp 1-59.
18. Doi H, Ibuki F, Kanamori M (1979) J. Dairy Sci. 62 (2):195-203.
19. Pujolle J, Ribadeau-Dumas B, Garnier J, Pion R (1966) Biochemical and Biophysical Research Communications 25 (3):285-290.
20. Woychik JH, Kalan EB, Noelken ME (1966) Biochemistry 5 (7):2276-2282.
21. Vreeman HJ, Both P, Brinkhuis JA, Van Der Spek C (1977) Biochim. Biophys. Acta - Protein Structure 491 (1):93-103.
22. Mackinlay AG, Wake RG (1965) Biochim. Biophys. Acta 104 (1):167-180.
23. Vreeman HJ, Visser S, Slangen CJ, van Riel JAM (1986) J. Biochem. 240:87-97.
24. Jolles J, Alais C, Jolles P (1968) Biochim. Biophys. Acta - Protein Structure 168 (3):591-593.
25. Delfour A, Jollès J, Alais C, Jollès P (1965) Biochemical and Biophysical Research Communications 19 (4):452-455.
26. Saito T, Itoh T (1992) J. Dairy Sci. 75 (7):1768-1774.
27. Fournet B, Fiat AM, Alais C, Jollès P (1979) Biochim. Biophys. Acta - Protein Structure 576 (2):339-346.
28. Jollès J, Schoentgen F, Alais C, Fiat AM, Jollès P (1972) Helvetica Chimica Acta 55 (8):2872-2883.
29. Tran VD, Baker BE (1970) J. Dairy Sci. 53 (8):1009-1012.

References

30.	Fiat A-M, Alais C, Jolles P (1972) European Journal of Biochemistry 27 (3):408-412.
31.	Jollès J, Fiat A-M, Alais C, Jollès P (1973) FEBS Letters 30 (2):173-176.
32.	Jollès P, Loucheux-Lefebvre M-H, Henschen A (1978) Journal of Molecular Evolution 11 (4):271-277.
33.	Fournet B, Fiat AM, Montreuil J, Jollès P (1975) Biochimie 57 (2):161-165.
34.	Molle D, Leonil J (1995) J. Chromatogr. A 708 (2):223-230.
35.	Walstra P (1990) J. Dairy Sci. 73 (8):1965-1979.
36.	Walstra P (1999) Int. Dairy J. 9 (3-6):189-192.
37.	Horne DS (1998) Int. Dairy J. 8 (3):171-177.
38.	Holt C, Horne DS (1996) Neth. Milk Dairy J. 50:85-111.
39.	Schmidt DG (1982) Food Microstructure 1:151-165.
40.	Holt C, Anfinsen CB, Edsall JD, Richards FK, Eisenberg DS (1992) Structure and stability of bovine casein micelles. In: Advances in Protein Chemistry, vol 43. Academic Press, pp 63-151.
41.	Fox PF, McSweeney PLH (1998) Dairy Chemistry and Biochemistry. First edn. Blackie Academic and Professional, London, Weinheim, New York, Tokyo, Melbourne, Madras.
42.	Park YW, Haenlein GFW (2006) Handbook of milk of non-bovine mammals. 1 edn. Blackwell Publishing.
43.	Law AJR, Tziboula A (1992) Milchwiss. 47 (9):558-562.
44.	Ono T, Creamer LK (1986) NZ J. Dairy Sci. Technol. 21:57-64.
45.	Richardson BC, Creamer LK, Munford RE (1973) Biochim. Biophys. Acta - Protein Structure 310 (1):111-117.
46.	Remeuf F, Lenoir J (1986) Bulletin of the International Dairy Federation 202:68-72.
47.	Jaubert A, Durier C, Kobilinsky A, Martin P (1999) Int. Dairy J. 9 (3-6):369-370.
48.	Senge B (2009) Materialsammlung zur Vorlesung Molkereitechnologie. TU Berlin
49.	Flueler O (1982) Deutsche Molkereizeitung 103:1172-1178.
50.	Dalgleish DG (2003) The enzymatic coagulation of milk. In: Fox PF, McSweeney PLH (eds) Advanced Dairy Chemistry Volume 1: Proteins, Part B, vol 1. 3 edn. Kluwer Academic/Plenum Publishers, New York, pp 579-619.
51.	Lieske B (1997) Lait 77:201-209.
52.	Hyslop DB (2003) Enzymatic coagulation of milk. In: Fox PF, McSweeney PLH (eds) Advanced Dairy Chemistry Volume 1: Proteins, Part B, vol 1. 3 edn. Kluwer Academic/Plenum Publishers, New York, pp 839-878.
53.	Lieske B, Faber W, Konrad G (1996) Milchwiss. 51 (10):548-551.
54.	Swaisgood HE (2003) Chemistry of the caseins. In: Fox PF, McSweeney PLH (eds) Advanced dairy chemistry - 1.: Proteins. - Part A. 3rd edn. Kluwer Academic / Plenum Publishers, New York.
55.	Kammerlehner J (1994) Labkäsetechnologie. Verlag Thomas Mann, Gelsenkirchen-Buer.
56.	Kirchmeier O (1987) Phasenumwandlungen in der Technologie der Milch. Volkswirtschaftlicher Verlag, München.
57.	Kroeker EM, Ng-Kwai-Hang KF, Hayes JF, Moxley JE (1985) J. Dairy Sci. 68 (7):1752-1757.
58.	Ng-Kwai-Hang KF, Hayes JF, Moxley JE, Monardes HG (1984) J. Dairy Sci. 67 (2):361-366.
59.	Grandison AS, Ford GD, Millard D, Owen AJ (1984) J. Dairy Res. 51 (03):407-416.
60.	Grandison AS, Ford GD (1986) J. Dairy Res. 53 (04):645-655.

61. Munro GL, Grieve PA, Kitchen BJ (1984) Aust. J. Dairy Tech. 39:7-16.
62. Ali AE, Andrews AT, Cheeseman GC (1980) J. Dairy Res. 47:393-400.
63. Ng-Kwai-Hang KF, Hayes JF, Moxley JE, Monardes HG (1984) J. Dairy Sci. 67 (4):835-840.
64. Banks JM, Muir DD (1984) Dairy Industries International 49 (9):17-36.
65. Marziali AS, Ng-Kwai-Hang KF (1986) J. Dairy Sci. 69 (7):1793-1798.
66. Okigbo LM, Richardson GH, Brown RJ, Ernstrom CA (1985) J. Dairy Sci. 68 (4):822-828.
67. Storry JE, Ford GD (1982) J. Dairy Res. 49 (3):469-477.
68. Storry JE, Grandison AS, Millard D, Owen AJ, Ford GD (1983) J. Dairy Res. 50 (2):215-229.
69. Politis I, Ng-Kwai-Hang KF (1988) J. Dairy Sci. 71 (7):1740-1746.
70. McDowell AKR, Pearce KN, Creamer LK (1969) NZ J. Dairy Sci. Technol. 4:166.
71. Lomholt SB, Worning P, Ogendal L, Qvist KB, Hyslop DB, Bauer R (1998) J. Dairy Res. 65 (4):545-554.
72. Schulz D, Senge B, Krenkel K (1997) Milchwiss. 52 (6):303-306.
73. Reuter H, Hisserich D, Prokopek D (1981) Milchwiss. 36 (1).
74. Coulon J-B (2004) Lait 84:221-242.
75. Coulon J-B, Gasqui P, Barnouin J, Ollier A, Pradel P, Pomiès D (2002) Anim. Res. 51:383-393.
76. Harmon RJ (1994) J. Dairy Sci. 77 (7):2103-2112.
77. Lüthje P, Schwarz S (2006) J. Antimicrob. Chemother. 57 (5):966-969.
78. Östensson K, Hagelton M, Aström G (1988) Acta Vet. Scand. 29:493-500.
79. Leitner G, Chaffer M, Krifucks O, Glickman A, Ezra E, Saran A (2000) Journal of Veterinary Medicine 47:133-138.
80. Vangroenweghe F, Dosogne H, Burvenich C (2002) The Veterinary Journal 164 (3):254-260.
81. Urech E, Puhan Z, Schallibaum M (1999) J. Dairy Sci. 82 (11):2402-2411.
82. Korhonen H, Kaartinen L (1995) Changes in the composition of milk induced by mastitis. In: Sandholm M, Honkanen-Buzalski T, Kaartinen L, Pyörälä S (eds) The bovine udder and mastitis. University of Helsinki, Faculty of Vetrinary Medicine, Helsinki, pp 76-82.
83. Somers JM, O'Brien B, Meaney WJ, Kelly AL (2003) J. Dairy Res. 70 (01):45-50.
84. Grönlund U, Hultén C, Eckersall PD, Hogarth C, Waller KP (2003) J. Dairy Res. 70 (04):379-386.
85. Wendt K (1998) Handbuch Mastitis. Kamlage Verlag, Osnabrück.
86. Spreer E (1995) Technologie der Milchverarbeitung. 7. edn. Behr, Hamburg.
87. Politis I, Lachance E, Block E, Turner JD (1989) J. Dairy Sci. 72 (4):900-906.
88. Bastian ED, Brown RJ, Ernstrom CA (1991) J. Dairy Sci. 74 (11):3677-3685.
89. Verdi RJ, Barbano DM (1991) J. Dairy Sci. 74 (3):772-782.
90. Donnelly WJ, Barry JG (1983) J. Dairy Res. 50 (04):433-441.
91. Barry JG, Donnelly WJ (1981) J. Dairy Res. 48 (03):437-446.
92. Auldist MJ, Coats S, Sutherland BJ, Mayes JJ, McDowell GH, Rogers GL (1996) J. Dairy Res. 63 (02):269-280.
93. Auldist MJ, Hubble IB (1998) Aust. J. Dairy Tech. 53:28-36.
94. De Marchi M, Dal Zotto R, Cassandro M, Bittante G (2007) J. Dairy Sci. 90 (8):3986-3992.
95. Cooney S, Tiernan D, Joyce P, Kelly AL (2000) J. Dairy Res. 67 (02):301-307.
96. Barbano DM, Rasmussen RR, Lynch JM (1991) J. Dairy Sci. 74 (2):369-388.

97. Klei L, Yun J, Sapru A, Lynch J, Barbano D, Sears P, Galton D (1998) J. Dairy Sci. 81 (5):1205-1213.
98. Formaggioni P, Malacarne M, Summer A, Fossa E, Mariani P (2001) Ann. Fac. Med. Vet. Univ. Parma 21:261–268.
99. Summer A, Malacarne M, Martuzzi F, Mariani P (2002) Ann. Fac. Med. Vet. Univ. Parma. 22:163-174.
100. Van Hooydonk ACM, Walstra P (1987) Neth. Milk Dairy J. 41:19-47.
101. Caron A, St-Gelais D, Pouliot Y (1997) Int. Dairy J. 7 (6-7):445-451.
102. Okigbo LM, Richardson GH, Brown RJ, Ernstrom CA (1985) J. Dairy Sci. 68 (8):1887-1892.
103. Tyriseva AM, Vahlsten T, Ruottinen O, Ojala M (2004) J. Dairy Sci. 87 (11):3958-3966.
104. Tyrisevä A-M, Ikonen T, Ojala M (2003) J. Dairy Res. 70 (01):91-98.
105. Mariani P, Losi G, Russo V, Castagnetti GB, Grazia L, Morini D, Fossa E (1976) Scienza E Tecnica Lattero-Casearia 27 (3):208-277.
106. Davoli R, Dall'Olio S, Russo V (1990) Journal of Animal Breeding and Genetics 107:458-464.
107. Ikonen T, Morri S, Tyriseva AM, Ruottinen O, Ojala M (2004) J. Dairy Sci. 87 (2):458-467.
108. Lindström UB, Antila V, Syväjärvi J (1984) Acta Agric. Scand. 34:349-355.
109. Tervala HL, Antila V (1985) Meijeritieteellinen Aikakauskirja XLIII:16-25.
110. Van Hooydonk ACM, Olieman C (1982) Neth. Milk Dairy J. 36:153-158.
111. Lieske B, Konrad G (1996) Milchwiss. 51 (8):431-435.
112. Lieske B, Konrad G, Faber W (1997) Int. Dairy J. 7 (12):805-812.
113. Lieske B, Konrad G, Kleinschmidt T (2004) Milchwiss. 59 (3/4):172-175.
114. Dalgleish DG (1986) J. Dairy Res. 53 (1):43-51.
115. Leonil J, Molle D (1991) J. Dairy Res. 58 (3):321-328.
116. Molle D, Leonil J (2005) Int. Dairy J. 15 (5):419-428.
117. Fox PF, Guinee TP, Cogan TM, McSweeney PLH (2000) Fundamentals of cheese science. Aspen Publishers Inc., Gaithersburg, Maryland.
118. Lucey JA (2002) J. Dairy Sci. 85 (2):281-294.
119. O'Callaghan DJ, O'Donnell CP, Payne FA (2000) Journal of Food Engineering 43 (3):155-165.
120. Thomasow J, Voss E (1977) Bulletin of the International Dairy Federation 99:1-7.
121. van Hooydonk ACM, van den Berg G (1988) Bulletin of the International Dairy Federation 225:2-10.
122. O`Callaghan DJ (1999) On-line measurement of curd firming during cheese manufacture. Doctoral Dissertation, University College Dublin, Ireland,
123. Schulz D (2000) Untersuchung von Strukturierungsvorgängen bei der Lab- und Säuregerinnung von Milch. Doctoral Dissertation, Technische Universität Berlin, Berlin
124. Sharma SK, Hill AR, Goff HD, Yada R (1989) Milchwiss. 44:682-685.
125. Sharma SK, Hill AR, Mittal GS (1993) Food Research International 26 (2):81-87.
126. Hori T (1985) Journal of Food Science 50:911-917.
127. Ustunol Z, Hicks CL, Payne FA (1991) Journal of Food Science 56 (2):411-420.
128. Payne FA, Hicks CL, Shen P-S (1993) J. Dairy Sci. 76 (1):48-61.
129. Laporte M-F, Martel R, Paquin P (1998) Int. Dairy J. 8 (7):659-666.
130. Lucey JA (2004) Int. J. Dairy Technol. 57 (2-3):77-84.
131. Weipert D, Tscheuschner H-D, Windhab E (1993) Rheologie der Lebensmittel. Behr´s Verlag.

References

132.	Banon S, Hardy J (1992) J. Dairy Sci. 75 (4):935-941.
133.	Schulz-Collins D, Senge B (2004) Acid- and acid/rennet-curd cheeses. Part A: Quark, Cream cheese and related varieties. In: Fox PF, McSweeney PLH, Cogan TM, Guinee TP (eds) Cheese Chemistry, Physics and Microbiology, vol 2. Major Cheese Groups, 3 edn. Elsevier Academic Press, Amsterdam.
134.	Schwurack B (2010) Steigerung der Quarkausbeute durch Optimierung der Säuerungskultur. Diploma Thesis, Technische Universität Berlin, Berlin
135.	Ott H (1977) Deutsche Milchwirtschaft 22:721-722.
136.	Ramet JP (1990) Dairy Industries International 55 (6):49-52.
137.	Jelen P, Renz-Schauen A (1989) Food Technology 43:74-81.
138.	Dolle E (1977) Deutsche Milchwirtschaft 22:709-712.
139.	Kroger M (1980) Cult. Dairy Prod. J. 15 (8):11-14.
140.	Spreer E (2005) Technologie der Milchverarbeitung, vol 8. . Behr's, Hamburg.
141.	Rohm H (1990) Textureigenschaften und Milchprodukte, vol 86/87. Verlag Th. Mann, Gelsenkirchen-Buer.
142.	Schmidt RH, Packard VS, Morris HA (1984) J. Dairy Sci. 67 (11):2723-2733.
143.	Kosikowski FV (1979) J. Dairy Sci. 62 (7):1149-1160.
144.	Marshall KR (1982) Industrial isolation of milk proteins: whey proteins. In: Fox PF (ed) Developments in dairy chemistry-1. Proteins. Appl. Sci. Publ., New York, NY, pp 339-373.
145.	Zall RR (1984) J. Dairy Sci. 67 (11):2621-2629.
146.	De Wit JN (1998) J. Dairy Sci. 81 (3):597-608.
147.	Morr CV, Ha EYW (1993) Critical Reviews in Food Science and Nutrition 33 (6):431-476.
148.	Kinsella JE, Whitehead DM (1989) Advances in Food and Nutrition Research 33:343-438.
149.	Wang T, Lucey JA (2003) J. Dairy Sci. 86 (10):3090-3101.
150.	Morr CV, Foegeding EA (1990) Food technology 44 (4):100-112.
151.	Baker HJ, Mickle JB, Leidigh ME, Morrison RD (1966) Journal of Home Economics 58 (6):468-473.
152.	Zadow JG (1986) Aust. J. Dairy Tech. 41 (4):96-99.
153.	Kessler HG (1996) Lebensmittel- und Bioverfahrenstechnik – Molkereitechnologie, vol 4. überarbeitete und erweiterte Auflage. Kessler, A., München.
154.	Morr CV, Swenson PE, Richter RL (1973) Journal of Food Science 38:324-330.
155.	Modler HW, Jones JD (1987) Food technology 41 (10):114-117.
156.	Matthews ME (1984) J. Dairy Sci. 67 (11):2680-2692.
157.	De Wit JN (1990) J. Dairy Sci. 73 (12):3602-3612.
158.	Modler HW (1985) J. Dairy Sci. 68 (9):2195-2205.
159.	Morr CV (1979) NZ J. Dairy Sci. Technol. 14:185-194.
160.	Dybing ST, Smith DE (1991) Cult. Dairy Prod. J. 28:4-12.
161.	Deshler M (1999) Whey Protein Isolates - Production, Composition And Nutritional Facts.
162.	Huffman LM, Harper WJ (1999) J. Dairy Sci. 82 (10):2238-2244.
163.	Morr CV (1987) Journal of Food Science 52 (2):312-317.
164.	Onwulata CI, Konstance RP, Tomasula PM (2004) J. Dairy Sci. 87 (3):749-756.
165.	Patel MT, Kilara A, Huffman LM, Hewitt SA, Houlihan AV (1990) J. Dairy Sci. 73 (6):1439-1449.
166.	Morr CV (1985) J. Dairy Sci. 68 (10):2773-2781.
167.	Holt C, McPhail D, Nevison I, Nylander T, Otte J, Ipsen RH, Bauer R, Ogendal L, Olieman K, Kruif KG, Leonil J, Molle D, Henry G, Maubois JL, Perez MD, Puyol P, Calvo M, Bury SM, Kontopidis G, McNae I, Sawyer L, Ragona L, Zetta

L, Molinari H, Klarenbeek B (1999) International Journal of Food Science & Technology 34 (5-6):543-556.

168. Holt C, McPhail D, Nylander T, Otte J, Ipsen R, Bauer R, Ogendal L, Olieman K, De Kruif KG, Leonil J, Molle D, Henry G, Maubois JL, Perez MD, Puyol P, Calvo M, Bury SM, Kontopidis G, McNae I, Sawyer L, Ragona L, Zetta L, Molinari H, Klarenbeek B, Jonkman MJ, Moulin J, Chatterton D (1999) International Journal of Food Science & Technology 34:587-601.

169. De Wit JN, Hontelez-Backx E, Adamse M (1988) Neth. Milk Dairy J. 42:155-172.

170. Thies C (2001) Microencapsulation: What it is and Purpose. In: Vilstrup P (ed) Microencapsulation of Food Ingredients. Leatherhead Publishing, Surrey, England, pp 1-30.

171. Masters K (1991) Spray Drying Handbook, vol Fifth edition. Longman Scientific & Technical and John Wiley & Sons Inc. , Essex, UK.

172. Písecký J (1997) Handbook of milk powder manufacture. Niro A/S, Copenhagen, Denmark.

173. Hempel P (2005) Lebensmittelwissenschaftliche Untersuchungen zur Trocknung von Hefeautolysaten. Diploma Thesis, Technische Universität, Berlin

174. Nasr GG, Yule AJ, Bendig L (2002) Industrial Sprays and Atomization. Springer Verlag, London, Berlin, Heidelberg.

175. Bloore CG, Boag IF (1982) NZ J. Dairy Sci. Technol. 17:103-120.

176. Lefebvre AH (1989) Atomization and Sprays. Hemisphere Publishing Corporation, New York.

177. Duffie JA, Marshall WRJ (1953) Chemical Engineering Progress 49 (8):417-486.

178. Augustin MA, Clarke PT, Craven H (2003) Powdered Milk: Characteristics of milk powders. Encyclopedia of Food Science and Nutrition. Elsevier, Amsterdam

179. Woodhams DJ, Murray MJ (1974) NZ J. Dairy Sci. Technol. 9:172-178.

180. Carić M, Milanović S (2004) Milk Powders: Physical and functional properties. Encyclopedia of Dairy Sciences. Elsevier, Amsterdam

181. Schubert H, Ax K, Behrend O (2003) Trends in Food Science & Technology 14:9-16.

182. Freudig B, Hogekamp S, Schubert H (1999) Chemical Engineering and Processing 38:525-532.

183. Hogekamp S, Schubert H (2003) Food Science and Technology International 9 (3):223-235.

184. Schubert H (1993) International chemical engineering 33:28-45.

185. Wollny M (2002) Über das Gestalten der Eigenschaften von Instantprodukten mit dem Verfahren der Strahlagglomeration. Doctoral Dissertation, Universität Karlsruhe

186. Gaiani C, Schuck P, Scher J, Desobry S, Banon S (2007) J. Dairy Sci. 90 (2):570-581.

187. Palzer S (2000) Anreichern und Benetzen von pulverförmigen Lebensmitteln mit Flüssigkeiten in diskontinuierlichen Mischaggregaten. Doctoral Dissertation, Müchen

188. Stieß M (1994) Mechanische Verfahrenstechnik 2. 1. edn. Springer, Berlin, Heidelberg, New York.

189. Kurzhals H-A (2003) Lexikon Lebensmitteltechnik, vol 1. Auflage. B. Behr's, Hamburg.

190. Baldwin AJ, Truong GNT (2007) Food and Bioproducts Processing 85 (3):202-208.

References

191. Havea P, Singh H, Creamer LK, Campanella OH (1998) J. Dairy Res. 65:79-91.
192. De Wit JN, Klarenbeek G (1984) J. Dairy Sci. 67 (11):2701-2710.
193. Schokker EP, Singh H, Pinder DN, Norris GE, Creamer LK (1999) Int. Dairy J. 9 (11):791-800.
194. Shimada K, Cheftel JC (1989) J. Agric. Food Chem. 37:161-168.
195. Hecht JP, King CJ (2000) Industrial & Engineering Chemistry Research 39 (6):1756-1765.
196. Carpenter JF, Prestrelski SJ, Arakawa T (1993) Archives of Biochemistry and Biophysics 303 (2):456-464.
197. Prestrelski SJ, Tedeschi N, Arakawa T, Carpenter JF (1993) Biophysical Journal 65 (2):661-671.
198. Allison SD, Dong A, Carpenter JF (1996) Biophysical Journal 71 (4):2022-2032.
199. Allison SD, Chang B, Randolph TW, Carpenter JF (1999) Archives of Biochemistry and Biophysics 365 (2):289-298.
200. Rattray W, Jelen P (1995) Int. Dairy J. 5 (7):673-684.
201. Garrett JM, Stairs RA, Annett RG (1988) J. Dairy Sci. 71 (1):10-16.
202. Spiegel T (1999) International Journal of Food Science & Technology 34 (5-6):523-531.
203. Plock J, Spiegel T, Kessler HG (1998) Milchwiss. 53 (7):389-393.
204. Jou KD, Harper WJ (1996) Milchwiss. 51 (9):509-512.
205. Bernal V, Jelen P (1985) J. Dairy Sci. 68 (11):2847-2852.
206. Lieske B (2006) Information on a complexometric method for the determination of Calcium in milk. Berlin
207. Tolstogzov VB (1991) Food Hydrocolloids 4 (6):429-468.
208. ISO (2002) 15323:2002. Dried milk protein products – Determination of nitrogen solubility index. ISO 13320:2002, 1st edn. International Organisation for Standardization.
209. Wydro P, Krajewska B, Hac-Wydro K (2007) Biomacromolecules 8:2611-2617.
210. Ausar SF, Bianco ID, Badini RG, Castagna LF, Modesti NM, Landa CA, Beltramo DM (2001) J. Dairy Sci. 84 (2):361-369.
211. Fernandez M, Fox PF (1997) Food Chem. 58 (4):319-322.
212. Muzzarelli RAA (1996) Carbohydrate Polymers 29 (4):309-316.
213. Ventura P Lipid lowering activity of chitosan, a new dietary integrator. In: Muzzarelli RAA (ed) International symposium on Chitin Enzymology, Senigallia, Italy, 1996. Atec Edizioni, pp 55-62.
214. Guzey D, McClements DJ (2006) Food Hydrocoll. 20 (1):124-131.
215. Delben F, Stefancich S (1998) Food Hydrocoll. 12 (3):291-299.
216. Bough WA, Landes DR (1976) J. Dairy Sci. 59 (11):1874-1880.
217. Hwang D-C, Damodaran S (1995) J. Agric. Food Chem. 43:33-37.
218. Hattori M, Numamoto K-i, Kobayashi K, Takahashi K (2000) J. Agric. Food Chem. 48 (6):2050-2056.
219. Casal E, Montilla A, Moreno FJ, Olano A, Corzo N (2006) J. Dairy Sci. 89 (5):1384-1389.
220. Aoki T, Yamada N, Tomita I, Kako Y, Imamura T (1987) Biochim. Biophys. Acta - Protein Structure and Molecular Enzymology 911 (2):238-243.
221. Hollar CM, Law AJR, Dalgleish DG, Brown RJ (1991) J. Dairy Sci. 74 (8):2403-2409.
222. Hollar CM, Law AJR, Dalgleish DG, Medrano JF, Brown RJ (1991) J. Dairy Sci. 74 (10):3308-3313.
223. Chaplin LC (1986) J. Chromatogr. A 363 (2):329-335.
224. Guillou H, Miranda G, Pelissier JP (1987) Lait 67 (2):135-148.
225. Creamer LK, Matheson AR (1981) J. Chromatogr. A 210 (1):105-111.

226. Syväoja E-L (1992) Milchwiss. 47 (9):563-566.
227. Lieske B, Valbuena R (2008) Milchwiss. 63 (2):178-181.
228. Bramanti E, Sortino C, Onor M, Beni F, Raspi G (2003) J. Chromatogr. A 994 (1-2):59-74.
229. Schägger H, von Jagow G (1987) Analytical Biochemistry 166 (2):368-379.
230. Veith PD, Reynolds EC (2004) J. Dairy Sci. 87 (4):831-840.
231. Roufik S, Paquin P, Britten M (2005) Int. Dairy J. 15 (3):231-241.
232. van Vliet T, Roefs S, Zoon P, Walstra P (1989) J. Dairy Res. 56 (3):529-534.
233. Senge B, Krenkel K, Schwarzlos M, Schulze W-K, Sienkiewicz T (1996) Verfahren zur Kontrolle der Verarbeitungstauglichkeit von Milch durch inline-online Bestimmung des Gerinnungsverhaltens. Berlin Patent DE 195 16 615 A1,
234. Kromidas S (1995) Qualität im analytischen Labor. VCH, Weinheim.
235. Kromidas S (2000) Handbuch Validierung in der Analytik. VCH, Weinheim.
236. Funk W, Dammann C, Oehlmann G (1985) Statistische Methoden in der Wasseranalytik: Begriffe, Statistik, Anwendungen. VCH, Weinheim.
237. Senge B, Blochwitz R, Bentlin S (2004) Deutsche Milchwirtschaft 7:256-260
238. Senge B, Blochwitz R (2009) Deutsche Milchwirtschaft 60 (13):479-483.
239. Senge B, Blochwitz R (2009) Deutsche Milchwirtschaft 60 (14):517-520.
240. Senge B, Blochwitz R (2009) Deutsche Milchwirtschaft 60 (15):553-557.
241. Merkus HG (2009) Particle Size Measurements - Fundamentals, Practice, Quality, vol 17. Particle Technology Series, 1 edn. Springer, Dordrecht.
242. Allen T (1997) Particle Size Measurement - Powder sampling and particle size measurement, vol 1. Powder Technology Series, 5 edn. Chapman and Hall, London, Weinheim, New York.
243. Mie G (1908) Ann. Phys. 330 (3):377-445.
244. Müller RH, Schuhmann R (1996) Teilchengrößenmessung in der Laborpraxis, vol 38. wissenschaftliche Verlagsgesellschaft mbH Stuttgart.
245. Michalski MC, Briard V, Michel F (2001) Lait 81 (6):787-796.
246. Mimouni A, Schuck P, Bouhallab S (2005) Lait 85:253-260.
247. Huppertz T, de Kruif CG (2007) Int. Dairy J. 17 (5):436-441.
248. Gaucher I, Piot M, Beaucher E, Gaucheron F (2007) Int. Dairy J. 17 (12):1375-1383.
249. Saveyn H, Thu TL, Govoreanu R, Van der Meeren P, Vanrolleghem PA (2006) Particle & Particle Systems Characterization 23 (2):145-153.
250. Ahmad S, Gaucher I, Rousseau F, Beaucher E, Piot M, Grongnet JF, Gaucheron F (2008) Food Chem. 106 (1):11-17.
251. Ennis MP, O'Sullivan MM, Mulvihill DM (1998) Food Hydrocoll. 12 (4):451-457.
252. Kravtchenko TP, Renoir J, Parker A, Brigand G (1999) Food Hydrocoll. 13 (3):219-225.
253. Gaiani C, Banon S, Scher J, Schuck P, Hardy J (2005) J. Dairy Sci. 88 (8):2700-2706.
254. Povey MJW, Golding M, Higgs D, Wang Y (1999) Int. Dairy J. 9 (3-6):299-303.
255. Davenel A, Schuck P, Marchal P (1997) Milchwiss. 52 (1):35-39.
256. Schuck P, Davenel A, Mariette F, Briard V, Mejean S, Piot M (2002) Int. Dairy J. 12 (1):51-57.
257. Mimouni A, Deeth HC, Whittaker AK, Gidley MJ, Bhandari BR (2009) Food Hydrocoll. 23 (7):1958-1965.
258. Moughal KI, Munro PA, Singh H (2000) Int. Dairy J. 10 (10):683-690.
259. Gaiani C, Scher J, Schuck P, Hardy J, Desobry S, Banon S (2006) Int. Dairy J. 16:1427-1434.

260. ISO (1999) 13320-1:1999. Particle size analysis - Laser diffraction methods - Part 1: General principles. . ISO 13320-1:1999 (E), 1st edn. International Organisation for Standardization.

261. Bortz J, Lienert GA, Boehnke K (2000) Verteilungsfreie Methoden in der Biostatistik. 2. edn. Springer Verlag, Berlin Heidelberg NY.

262. Kubinger KD (1986) Biom. J. 28 (1):67-72.

263. Kubinger K, Häusler J (2001-2003) Multiple Rang Kovarianzanalyse mKVA. 1.4.20 edn. Psychologische Diagnostik, Universität Wien, Wien

264. Wilcoxon F, Wilcox RA (1964) Some rapid approximate statistical Procedures. Lederle Laboratories Pearl River, N. Y. .

265. Schaich E, Hamerle A (1984) Verteilungsfreie statistische Prüfverfahren. Springer Berlin.

266. Wedholm A (2008) Variation in milk protein composition and its importance for the quality of cheese milk Doctoral Dissertation, Acta Universitatis agriculturae Sueciae

267. Ferron-Baumy C, Molle D, Garric G, Maubois JL (1992) Lait 72:165-173.

268. Okigbo LM, Richardson GH, Brown RJ, Ernstrom CA (1985) J. Dairy Sci. 68 (8):1893-1896.

269. Jenness R, Patton S (1967) Grundzüge der Milchchemie. Bayerischer Landwirtschaftsverlag, München, Basel, Wien.

270. Wiedemann M (2004) Überwachung der Eutergesundheit bei Milchkühen durch Kombination verschiedener chemisch-physikalischer Messwerte. Doctoral Dissertation, Technische Universität München

271. Richtlinie 92/46/EWG: Hygienevorschriften für die Herstellung und Vermarktung von Rohmilch, wärmebehandelter Milch und Erzeugnissen auf Milchbasis (1992). Europäischer Rat,

272. Verordnung über Hygiene- und Qualitätsanforderungen an Milch und Erzeugnisse auf Milchbasis (2000). BMVEL,

273. Smith KL, Hillerton JE, Harmon RJ (2001) Guidelines on normal and abnormal raw milk based on somatic cell counts and signs of clinical mastitis National Mastitis Council,

274. Hillerton JE (1999) Bulletin of the International Dairy Federation 345:4-6.

275. Lieske B, Valbuena R (2008) Milchwiss. 63 (3):247-250.

276. Dupont D, Grappin R (1998) J. Dairy Res. 65 (4):643-651.

277. Ogola H, Shitandi A, Nanua J (2007) J. Vet. Sci. 8 (3):237-242.

278. Kitchen BJ (1981) J. Dairy Res. 48 (01):167-188.

279. Dang AK, Kapila S, Singh C, Sehgal JP (2008) Milchwiss. 63 (3):239-242.

280. Verdi RJ, Barbano DM, Dellavalle ME, Senyk GF (1987) J. Dairy Sci. 70 (2):230-242.

281. Ikonen T, Ahlfors K, Kempe R, Ojala M, Ruottinen O (1999) J. Dairy Sci. 82 (1):205-214.

282. Lundstedt E (1978) Cult. Dairy Prod. J.:10-15.

283. Gilles J, Lawrence RC (1985) NZ J. Dairy Sci. Technol. 20:205-214.

284. Marziali AS, Ng-Kwai-Hang KF (1986) J. Dairy Sci. 69 (5):1193-1201.

285. Hallén E, Lundén A, Allmere T, Andrén A (2010) J. Dairy Res. 77 (01):71-76.

286. Ikonen T, Ojala M, Syväoja E-L (1997) Agric. Food Sci. Finl. 6:283-294.

287. Aleandri R, Schneider JC, Buttazzoni LG (1989) J. Dairy Sci. 72 (8):1967-1975.

288. Moreno FJ, Recio I, Olano A, López-Fandino R (2001) J. Dairy Res. 68 (02):197-208.

289. Addeo F, Soulier S, Pelissier J-P, Chobert J-M, Mercier J-C, Ribadeau-Dumas B (1978) J. Dairy Res. 45 (02):191-196.

290. Recio I, Perez-Rodriguez ML, Amigo L, Ramos M (1997) J. Dairy Res. 64 (4):515-523.

291. Tamime A, Robinson RK (1999) Yoghurt-Science and Technology. 2 edn. Woodhead Publishing Ltd., Cambridge England.

292. De la Fuente MA, Hemar Y, Tamehana M, Munro PA, Singh H (2002) Int. Dairy J. 12 (4):361-369.

293. Tamime A (2006) Fermented milks. Blackwell Science Ltd., Oxford.

294. Mrowetz G, Klostermeyer H, Thomasow J (1972) Zeitschrift für Lebensmitteluntersuchung und -Forschung A 149 (6):341-346.

295. Banavara DS, Anupama D, Rankin SA (2003) J. Dairy Sci. 86 (12):3866-3875.

296. Johnson ME, Chen CM, Jaeggi JJ (2001) J. Dairy Sci. 84 (5):1027-1033.

297. Moore KJ, Johnson MG, Sistrunk WA (1987) Journal of Food Science 52 (2):491-492.

298. O´Melia CR (1972) Coagulation and flocculation. In: Weber WJJ (ed) Physicochemical processes for water quality control. vol Environmental science and technology. John Wiley & Sons, Inc., New York, pp 61-109.

299. Parris N, Anema SG, Singh H, Creamer LK (1993) J. Agric. Food Chem. 41:460-464.

300. Hollar CM, Parris N, Hsieh A, Cockley KD (1995) J. Dairy Sci. 78 (2):260-267.

301. Law AJR, Leaver J, Banks JM, Horne DS (1993) Milchwiss. 48 (12):663-666.

302. Andrews AT, Taylor MD, Owen AJ (1985) J. Chromatogr. A 348:177-185.

303. Basch JJ, Douglas FW, Jr., Procino LG, Holsinger VH, Farrell HM, Jr. (1985) J. Dairy Sci. 68 (1):23-31.

304. Attaie R, Richter RL (2000) J. Dairy Sci. 83 (5):940-944.

305. Gaucher I, Molle D, Gagnaire V, Leonil J, Rousseau F, Gaucheron F (2009) Milchwiss. 64 (1):43-47.

306. Brew K, Grobler JA (1992) a-Lactalbumin. In: Fox PF (ed) Advances in Dairy Chemistry-1. Elsevier Appl. Sci, London, England, pp 191-229.

307. Carter DC, He XM (1990) Science 249 (4966):302-303.

308. Goodsell DS, Olson AJ (1993) Trends in Biochemical Sciences 18 (3):65-68.

309. McKenzie HA (1971) beta-Lactoglobulin. In: McKenzie HA (ed) Milk Proteins, Chemistry and Molecular Biology. Academic Press, New York, NY, pp 257-330.

310. HORIBA Instruments (2008) Understanding the Chi Square and R Parameter Calculations in the LA-950 Software. Technical Note TN153.

311. Poste G, Moss C (1972) Progress in Surface Science 2 (Part 3):139-232.

312. Voros J (2004) Biophys. J. 87:553-561.

313. Kennel R (1994) Hitzeinduzierte Aggregatbildung von Molkenproteinen - Größenbestimmung und Strukturanalyse. Doctoral Dissertation, Technische Universität München,

314. Kinsella JE (1984) CRC Critical Reviews in Food Science and Nutrition 21 (3):197-262.

315. Morr CV (1989) J. Dairy Sci. 72 (2):575-580.

316. Robin O, Turgeon S, Paquin P (1993) Functional properties of milk proteins. In: Hui YH (ed) Dairy Science and Technology Handbook, vol 1. Principles and Properties. VCH Publishers Inc., New York, pp 277-353.

317. De Wit JN, Klarenbeek G, Adamse M (1986) Neth. Milk Dairy J. 40:41-56.

318. Onwulata CI, Tomasula PM (2006) International Journal of Dairy Science 1 (1):1-8.

319. El-Sayed TM, Wallack DA, King CJ (1990) Industrial & Engineering Chemistry Research 29 (12):2346-2354.

320. Adhikari B, Howes T, Shrestha A, Bhandari BR (2007) J. Food Eng. 79:1136-1143.

321. Mulhelm B, Fritsching U, Schulte G, Bauckhage K (2003) Atomization and Sprays 13:321-343.
322. Hecht JP, Bayly AE (2009) Atomization for spray drying: Unanswered questions and industrial needs. Paper presented at the International Conference on Liquid Atomization and Spray Systems, Vail, Colorado, Sunday, July 26-Thursday, July 30, 2009

Chapter 12: Appendix

HPSEC
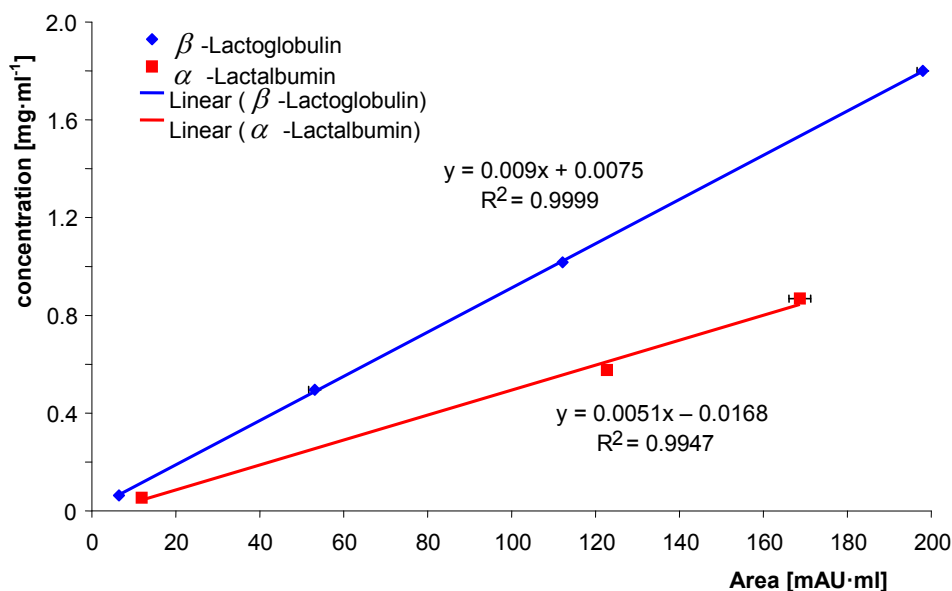
Figure 12-1: Regression lines of the main whey proteins used in the HPSEC

Figure 12-2 displays the UV response at 280 nm of the standard proteins IgG (c = 2 mg·ml^{-1}), BSA (c = 2 mg·ml^{-1}), β-Lg (c = 1.8 mg·ml^{-1}) and α-La (c = 0.85 mg·ml^{-1}).
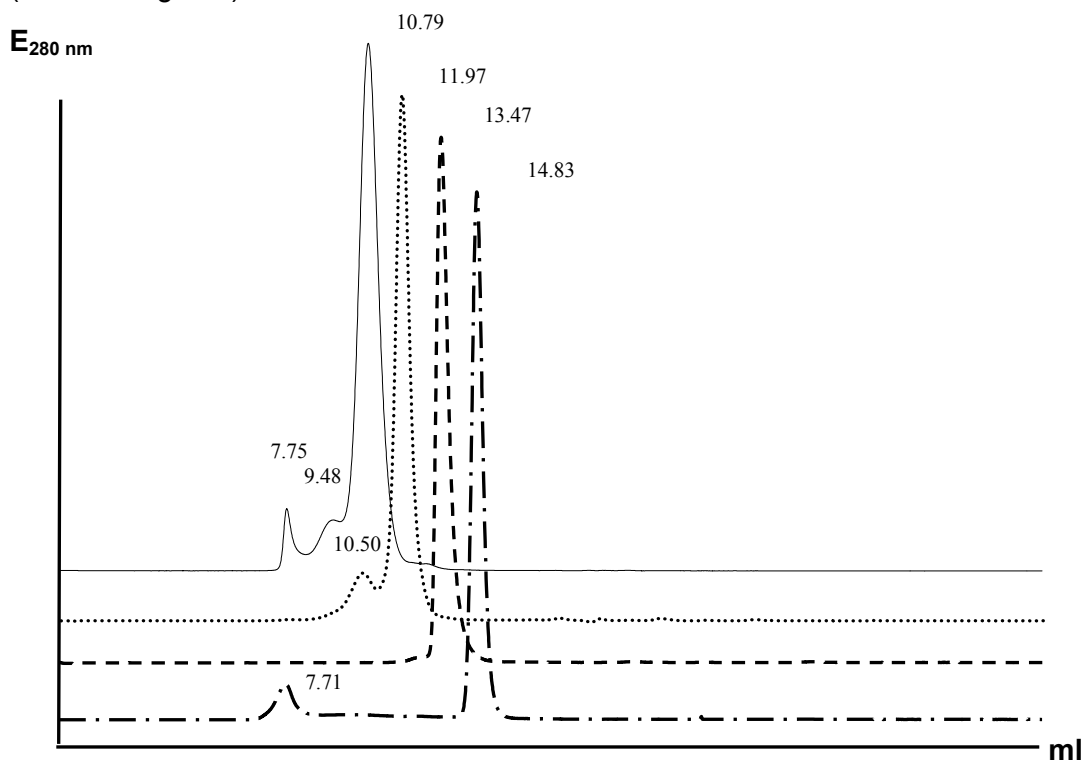
Figure 12-2: Elution curves of standard proteins separated individually
(— · -) α-Lactalbumin, (– – –) β-Lactoglobulin, (..........) BSA, (———) IgG

Rheological measurements

Figure 12-3 displays the mean value of the process viscosity during the rennet-induced coagulation (N = 3) ± s.
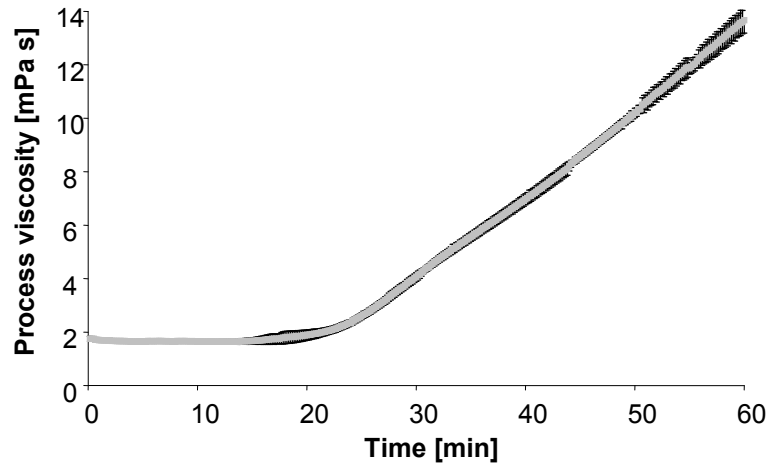
Figure 12-3:   Process viscosity of commercial milk during rennet-induced coagulation

Rennet-induced coagulation

Table 12-1:   **Allocation of the cow type to the sample number, the medication with antibiotics, and the length of medication of milk from infected udder quarters**

No.	Cow	Antibiotics	Length of medication days
9	C	None	0
10	D	Benzylpenicillin-Procain 1 H_2O	2
11	E	Benzylpenicillin-Procain 1 H_2O	4
12	F	Benzylpenicillin-Procain 1 H_2O	2
13	H	None	0
A1	A	none	0
A2	A	Benzylpenicillin-Procain 1 H_2O	5
A3	A	Benzylpenicillin-Procain 1 H_2O	7
B1	B	Benzylpenicillin-Procain 1 H_2O	2
B2	B	Benzylpenicillin-Procain 1 H_2O	9
		End of waiting time	
B3	B	None	0
B4	B	Cefquinonsulfat	2
B5	B	Cefquinonsulfat	7
B6	B	None	0
G1	G	None	0
G2	G	Benzylpenicillin-Procain 1 H_2O	1
G3	G	Benzylpenicillin-Procain 1 H_2O	2
G4	G	Benzylpenicillin-Procain 1 H_2O	3
G5	G	Benzylpenicillin-Procain 1 H_2O	4
G6	G	Benzylpenicillin-Procain 1 H_2O	7
G7	G	None	0

Table 12-2: **Results of the regression**

	Section 2.1 12min $\leq t \leq$ 16 min	Section 2.2 16 min$\leq t \leq$22 min	Section 2.3 22 min$\leq t \leq$26 min	Section 3 26 min$\leq t \leq$60 min
1	$\eta(t) = 0.032t + 0.882$	$\eta(t) = 0.4495e^{0.068t}$	$\eta(t) = 0.293t - 4.337$	$\eta(t) = 0.503t - 11.00$
	$R^2 = \quad 0.8606$	$R^2 = \quad 0.9504$	$R^2 = \quad 0.9995$	$R^2 = \quad 0.9923$
2	$\eta(t) = 0.039t + 0.917$	$\eta(t) = 0.2807e^{0.1045t}$	$\eta(t) = 0.278t - 3.258$	$\eta(t) = 0.469t - 8.959$
	$R^2 = \quad 0.9393$	$R^2 = \quad 0.9905$	$R^2 = \quad 0.9995$	$R^2 = \quad 0.9979$
3	$\eta(t) = 0.096t + 0.172$	$\eta(t) = 0.213e^{0.134t}$	$\eta(t) = 0.393t - 4.850$	$\eta(t) = 0.470t - 6.102$
	$R^2 = \quad 0.9499$	$R^2 = \quad 0.9921$	$R^2 = \quad 0.9946$	$R^2 = \quad 0.9757$
4	$\eta(t) = 0.013t + 1.247$	$\eta(t) = 0.3812e^{0.0815t}$	$\eta(t) = 0.287t - 3.898$	$\eta(t) = 0.409t - 7.847$
	$R^2 = \quad 0.7581$	$R^2 = \quad 0.9693$	$R^2 = \quad 0.9994$	$R^2 = \quad 0.995$
5	$\eta(t) = 0.022t + 1.159$	$\eta(t) = 0.5119e^{0.065t}$	$\eta(t) = 0.314t - 4.680$	$\eta(t) = 0.475t - 9.825$
	$R^2 = \quad 0.6703$	$R^2 = \quad 0.9405$	$R^2 = \quad 0.9967$	$R^2 = \quad 0.9941$
6	$\eta(t) = 0.024t + 0.976$	$\eta(t) = 0.2511e^{0.1028t}$	$\eta(t) = 0.390t - 6.047$	$\eta(t) = 0.602t - 12.43$
	$R^2 = \quad 0.9363$	$R^2 = \quad 0.9788$	$R^2 = \quad 0.9999$	$R^2 = \quad 0.9978$
7	$\eta(t) = 0.035t + 0.875$	$\eta(t) = 0.2962e^{0.0949t}$	$\eta(t) = 0.380t - 5.831$	$\eta(t) = 0.622t - 12.92$
	$R^2 = \quad 0.901$	$R^2 = \quad 0.9611$	$R^2 = \quad 0.9997$	$R^2 = \quad 0.9979$
8	$\eta(t) = 0.033t + 0.880$	$\eta(t) = 0.3099e^{0.0912t}$	$\eta(t) = 0.375t - 5.78$	$\eta(t) = 0.586t - 12.22$
	$R^2 = \quad 0.8947$	$R^2 = \quad 0.9442$	$R^2 = \quad 0.9997$	$R^2 = \quad 0.9975$
9	$\eta(t) = 0.034t + 1.067$	$\eta(t) = 0.2406e^{0.117t}$	$\eta(t) = 0.338t - 4.162$	$\eta(t) = 0.527t - 9.840$
	$R^2 = \quad 0.8286$	$R^2 = \quad 0.9888$	$R^2 = \quad 0.9997$	$R^2 = \quad 0.9983$
10	$\eta(t) = 0.039t + 1.058$	$\eta(t) = 0.3035e^{0.1057t}$	$\eta(t) = 0.347t - 4.483$	$\eta(t) = 0.546t - 10.419$
	$R^2 = \quad 0.9415$	$R^2 = \quad 0.9884$	$R^2 = \quad 0.9996$	$R^2 = \quad 0.9978$
11	$\eta(t) = 0.015t + 1.253$	$\eta(t) = 0.2569e^{0.1069t}$	$\eta(t) = 0.305t - 3.870$	$\eta(t) = 0.504t - 9.864$
	$R^2 = \quad 0.5314$	$R^2 = \quad 0.9729$	$R^2 = \quad 0.9955$	$R^2 = \quad 0.9975$
12	$\eta(t) = 0.030t + 1.001$	$\eta(t) = 0.3313e^{0.0903t}$	$\eta(t) = 0.246t - 2.880$	$\eta(t) = 0.382t - 7.209$
	$R^2 = \quad 0.8823$	$R^2 = \quad 0.9769$	$R^2 = \quad 0.9917$	$R^2 = \quad 0.9958$
13	$\eta(t) = 0.010t + 1.227$	$\eta(t) = 0.6815e^{0.0445t}$	$\eta(t) = 0.250t - 3.675$	$\eta(t) = 0.369t - 7.507$
	$R^2 = \quad 0.8739$	$R^2 = \quad 0.9828$	$R^2 = \quad 0.9962$	$R^2 = \quad 0.9887$
14	$\eta(t) = 0.027t + 1.212$	$\eta(t) = 0.5958e^{0.0607t}$	$\eta(t) = 0.323t - 4.762$	$\eta(t) = 0.446t - 8.704$
	$R^2 = \quad 0.9726$	$R^2 = \quad 0.9474$	$R^2 = \quad 0.9983$	$R^2 = \quad 0.9951$
16	$\eta(t) = 0.022t + 1.158$	$\eta(t) = 0.4914e^{0.0675t}$	$\eta(t) = 0.322t - 4.905$	$\eta(t) = 0.582t - 12.97$
	$R^2 = \quad 0.9687$	$R^2 = \quad 0.9717$	$R^2 = \quad 0.9972$	$R^2 = \quad 0.9922$

Table 12-3 to Table 12-6 display the process viscosities (mPa·s) of the milk samples of infected udder quarters after classification.

Table 12-3: **Class I milk**

No.	starting viscosity	η 12 min	η 16 min	η 22 min	η 26 min	η 60 min	η 100 min
B2	1.33	4.06	8.71	17.5	22.6	41.6	55.1
B5	1.49	1.48	2.14	5.2	8.72	41.5	57.1
10	1.9	2.05	2.23	4.37	7.04	49.2	64.9
11	1.48	1.59	2.92	6.69	10.3	41.3	56.1
$\overline{X}$	1.55	2.30	4.00	8.44	12.17	43.40	58.30
s	0.24	1.20	3.16	6.12	7.08	3.87	4.48

Table 12-4: **Class II milk**

No.	starting viscosity	η 12 min	η 16 min	η 22 min	η 26 min	η 60 min	η 100 min
3	1.54	1.5	1.84	4	6	35	50
5	1.4	1.41	1.67	3.86	5.99	33.2	48.7
6	1.46	1.49	1.56	2.31	3.58	26.7	40.6
7	1.36	1.42	1.65	2.92	4.33	25.1	34
9	1.42	1.39	1.44	1.86	2.98	24.1	38.5
G3	1.4	6.07	8.67	12.4	14.7	28.1	34.2
G5	1.32	2.14	3.52	5.7	7.63	24	32.1
G7	1.4	1.43	2.11	4.49	6.35	27.2	40
$\overline{X}$	1.41	2.11	2.81	4.68	6.47	27.91	39.79
s	0.07	1.62	2.46	3.35	3.67	4.08	6.70

Table 12-5: **Class III milk**

No.	starting viscosity	η 12 min	η 16 min	η 22 min	η 26 min	η 60 min	η 100 min
8	1.33	1.28	1.3	1.45	1.84	17.2	29
12	1.38	1.36	1.46	2.42	3.47	19.4	31.4
13	1.47	1.55	2.14	3.83	4.91	18.9	28
A2	1.3	1.89	3.34	5.33	7.04	19.5	26.3
B3	1.52	1.45	1.48	1.6	1.67	11.9	26.7 (97. min)
B4	1.49	1.4	1.42	1.61	1.94	15.3	32.1
G1	1.41	1.4	1.43	1.58	1.94	10.4	23.6
G2	1.35	1.31	1.35	1.71	2.44	12.9	25.1
G4	1.36	1.79	2.64	3.7	4.25	12.5	19.1
G6	1.37	1.43	1.9	3.64	4.69	19	28.1
$\overline{X}$	1.40	1.49	1.85	2.69	3.42	15.70	26.97
s	0.07	0.20	0.68	1.35	1.78	3.53	4.03

Table 12-6: **Class IV milk**

No.	starting viscosity	η 12 min	η 16 min	η 22 min	η 26 min	η 60 min	η 100 min
1	1.58	1.61	1.61	1.66	1.67	1.91	2.86
A1	1.39	1.4	1.4	1.43	1.38	1.41	1.58
A3	1.86	2	2.01	1.98	1.98	2.12	2.17
B1	1.51	1.38	1.37	1.36	1.4	1.53	
B6	1.66	1.48	1.46	1.6	1.86	3.54	7.03
$\overline{X}$	1.60	1.57	1.57	1.61	1.66	2.10	3.41
s	0.18	0.25	0.26	0.24	0.27	0.85	2.47

Quality investigations of dairy powders

Table 12-7:   Results of the chitosan treatment of selected WPCs I

WPC 35 1 Chitosan (%)	$E_{500\,nm}$	% of initial turbidity	$E_{660\,nm}$	% of initial turbidity
0	0.14	100.00	0.10	100.00
0.01	0.03	18.75	0.02	21.88
0.013	0.03	17.36	0.02	20.83
0.015	0.03	17.36	0.02	20.83
0.018	0.02	15.97	0.02	19.79
0.021	0.03	17.36	0.02	20.83
0.022	0.03	17.36	0.02	20.83
0.025	0.03	18.06	0.02	21.88
0.031	0.03	18.06	0.02	20.83
WPC 35 3				
0	0.927	100.00	0.513	100.00
0.01	0.124	13.38	0.077	15.01
0.016	0.051	5.50	0.035	6.82
0.021	0.056	6.04	0.037	7.21
0.025	0.055	5.93	0.037	7.21
0.031	0.05	5.39	0.035	6.82
WPC 60 1				
0	0.848	100.00	0.542	100.00
0.01	0.043	5.07	0.03	5.54
0.013	0.032	3.77	0.023	4.24
0.015	0.038	4.48	0.026	4.80
0.018	0.033	3.89	0.023	4.24
0.02	0.032	3.77	0.023	4.24
WPC 60 2				
0	0.055	100.00	0.039	100.00
0.01	0.029	52.73	0.022	56.41
0.013	0.033	60.00	0.025	64.10
0.015	0.031	56.36	0.023	58.97
0.018	0.036	65.45	0.026	66.67
0.02	0.031	56.36	0.022	56.41
WPC 80 1				
0	0.045	100.00	0.032	100.00
0.01	0.032	22.22	0.025	26.04
0.013	0.034	23.61	0.024	25.00
0.015	0.039	27.08	0.026	27.08
0.018	0.043	29.86	0.028	29.17
0.02	0.043	29.86	0.028	29.17
WPC 80 5				
0	0.051	100.00	0.033	100.00
0.01	0.032	62.75	0.024	72.73
0.012	0.035	68.63	0.024	72.73
0.015	0.037	72.55	0.025	75.76
0.018	0.048	94.12	0.031	93.94
0.02	0.052	101.96	0.034	103.03

Table 12-8:   **Results of the chitosan treatment of selected WPCs II**

WPC 35 2				
Chitosan (%)	$E_{500 nm}$	% of initial turbidity	$E_{660 nm}$	% of initial turbidity
0	0.088	100.00	0.054	100.00
0.011	0.035	39.77	0.025	46.30
0.013	0.037	42.05	0.026	48.15
0.016	0.031	35.23	0.022	40.74
0.018	0.033	37.50	0.023	42.59
0.02	0.032	36.36	0.023	42.59
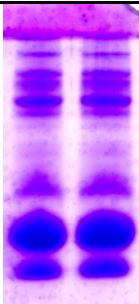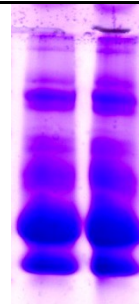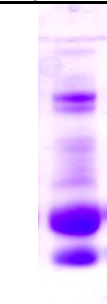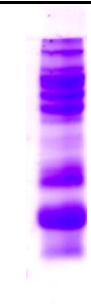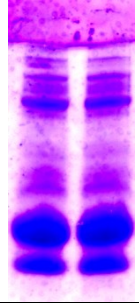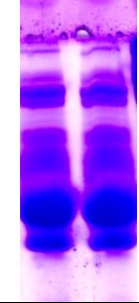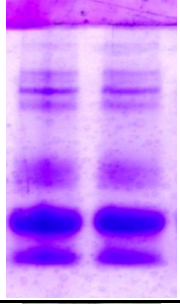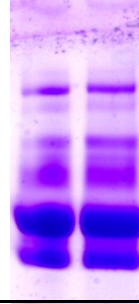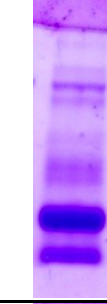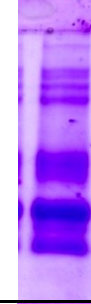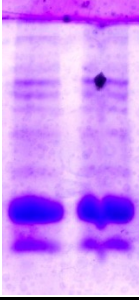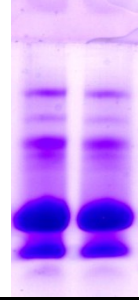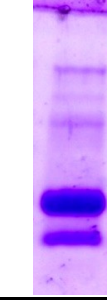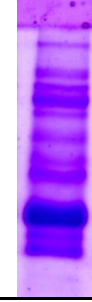
Table 12-9:   **Amount of chitosan used in case of HPLC analysis and appropriate residual fat content in the supernatant in %**

Sample	Chitosan	Residual fat in the supernatant
WPC 35 1	0.018	0.59
WPC 35 2	0.015	0.14
WPC 35 3	0.015	1.43
WPC 60 1	0.015	0.7
WPC 60 2	0.01	1.46
WPC 70 1	0.01	0.49
WPC 80 1	0.01	2.44
WPC 80 5	0.01	0.49
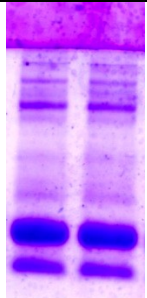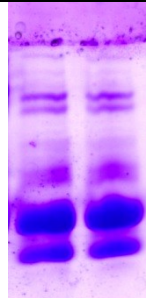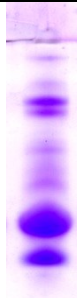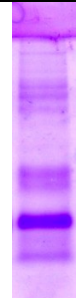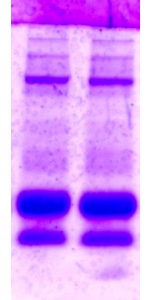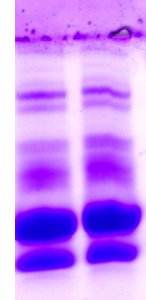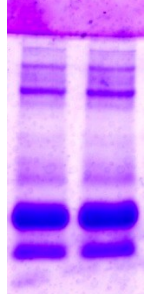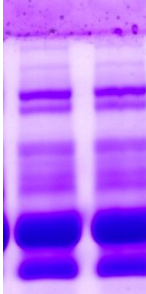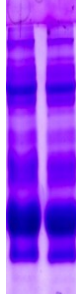
The SDS-PAGE profiles of selected samples in native state, after pH 4.6 adjustment, and after chitosan treatment (supernatant and sediment) are displayed in Table 12-10 and Table 12-11.

Table 12-10: **SDS-PAGE profiles of selected samples in native state, after pH 4.6 adjustment, and after chitosan treatment (supernatant and sediment), I**

Table 12-11: SDS-PAGE profiles of selected samples in native state, after pH 4.6 adjustment, and after chitosan treatment (supernatant and sediment), II

Sample	Native	pH 4.6	Chitosan Supernatant	Chitosan Sediment
WPC 80 5				
WPC 60 1				
WPC 60 2				

Table 12-12: D_{10}, D_{50}, D_{90} (μm), the specific surface (cm²·cm^{-3}), and the standard deviation (μm) of the dry measurements under vacuum
Values are averages of three replicates ± *s*

Sample	D_{10}	±	D_{90}	±	D_{50}	±	Spec. surf.	±	Std. dev.
SWP 131	43.44	1.81	225.59	4.82	110.18	1.29	820.00	22.49	76.63
SWP 132	47.02	1.38	231.89	1.78	111.86	1.26	758.40	14.94	78.71
SWP 133	71.27	0.48	320.16	4.31	154.09	2.14	500.00	5.66	106.02
SMP	32.48	0.74	238.92	4.55	86.65	1.55	927.33	16.92	87.13
WPC 351	24.63	0.43	131.11	0.24	57.08	0.62	1291.25	16.64	47.00
WPC 352	26.61	0.70	227.13	3.20	90.86	2.26	1016.25	23.33	84.04
WPC 353	34.65	0.98	201.63	14.11	77.82	3.87	943.80	37.47	70.61
WPC 354	30.56	0.17	237.35	0.02	98.50	0.20	944.50	2.50	84.62
WPC 355	24.10	0.21	129.31	2.06	56.49	0.58	1317.00	6.24	46.57
WPC 356	51.23	0.90	234.99	1.15	118.85	0.75	695.00	6.24	77.63
WPC 357	34.04	0.74	265.83	8.90	98.48	1.77	861.00	14.73	97.95
WPC 601	21.83	0.31	71.12	0.49	41.64	0.37	1681.00	20.00	20.77
WPC 602	21.46	0.67	80.55	1.25	44.50	0.84	1617.50	38.96	26.18
WPC 603	30.32	0.74	157.32	3.04	68.84	1.24	1075.00	19.85	54.36
WPC 604	29.91	0.12	190.73	7.00	73.50	1.35	1039.67	15.57	68.27
WPC 605	27.96	0.02	152.46	3.38	66.01	0.66	1133.67	6.11	53.77
WPC 701	22.72	0.22	96.29	0.30	48.75	0.32	1506.50	11.50	34.19
WPC 702	23.25	1.08	89.60	2.01	48.81	3.20	1470.00	121.19	31.44
WPC 801	30.97	0.75	111.02	1.13	60.20	1.02	1171.67	23.50	36.05
WPC 802	53.04	1.02	362.18	1.23	194.32	0.57	514.25	8.06	123.38
WPC 803	30.94	0.48	169.51	2.89	72.02	0.69	1066.33	13.01	59.49
WPC 804	23.78	0.80	89.10	1.66	49.34	1.13	1461.75	40.58	29.51
WPC 805	24.62	0.47	91.36	0.93	50.05	0.44	1421.80	17.77	30.13

Table 12-13: D_{10}, D_{50}, D_{90} (µm), the specific surface (cm²·cm⁻³), and the standard deviation (µm) of the dry measurements under pressure of 0.1 MPa Values are averages of three replicates ± *s*

Sample	D_{10}	±	D_{90}	±	D_{50}	±	Spec. surf.	±	Std. dev.
SWP 131	41.61	0.15	229.75	0.21	112.86	0.07	866.00	3.00	79.00
SWP 132	44.84	0.11	230.20	2.24	112.80	0.22	817.00	2.00	78.43
SWP 133	72.14	1.41	313.88	8.45	152.94	4.28	517.50	4.36	103.80
SMP	28.69	0.79	247.77	6.82	88.20	3.73	984.25	30.46	92.04
WPC 351	21.75	0.10	133.26	1.06	55.84	0.29	1394.00	2.00	48.51
WPC 352	23.80	0.22	232.15	1.83	93.61	0.52	1071.67	8.08	86.36
WPC 353	31.85	0.01	204.00	0.12	76.41	0.18	995.50	0.50	72.73
WPC 354	26.52	0.31	240.41	1.84	101.55	0.63	1013.25	4.86	85.98
WPC 355	21.51	0.05	130.97	0.67	54.49	0.23	1419.00	1.00	47.95
WPC 356	49.97	0.17	236.50	0.84	120.92	0.13	735.50	1.50	78.21
WPC 357	30.81	0.31	273.17	2.84	101.14	1.04	908.33	7.37	101.78
WPC 601	18.81	1.15	65.33	1.00	37.32	1.34	1900.67	88.22	19.60
WPC 602	19.64	0.10	78.88	0.64	41.94	0.11	1733.75	6.29	26.38
WPC 603	25.22	0.32	156.00	1.41	63.26	0.61	1222.00	15.00	55.87
WPC 604	27.48	5.69	188.45	3.66	71.95	6.98	1115.25	142.21	67.86
WPC 605	24.26	0.46	150.99	3.01	60.60	2.16	1265.50	30.35	54.87
WPC 701	18.92	0.01	95.17	0.27	44.91	0.11	1701.00	2.00	35.53
WPC 702	19.04	0.20	83.15	2.14	41.72	0.88	1765.50	26.50	30.23
WPC 801	26.59	0.11	108.68	0.02	55.69	0.08	1302.50	3.50	36.82
WPC 802	49.23	0.47	364.86	1.86	199.18	1.15	541.00	4.00	124.20
WPC 803	25.51	0.18	176.55	7.20	68.55	0.48	1193.67	5.51	64.07
WPC 804	21.16	0.14	86.36	0.35	45.73	0.21	1599.00	10.61	29.43
WPC 805	20.88	0.57	90.40	1.18	46.22	0.53	1593.40	30.86	31.79

Table 12-14: D_{10}, D_{50}, D_{90} (µm), the specific surface (cm²·cm^{-3}), and the standard deviation (µm) of the dry measurements under pressure of 0.3 MPa Values are averages of three replicates ± *s*

Sample	D_{10}	±	D_{90}	±	D_{50}	±	Spec. surf.	±	Std. dev.
SWP 131	39.56	1.06	233.20	0.07	114.52	1.03	904.50	8.50	80.36
SWP 132	44.70	0.29	236.30	0.93	114.82	0.63	835.00	1.00	80.64
SWP 133	72.17	0.65	323.47	3.02	156.29	0.97	529.33	4.16	107.34
SMP	27.45	0.30	242.78	1.23	88.56	1.11	1010.00	11.00	89.90
WPC 351	20.84	0.04	132.53	0.14	56.23	0.10	1427.00	3.00	48.10
WPC 352	22.25	0.11	224.85	5.29	92.85	1.30	1116.67	8.33	82.40
WPC 353	30.77	0.09	205.04	0.61	77.51	0.00	1016.00	1.00	73.18
WPC 354	24.20	0.25	237.60	1.59	101.32	0.75	1071.00	8.00	85.49
WPC 355	20.87	0.14	134.34	0.68	56.52	0.46	1422.00	10.00	49.04
WPC 356	50.45	0.12	235.03	0.24	121.53	0.27	747.00	0.00	77.48
WPC 357	29.36	0.05	267.16	1.15	100.96	0.54	944.00	1.73	99.92
WPC 601	16.56	0.05	63.46	0.18	34.87	0.11	2080.00	6.00	19.59
WPC 602	18.77	0.03	77.07	0.43	40.60	0.15	1797.00	5.00	24.89
WPC 603	23.36	0.12	155.29	0.93	61.92	0.14	1285.00	4.00	56.03
WPC 604	23.59	0.09	182.75	1.35	67.55	0.45	1224.50	6.50	66.75
WPC 605	23.47	0.03	154.58	1.30	62.88	0.15	1272.50	1.50	56.00
WPC 701	18.09	0.04	96.37	2.20	44.37	0.62	1748.33	7.09	36.38
WPC 702	17.41	0.03	84.49	0.16	40.28	0.02	1874.50	1.50	31.63
WPC 801	24.89	0.01	108.25	0.26	54.31	0.01	1356.00	0.00	36.86
WPC 802	47.37	0.18	360.44	0.59	198.04	0.03	563.50	1.50	122.87
WPC 803	22.52	0.28	176.75	3.01	66.51	0.50	1292.50	12.50	64.93
WPC 804	20.41	0.13	86.13	0.47	44.92	0.18	1641.50	9.26	29.31
WPC 805	19.86	0.09	89.33	1.53	44.59	0.13	1662.50	7.14	31.50

Table 12-15: Results of the statistical analysis of the dry measurements

	Influence pressure	Influence protein	Interaction
D_{10}, average	sig.	sig.	not sig.
D_{50}, average	not sig.	sig.	not sig.
D_{90}, average	not sig.	sig.	not sig.
Specific surface, average	not sig.	sig.	not sig.
Standard deviation	not sig.	sig.	not sig.

Table 12-16: D_{10}, D_{50}, D_{90} (µm), the specific surface (cm²·cm⁻³), and the standard deviation (µm) of the dry measurements under pressure of 0.1 MPa. Values are averages of three replicates ± *s*

Sample	D_{10}	±	D_{90}	±	D_{50}	±	Spec. surf.	±	Std. dev.
WPC30	24.08	0.64	133.75	1.47	68.23	1.75	1236.33	33.25	46.10
WPC358	28.67	6.20	138.13	2.90	73.56	3.44	1098.00	148.29	45.36
WPC359	25.18	0.05	179.85	0.79	76.99	0.88	1122.67	4.51	64.20
WPC3510	23.80	0.49	173.89	0.33	74.47	0.46	1169.67	20.50	62.95
WPC3511	31.99	0.73	415.90	20.06	187.52	7.67	750.67	12.50	151.13
WPC3512	12.18	0.34	140.45	0.81	28.91	0.48	2459.00	59.02	59.37
WPC3513	18.83	1.40	180.16	3.43	71.31	2.56	1378.33	84.32	67.08
WPC3514	17.57	0.16	277.43	1.47	109.94	0.69	1244.67	5.51	106.43
WPC606	19.97	0.92	203.63	11.95	58.16	3.35	1419.67	75.10	78.55
WPC607	27.98	0.04	314.71	1.31	95.84	0.18	954.33	1.53	122.07
WPC806	23.83	0.34	110.63	1.98	53.33	0.33	1392.33	18.45	39.06

Table 12-17: Parameter taken from the PSD of the raw material whey

	D_{10} µm	D_{50} µm	D_{90} µm	Share of the first peak %
Peak 1				
$\overline{x}$, thin whey	0.083	0.145	0.251	85.230
s	0.000	0.000	0.000	0.360
$\overline{x}$, whey concentrate	0.078	0.135	0.236	72.955
s	0.000	0.001	0.003	0.125
$\overline{x}$, final mixed whey	0.079	0.136	0.233	89.753
s	0.000	0.000	0.001	0.779
Peak 2				
$\overline{x}$, thin whey	1.129	1.984	3.401	14.77
s	0.020	0.022	0.050	
$\overline{x}$, whey concentrate	1.061	2.267	4.734	27.045
s	0.048	0.318	1.195	
$\overline{x}$, final mixed whey	1.029	1.870	3.312	10.247
s	0.042	0.093	0.211	

Table 12-18:   Parameter of the PSD of final mixed whey after different periods of time

	D_{10} µm	D_{50} µm	D_{90} µm	Share of the first peak %
Peak 1				
Final mixed whey 10/05/2009	0.080	0.139	0.247	89.12
Final mixed whey 10/05/2009	0.080	0.139	0.248	89.46
Final mixed whey 10/05/2009	0.080	0.139	0.247	89.19
Final mixed whey 10/06/2009	0.081	0.143	0.255	87.2
Final mixed whey 10/06/2009	0.081	0.143	0.256	86.67
Final mixed whey 10/07/2009	0.081	0.143	0.255	87.91
Final mixed whey 10/07/2009	0.081	0.143	0.255	88.24
Final mixed whey 10/13/2009	0.081	0.142	0.250	87.81
Final mixed whey 10/13/2009	0.080	0.140	0.246	87.52
Final mixed whey 11/02/2009	0.079	0.135	0.232	85.59
Final mixed whey 11/02/2009	0.079	0.136	0.234	84.87
$\overline{x}$	**0.080**	**0.140**	**0.248**	**87.598**
s	**0.001**	**0.003**	**0.008**	**1.462**
Peak 2				
Final mixed whey 10/05/2009	0.924	1.988	5.021	
Final mixed whey 10/05/2009	0.907	1.813	3.913	
Final mixed whey 10/05/2009	0.927	1.984	4.773	
Final mixed whey 10/06/2009	0.989	2.288	6.193	
Final mixed whey 10/06/2009	0.999	2.440	7.882	
Final mixed whey 10/07/2009	0.972	2.104	4.702	
Final mixed whey 10/07/2009	0.949	2.060	5.040	
Final mixed whey 10/13/2009	1.033	2.235	4.845	
Final mixed whey 10/13/2009	1.049	2.254	4.901	
Final mixed whey 11/02/2009	0.987	1.777	3.101	
Final mixed whey 11/02/2009	1.071	1.963	3.523	
$\overline{x}$	**0.982**	**2.082**	**4.899**	
s	**0.053**	**0.206**	**1.295**	

Table 12-19: D_{10}, D_{50}, D_{90} (µm) of the first peak of the wet measurements after the start of rehydration, 10 min, and full rehydration of the SWP, SMP, and WPC 35

| | start | 10min | rehy. | start | 10min | rehy. | start | 10min | rehy. |
	D_{50}	D_{50}	D_{50}	D_{10}	D_{10}	D_{10}	D_{90}	D_{90}	D_{90}
SWP131	0.227	0.211	0.126	0.159	0.126	0.077	0.315	0.304	0.208
	0.568	0.228	0.130	0.414	0.158	0.077	0.805	0.318	0.218
	0.341	0.143	0.128	0.250	0.083	0.077	0.445	0.238	0.213
SWP132	0.563	0.336	0.134	0.432	0.243	0.079	0.757	0.439	0.221
	0.627	0.550	0.135	0.454	0.466	0.079	0.953	0.643	0.223
	0.542	0.215	0.152	0.425	0.143	0.093	0.696	0.304	0.241
SWP133	0.194	0.193	0.192	0.100	0.100	0.099	0.366	0.358	0.365
	0.288	0.195	0.192	0.191	0.101	0.099	0.432	0.362	0.365
	0.205	0.193	0.192	0.108	0.100	0.099	0.383	0.359	0.361
SMP	0.133	0.131	0.129	0.082	0.081	0.080	0.205	0.204	0.197
	0.130	0.130	0.128	0.081	0.081	0.080	0.198	0.200	0.196
	0.131	0.121	0.125	0.081	0.078	0.079	0.204	0.185	0.192
WPC30	0.247	0.272	0.204	0.148	0.158	0.121	0.364	0.385	0.313
	0.225	0.325	0.222	0.133	0.228	0.133	0.336	0.443	0.336
	0.247	0.328	0.251	0.148	0.233	0.156	0.364	0.448	0.360
WPC351	0.193	0.226	0.215	0.121	0.136	0.129	0.289	0.334	0.321
	0.206	0.158	0.161	0.123	0.091	0.092	0.313	0.254	0.256
	0.181	0.180	0.192	0.105	0.105	0.121	0.279	0.279	0.285
WPC352	0.172	0.169	0.166	0.091	0.090	0.090	0.327	0.319	0.304
	0.170	0.168	0.166	0.091	0.089	0.089	0.322	0.316	0.305
	0.168	0.170	0.168	0.090	0.091	0.091	0.310	0.320	0.308
WPC353	0.161	0.212	0.143	0.092	0.139	0.082	0.259	0.333	0.243
	0.183	0.184	0.144	0.113	0.112	0.084	0.289	0.289	0.240
	0.219	0.187	0.153	0.146	0.115	0.088	0.340	0.297	0.258
WPC354	0.143	0.145	0.149	0.083	0.084	0.086	0.234	0.238	0.246
	0.145	0.148	0.147	0.085	0.086	0.086	0.238	0.245	0.244
	0.147	0.148	0.147	0.086	0.086	0.085	0.243	0.249	0.244
WPC355	0.190	0.159	0.192	0.120	0.091	0.122	0.284	0.257	0.285
	0.207	0.206	0.197	0.124	0.124	0.125	0.314	0.311	0.288
	0.159	0.193	0.197	0.091	0.120	0.122	0.257	0.291	0.294
WPC356	0.202	0.179	0.211	0.122	0.103	0.130	0.295	0.276	0.309
	0.210	0.206	0.188	0.130	0.126	0.109	0.306	0.300	0.287
	0.222	0.202	0.214	0.141	0.122	0.132	0.317	0.295	0.314
WPC357	0.155	0.163	0.154	0.084	0.086	0.084	0.293	0.435	0.291
	0.158	0.155	0.165	0.086	0.085	0.087	0.300	0.287	0.430
	0.185	0.157	0.156	0.127	0.085	0.084	0.261	0.296	0.296
WPC358	0.199	0.208	0.246	0.125	0.125	0.150	0.293	0.312	0.350
	0.219	0.216	0.245	0.132	0.130	0.148	0.323	0.320	0.351
	0.240	0.236	0.254	0.144	0.142	0.153	0.348	0.343	0.365
WPC359	0.162	0.162	0.162	0.089	0.088	0.089	0.290	0.294	0.293
	0.168	0.166	0.167	0.090	0.089	0.090	0.316	0.314	0.306
	0.170	0.168	0.166	0.091	0.090	0.089	0.317	0.307	0.302
WPC3510	0.224	0.245	0.229	0.130	0.136	0.132	0.420	0.429	0.428
	0.183	0.177	0.178	0.094	0.091	0.092	0.376	0.358	0.354
	0.248	0.246	0.176	0.137	0.137	0.091	0.439	0.433	0.357
WPC3511	0.143	0.144	0.144	0.081	0.081	0.081	0.258	0.262	0.263
	0.147	0.141	0.146	0.083	0.080	0.082	0.264	0.254	0.270
	0.146	0.142		0.082	0.080		0.266	0.257	
WPC3512	0.142	0.142	0.143	0.081	0.081	0.081	0.253	0.253	0.257
	0.144	0.142	0.144	0.081	0.081	0.081	0.258	0.255	0.258
	0.146	0.143		0.082	0.081		0.259	0.255	
WPC3513	0.146	0.145	0.144	0.083	0.082	0.081	0.258	0.259	0.259
	0.149	0.144	0.143	0.083	0.081	0.081	0.266	0.256	0.257
	0.149	0.144	0.143	0.084	0.081	0.081	0.265	0.258	0.254
WPC3514	0.147	0.142	0.144	0.083	0.081	0.082	0.262	0.248	0.257
	0.148	0.143	0.145	0.084	0.081	0.082	0.263	0.250	0.257
	0.247	0.147	0.147	0.173	0.083	0.083	0.342	0.259	0.263

Table 12-20: *D_{10}, D_{50}, D_{90} (µm) of the first peak of the wet measurements after the start of rehydration, 10 min, and full rehydration of the WPC 60, 70, and 80*

	start	10min	rehy.	start	10min	rehy.	start	10min	rehy.
	D_{50}	D_{50}	D_{50}	D_{10}	D_{10}	D_{10}	D_{90}	D_{90}	D_{90}
WPC601	0.166	0.166	0.204	0.091	0.090	0.121	0.295	0.294	0.333
	0.241	0.165	0.237	0.140	0.090	0.139	0.381	0.294	0.372
	0.265	0.240	0.164	0.146	0.139	0.090	0.459	0.382	0.291
WPC602	0.251	0.164	0.163	0.143	0.088	0.087	0.412	0.299	0.306
	0.166	0.163	0.161	0.089	0.088	0.086	0.311	0.301	0.304
	0.164	0.166	0.163	0.088	0.089	0.087	0.304	0.312	0.304
WPC603	0.318	0.309	0.203	0.231	0.209	0.129	0.418	0.416	0.297
	0.320	0.218	0.185	0.233	0.138	0.115	0.421	0.313	0.285
	0.317	0.221	0.163	0.231	0.141	0.097	0.417	0.315	0.267
WPC604	0.305	0.307	0.311	0.210	0.214	0.216	0.400	0.401	0.411
	0.303	0.311	0.314	0.205	0.220	0.223	0.400	0.408	0.412
	0.304	0.329	0.310	0.207	0.241	0.214	0.400	0.428	0.411
WPC605	0.175	0.175	0.176	0.095	0.095	0.096	0.297	0.300	0.301
	0.176	0.174	0.174	0.096	0.095	0.095	0.302	0.297	0.296
	0.172	0.174	0.175	0.095	0.095	0.096	0.291	0.296	0.299
WPC606	0.146	0.142	0.141	0.082	0.081	0.080	0.260	0.254	0.252
	0.232	0.144	0.142	0.157	0.081	0.080	0.373	0.258	0.253
	0.085	0.145	0.141	0.059	0.081	0.080	0.119	0.267	0.251
WPC607	0.159	0.154	0.150	0.088	0.085	0.083	0.288	0.276	0.275
	0.152	0.155	0.147	0.086	0.085	0.083	0.267	0.285	0.266
	0.164	0.148	0.153	0.110	0.083	0.084	0.232	0.270	0.279
WPC701	0.118	0.117	0.116	0.074	0.073	0.073	0.190	0.188	0.188
	0.117	0.119	0.116	0.074	0.074	0.073	0.188	0.191	0.186
	0.118	0.117	0.119	0.074	0.073	0.074	0.189	0.188	0.194
WPC702	0.119	0.117	0.117	0.074	0.073	0.073	0.192	0.189	0.188
	0.119	0.117	0.117	0.074	0.073	0.073	0.193	0.189	0.190
	0.118	0.118	0.116	0.074	0.073	0.072	0.192	0.191	0.188
WPC801	0.158	0.159	0.163	0.087	0.088	0.088	0.285	0.287	0.297
	0.160	0.160	0.158	0.088	0.088	0.086	0.288	0.291	0.287
	0.164	0.163	0.158	0.088	0.088	0.086	0.300	0.293	0.288
WPC802	0.154	0.156	0.150	0.088	0.088	0.083	0.263	0.275	0.268
	0.154	0.153	0.151	0.086	0.085	0.084	0.272	0.270	0.270
	0.153	0.154	0.151	0.085	0.085	0.084	0.272	0.274	0.271
WPC803	77.65	80.35	92.70	18.25	19.82	21.66	194.84	200.07	233.59
	83.13	82.39	97.28	19.25	18.65	23.29	212.63	214.34	237.60
	87.17	87.29	85.94	22.73	23.72	21.61	218.12	224.86	213.98
WPC804	0.168	0.167	0.162	0.087	0.087	0.086	0.342	0.340	0.321
	0.159	0.167	0.162	0.087	0.087	0.086	0.294	0.338	0.321
	0.168	0.167	0.162	0.087	0.087	0.086	0.339	0.336	0.321
WPC805	0.155	0.155	0.152	0.085	0.085	0.083	0.288	0.286	0.285
	0.160	0.158	0.152	0.086	0.085	0.084	0.306	0.301	0.282
	0.163	0.158	0.152	0.087	0.085	0.083	0.319	0.300	0.281
WPC806	0.151	0.151	0.156	0.087	0.085	0.087	0.260	0.261	0.279
	0.154	0.152	0.156	0.088	0.086	0.087	0.269	0.265	0.278
	0.154	0.152	0.153	0.088	0.086	0.086	0.267	0.264	0.269

Table 12-21: D_{10}, D_{50}, D_{90} (µm) of the second peak of the wet measurements after the start of rehydration, 10 min, and full rehydration of the SWP, SMP, and WPC 35

	start D_{50}	10min D_{50}	rehy. D_{50}	start D_{10}	10min D_{10}	rehy. D_{10}	start D_{90}	10min D_{90}	rehy. D_{90}
SWP131	9.376	6.467	4.315	4.112	3.195	2.338	18.704	14.103	7.771
	46.757	7.444	4.059	19.492	3.447	2.097	78.935	16.713	7.553
	44.474	5.237	3.784	10.573	2.785	2.233	93.179	10.597	6.103
SWP132	41.854	7.835	4.706	14.544	3.776	2.627	77.175	16.779	8.466
	50.395	5.989	4.422	14.181	2.688	2.557	143.22	14.752	7.507
	48.587	7.951	6.413	19.869	3.705	3.463	80.364	17.467	11.723
SWP133	6.037	3.818	3.749	1.793	1.603	1.499	22.950	8.434	11.510
	17.224	3.916	3.749	2.927	1.646	1.499	52.470	8.479	11.510
	9.469	4.867	4.496	2.159	1.634	1.591	31.617	14.322	21.944
SMP	13.033	17.385	20.997	6.616	7.195	12.256	29.353	60.154	33.328
	16.047	15.640	11.098	8.064	7.788	7.733	37.265	36.414	15.501
	15.462	15.758	7.525	7.276	7.923	5.632	36.421	33.769	10.300
WPC30	3.552	4.661	4.199	2.126	2.352	2.424	5.804	9.548	7.185
	4.079	4.227	4.431	2.322	2.236	2.500	7.198	7.766	7.759
	3.552	3.867	3.819	2.126	2.149	2.272	5.804	6.629	6.319
WPC351	4.602	4.695	4.924	2.602	2.657	2.812	8.019	8.247	8.488
	4.003	4.436	5.133	2.427	2.626	2.873	6.481	7.398	9.219
	4.522	4.413	4.480	2.609	2.601	2.661	7.590	7.251	7.357
WPC352	3.340	2.882	2.873	1.228	1.204	1.262	12.679	7.826	6.579
	3.459	3.342	2.797	1.273	1.269	1.298	14.830	11.808	5.857
	3.279	3.255	3.839	1.369	1.353	1.357	7.665	7.833	23.624
WPC353	11.350	12.801	3.582	5.001	5.577	1.590	35.933	30.673	7.921
	11.874	11.987	5.210	5.404	5.175	2.211	29.124	30.369	11.684
	13.131	12.017	12.366	5.742	5.180	4.476	30.139	28.821	29.405
WPC354	4.036	4.821	6.607	2.622	3.036	3.453	5.897	7.331	13.019
	5.892	6.943	6.355	3.432	3.595	3.361	9.847	13.945	12.145
	6.241	7.374	5.408	3.510	3.553	3.140	10.872	23.554	8.848
WPC355	4.351	4.823	4.538	2.562	2.675	2.685	7.233	8.799	7.455
	4.346	4.051	4.352	2.557	2.459	2.630	7.323	6.536	7.054
	4.823	4.958	5.361	2.675	2.691	2.866	8.799	8.962	9.781
WPC356	12.410	11.706	11.680	6.065	5.597	5.618	26.695	28.907	22.994
	12.511	11.747	10.895	6.099	5.854	5.374	25.679	22.700	21.807
	12.869	11.850	11.721	6.119	5.845	5.557	26.122	23.906	23.211
WPC357	2.313	27.279	2.275	1.057	19.083	1.078	7.435	39.557	5.063
	2.482	2.609	29.986	1.073	1.134	17.716	8.176	5.994	48.505
	0.928	2.369	2.229	0.518	1.087	1.070	1.930	5.895	5.020
WPC358	6.049	4.502	5.678	3.100	2.658	3.155	11.225	7.441	9.815
	5.293	5.075	5.727	2.983	2.885	3.136	9.123	8.644	10.056
	5.424	5.076	6.355	2.976	2.828	3.262	9.695	8.791	11.990
WPC359	3.382	2.594	4.525	1.635	1.356	1.777	6.022	4.422	9.983
	2.105	1.411	3.141	1.011	0.813	1.564	4.929	2.637	5.489
	6.044	4.160	3.646	1.817	1.761	1.662	29.220	8.674	6.980
WPC3510	2.149	2.245	4.119	1.061	1.121	1.441	5.157	5.042	10.707
	2.467	2.606	3.769	1.097	1.158	1.347	5.457	6.272	9.905
	2.331	2.031	3.148	1.102	1.092	1.210	5.284	4.127	8.722
WPC3511	1.550	1.445	1.383	0.836	0.827	0.814	3.840	2.943	2.770
	1.684	1.348	1.510	0.841	0.751	0.832	4.759	2.694	3.274
	1.737	1.317		0.860	0.742		5.491	2.679	
WPC3512	1.681	1.596	1.674	0.881	0.864	0.874	3.450	3.241	3.524
	2.091	1.610	1.561	0.909	0.866	0.853	7.039	3.258	3.175
	1.892	1.676		0.885	0.880		5.434	3.481	
WPC3513	1.945	2.003	1.539	0.936	0.963	0.864	4.709	4.315	3.014
	1.812	2.034	1.403	0.887	0.952	0.836	5.511	4.924	2.569
	2.216	1.728	1.767	0.957	0.899	0.909	6.900	3.685	3.728
WPC3514	2.250	3.463	2.660	0.964	1.626	1.208	5.679	6.347	5.560
	2.515	3.068	3.896	1.010	1.374	1.297	7.831	6.368	10.782
	3.421	3.905	2.086	2.085	1.331	0.925	5.260	9.378	5.105

Table 12-22: D_{10}, D_{50}, D_{90} (µm) of the second peak of the wet measurements after the start of rehydration, 10 min, and full rehydration of the WPC 60, 70, and 80

	start D_{50}	10min D_{50}	rehy. D_{50}	start D_{10}	10min D_{10}	rehy. D_{10}	start D_{90}	10min D_{90}	rehy. D_{90}
WPC601	2.381	2.407	2.043	1.280	1.288	1.177	4.557	4.705	3.525
	2.488	2.163	2.433	1.355	1.219	1.357	5.025	3.778	4.587
	2.433	2.116	23.714	1.356	1.242	12.871	4.876	3.594	44.595
WPC602	1.558	1.588	1.811	0.940	0.910	1.010	2.605	2.784	3.476
	1.814	1.551	1.664	1.008	0.895	0.972	3.484	2.733	2.928
	1.578	1.707	1.650	0.899	0.973	0.922	2.802	3.141	2.948
WPC603	20.397	19.212	16.613	9.236	8.494	5.979	40.058	42.628	36.733
	23.804	18.781	16.210	10.094	8.295	5.661	85.186	43.768	39.097
	21.198	19.424	17.214	9.457	8.370	5.165	44.691	52.844	53.166
WPC604	19.808	20.548	20.444	8.737	9.096	8.897	62.589	64.824	61.171
	19.093	21.098	21.571	8.546	9.065	9.240	54.155	68.075	74.713
	19.047	21.775	20.190	8.431	9.295	8.656	59.954	76.061	61.102
WPC605	7.326	7.166	5.613	3.022	2.900	2.655	18.020	19.558	10.707
	7.288	6.221	5.138	2.933	2.846	2.574	18.785	12.513	9.411
	5.948	7.376	6.674	2.981	2.918	2.789	10.980	21.972	14.777
WPC606	2.839	2.491	2.800	1.130	1.079	1.088	7.241	5.143	7.341
	55.507	2.665	2.510	19.566	1.088	1.097	150.48	6.422	5.090
	0.275	1.729	2.487	0.166	0.939	1.089	0.487	3.395	5.090
WPC607	18.693	3.290	1.622	2.435	1.314	0.855	51.333	6.895	3.375
	34.034	2.004	1.508	6.174	0.994	0.843	82.158	4.403	2.920
	0.373	1.262	1.887	0.278	0.793	0.889	0.610	2.267	4.564
WPC701	9.373	7.171	4.181	3.879	3.626	2.186	23.241	13.452	7.905
	10.931	8.037	4.388	4.459	3.694	2.245	28.487	16.238	8.329
	14.009	8.854	3.755	5.492	3.829	2.102	31.585	22.120	6.306
WPC702	6.393	6.000	4.451	2.941	2.770	2.243	12.552	12.277	9.005
	41.054	5.974	3.803	7.531	2.774	2.014	85.784	12.233	7.244
	5.305	4.947	3.643	2.421	2.477	1.932	9.891	9.488	6.837
WPC801	11.629	12.856	8.569	2.290	2.681	2.328	30.354	29.981	19.090
	15.355	8.848	5.399	3.236	2.445	1.877	34.349	19.078	11.904
	11.267	6.022	5.075	2.440	2.183	1.526	26.491	12.330	13.428
WPC802	3.695	4.458	2.645	1.798	1.507	1.266	6.988	14.540	6.268
	3.524	2.782	2.308	1.356	1.230	1.185	13.614	8.840	4.569
	2.738	2.707	2.397	1.205	1.195	1.199	8.795	8.805	4.960
WPC803									
WPC804	0.969	0.989	1.010	0.663	0.667	0.673	1.619	1.722	1.796
	1.125	0.950	1.029	0.699	0.660	0.676	2.338	1.507	1.894
	1.016	1.002	1.025	0.672	0.669	0.675	1.852	1.786	1.875
WPC805	1.548	2.029	1.225	0.883	0.943	0.779	3.490	5.652	2.244
	1.641	2.280	1.410	0.890	0.944	0.807	3.941	12.858	2.995
	1.783	1.823	1.335	1.002	0.910	0.804	3.680	6.774	2.613
WPC806	24.330	4.479	6.752	3.757	1.945	1.723	48.243	8.646	20.234
	20.566	7.179	6.571	3.618	2.024	1.776	37.614	18.422	19.804
	20.366	4.745	5.352	3.785	2.017	1.822	36.218	9.396	12.751

Table 12-23: *D_{10}, D_{50}, and D_{90} (μm) of the third peak after the start of rehydration, 10 min, and full rehydration*

| | start | 10min | rehy | start | 10min | rehy | start | 10min | rehy |
	D_{50}	D_{50}	D_{50}	D_{10}	D_{10}	D_{10}	D_{90}	D_{90}	D_{90}
SWP131	119.356	271.191	192.585	44.707	118.163	99.918	408.184	469.247	271.501
		111.054	140.811		53.799	87.694		303.386	201.132
		186.326			77.914			336.932	
SWP132		86.675	149.378		58.540	80.934		131.795	230.819
		80.448	159.297		53.721	99.842		123.635	205.479
		88.214	185.036		53.126	92.732		140.854	285.274
SWP133	102.473		56.109	60.065		31.753	221.262		87.373
	210.428		56.109	107.314		31.753	383.004		87.373
	178.895			73.130			305.719		
SMP	70.905			49.603			97.058		
		95.903			65.392			237.024	
	80.428	78.627		56.997	51.226		162.017	190.764	
WPC356	90.784		161.833	58.738		80.102	151.657		272.892
	117.839	168.782	140.884	66.546	89.590	70.078	220.689	262.393	259.681
	191.340	116.055	161.219	88.404	66.487	80.728	327.563	229.481	270.047
WPC357	46.499			27.522			72.025		
	52.857	204.275		31.074	85.110		83.803	582.570	
	125.349	74.584		26.308	49.152		817.589	97.255	
WPC359	46.483			31.839			67.026		
WPC3510	35.826			13.245			54.487		
	24.829			9.534			48.095		
	25.275			10.103			39.560		
WPC3511	40.675			27.063			57.803		
	45.011			25.750			79.899		
	46.309			26.597			74.881		
WPC3512	24.184			15.286			36.845		
	37.112			18.483			62.551		
WPC3513	55.875			36.435			81.039		
	37.682			24.344			52.881		
	51.304			28.980			84.146		
WPC3514	39.050	21.428		15.805	13.152		76.124	40.205	
	45.841			24.712			74.071		
	107.339			27.631			1176.113		
WPC603	107.647		173.896	60.041		92.401	224.291		272.807
	213.305	235.005	113.555	163.208	169.697	84.016	288.431	307.129	212.981
	114.976	202.420		67.158	161.752		229.838	249.119	
WPC606	65.681			39.109			94.543		
	90.891			11.380			155.003		
WPC607	40.332			9.252			139.589		
WPC701			96.878			72.482			163.555
	80.017	61.841	114.789	47.417	29.757	79.857	182.100	91.921	196.006
	91.019	87.355		51.246	45.195		229.053	205.540	
WPC702	49.049	40.892	53.406	23.678	19.773	34.920	83.586	75.116	78.166
	824.944	38.521		551.982	19.730		1120.173	65.532	
	24.013			13.793			38.597		
WPC802		34.206			22.367			53.933	
	53.549	46.867		26.574	24.763		86.851	79.261	
WPC805	18.442	43.117		7.067	13.230		31.778	86.531	
	14.598			6.589			26.661		
	11.054	26.925		5.460	14.546		21.160	45.454	

Table 12-24: Results of the contrast analysis regarding the rehydration time

	between start and 10 min	between start and rehydrated	between 10 min and rehydrated
D_{10} Peak 1	Sig.	Sig.	Sig.
D_{50} Peak 1	Sig. (α = 0.05)	Sig.	Sig.
D_{90} Peak 1	Sig.	Sig.	Sig.
D_{10} Peak 2	Sig.	Sig.	Sig.
D_{50} Peak 2	Sig.	Sig.	Sig. (α = 0.05)
D_{90} Peak 2	Sig.	Sig.	Sig. (α = 0.05)

Table 12-25:   Results of the contrast analysis regarding the protein contents

Compared samples	Peak 1			Peak 2		
	D_{10}	D_{50}	D_{90}	D_{10}	D_{50}	D_{90}
SWP13/35	sig	sig	sig	sig	sig	sig
SWP13/60	sig	sig	sig	sig	sig	sig
SWP13/70	sig	sig	sig	sig	sig	sig
SWP13/80	sig	sig	sig	sig	Not sig	Not sig
35/60	sig	sig	sig	sig	sig	sig
35/70	sig	sig	sig	sig	sig	sig
35/80	sig	sig	sig	sig	sig	sig
60/70	sig	sig	sig	sig	sig	sig
60/80	sig	sig	sig	sig	sig	sig
70/80	sig	sig	sig	Not sig	sig	sig

Table 12-26:   V.c. (%) of peak 1, peak 2, and peak 3 in the course of rehydration

	start			10 min			rehydrated		
	1. Peak	2. Peak	3. Peak	1. Peak	2. Peak	3. Peak	1. Peak	2. Peak	3. Peak
13 1	12.1	65.3	22.6	24.8	8.5	66.8	77.1	17.6	5.4
13 2	1.4	98.6		15.8	15.0	69.2	58.4	32.2	9.4
13 3	42.9	33.1	24.0	67.6	32.4		63.2	32.9	4.0
30	40.4	59.6		42.3	57.7		38.6	61.4	
SMP	82.5	15.5	2.0	85.5	12.1	2.4	98.8	1.2	
35 1	38.0	62.0		40.6	59.4		35.9	64.1	
35 2	73.4	26.6		74.3	25.8		74.3	25.7	
35 3	45.8	54.2		47.0	53.0		71.7	28.3	
35 4	71.8	28.2		68.7	31.3		69.9	30.1	
35 5	37.5	62.5		37.1	62.9		36.3	63.7	
35 6	30.6	51.0	18.3	35.9	55.0	13.6	35.9	49.0	15.1
35 7	59.4	9.3	31.3	80.1	3.8	16.1	95.4	4.6	
35 8	32.2	67.8		33.4	66.6		25.3	74.7	
35 9	77.9	17.5	14.0	85.2	14.8		81.2	18.8	
35 10	62.3	12.4	25.3	81.5	18.5		78.8	21.2	
35 11	73.1	7.7	19.2	91.0	9.0		90.4	9.6	
35 12	86.5	8.3	7.7	91.6	8.4		91.3	8.7	
35 13	64.2	7.7	28.1	89.0	11.0		90.2	9.6	
35 14	54.4	6.3	39.4	82.4	14.8	8.4	83.1	14.1	
60 1	54.5	45.5		58.8	41.2		57.5	42.5	
60 2	65.2	34.8		69.2	30.8		67.7	32.3	
60 3	13.3	63.5	23.2	25.9	72.5	1.6	41.6	53.7	4.7
60 4	15.4	84.6		14.2	85.8		16.5	83.5	
60 5	56.0	44.0		56.4	43.6		59.7	40.3	
60 6	44.4	35.1	30.8 (53,18)	93.0	7.0		92.7	7.4	
60 7	52.5	29.8	only for one sample	90.7	9.3		90.8	8.7	
70 1	83.6	9.5	6.9	85.0	6.8	8.2	91.7	4.2	4.1
70 2	82.4	7.5	10.2	93.6	3.5	2.9	96.3	3.3	0.4
80 1	71.8	28.2		74.6	25.4		78.2	21.8	
80 2	68.5	28.9	2.5	68.2	28.7	3.1	69.6	30.4	
80 3	-	-	-	-	-	-	-	-	-
80 4	83.9	16.1		82.9	17.1		84.2	15.8	
80 5	87.0	5.7	7.3	87.2	7.7	5.1	92.3	7.7	
80 6	60.6	39.4		80.6	19.4		75.0	25.0	

Figure 12-4 to Figure 12-9 display the PSD of the sweet whey powders (SWP) and the WPC immediately after rehydration (1 min; blue curve) designated by 'start', after complete rehydration (24 h; black curve) designated by 'rehydrated', and of the dry sample indicated by the dispersion pressure in MPa (red curve).
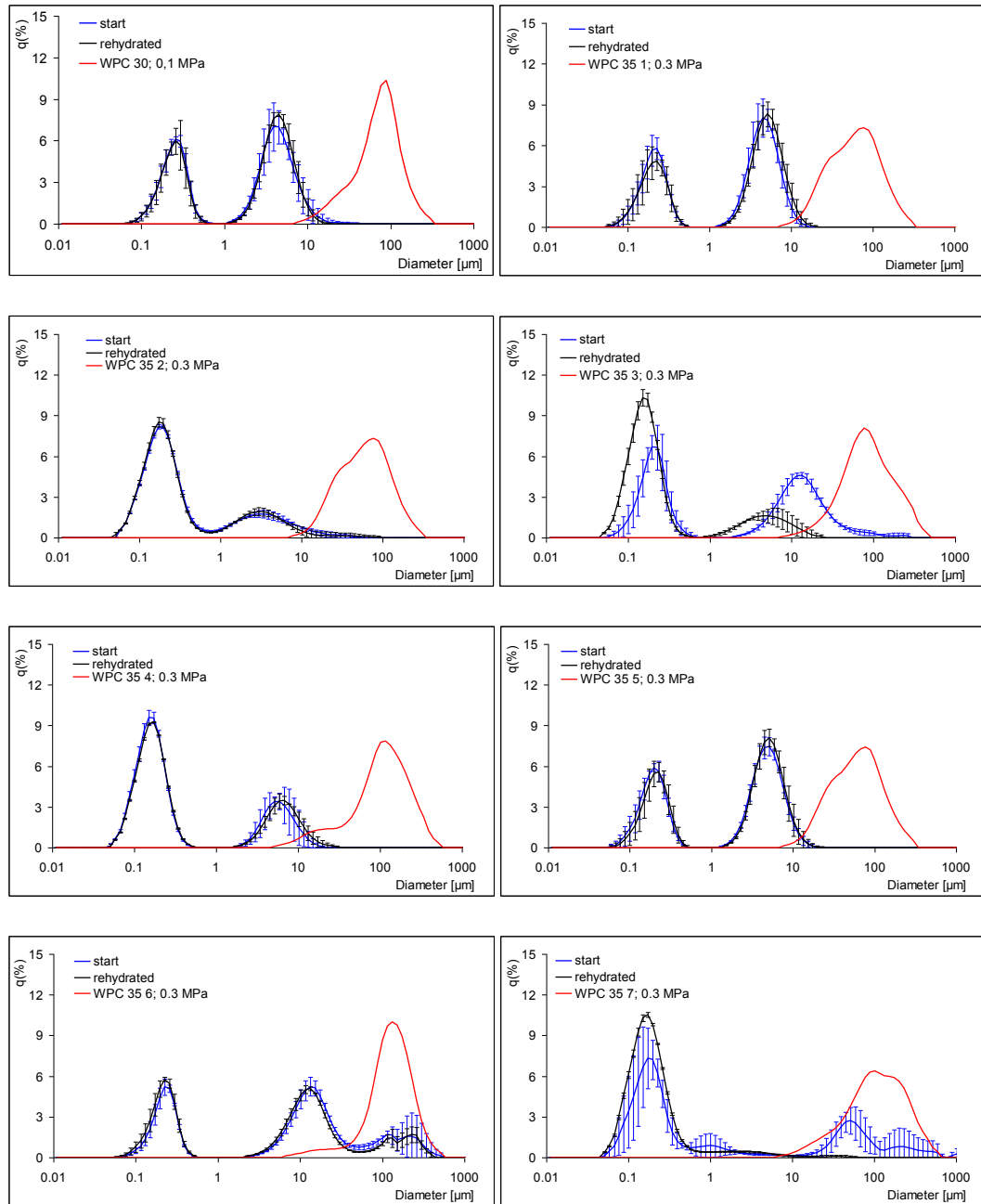
SWP
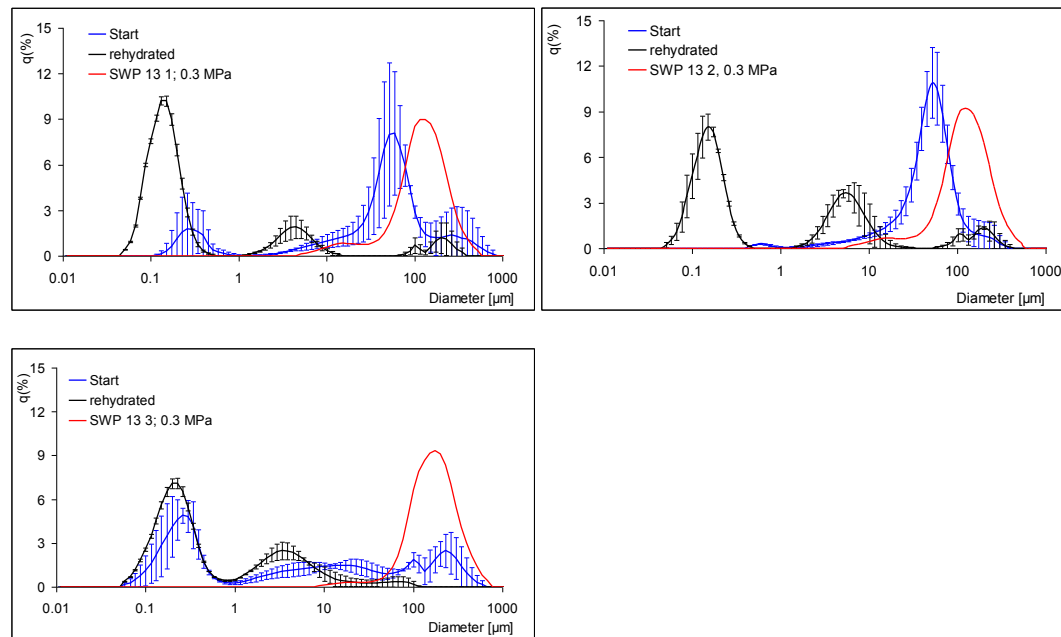
Figure 12-4:   PSD of SWP 13 1, 13 2, and 13 3 after the start and complete rehydration (N = 3 ± *s*); the distribution of the dry powder is given in red
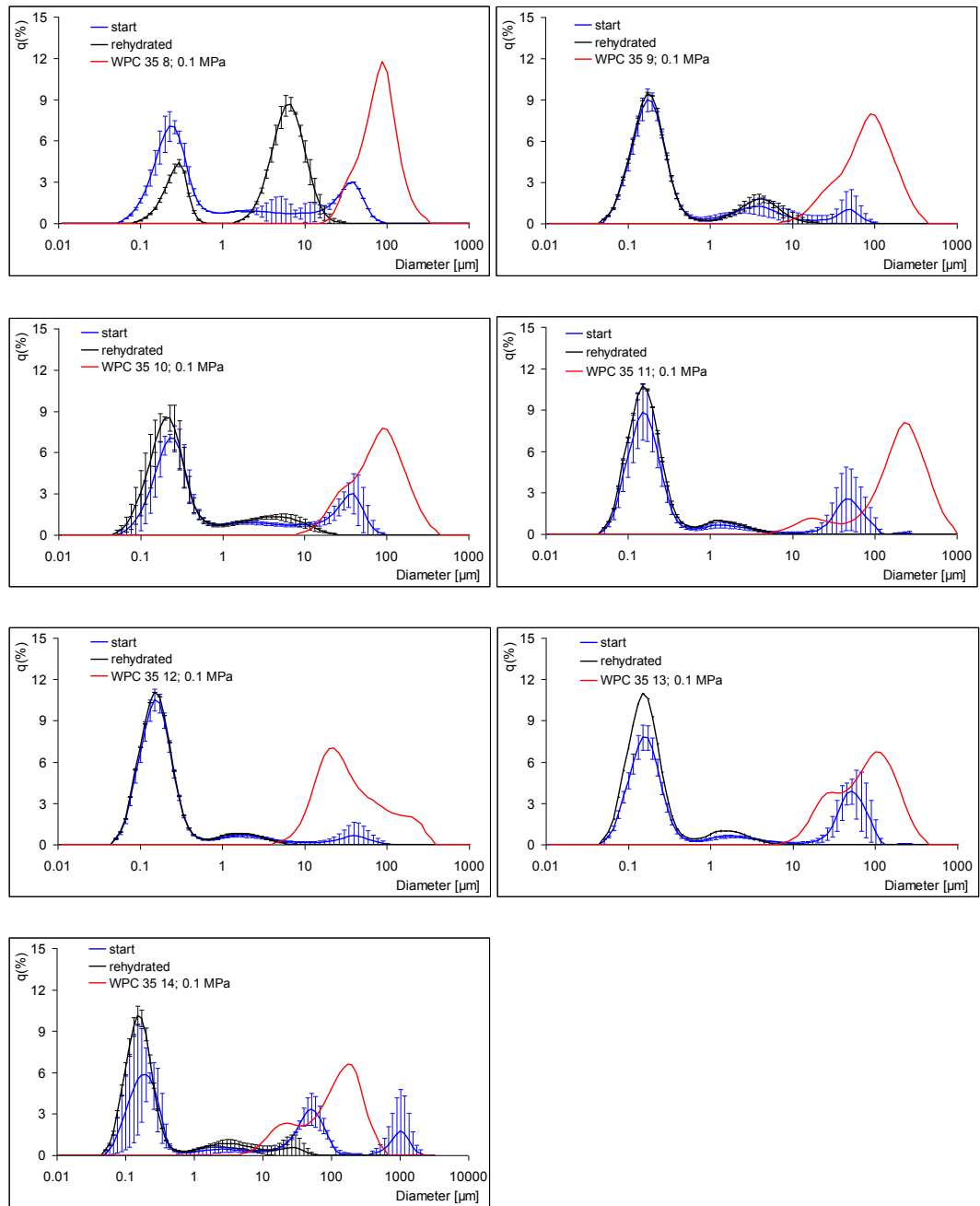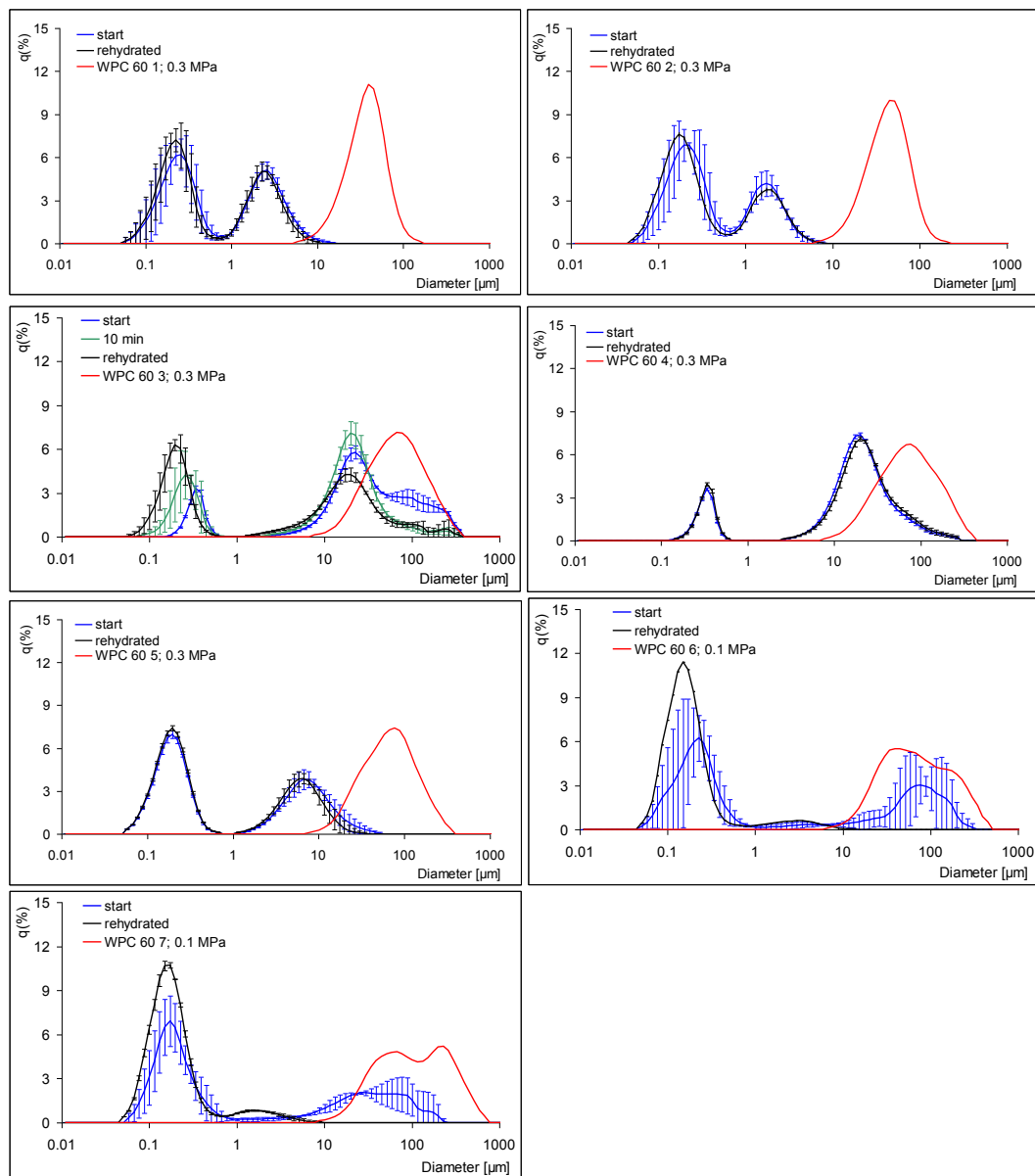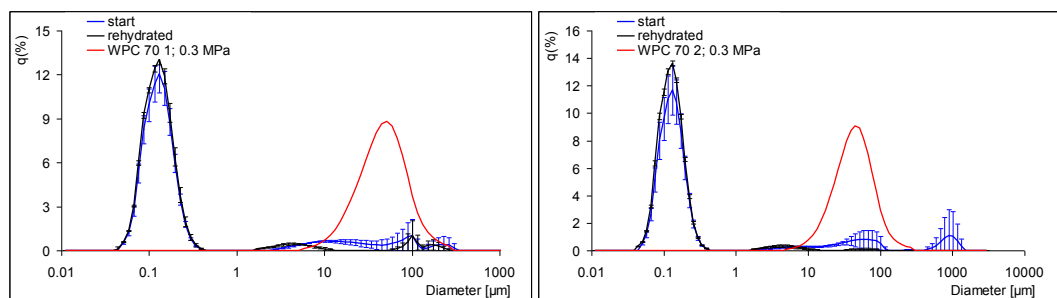
WPC 30 and 35

Figure 12-5: **PSD of the WPC 30 and 35 1 to 7 after the start and complete rehydration ($N = 3 \pm s$); the distribution of the dry powder is given in red**

Figure 12-6: PSD of the WPC 35 8 to 14 after the start and complete rehydration ($N = 3 \pm s$); the distribution of the dry powder is given in red

WPC 60

Figure 12-7: **PSD of the WPC 60 after the start and complete rehydration (*N* = 3 ± *s*); the distribution of the dry powder is given in red**

WPC 70

Figure 12-8: **PSD of the WPC 70 after the start and complete rehydration (*N* = 3 ± *s*); the distribution of the dry powder is given in red**
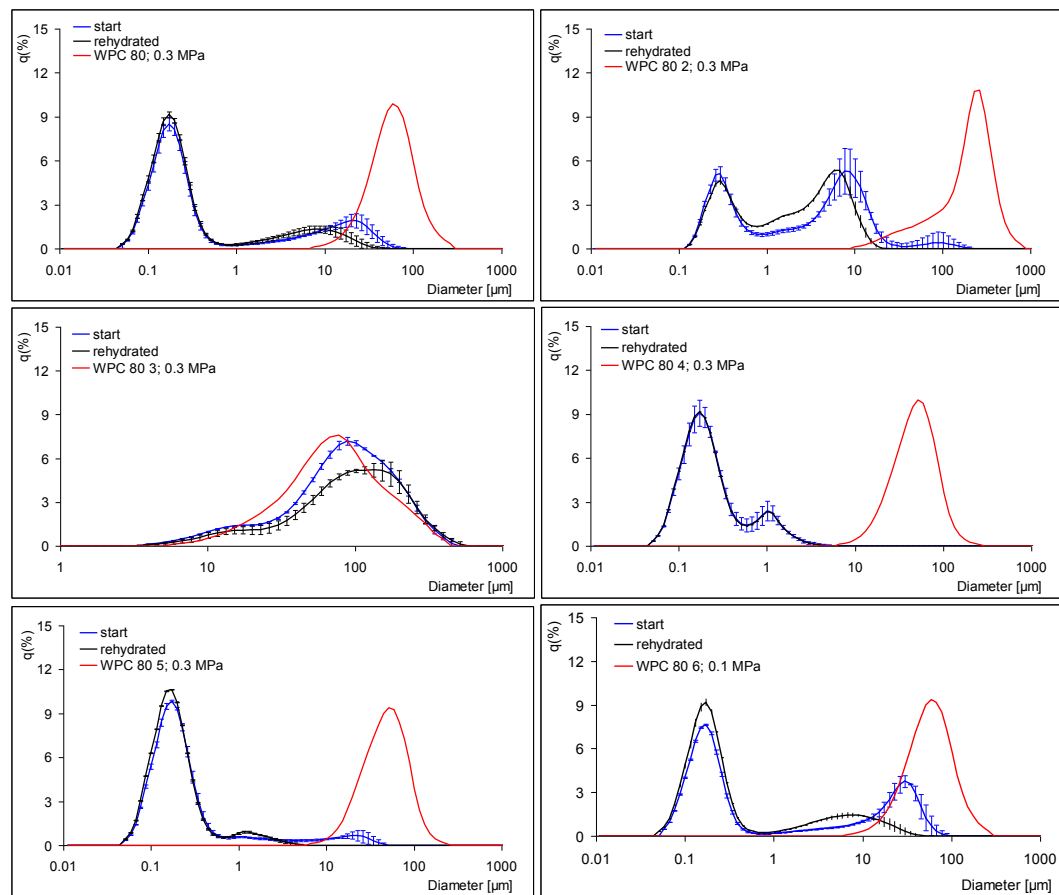
WPC 80

Figure 12-9:   PSD of the WPC 80 after the start and complete rehydration
(*N* = 3 ± *s*); the distribution of the dry powder is given in red

Production of quark

Scale-up: production of quark powder on a pilot plant and small-scale dryer

Table 12-27:   Warming parameters of quark in scraped SHE

$T_{heat\ exchanger\text{-}inlet}$	T_{outlet}	$\dot{V}$	Comment: medium
°C	°C	l·h⁻¹	
Variant I			
48.8	42.9	515	Water
51.8	38.5	480-550	
54.1	39.8	390-480	
58.1	43.4	420-515	
62.1	47.3	400-500	
62.5	51.5	380-500	
51.5	52.8	420-520	Quark
60.3	53.7	440-520	mixed
61.2	54.0	490-610	with
62.4	54.7	450-550	water
64.3	55.9	350-400	
65.9	57.5	410-660	
66.7	58.4	400-470	
67.6	59.7	350-450	Quark
68.3	61.5	300-400	350
68.3	62.0	300-500	400
68.6	63.3	300-500	400
69.5	65.0	360-430	390
69.4	64.3	350	350
Variant II: air input: 20 standard cubic meter			
68.0	65.0	260-430	330 Quark
67.6	64.5	330-430	380
67.5	64.4	350-450	400
67.4	64.2	350-450	400

Comment: stable atomization of quark at a primary pressure of 3.6 … 3.8 bar, acceptable, not expected atomization

Scale-up: production of quark powder on large-scale dryer

Table 12-28:   Warming parameters of quark in scraped SHE, large-scale dryer

$T_{incoming}$	T_{Quark}	$\dot{V}$	Comments
°C	°C	l·h^{-1}	
			Warming-up of the plant components with water
			Feeding of quark into the reservoir
65.9	54.2	2054	
66.2	53.7	2034	
66.6	53.4	2028	
67.4	53.2	2022	65% regulator
69.5	53.4	2035	
72.2	53.9	2045	
73.3	54.4	2025	
74.4	55.9	2028	
75.5	57.2	2013	
76.3	58.1	2028	61% regulator
75.7	59.1	2025	
75.6	59.4	2037	
75.5	59.7	2039	
75.4	59.6	2054	After pipe 54°C/905
75.7	59.6	2031	
76.1	59.6	2034	
76.0	59.9	2018	
76.3	60.2	2033	
76.4	60.3	2008	
			Feeding of the large-scale dryer
77.0	61.4	2013	
77.1	61.4	2020	
77.1	61.4	2005	
77.2	61.9	~2005	Break off

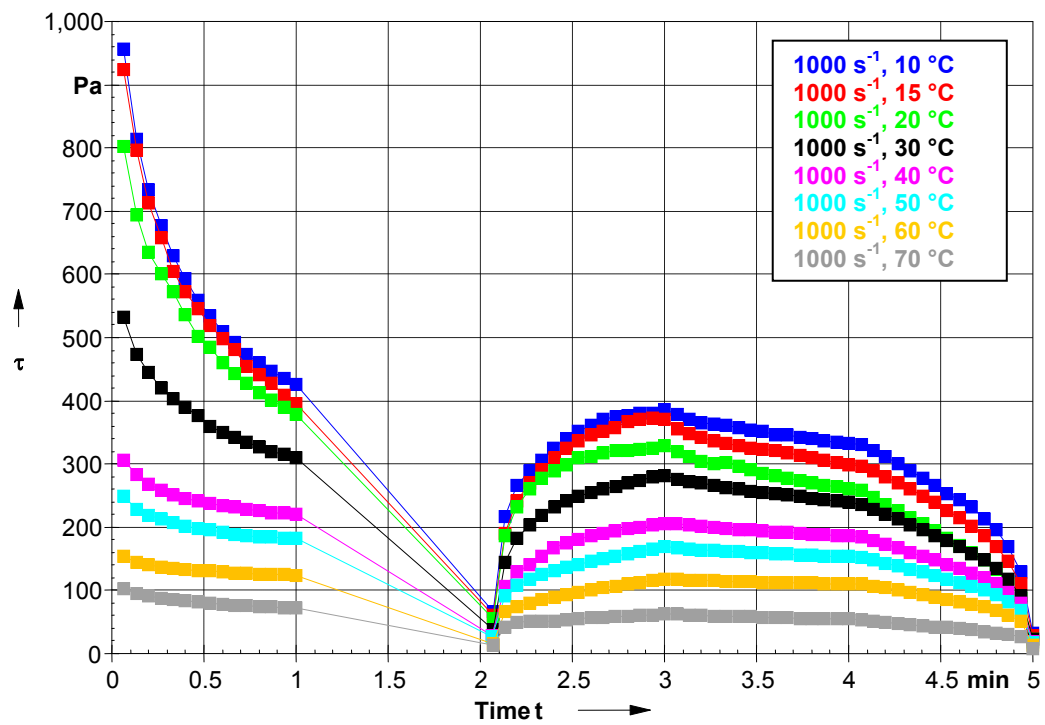*Influence of thermal and mechanical parameters on the low fat quark matrix*
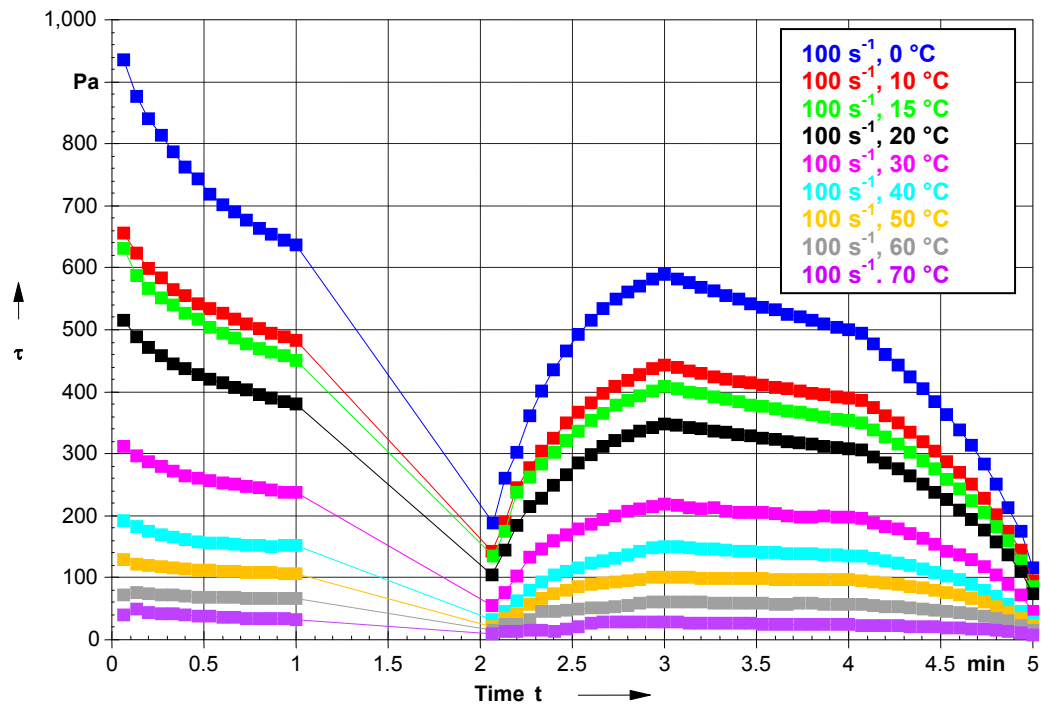
Figure 12-10: **Shear stress behavior at** $\dot{\gamma}_{max}$ **= 100 s^{-1}, temperature range 0…70 °C**
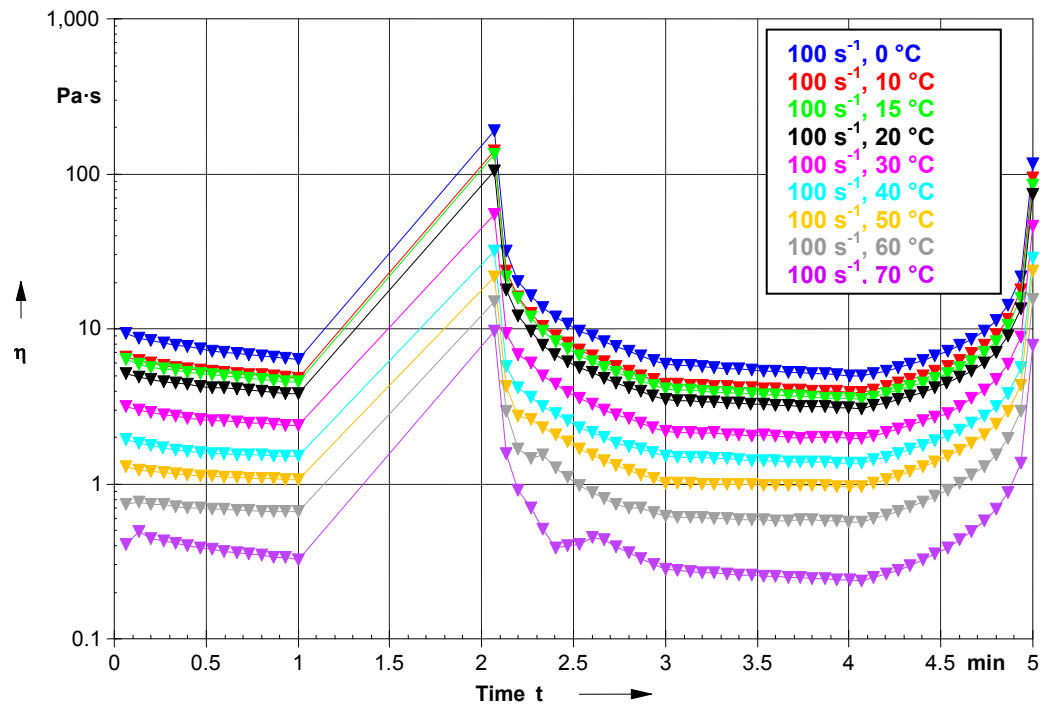
Figure 12-11: **Viscosity behavior at** $\dot{\gamma}_{max}$ **= 100 s^{-1}, temperature range 0…70 °C**
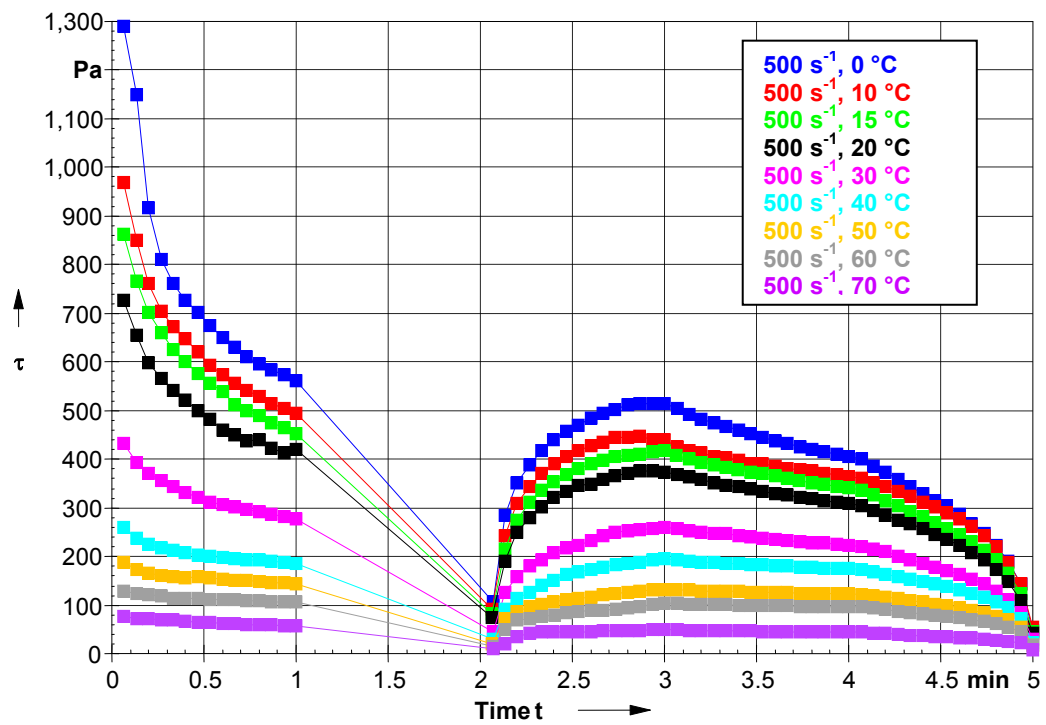
Figure 12-12: Shear stress behavior at $\dot{\gamma}_{max}$ = 500 s^{-1}, temperature range 0...70 °C
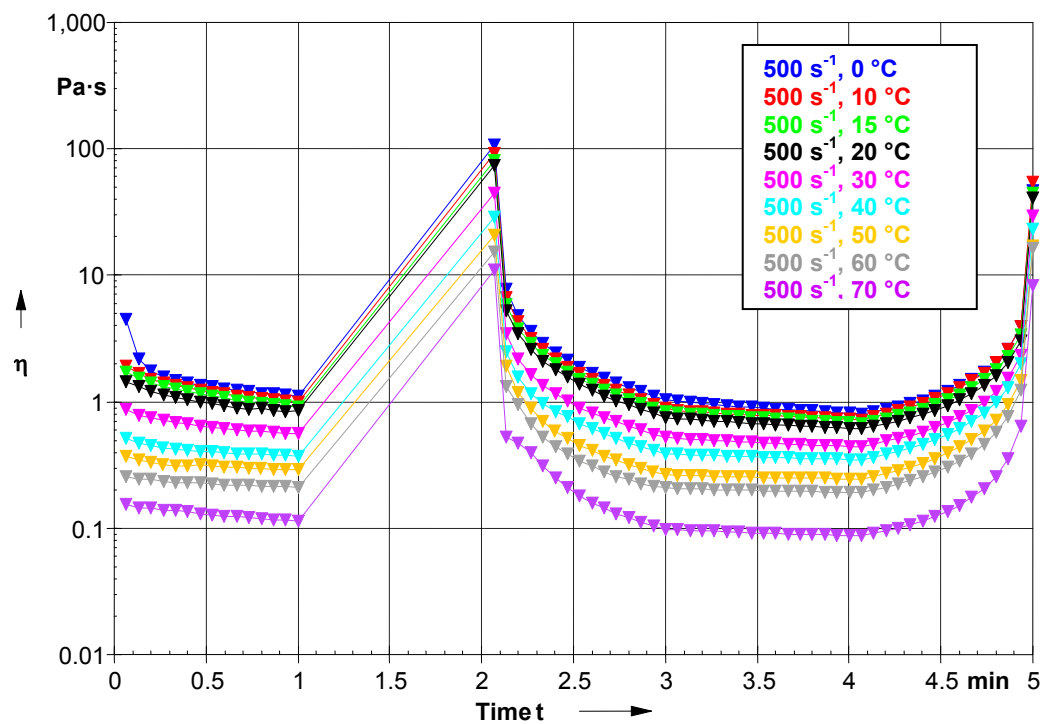
Figure 12-13: Viscosity behavior at $\dot{\gamma}_{max}$ = 500 s^{-1}, temperature range 0...70 °C

Figure 12-14: Shear stress behavior at $\dot\gamma_{max}$ = 1000 s^{-1}, temperature range 0…70 °C
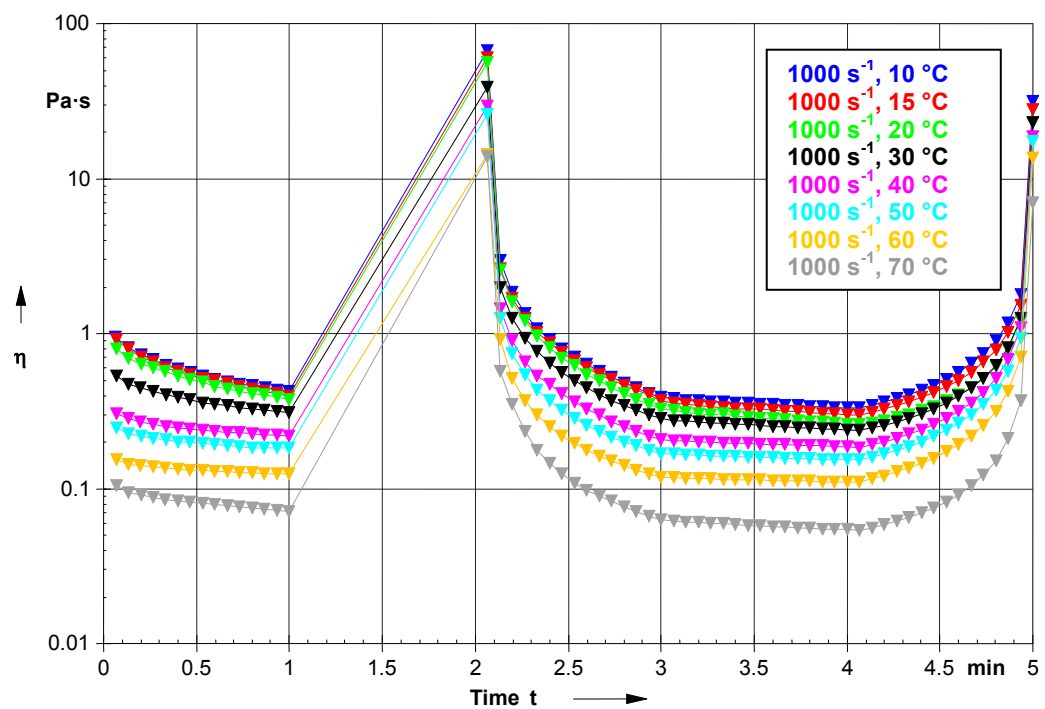
Figure 12-15: Viscosity behavior at $\dot\gamma_{max}$ = 1000 s^{-1}, temperature range 0…70 °C

Detection of interactions between mechanical energy and temperature
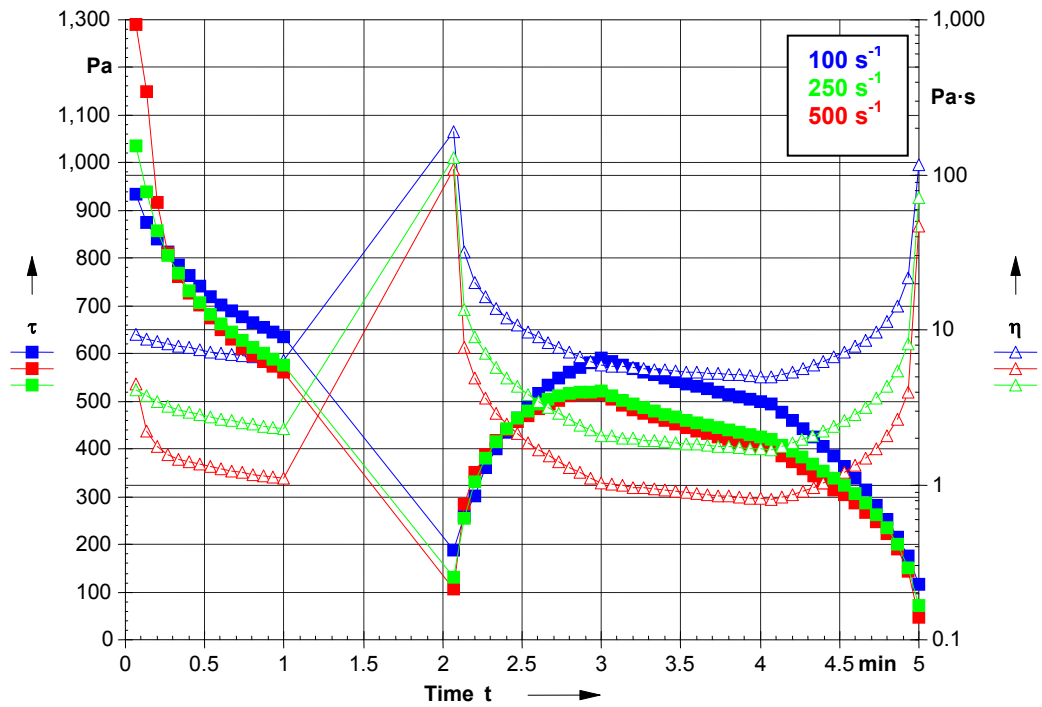
Figure 12-16:   Flow behavior in dependence on shear velocity at 0 °C
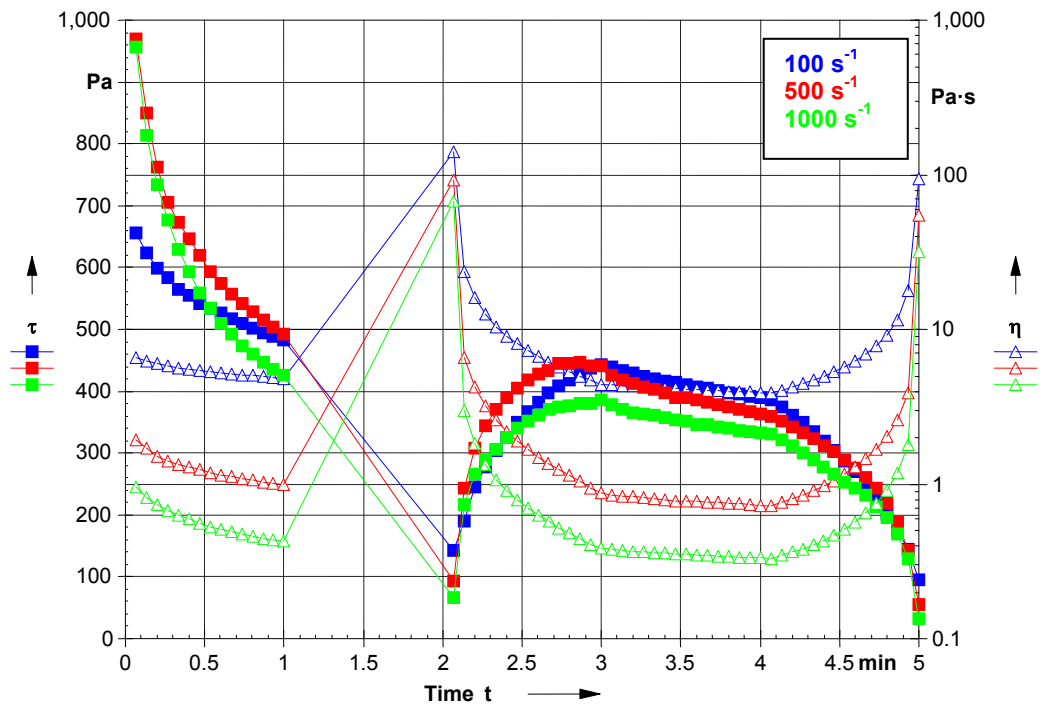
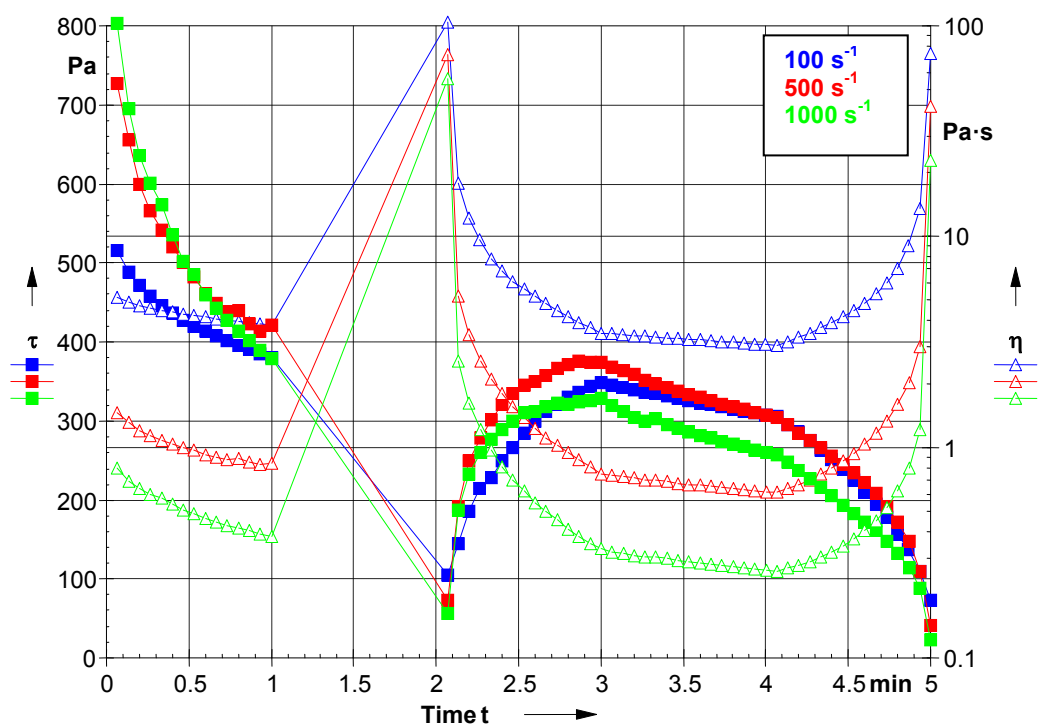**Figure 12-17:   Flow behavior in dependence on shear velocity at 10 °C**
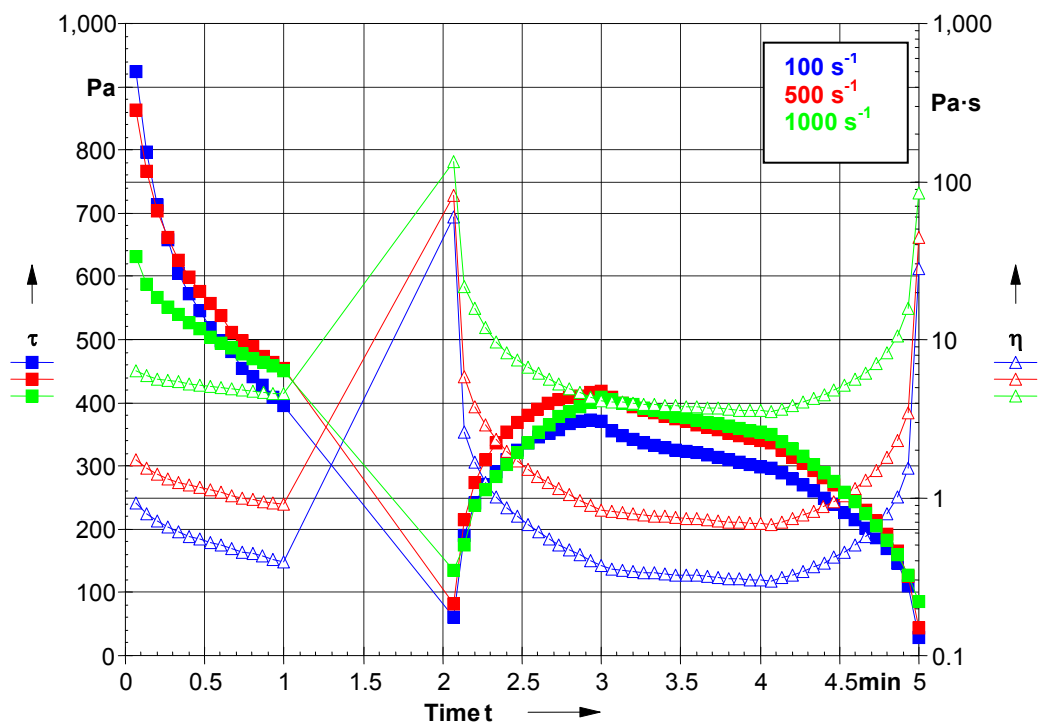
Figure 12-18: Flow behavior in dependence on shear velocity at 15 °C

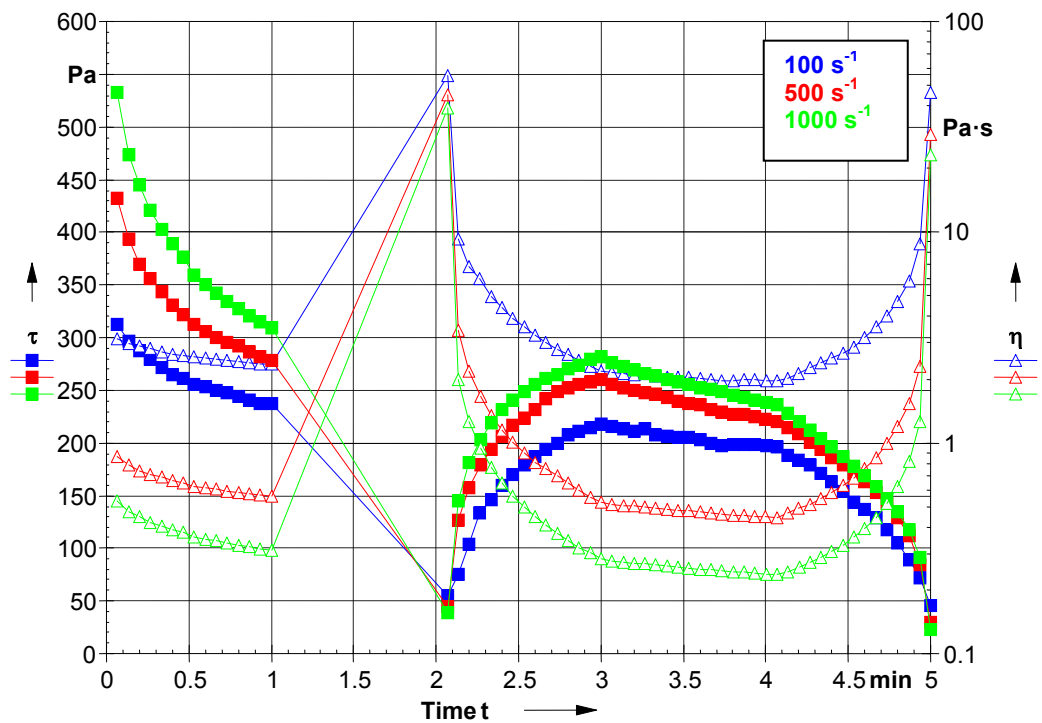**Figure 12-19: Flow behavior in dependence on shear velocity at 20 °C**

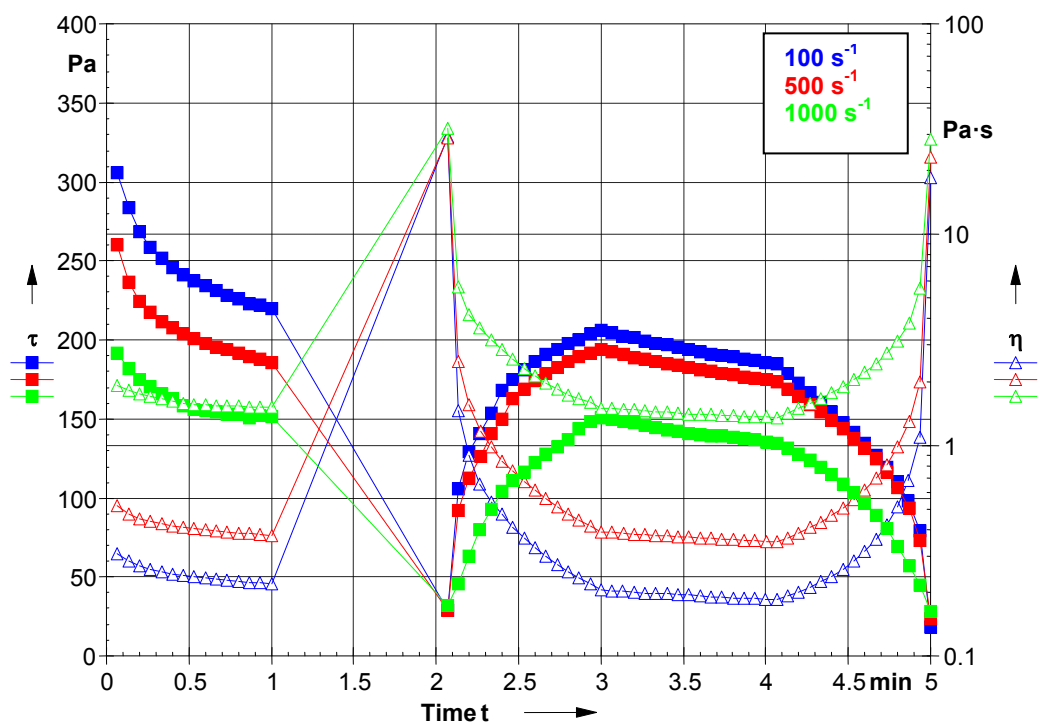**Figure 12-20: Flow behavior in dependence on shear velocity at 30 °C**

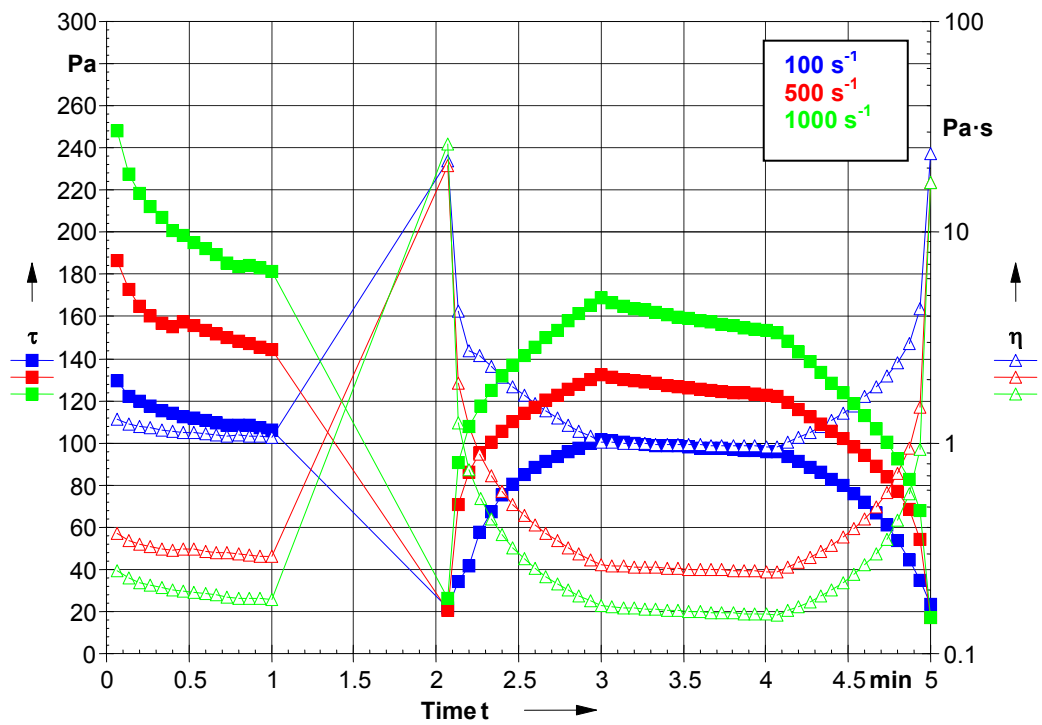**Figure 12-21: Flow behavior in dependence on shear velocity at 40 °C**

Figure 12-22:   Flow behavior in dependence on shear velocity at 50 °C
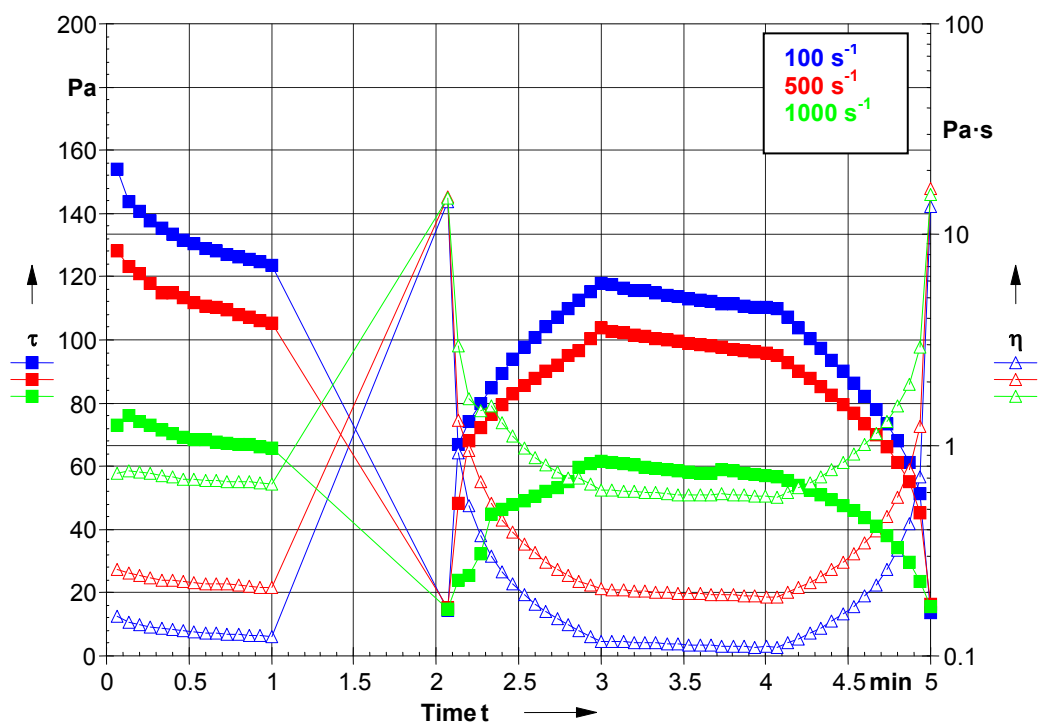

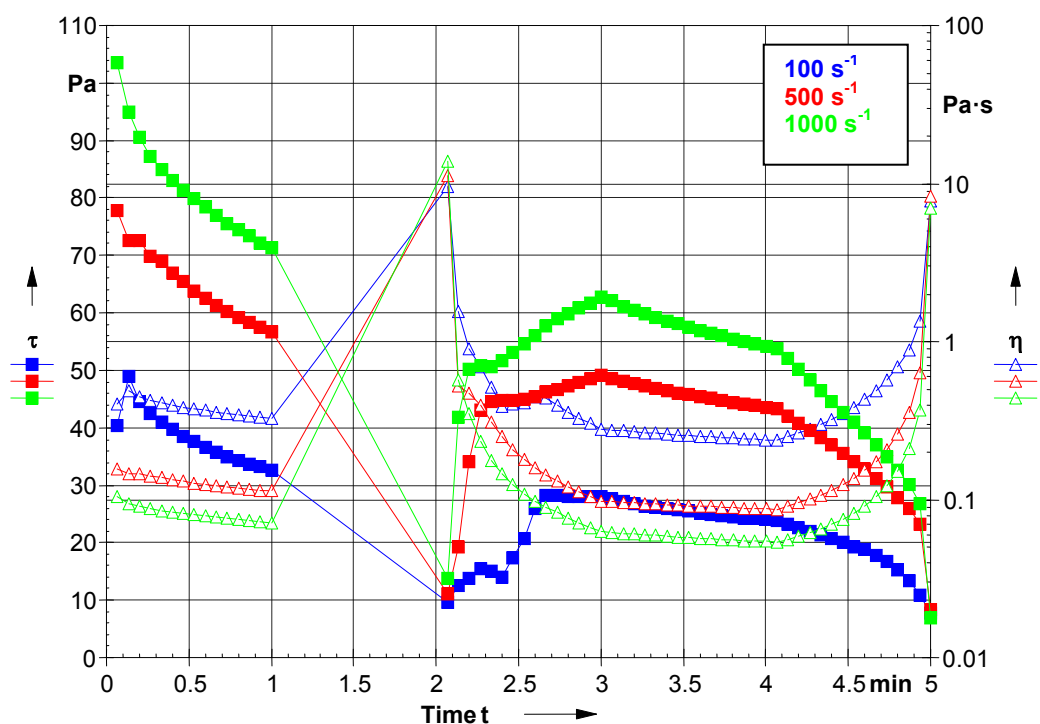**Figure 12-23:   Flow behavior in dependence on shear velocity at 60 °C**

Figure 12-24:   Flow behavior in dependence on shear velocity at 70 °C

Eidesstattliche Erklärung

Ich erkläre an Eides Statt, daß die vorliegende Dissertation in allen Teilen von mir selbständig angefertigt wurde und die benutzten Hilfsmittel vollständig angegeben worden sind.

Weiter erkläre ich, daß ich nicht schon anderweitig einmal die Promotionsabsicht angemeldet oder ein Promotionseröffnungsverfahren beantragt habe.

Veröffentlichungen von irgendwelchen Teilen der vorliegenden Dissertation sind von mir wie folgt vorgenommen worden.

Berlin,

Monika Stephanie Brückner-Gühmann geb. Brückner

List of Publications

Brückner Monika & Senge Bernhard (2007). Casein and structural changes during the rennet-induced coagulation of bulk raw milk from infected udder quarters of cows. Milchwissenschaft, 62, 245-249.

Brückner-Gühmann Monika, Grohmann Anne & Senge B. (2009). Untersuchung des Rehydratationsverhaltens von Molkenpulvern mittels Laserdiffraktometrie. Deutsche Molkereizeitung, Teil I 130 S. 20-23 Teil II 130 S. 20-24

Pesentations

Oral presentations

1. **Monika Brückner, Bernhard Senge** (2006). Kasein- und Strukturveränderungen bei der labinduzierten Gerinnung von verkehrsfähiger und nicht-verkehrsfähiger Rohmilch. Oral presentation at Innofood, Köthen, Germany
2. **Bernhard Senge, Reinhard Blochwitz, Monika Brückner** (2006). Optimierung der Linientechnologie bei der Rührjoghurtherstellung. Oral presentation at Innofood, Köthen, Germany
3. **Bernhard Senge und Monika Brückner** (2007). Kasein- und Strukturveränderungen bei der labinduzierten Gerinnung von verkehrsfähiger/ nicht-verkehrsfähiger Kuhmilch und Ziegenmilch. Oral presentation at Milchkonferenz, Wien, Austria
4. **Monika Brückner, Bernhard Senge** (2007). Untersuchung von Milchproteinumwandlungen aus struktureller und chemischer Sicht bei der labinduzierten Gerinnung von verkehrsfähiger und nicht-verkehrsfähiger Milch. Oral presentation at GDL-Kongress, Hamburg, Germany

Poster presentations

1. **Bernhard Senge, Reinhard Blochwitz, Monika Brückner and Bärbel Lieske** (2006). Structure formation and structure kinetic on acidification of milk. Poster presented at ISFRS, Zürich, Switzerland
2. **Bernhard Senge, Reinhard Blochwitz, Monika Brückner and Bärbel Lieske** (2006). Structure formation and structure kinetic on acidification of milk. Poster presented at GDCh Gemeinsame Regionalverbandstagung Nord-Ost und Süd-Ost, Berlin, Germany
3. **Bernhard Senge, Reinhard Blochwitz und Monika Brückner** (2007). Temperatur- und Scherbelastungsabhängigkeit der Strukturparameter von Rührjoghurt und Magerquark. Oral presentation at Milchkonferenz, Wien, Austria
4. **Grohmann, Anne; Brückner-Gühmann, Monika; Senge, B.** (2009). Particle Size as Important Parameter for Rehydration of Milk- and Whey Protein Powders. Presented at EFFoST - the European Federation of Food Science and Technology, Budapest, Hungary